Measuring the susceptibility and adhesion of microorganisms to light-activated antimicrobial surfaces

A thesis presented to University College London in partial fulfilment of the requirements for the degree of Doctor of Philosophy

Zoie Alexandra Aiken

Division of Microbial Diseases, UCL Eastman Dental Institute

Supervised by

Doctor Jonathan Pratten

Division of Microbial Diseases, UCL Eastman Dental Institute

Professor Michael Wilson

Division of Microbial Diseases, UCL Eastman Dental Institute

2012

Declaration

I, Zoie Alexandra Aiken, confirm that the work presented in this thesis is my own. Where information has been derived from other sources, I confirm that this has been indicated in the thesis.

Abstract

The prevention of healthcare-associated infections (HCAIs) is a major challenge currently being faced by hospitals in both the UK and worldwide. The hospital environment acts as a reservoir for nosocomial organisms contributing towards the transmission of bacteria and thus the colonisation and infection rates of the patient population. Therefore, it is desirable to implement measures to decrease the microbial load within the hospital environment as a whole and particularly on frequently touched surfaces. Antimicrobial coatings could be applied to these surfaces, and used as an adjunct to other infection control policies to reduce the incidence of HCAIs.

Novel nitrogen-doped, sulfur-doped and silver-coated titanium dioxide photocatalytic thin films were generated by sol-gel or chemical vapour deposition. The materials exhibited antibacterial properties after exposure to a white light commonly used in UK hospitals. However, it was difficult to synthesise reproducible thin films using the CVD method of deposition. An additional antibacterial material was generated with the potential to be used in endotracheal tubes to reduce the incidence of HCAIs such as ventilator-associated pneumonia. The novel polymer was impregnated with a photosensitiser using a swell encapsulation method, and activated with laser light; the antibacterial and anti-adhesive properties were then assessed.

Sampling the test surfaces by swabbing and subsequently performing viable counts was shown to provide an adequate estimate of concentration of bacteria on a test surface. The nitrogen- and sulfur-doped titanium dioxide coatings displayed significant photocatalytic activity against *Escherichia coli* after exposure to a white light source,

which demonstrate d a shift in the band gap from the UV to the visible region of the electromagnetic spectrum. Visible light photocatalysis was confirmed on the silver-coated titania thin films when a UV filter was used to block out the minimal UV component of the white light source, in the form of photo-oxidation of stearic acid, a reduction in the water contact angle and photocatalytic activity against an epidemic strain of meticillin resistant *Staphylococcus aureus* (EMRSA-16). This is the first example of unambiguous visible light photocatalysis and photo-induced superhydrophilicity alongside a titanium dioxide control that shows no activation. A reduction in the viability of EMRSA-16 adhered onto the surface of the irradiated silver-coated titania thin films was also demonstrated.

A significant reduction in the recovery of *Pseudomonas aeruginosa, Stenotrophomonas maltophilia, Acinetobacter baumannii* and *Candida albicans* was observed on TBO-impregnated polymers, after irradiation with a HeNe laser light. A recently isolated clinical strain of *P. aeruginosa* showed decreased susceptibility to the photo-activity of the TBO-impregnated polymers compared with a laboratory type strain. Finally, a significant reduction in the adhesion of *P. aeruginosa* on the TBO-impregnated polymers was demonstrated after a 3-step irradiation schedule. A photo-bleaching effect was noted after light exposure that reduced the antibacterial activity of the polymers, which demonstrates the requirement for further modification to retain the photosensitiser within the polyurethane matrix.

These novel materials have the potential to be used as anti-microbial surfaces in healthcare environments.

Acknowledgements

I would like to thank my supervisors Dr Jonathan Pratten and Professor Mike Wilson for their support over the last four years. It has been an eventful journey and I thank you for all the knowledge and wisdom you have shared with me. Thanks to Dr. Charlie Dunnill and Dr. Geoff Hyett for synthesising the CVD thin films and to Charlie for the assistance with theoretical concepts, especially during my writing up period – it has been invaluable. Thanks to Professor Ivan Parkin, Dr. Kristopher Page, and Dr. Stefano Perni for teaching materials chemistry to a microbiologist – it can't have been easy! I would like to acknowledge the Engineering and Physical Sciences Research Council for financial support, Dr. Aviva Petrie for providing statistical assistance and Dr. Nicky Mordan for preparing samples for SEM analysis and help in analysing the generated images.

I would like to thank the staff from the Division of Microbial Diseases at The Eastman Dental Institute, past and present who made the experience more enjoyable, especially Mike Brouwer (for motivating tea breaks, Body Combat, Stroopwafels, Bastongne & beer), Dr. Sarah Tubby, Linda Dekker, Dr. Katherine McCurrie, Salim Ismal, Dr. Lena Ciric, Dr Rachael Whealan, Dr. Florent Chang Pi, Dr. John Wright and Dr. Gil Shalom. Thanks to Dr. Tom Morgan and Dr. Will Koning for challenging my views on statistical analysis.

Thank you to Kerry Williams, Rebecca Gorton, Michelle Cairns and Dr. Cassie Pope for your friendship, support, love and scientific advice – my (other) London family! Thanks to Samantha Kaiser, Helen Castle, Catriona Wright, Alice O'Sullivan and Becca Owen

for your continued friendship and patience during the tough times. Thanks to Emiel Aiken, Dad, Mike Nelson, and also to the Derbyshire family for your laughter and continued support.

I'm indebted to Dr. Tim McHugh for helping me to believe that I could do a PhD, and to Dr. Clare Ling and Simon Rattenbury for hiring me as a trainee Clinical Scientist all those years ago, supporting me since and allowing me to pursue a career in Microbiology. Thanks to Dr. Mathew Diggle and Dr. Katrina Levi for your flexibility and understanding during my write-up period.

Finally, thank you to my Mum for being a constant support in my life. I've enjoyed sharing my positive results with you and your words of encouragement have kept me going through the bad times. I could not have done this without you. This is dedicated to you, and to Nanny, Grandad and Auntie Ann, who would have loved to be around to read this.

Table of contents

List of figures

List of tables

1 Introduction

1.1 Healthcare-associated infections

Healthcare-associated infections (HCAIs) are defined by the Department of Health as "any infection by any infectious agent acquired as a consequence of a person's treatment in healthcare" (Department of Health, 2008) and they are among the most common adverse events in hospitalised patients (Leape et al., 1991). Organisms that cause HCAIs are able to cause disease in the susceptible host and survive in the hospital environment for long periods of time (Dancer, 2011). The prevention and control of HCAIs within healthcare institutions both in the UK and worldwide, is a major priority and the recently revised document from the Department of Health, 'The Health Act 2006: Code of Practice for the Prevention and Control of Healthcare-Associated Infections' details standards required to achieve these aims (Department of Health, 2008). Mandatory surveillance of certain infections such as orthopaedic surgical site infections, and those caused by specific bacteria such as meticillin-resistant *Staphylococcus aureus* (MRSA) and *Clostridium difficile* have been introduced because of the morbidity and mortality associated with those infections (Report by the Comptroller and Auditor General - HC Session 2003-2004). Surveillance data are updated fortnightly and are available at www.data.gov.uk. The mandatory surveillance scheme was extended in June 2011 to include rates of *Escherichia coli* and meticillin-sensitive *S. aureus* bacteraemia (Health Protection Agency, 2011a). Government targets are also in place to reduce the incidence of infections caused by *S. aureus* and *C. difficile*. Both of these organisms can reside in harmony within healthy human hosts but cause serious problems when growth is uncontrolled or permitted outside their usual niches.

Approximately 1.7 million HCAIs are acquired annually in the American healthcare environment resulting in nearly 99,000 deaths a year, greater than the number of cases of any notifiable disease, with an associated cost per patient of between $16,359 and $19,430 (Scott II, 2009). When this figure is scaled up it amounts to a cost of between $28.4 to 33.8 billion dollars per annum (Klevens et al., 2007; Scott II, 2009). In response to the rising cost of in-patient care, the Centers for Medicare and Medicaid Services which provide health insurance for certain sections of the American population, have discontinued payment to hospitals if the patient is afflicted by one of eight 'preventable complications' during their stay (Rosenthal, 2007). The HCAIs included in this list are catheter associated urinary tract infections and vascular catheter-associated infections. An estimated 13,000 deaths were caused by urinary tract infection alone in 2002 (Klevens et al., 2007).

In England, approximately 1 in 10 patients have an HCAI at any one time, accounting for 100,000 cases and 5,000 deaths per annum (Report by the Comptroller and Auditor General - HC 230 Session 1999-2000; Report by the Comptroller and Auditor General - HC Session 2003-2004). Patients that acquire an HCAI are required to stay in hospital for an average of eleven additional days and incur treatment costs of nearly three times that of an uninfected patient; they are also seven times more likely to die than patients that did not acquire an HCAI (Plowman et al., 2000; Report by the Comptroller and Auditor General - HC Session 2003-2004, 2004). The financial cost of HCAIs in England has been calculated to be approximately £1 billion per annum and up to 30% of these infections can be prevented (Plowman et al., 2000). Introducing preventative measures costs less than treating the infection itself so intensive efforts are in place to

reduce infection rates (Report by the Comptroller and Auditor General - HC Session 2003-2004, 2004).

1.1.1 Organisms causing HCAIs

1.1.1.1 Meticillin-resistant *S. aureus* (MRSA)

S. aureus is found in the anterior nares of 20% of the population (Report by the Comptroller and Auditor General - HC Session 2003-2004, 2004; Alekshun and Levy, 2006) but causes infection in wounds, which can lead to osteomyelitis if it reaches the bone, abscesses if it penetrates deep into the tissues, bacteraemia and septicaemia if it gets into the bloodstream and from this point it could seed into any organ and cause disseminated disease. Meticillin-resistant *S. aureus* (MRSA) is resistant to the β-lactam group of antibiotics, which was the first line therapy before the widespread development of resistance. This resistance decreases the number of available treatment options, requiring the use of antibiotics with greater side effects, which can prolong the duration of treatment and the time spent in hospital.

MRSA is most commonly transmitted between patients via contaminated hands, but the persistence of the organism in the environment also provides an important source. Additionally, the presence of MRSA in the nasal passages of colonised patients enables spread via respiratory droplet nuclei. For these reasons, the near patient environment is often contaminated with bacteria and the most likely sources of MRSA/meticillin-sensitive (MSSA) contamination in colonised patients are the floor and bedframe, followed by the patient locker and the overbed table (Mulvey et al., 2011).

1.1.1.2 Glycopeptide-resistant enterococci

Glycopeptide-resistant enterococci (GRE) predominantly cause infections of the bloodstream, abdomen, pelvis or open wounds in immunocompromised patients. This patient group is likely to have had previous antibiotic treatment and a prolonged hospital stay, due to significant co-morbidities such as liver or renal disease, haematological malignancies or diabetes (Han et al., 2009) usually in a specialist ward such as intensive care or a renal unit (Health Protection Agency, 2011b). GRE are resistant to the glycopeptide group of antibiotics, which includes vancomycin and teicoplanin. Infections are usually either nosocomial or due to endogenous inoculation and are difficult to treat due to the lack of treatment options and the vulnerability of the affected patient.

The first reports of glycopeptide resistant enterococci were documented in the mid-1980s (Uttley et al., 1988) and there has been a significant increase in the incidence of both GRE colonisation and infection since; between 1989 and 1995 the proportion of glycopeptide-resistant strains of enterococci isolated in the United States rose from 0.3% to 10.4% (Gaynes et al., 1996). The emergence of GRE coincided with an increase in the use of vancomycin (Ena et al., 1993) and it is possible that sub-inhibitory concentrations of vancomycin were generated in the tissues of these patients so that vancomycin-resistance was selected alongside an overgrowth of the resistant *Enterococcus faecalis* (Uttley et al., 1988). A recent 10-year study calculated the 60-day mortality of patients with GRE bacteraemia at 57% and as standard empirical therapy often does not include cover for GRE, suitable antimicrobial therapy is often delayed which further increases mortality (Han et al., 2009).

GRE have increased tolerance to environmental conditions and therefore have an improved survival rate compared with MRSA. However, transmission of GRE is less frequent because the colonisation site is usually the gastrointestinal tract whereas MRSA commonly colonises the nasal passages allowing for transmission via respiratory droplets (Dancer, 2002). Unwashed hands remain an important fomite in the transmission of GRE.

1.1.1.3 C. difficile

C. difficile can be found in small numbers in the large intestines of some healthy humans. However, when the normal microbiota of the gut is compromised either by the use of broad spectrum antibiotics such as cephalosporins due to co-morbidities, or old age, the colonisation resistance effect of the gut is depleted which allows *C. difficile* to proliferate (Wilcox, 1996). The clinical presentation ranges from asymptomatic carriage, through to profuse diarrhoea and in serious cases toxic megacolon and pseudomembranous colitis which carries a significant mortality rate (Alekshun and Levy, 2006). *C. difficile* produces toxins during growth which damage the integrity of the colon and this damage contributes to the clinical symptoms. *C. difficile* is capable of entering a dormant phase during which the bacterial cells sporulate, and these spores have increased resistance to harsh environmental conditions such as desiccation, extremes in temperature and disinfectants. Spores are often found in high numbers in the areas surrounding *C. difficile* positive patients (Dancer, 1999) and elimination of this environmental source has been cited as a contributing factor in halting the onward transmission of infection (Samore et al., 1996).

1.1.1.4 Organisms causing ventilator-associated pneumonia

Ventilator-associated pneumonia (VAP) is a nosocomial bacterial infection of the lungs with a multifactorial etiology. An endotracheal tube (ETT) is placed along the trachea and is connected to a ventilator to allow mechanically assisted breathing. The physical presence of the tube interferes with the normal clearing of secretions such as mucus from the upper airways and allows micro-aspiration of contaminated subglottic secretions into the lungs. These secretions are contaminated with commensal bacteria which provide a source for a pulmonary infection. The lumen of the ETT itself can become colonised with bacteria, providing an additional source of infection. The organisms most commonly implicated are *S. aureus*, *Pseudomonas aeruginosa, Acinetobacter species* and *Stenotrophomonas maltophilia* (Johanson et al., 1972; Weber et al., 2007; Bouadma et al., 2010); these organisms are not usual commensals of the upper respiratory tract but the normal flora of hospitalised patients tends to contain a greater proportion of Gram-negative bacilli, which are also likely to display multidrug resistance phenotypes. VAP is the most common HCAI in the intensive care unit, accounting for 30 - 50% of infections and is associated with increased duration of intubation and increased length of hospital stay (Kollef et al., 2008; Bouadma et al., 2010).

The estimated number of infections caused by VAP in the United States is 52,543, with an attributable cost of between $14,806 and $27,520 per patient (Klevens et al., 2007). When all nosocomial pneumonias were considered, there were nearly 36,000 deaths in the United States and of the patients that survived, the extra length of stay in the hospital was 9 days (Wenzel, 1995).

1.2 Relevance of the environment in HCAIs

Dr Ignac Semmelweis, dubbed the 'Father of Infection Control', first described the importance of clean hands in the prevention of infection in 1861 (Semmelweis, 1861). He noticed an increased rate of puerperal fever in a labour ward attended exclusively by clinicians compared to a neighbouring ward attended exclusively by nursing staff. The clinicians performed autopsies on cadavers before attending to parturient patients but did not wash their hands after the investigations, thus allowing the transfer of the 'cadaveric particles' to the women in labour. Semmelweis proposed that all examiners should wash their hands in a solution of chlorinated lime to destroy the cadaveric material adhering to the hands. By introducing this measure, he reduced the rates of childhood mortality from 11.4% in 1846 to 1.8% in 1848 (Semmelweis, 1861).

More recently, the NHS National Patient Safety Agency launched the 'clean**your**hands' campaign, with the aim to improve the hand hygiene of healthcare workers in order to reduce the incidence of HCAIs (NHS National Patient Safety Agency, 2004). Hand hygiene plays an essential role in preventing the transmission of microorganisms (Casewell and Phillips, 1977; Hayden et al., 2006; Dancer, 2010) and it is recommended both in the scientific literature and by the World Health Organisation that hands should be decontaminated before and after touching a patient, before any aseptic procedure and after exposure to body fluids, as detailed in Figure 1.1.

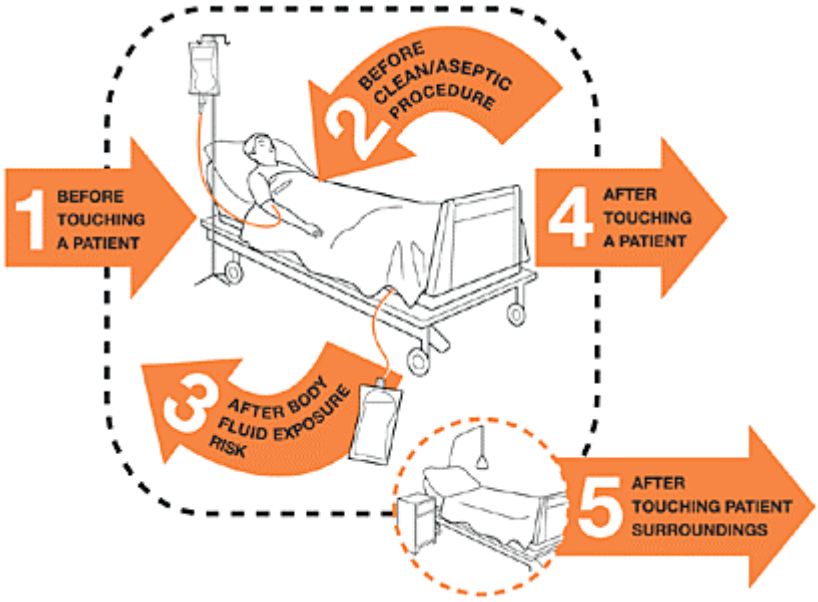

Figure 1.1 The World Health Organisation Five Moments for Hand Hygiene recommend hand decontamination after touching the near patient environment (Pittet et al., 2009)

The guidelines also recommend that hands should be decontaminated after contact with the environment surrounding a patient as evidence shows that sites close to the patient can be heavily contaminated with bacteria or bacterial spores (Samore et al., 1996; Weber and Rutala, 1997; Devine et al., 2001; Boyce and Pittet, 2002; Oie et al., 2007; Dancer et al., 2008; Pittet et al., 2009). The role of the environment in the transmission of HCAIs has been demonstrated in the scientific literature, and is illustrated in Figure 1.2.

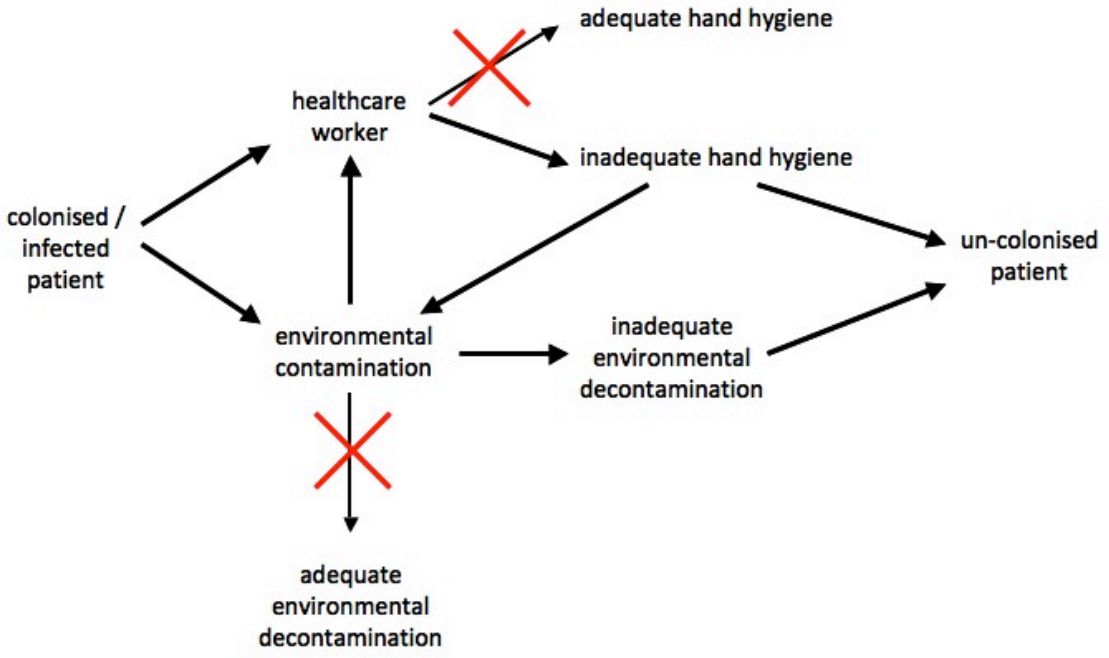

Figure 1.2 Transmission routes of pathogens within a hospital environment. Bold arrows indicate potential routes of pathogen transfer, and red crosses denote a disruption in transmission

Two independent routes have been described (Talon, 1999; Boyce and Pittet, 2002; Boyce, 2007; Dancer, 2008):

1. A healthcare worker (HCW) contaminates their hands by touching the environment, then touches a patient, leading to microbial transfer, or

2. A susceptible patient touches a contaminated surface and the microorganisms are transferred directly from the environment to the same patient.

Surfaces that are frequently touched by people in the hospital environment are termed 'hand-touch surfaces' and those that have been studied in the most detail to determine levels of microbial contamination include the bed-frame, bedside tables, door handles, toilet rails and toilet seats (Dancer, 2004; Denton et al., 2004; Boyce et

al., 2008; Dancer et al., 2008; Huslage et al., 2010). Hand-touch surfaces in the hospital environment are being increasingly implicated in the transmission of nosocomial pathogens, patient colonisation by these organisms and outbreaks of HCAIs (Boyce et al., 1994; Weber and Rutala, 1997; Bartley et al., 2001; Department of Health, 2001; Rampling et al., 2001; French et al., 2004; Johnston et al., 2006; Dancer, 2010; Dancer and Carling, 2010). In reality, adherence to hand washing practices has remained substandard but even exemplary hand hygiene cannot stop transmission if the environment has a high bacterial load (Dharan et al., 1999; Boyce and Pittet, 2002; Dancer, 2004, 2010; Erasmus et al., 2010).

The risk of acquiring MRSA, GRE or *C. difficile* has been demonstrated to be significantly higher in patients admitted to a room whose previous occupant had been MRSA, GRE or *C. difficile* positive (McFarland et al., 1989; Huang et al., 2006; Dancer, 2009; Carling and Bartley, 2010; Shaughnessy et al., 2011). Drees et al., (2008) showed patients who acquired GRE during their hospital stay were more likely to be in a room in which a GRE-positive patient had previously occupied, and GRE was isolated from the near-patient environment in 25% of cases. Bacteria are frequently found to contaminate hand-touch surfaces, even after cleaning, and organisms commonly found include MRSA, GRE and other causes of HCAIs such as MSSA and *Acinetobacter baumannii* (Denton et al., 2004; Lewis et al., 2008; Boyce et al., 2009; Mulvey et al., 2011).

The environment has also been shown to play a role in the transmission of infection outside a hospital setting. An American study showed an increased rate of diarrhoeal disease in children attending day care centres where the environment was found to be

contaminated with faecal coliforms (Laborde et al., 1993). The environmental sources implicated were moist sites such as sinks and taps and a two-fold increase in the rate of diarrhoea was found in children attending these facitilites, compared to centres with an uncontaminated environment. In a separate study of household cases of infant salmonellosis, the serotype of Salmonella excreted by the infected individual was also isolated from the environment (van Schothorst et al., 1978). Chopping boards have been commonly implicated in the spread of gastroenteritis. For example, inadequate cleaning of a chopping board contaminated with juices from raw turkeys led to an outbreak of gastroenteritis when the chopping board was later used to prepare sandwiches. Additionally, an individual investigating the outbreak also developed symptoms after touching the chopping board before smoking (Sanborn, 1963).

The risk of acquiring an infection from a contaminated environment is multifactorial and difficult to directly assess (Boyce, 2007; Lewis et al., 2008). However, it is likely to be linked to:

- the ability of the organism to survive desiccation;
- the frequency and level of cleaning;
- the level of surface contamination;
- the frequency of recontamination after cleaning;
- the frequency of contact with the hand-touch surface by healthcare workers, patients and visitors;
- the hygiene practices of the healthcare workers, patients and visitors.

1.2.1 Bacterial survival of desiccation

Some bacterial strains are more resilient to desiccation because of the ecological niche they occupy. For example, staphylococcal species are well adapted for survival on the arid environment of the skin and on environmental surfaces, which is likely to be linked to matric and ionic stress resistance (Chaibenjawong and Foster, 2011). MRSA has been shown to survive for over 2 months on a cotton-blanket (Duckworth and Jordens, 1990), GRE has been shown to survive for up to 4 months on a polyvinyl chloride surface (PVC) (Wendt et al., 1998) and *A. baumannii* was recovered from a patients room 6 months after discharge (Zanetti et al., 2007). Conversely, *Neisseria gonorrhoeae* thrives in the moisture-rich environment of the genital and buccal tracts but is not so well adapted for survival on the predominantly dry hospital surfaces

(Griffith et al., 2000). Furthermore, some epidemic strains of MRSA (EMRSA) have been shown to have an increased survival rate, and can survive in the environment at higher concentrations than sporadic strains (Farrington et al., 1992; Wagenvoort et al., 2000). This provides a selective advantage and contributes towards its persistence and endemicity in the hospital environment (Talon, 1999). *C. difficile* spores can survive in the environment for many years and spores are resistant to hand decontamination products such as alcohol hand gels, which further contributes to the persistence of these organisms in the environment (BAPS, 1994).

1.2.2 Cleaning frequency and standards

The purpose of cleaning is twofold: the microbiological purpose is to reduce both the microbial load and any nutrients which support bacterial growth or substances that inhibit the activity of disinfectants; the non-microbiological purpose is aesthetic and is to restore the appearance of the material and prevent deterioration (Collins, 1988). As thorough cleaning can reduce the microbial load then it can assist in breaking the cycle of transmission of infection within the hospital environment (Dancer, 2002; Lewis et al., 2008). Indeed, regular disinfection of surfaces has been shown to reduce the transmission of hospital pathogens by 40% and enhanced cleaning of the patient environment reduces acquisition of bacteria known to cause HCAIs (Hayden et al., 2006; Boyce, 2007; Carling and Bartley, 2010). Despite this, the frequency and standard of cleaning has decreased in recent years due to out-sourcing of contracts and limitations on cleaning budgets (Dancer, 1999; Carling et al., 2008; Dancer, 2008).

Cleaning with a detergent solution is usually sufficient, but the use of detergent alone has been shown to lead to an increase in bacterial contamination of hospital surfaces (Dharan et al., 1999; Dancer, 2011). A sporicidal agent, such as a chlorine containing formulation is required when the environment is contaminated with *C. difficile* (Weber and Rutala, 2011).

Using ATP to assess the cleaning process is an effective tool as the total organic soiling of a surface can be determined (Hawronskyj and Holah, 1997). A surface could be free from microbial contamination but could still contain a high level of organic soil originating from food residues which would provide nutrients to support microbial growth (Whitehead et al., 2008). Dead bacteria and viable but non-cultivable (VBNC) organisms can also be detected using ATP bioluminescence and would be missed by traditional culturing methods (Poulis et al., 1993). ATP bioluminescence has been shown to be a good indicator of the cleanliness of a surface and of likely bacterial contamination (Griffith et al., 2000; Malik et al., 2003; Anderson et al., 2011).

The Department of Health has drawn up a set of 'Standard Principles for the Prevention of Healthcare-Associated Infections' for hospitals to adhere to (Department of Health, 2001; NHS Estates, 2004). The first guideline covers the maintenance of a clean hospital environment and describes the potential link between inadequate environmental hygiene and the spread of microorganisms capable of causing HCAIs. It recommends that the hospital environment should be visibly clean and free from soilage and dust, but no microbiological guidance is provided (Department of Health, 2001). More recent guidance states that hospitals also have to provide and maintain a clean and appropriate environment for healthcare (Department of Health, 2008),

although no specific recommendation on the cleanliness of the environment is given. The American based Centers for Disease Control and Prevention have acknowledged this association in a set of guidelines which recommend cleaning or disinfection of environmental surfaces on a regular basis in addition to when visibly soiled (Rutala et al., 2008) and more frequent cleaning and disinfection of high-touch surfaces than minimal touch surfaces (Sehulster et al, 2003). These recommendations are all based on visual assessment to determine the cleanliness of the environment, which is a poor indication of the efficiency of the cleaning process (Malik et al., 2003).

However, proposed cleaning standards are not always adhered to. This is demonstrated by an environmental audit of a renal unit in an Australian hospital that showed just 43% of the minimum standards were being met during an outbreak of GRE (Bartley et al., 2001). The epidemic was terminated with a combination of measures including enhanced environmental cleaning and isolation of colonised patients to prevent onward transmission

1.2.3 Level of surface contamination

The level of environmental contamination is partly dependent on the patients' site of colonisation or infection; patients with MRSA in the urine, stools or in a wound display higher levels of environmental contamination than patients with MRSA isolated from other body sites (Rutala et al., 1983; Boyce et al., 1997; 2007; 2007; 2008). The environment surrounding a GRE-positive patient was seven times more likely to be contaminated with GRE than an un-colonised patient (Hayden et al., 2006) and when the routine environmental cleaning regimen was improved a decrease in

environmental contamination was observed. Certainly contaminated rooms are a risk factor for the acquisition of nosocomial pathogens (Hota, 2004) and a positive correlation has been demonstrated between the level of *A. baumannii* environmental contamination and the number of patients colonised or infected with *A. baumannii* (Denton et al., 2004).

The minimum level of contamination on a surface needed to initiate colonisation of a patient, which could lead to an infection, has not been quantified and is difficult to measure. Microbiological standards have been proposed for hand-touch surfaces in hospitals in an attempt to determine whether the microbial contamination of a given surface presents a risk of infection for any patients in that vicinity (Dancer, 2004; Mulvey et al., 2011). It was proposed that an integrated and risk based approach should be used encompassing visual assessment, rapid assays to detect organic soil and microbiological testing. The standards for the microbiological assessment were split into two sections: (i) the presence of indicator organisms and (ii) the total aerobic colony count.

Indicator organisms are pathogens that pose a significant threat to patients and include MSSA, MRSA, *C. difficile*, *Salmonella* species, multi-drug resistant Gram-negative bacilli, GRE and a number of other organisms that are important in certain clinical situations, such as *Aspergillus* species in a ward for severely immunocompromised patients. This standard was set at less than 1 cfu / cm^2. The second standard was set to provide an indication of the complete microbial load on a given surface, as a high microbial load on a hand-touch surface is likely to represent poor environmental cleaning and the heavy growth of other organisms may shield the

presence of an indicator organism (Dancer, 2004). This standard was set at less than 5 cfu / cm^2. These standards have since been tested and adapted in different hospitals using various detection systems to validate the set benchmarks and are still under review (Griffith et al., 2000; Malik et al., 2003; Aycicek et al., 2006; Griffith et al., 2007; Oie et al., 2007; Dancer et al., 2008; Lewis et al., 2008; Dancer, 2011; Mulvey et al., 2011).

1.2.4 Frequency of surface re-contamination post-cleaning

The hospital environment is rapidly re-contaminated after cleaning (Weber and Rutala, 1997) and hospital floors can become re-contaminated to the same level as before the cleaning event, within 2 hours (Collins, 1988; Dettenkofer and Spencer, 2007). Benchmarks could be used to establish how long it takes for a surface to become re-contaminated after cleaning so that the frequency of cleaning could be optimised (Lewis et al., 2008). Bed occupancy rates also have an effect on the microbial contamination of the hospital environment and the risk of infection with MRSA. One study demonstrated greater bacterial contamination of sampled hand-touch surfaces when bed occupancy rates were above 95% compared with bed occupancy rates of below 80%, and a separate study showed the risk of cross-infection with MRSA was increased for patients in a five-bedded bay compared with those in a four-bedded bay (Kibbler et al., 1998; Dancer et al., 2008). Bed making has also been shown to increase airborne levels of *S. aureus*, which then have the potential to settle on near-patient surfaces and further contaminate the environment (Shiomori et al., 2002; Hansen et al., 2010). Re-contamination of the patient environment is not surprising given that viable skin colonising microorganisms are carried on skin squames, one million of

which are shed from healthy skin each day, efficiently transferring bacteria into the immediate surroundings (Noble, 1975).

Bacterial contamination of the environment is not necessarily detrimental to a patient's health. Bacterial contamination of the hospital environment is ubiquitous even though the environment is dry and free from substances that encourage microbial growth (Collins, 1988; Dettenkofer et al., 2011). Gram-positive cocci are most commonly found and more than 99% are likely to be coagulase negative commensals and thus unlikely to cause serious disease. To create an environment completely free from bacteria would require sterilisation, which is both impractical and unnecessary. It would however be advantageous to create an environment where the bacterial population present does not contain pathogens and is unlikely to cause infection (Collins, 1988).

1.2.5 Frequency of contact with the hand-touch surface

By definition, hand contact upon hand-touch surfaces is frequent, so the numbers of occasions for the potential transfer of pathogens from contaminated hands to these surfaces, or vice versa, is high. The near-patient environment contains numerous hand-touch surfaces; on an intensive care unit for example, there are various items of instrumentation such as ventilators and monitors that could be potential reservoirs of infection (Dancer, 2008). Nursing staff rather than domestic staff are usually responsible for cleaning these surfaces and it is often a low priority task, in fact only 40% of these surfaces were shown to be cleaned adequately (Dancer et al., 2008; Dancer, 2009; Carling and Bartley, 2010). Ten hand-touch surfaces were sampled in

two surgical units over a one year period and it was found that near-patient, hand-touch sites cleaned by trained nursing staff were most likely to fail microbiological hygiene standards as opposed to surfaces cleaned by domestic staff (Dancer et al., 2008). Denton et al., (2004) clearly defined the responsibility for cleaning these hand-touch surfaces to the different staff groups during an outbreak of *A. baumannii* and this measure along with a number of others, assisted in terminating the outbreak. Anderson et al., (2011) demonstrated more recently that surfaces cleaned by domestic staff are more likely to pass defined hygiene standards than surfaces which are cleaned by other staff such as nurses and clinical support workers.

Hands are an important fomite implicated in the transfer of pathogens between patients, and improvements in routine cleaning regimens have been associated with a decrease in the contamination on the hands of healthcare workers (Hayden et al., 2006). An association has been demonstrated between positive cultures from the hands of healthcare workers and *C. difficile* environmental contamination, which implies that the environment can play a role in contaminating the hands of the staff (Samore et al., 1996; Weber and Rutala, 2011). Bhalla et al., (2004) showed the transfer of pathogens from the near-patient environment to the hands of the investigators in over half of the sampling occasions and surprisingly, pathogen transfer occurred in occupied patient rooms, regardless of the colonisation or infection status of the patient. These examples demonstrate the importance of adhering to defined cleaning standards, with defined roles and responsibilities for staff members.

1.2.6 Hygiene practices of staff, patients and visitors

There is a large variation in the hand hygiene practices of healthcare workers and a recent systematic review of 96 studies reported hand hygiene compliance rates ranging from 4 – 100% with an overall average rate of 40% (Erasmus et al., 2010). Compliance was lower in the intensive care unit setting, amongst clinicians and before patient contact, even though this is the first of The World Health Organisation Five Moments for Hand Hygiene (Pittet et al., 2009; Erasmus et al., 2010). Intervention campaigns to improve hand-washing compliance are often effective during and immediately after the campaign (Cheng et al., 2011) but compliance rates often drop in the months after the intervention.

Educating staff about the importance of cleaning the hospital environment has resulted in improvements in the quality of cleaning as assessed by a number of methods: UV powders and gels have been applied to surfaces to assess the efficiency of the cleaning regimen and an increase in cleaning rates was achieved after feedback of surveillance results (Carling et al., 2008; Munoz-Price et al., 2011). ATP bioluminescence has also been used to assess contamination on hand-touch surfaces and a reduction in the relative light unit (RLU) values was observed after a similar education programmes (Poulis et al., 1993; Griffith et al., 2007; Boyce et al., 2009; Mulvey et al., 2011). Patient and visitor involvement in hand decontamination also decreases bacterial contamination of the healthcare environment.

1.3 Antimicrobial coatings

Antibacterial materials could be used to supplement cleaning of the hospital environment and The Centres for Disease Control and Prevention recommend further evaluating implementation of antimicrobial materials for use in the hospital environment (Rutala et al., 2008). It has been shown that bacteria can be spread from a contaminated area to a non-contaminated area during the cleaning process (Dharan et al., 1999). Recontamination of the hospital environment also occurs readily after cleaning events (Collins, 1988) and cleaning has often been found to be inadequate with studies showing only 34% compliance with policies (Carling and Bartley, 2010; Carling et al., 2010).

If hospital surfaces were coated with an antibacterial material, then the contaminated areas would be susceptible to the killing effect of the coating, and decontamination of the affected areas could occur in between cleaning events. Continuous protection of the hospital environment in this way has been proposed by a number of authors as an adjunct to other infection control procedures (Casey et al., 2010). Reducing the bacterial load in the environment can help to prevent person-to-person spread of bacteria and the development of infection.

MRSA has been isolated from computer keyboards within a hospital ward (Devine et al., 2001); however, when self-cleaning keyboards were used in a surgical ward in a Scottish hospital, sampled surfaces were consistently below the defined ATP benchmarks and passed the hygiene standards in the cleanliness audit (Anderson et al., 2011).

1.3.1 Silver as an antimicrobial agent

Silver has a broad spectrum of activity and is active against Gram-negative and -positive bacteria, fungi, viruses and protozoa (Davies and Etris, 1997; Martinez-Gutierrez et al., 2010). The antibacterial effect of silver has been known for centuries, and was used by the ancient Egyptians and Greeks to treat infectious ailments. For example, Hippocrates described the use of a silver powder to treat ulcers (Hippocrates, 400 BC) and at around the same time, Alexander the Great kept his drinking water clean by the use of silver water vessels (White, 2002). Silver was re-introduced for topical applications in the 1960s in the forms of silver nitrate or silver sulfadiazine, especially in the prevention of wound infections (Moyer et al., 1965; Fox et al., 1969). In more recent times, silver has been coated onto many substrates or impregnated throughout substances to provide antibacterial protection (Melaiye and Youngs, 2005). The use of silver nanoparticles is increasing due to their high antibacterial activity and small size, which provides a large surface area to volume ratio (Ruparelia et al., 2008; Lv et al., 2010).

1.3.1.1 Mechanism of action

The mechanism behind the antibacterial activity of silver and other metal ions is due to the oligodynamic effect, first described by Karl Wilhelm von Nägeli as the lethal effect that small metal ions exert on living cells (Kraemer, 1905). Silver binds to thiol groups on the bacterial proteins, including the ribosome and NADH dehydrogenase, which inhibits the expression of enzymes required in ATP production and prevents electron transfer and respiration, respectively (Davies and Etris, 1997; Plowman et al., 2000; Percival et al., 2005; Yamanaka et al., 2005; Kim et al., 2008; Liu et al., 2010). Oxidation

of key components of the respiratory pathway inhibits bacterial respiration (Bragg and Rainnie, 1974) and silver also reacts with microbial DNA to cause the free DNA to form a condensed Ag-DNA complex in the centre of the cell, which results in a loss in its replicative function (Feng et al., 2000; Melaiye and Youngs, 2005). Externally, silver targets the bacterial cell membrane and once bound, causes pitting and interference of membrane function, which has been visualised by electron microscopy (Clement and Jarrett, 1994; Lin et al., 1996; Percival et al., 2005; Kim et al., 2007). Interactions with the cell membrane also cause a collapse in the proton motive force, leading to the leakage of H^+, de-energisation of the membrane and cell death (Dibrov et al., 2002). Silver nanoparticles have also been shown to form silver-sulfur aggregates on the surface of bacterial cells, which interferes with the generation of free radicals, which can cause damage to bacterial cell membranes (Kim et al., 2007).

Serious adverse effects of silver in humans is limited to neurotoxicity, which is only experienced if the blood-brain barrier is breeched and *in vitro* toxicity to mammalian cells has not been replicated in the treatment of wound infections (Melaiye and Youngs, 2005; Taylor et al., 2009).

Zone of inhibition or agar pour plate tests were used to demonstrate the diffusible antibacterial activity of silver-based compounds against a range of bacteria including *E. coli, Klebsiella pneumoniae, P. aeruginosa, Streptococcus mutans, S. epidermidis, S. aureus, Bacillus anthracis, Acinetobacter baylyi, Mycobacterium fortuitum* and *Candida albicans* (Furno et al., 2004; Eby et al., 2009; Durucan and Akkopru, 2010; Gerasimchuk et al., 2010; Pollini et al., 2011; Rivero et al., 2011). This diffusible antibacterial activity would be advantageous for implants or surgical instruments to give an initial high dose

of silver to the surrounding environment, which would decrease the likelihood of resistance developing (Stobie et al., 2008). The release of silver from the surface can be further controlled by modifying the composition of the coating (Liu et al., 2010). Combining silver with an antibiotic agent can further enhance the antibacterial activity (Fox, 1968; Shahverdi et al., 2007; Kim et al., 2008).

1.3.1.2 Resistance to silver

Silver is a biocide and as such has multiple modes of action, unlike an antibiotic that tends to target a specific site (Percival et al., 2005). Biocides therefore have a broader spectrum of activity and resistance is less likely to occur. Silver resistance was not detected in any bacterial strains causing urinary tract infections in patients with silver-coated catheters *in situ* over a 12-month period (Rupp et al., 2004). However, resistance has been identified in many species of bacteria, mainly from burns units where silver-based dressings are used to prevent bacterial infection (Clement and Jarrett, 1994; Silver, 2003).

A strain of silver-resistant *Salmonella* was isolated from a hospital in Massachusetts and the resistance determinant was found to be a 180 kb plasmid pMG101 (McHugh et al., 1975). Much work has since been performed on this plasmid to elucidate the molecular basis for resistance, and the sequenced region is available on Genbank (Gupta et al., 1999). The gene cluster includes a periplasmic silver-specific binding protein (SilE) and two parallel efflux pumps (SilP and SilCBA) (Gupta et al., 1999) and amplification of these genes provides a rapid method of identifying resistant strains (Percival et al., 2008). Genotypic resistance does not typically translate directly into phenotypic resistance; three strains of *Enterobacter cloacae* isolated from burn

wounds were found to carry these resistant genes but still demonstrated susceptibility to therapeutic levels of silver *in vitro* (Percival et al., 2005). The widespread development of resistance to silver is unlikely as bacteria have been exposed to sub-inhibitory concentrations of this metal ion for centuries, however greater use will increase the likelihood of resistance developing (Percival et al., 2008).

1.3.1.3 Applications of silver as an antimicrobial material

1.3.1.3.1 Central venous catheters

Silver-coated catheters have been developed with the aim to reduce the probability of developing line-associated infections, which are a common cause of HCAIs (Noimark et al., 2009; Syed et al., 2009). Experimentally, silver-coated polyurethane catheters were inserted into a rat model, and bacteria could not be isolated from the surface of the lines after 6 weeks implantation in the internal jugular vein (Bambauer et al., 1997). A significant reduction in *E. coli* adhesion on silver-coated polyurethane catheters was demonstrated *in vitro* and of those bacteria that did adhere, a greater proportion of cells found on the silver-containing polymer were non-viable compared to the uncoated controls (Gray et al., 2003).

1.3.1.3.2 Urinary catheters

The American-based Healthcare Infection Control Practices Advisory Committee published guidelines detailing best practices in the prevention of catheter-associated urinary tract infection and the use of antimicrobial catheters were to be considered if other methods of decreasing rates of infection were failing (Gould et al., 2010). In the USA, a trial on the use of silver/hydrogel coated catheters was conducted compared

with standard silicone/hydrogel urinary catheters and the incidence of catheter-associated urinary-tract infections fell from 6.3 infections per 1000 catheter days to 2.6 infections per 1000 catheter days, achieving a 57% reduction overall (Rupp et al., 2004). In a separate study, a 60% reduction in catheter-associated urinary-tract infections was achieved following introduction of silver coated catheters, achieving an annual saving estimated to be in the region of £38,000, and the release of 192 bed days (Report by the Comptroller and Auditor General - HC Session 2003-2004).

1.3.1.4 Endotracheal tubes

An endotracheal tube (ETT) containing silver nitrate and sodium hydroxide reduced adhesion of *P. aeruginosa* (Monteiro et al., 2009) and a number of other studies have demonstrated clinical efficency of silver coated ETTs; this is further discussed in Section 1.4. Silver coated endotracheal tubes have been approved for clinical use in the USA, but the increased cost and risk of breakthrough events of VAP have prevented its' widespread use (Raad et al., 2011).

1.3.1.5 Environmental surfaces

Silver-based compounds can also be employed on inanimate surfaces which could potentially be added to hand-touch surfaces; sol-gel deposition was used to synthesise silver-doped phenyltriethoxysilane films that prevented *S. epidermidis* adhesion and biofilm formation over a 10-day period (Stobie et al., 2008). Silver-doped TiO_2 and titanium nitride thin films caused significant decreases in the viability of *S. aureus*, *E. coli, Streptococcus pyogenes* and *A. baumannii* (Kelly et al., 2009; Wong et al., 2010). *P. aeruginosa* appeared more sensitive to the titanium nitride films and growth was

inhibited for up to 7 days, supporting the hypothesis that Gram-positive bacteria are more resistant to the antibacterial effects of silver. This could be due to the larger amount of negatively-charged peptidoglycan in the thicker Gram-positive cell wall which could bind silver, thus reducing the silver available to act upon the interior of the cell to cause damage (Schierholz et al., 1998; Kawahara et al., 2000; Gray et al., 2003; Monteiro et al., 2009). However, other groups have shown that Gram-positive and -negative strains possess similar susceptibility to silver (Ruparelia et al., 2008; Wong et al., 2010). In a recent hospital study, a range of silver-coated products were placed in ward areas to monitor the effect on bacterial contamination of the environment and up to 98% fewer bacteria were recovered from the environment, compared with a control ward which contained uncoated products (Taylor et al., 2009). The antimicrobial activity lasted for the duration of the 12-month test period and adverse effects to silver were not reported.

1.3.1.6 Other applications

Surgical masks have been impregnated experimentally with titanium dioxide (TiO_2) and silver nanoparticles and no viable *S. aureus* or *E. coli* was detected after 48 hours. No adverse reactions were observed in human volunteers (Li et al., 2006). Silver has been incorporated into dental composite resins and a slow and sustained release of silver into the surrounding environment has been demonstrated with a 6-log reduction in *S. mutans* growth after 12 hours (Kawashita et al., 2000). These composites could potentially reduce infective causes of surgical implant failure (Flores et al., 2010). Silver nanoparticles have been incorporated with lysozyme and coated onto stainless steel surgical blades and needles and significant antibacterial activity against a panel of

Gram-positive and Gram-negative bacteria was observed (Eby et al., 2009). Silver was added to an ethanol-based disinfectant to generate additional residual antibacterial activity post-application (Brady et al., 2003). Silver nanoparticles have also been used in environmental settings such as in wastewater treatment (Lin et al., 1996; Davies and Etris, 1997).

1.3.2 Copper as an antimicrobial agent

The antibacterial activity of copper has also been known for centuries and Hippocrates described it as a cure for ulcers (Hippocrates, 400 BC). A wide range of microorganisms are susceptible to copper, including *S. aureus, E. coli, C. difficile, E. faecalis, E. faecium, Mycobacterium tuberculosis, Aspergillus fumigatus, C. albicans* and influenza A H1H1 (Grass et al., 2010). Copper-doped TiO_2 coatings were applied to a titanium alloy as a model for metal implants used for total joint arthroplasty, and a 6-log reduction in MRSA growth was observed after 24 hours compared with the TiO_2 coatings without the copper ions (Haenle et al., 2010). Noyce et al., (2006) inoculated MRSA onto copper surfaces and were unable to recover viable bacteria from the surfaces after 45 minutes incubation at room temperature. Significant reductions were also achieved at 4°C and from brass, which contains 80% copper, although extended exposure times were required.

Copper surfaces have been assessed for their use in the healthcare environment in the UK, USA, Chile and Japan (Prado et al., 2010; Schmidt et al., 2011; Keevil and Warnes, 2011). Copper-containing taps, door push plates and toilet seats were installed in an acute medical ward in the UK and compared with non-copper containing control

surfaces and the level of bacterial contamination found on the copper-containing surfaces was significantly lower than that found on the control surfaces (Casey et al., 2010). The toilet seat and tap handle surfaces passed the benchmark microbiological standards proposed by Dancer (2004) for hand-touch surfaces whereas 50% of the control surfaces failed. However, the cleanliness of the surface affects copper activity and cumulative soiling and cleaning of copper surfaces was shown to inhibit antibacterial activity; this decrease in antibacterial activity was not observed on stainless steel control surfaces (Airey and Verran, 2007).

The mechanism of activity of copper has been shown to be predominantly due to disruption of cellular respiration, DNA damage by the generation of reactive oxygen and ionic copper species, which cause damage to bacterial enzymes and proteins (Yoshida et al., 1993; Noyce et al., 2006; Weaver et al., 2010). The cell membrane may also be damaged during exposure to copper, which leads to rupture and loss of membrane potential (Grass et al., 2010), although this is not the main mechanism of cell death (Warnes and Keevil, 2011).

1.3.3 Titanium dioxide photocatalytic thin films

Titanium dioxide has inherent light-activated antibacterial activity and its functionalities have already been commercially exploited; TiO_2 coatings are available as self-cleaning glasses, with Pilkington Activ™ and Saint Gobain BIOCLEAN™ as the market leaders. The glass can be used in windows, conservatories and glass roofs and requires less frequent cleaning because of the dual photocatalytic and superhydrophilic activities of TiO_2. Modified TiO_2 has the potential for use in

healthcare institutions to reduce bacterial contamination of the environment, but to understand how the TiO_2 thin films are activated by light to exert an antibacterial effect it is first necessary to gain a basic understanding of band theory of solid state materials.

1.3.3.1 Band theory of solids

Solid state materials can be split into three categories; conductors, insulators and semiconductors (West, 1999). Their characterisation within these groups depends on the band structure which in turn depends on the positioning of the electrons within the atoms and molecules as they come together to make a solid material. Electrons are arranged into bands that contain space, or 'holes' for the electrons to exist in. No two electrons can occupy the same space and it is preferential for the electrons to exist in pairs. The category of the solid depends upon the number of spaces available and how many electrons there are to fill these spaces.

1.3.3.1.1 Conductors

Materials characterised as conductors have an 'unfilled conduction band' (Figure 1.3).

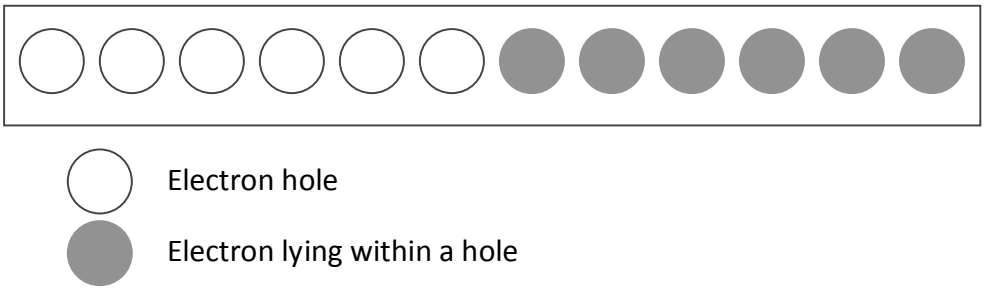

Figure 1.3 Schematic of a conduction band in a conductor

The electrons in conductors are free to move from one hole to another with no energy input, and a hole is left in the space from which the electron has moved (Figure 1.4). The electrons are able to transport charge because of this free movement and therefore the material is an electronic conductor. Metallic materials fall into this category.

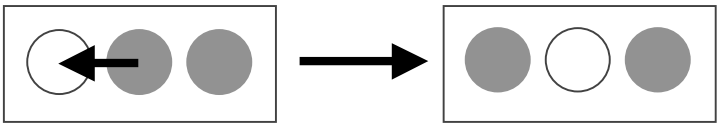

Figure 1.4 Free movement of electrons within a conductor

1.3.3.1.2 Insulators

If the conduction band of a material is full (Figure 1.5), the electrons are not able to move and so conduction of electricity will not be possible. This material is classified as an insulator.

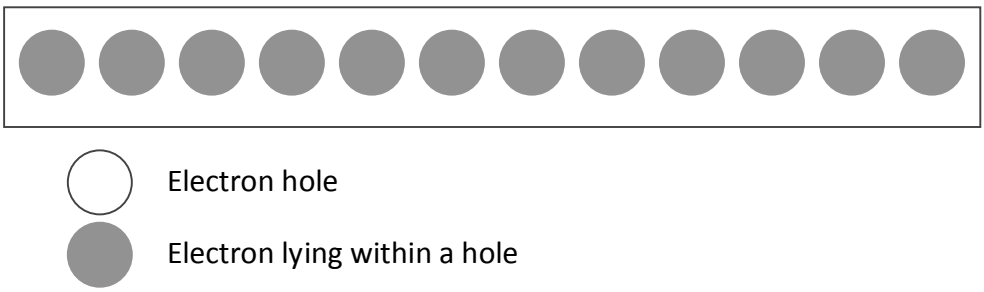

Figure 1.5 Schematic of a conduction band in an insulator

1.3.3.1.3 Semi-conductors

In addition to the previously described bands, an additional set of electron holes also exists above the conduction band, and there is a further set found above that. However, an input of energy is required in order to promote an electron from the valence band (highest band occupied by electrons) to the conduction band (lowest band with spaces for electrons (Figure 1.6)). This energy input is called the band gap.

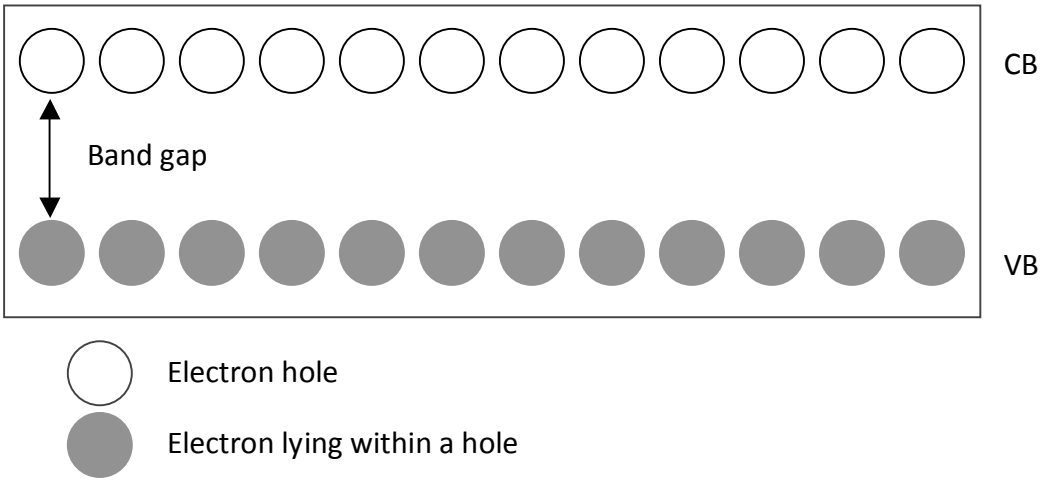

Figure 1.6 Schematic displaying the band gap within a solid state material, where CB = conduction band and VB = valence band.

The band gap of insulators like rubber is very high and a large input of energy is required to promote the electron to the conduction band. Semiconductors however have an accessible band gap (Figure 1.7); a small amount of energy is required to promote an electron to the conduction band and thus create a conductor out of an insulator (Carp et al., 2004). Once the electron has been promoted conduction can occur via two possible routes; either within the valence band using the positive holes created, or within the conduction bands through the movement of electrons.

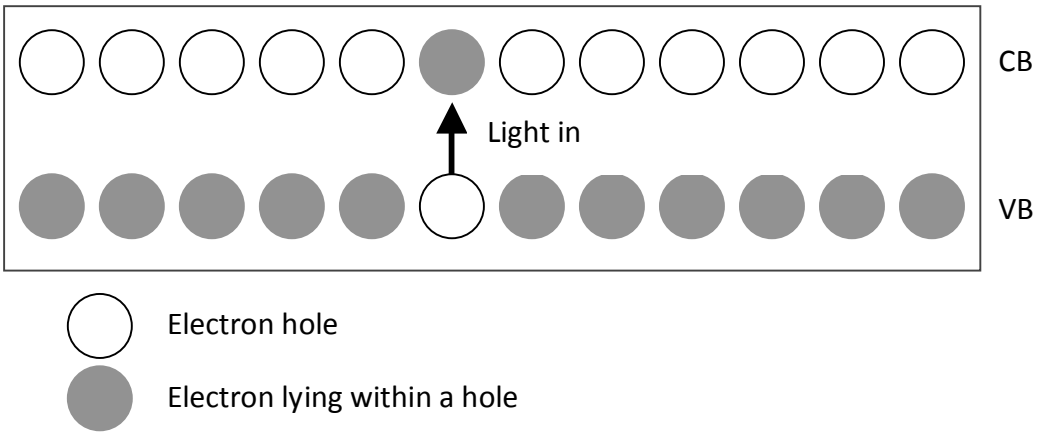

Figure 1.7 Promotion of an electron from the valence band (VB) to the conduction band (CB) in a semiconductor after absorption of light with a wavelength matching the band gap energy of the material

The excited electron can subsequently fall from the conduction band into a hole in the valence band, which results in the emission of light energy of the same wavelength as the absorbed incident ray. Alternatively, semi-conductor materials such as TiO_2 can be doped with elements so that the separation of the hole and electron can be stabilised and the absorbed energy can be utilised.

1.3.3.1.4 Doped Semiconductors

Doped semiconductors can be classified into one of two groups depending on the chemical properties of the dopant material; n-type semiconductors or p-type semiconductors. In an n-type semiconductor, the dopant material has a valence band which is slightly lower in energy than the conduction band of the semiconductor but higher in energy than the valence band of the semiconductor (Figure 1.8) (Carp et al., 2004). Conduction occurs when an electron is promoted from the valence band of the dopant to the conduction band of the semiconductor, which requires less energy than the normal electronic transition.

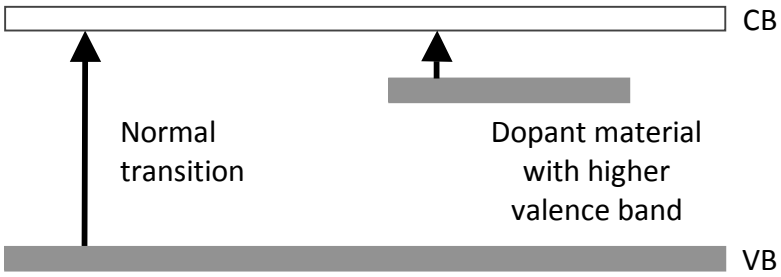

Figure 1.8 n-type semiconductors - positioning of the dopant valence band in relation to the semiconductor conduction band (CB) and valence band (VB)

Alternatively, in a p-type conductor the dopant material has a conduction band which is slightly lower in energy than the conduction band of the semiconductor (Figure 1.9). Electrons are trapped in the dopant conduction band and conduction occurs through the positive holes. The number of electrons should always equal the number of positive holes because the production of a single free electron results in the creation of a single positive hole.

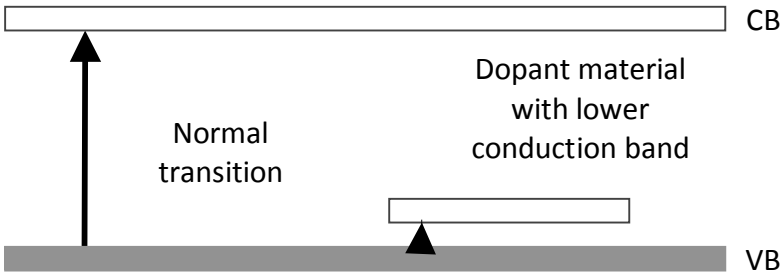

Figure 1.9 p-type semiconductors - positioning of the dopant conduction band in relation to the semiconductor conduction band (CB) and valence band (VB)

A number of processes can occur on the semiconductor after electronic excitation and these are summarised in Figure 1.10 (Mills and LeHunte, 1997). An electron (-) and a positive hole (+) are generated and as mentioned previously. The electron could return

to the valence band of the semiconductor, which is termed electron-hole recombination. This process could occur on the surface of the semiconductor (Figure 1.10, i), or within the bulk of the semiconductor (Figure 1.10, ii). Alternatively, the electron could reduce an electron acceptor in a redox reaction on the surface of the semiconductor (Figure 1.10, iii) or the positive hole could oxidise an electron donor on the surface of the semiconductor (Figure 1.10, iv).

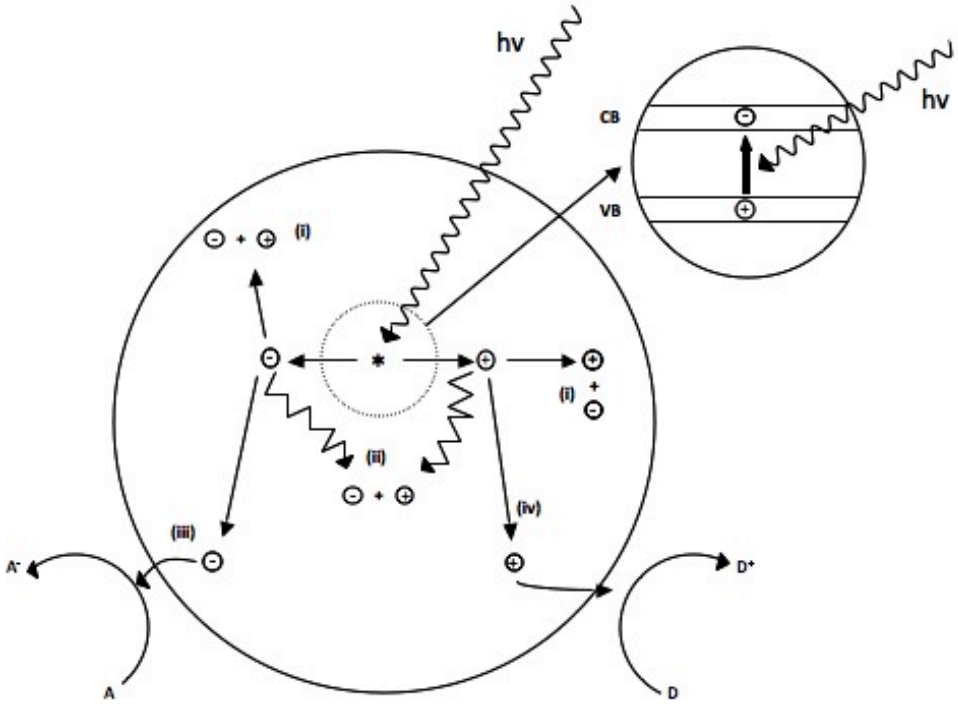

Figure 1.10 Diagram to illustrate the main reactions taking place on a semiconductor molecule after exposure to a light source causing electronic excitation: (i) electron hole recombination at the surface; (ii) electron-hole recombination in the bulk; (iii) reduction of an electron by an electron acceptor at the surface; (iv) oxidation of a positive hole by an electron donor at the surface. Figure amended from the semiconductor review by Mills and Le Hunt (Mills and LeHunte, 1997).

1.3.3.2 Titanium dioxide as a semiconductor

Titanium dioxide (TiO_2) is commonly used as a semiconductor as it is inexpensive, chemically stable, non-toxic, possesses a high refractive index and has excellent transmission in the infrared and visible regions (Dobosz and Sobczynski, 2003; Parkin and Palgrave, 2005; Dunnill et al., 2011). TiO_2 exists in many polymorphs, and the most abundant are anatase and rutile (Parkin and Palgrave, 2005). Pure anatase tends to display greater photocatalytic properties than rutile due to the faster electron-hole recombination rate of rutile titania (Mills and LeHunte, 1997; Allen et al., 2005; Brook

et al., 2007b). When TiO_2 in the anatase crystalline form is exposed to wavelengths of light below 385 nm, it behaves as an n-type semiconductor (Carp et al., 2004) and free electrons and positive holes are created in the following reaction:

$$TiO_2 \xrightarrow{\lambda < 385\ nm} h^+_{vb} + e^-_{cb}$$

The positive holes react with water present on the surface of the thin films in the following reactions to generate hydroxyl free radicals:

$$h^+_{vb} + H_2O_{adsorbed} \longrightarrow {}^{\cdot}OH + H^+$$

$$h^+_{vb} + {}^-OH_{surface} \longrightarrow {}^{\cdot}OH$$

The free electrons participate in the following reactions to generate the superoxide ion and subsequently, hydroxyl free radicals:

$$e^-_{cb} + O_2 \longrightarrow O_2^{\cdot -}$$

$$2O_2^{\cdot -} + 2H_2O \longrightarrow 2HO^{\cdot} + 2OH^- + O_2$$

The generated reactive oxygen species can react with organic material on the surface of the semiconductor, which undergo oxidation or reduction reactions. Photoreactions occurring on the surface of a catalyst such as TiO_2 are termed heterogeneous photocatalysis (Mills and LeHunte, 1997).

The generation of free electrons and positive holes in TiO_2 was first described in 1972 when water was decomposed after exposure to UV light (Fujishima and Honda, 1972).

This was followed in 1979 by research demonstrating the generation of the hydroxyl radical by electron spin resonance after irradiation of TiO_2 by UV light (Jaeger and Bard, 1979). The heterogeneous photocatalytic process is dependent on the presence of water on the surface of the catalyst and oxygen as an electron acceptor (Figure 1.10, iii).

1.3.3.3 Titanium dioxide-based antibacterial photoactivity

The bactericidal activity of the TiO_2 photocatalyst increases proportionately, as the concentration of oxygen is increased from 0% to 100% (Wei et al., 1994). Near UV light, with wavelengths between 300 and 400 nm is the light source most commonly used for bacterial photoinactivation experiments because UV light with wavelengths under 300 nm are absorbed by nucleic acids and can cause major damage to organisms (Saito et al., 1992). Near UV light is not absorbed by nucleic acids and so any observed damage can be attributed to the photoactivity of the catalyst and not the incident light source.

1.3.3.3.1 Demonstrating the loss of cell viability

The seminal paper in the field of photocatalysis described the photoinactivation of the Gram-positive bacterium *Lactobacillus acidophilus*, the Gram-negative bacterium *E. coli*, the yeast *Saccharomyces cerevisiae* and the green alga *Chlorella vulgaris* (Matsunaga et al., 1985). A suspension of platinum-loaded titanium oxide was added to each microbial suspension before a UV light source was applied; a reduction in the viability of all organisms was observed. The concentration of coenzyme A (CoA) generated throughout the course of the experiment was monitored and a decrease in

CoA concentration was associated with a loss of cell viability. They postulated that the mechanism of action was the photoelectrochemical oxidation of CoA, which resulted in a decrease in the metabolic activity of the cells and subsequent cell death.

The group followed up these experiments by immobilising the TiO_2 particles within a membrane in a continuous flow system which was used to sterilise water spiked with *E. coli* (Matsunaga et al., 1988). A decrease in CoA concentration was again observed and reactive oxygen species were implicated in the photoinactivation of *E. coli*. The electron donor, CoA, was oxidised by the positively-charged holes in the valence band.

A similar experimental rig was used by Ireland et al., (1993) to further elucidate the mechanism of the photocatalytic bactericidal activity of TiO_2. *E. coli* in an aqueous suspension was photoinactivated and after a 9 minute exposure time a 9 $\log_{10}$ reduction was observed. When hydrogen peroxide (H_2O_2) was added to the system, it acted as an irreversible electron acceptor and participated in the following reactions:

$$H_2O_2 + e^-_{cb} \longrightarrow {}^{\cdot}OH + OH^-$$

$$H_2O_2 + O_2^{\cdot -} \longrightarrow {}^{\cdot}OH + OH^- + O_2$$

The generation of hydroxyl radicals was promoted, which in turn reduced the rate of electron-hole recombination, which was accompanied by an increase in photocatalytic activity. Photoinactivation of *Streptococcus sobrinus* was also demonstrated after exposure to 21 nm diameter particles of TiO_2 and UV light; a 5 $\log_{10}$ decrease in viable bacteria was seen after just 1 minute at a bacterial concentration of 10^5 cfu / mL. Photocatalytic activity was reduced when the bacterial inoculum was higher and it

took 60 minutes to achieve a 5 $\log_{10}$ decrease in *S. sorbrinus* when a 10^9 cfu / mL inoculum was used (Saito et al., 1992).

A combination of reactive oxygen species is necessary to exert a photocatalytic bactericidal effect, with the hydroxyl radical as the primary radical acting directly on the cell (Yan et al., 2009). Hydrogen peroxide has also been postulated to directly contribute towards the bactericidal activity, as an increase in the concentration of catalase, which degrades hydrogen peroxide to water and oxygen, increased the survival rate of *E. coli* (Kikuchi et al., 1997). Therefore, hydrogen peroxide could provide a source of hydroxyl radicals and act as a direct attacking agent (Yan et al., 2009).

Viruses have also been shown to be susceptible to the photocatalytic effect of irradiated TiO_2. The non-enveloped polio virus was spiked into wastewater samples containing a stock solution of anatase TiO_2 and a rapid inactivation of the polio virus was observed (Watts et al., 1995). A 2 $\log_{10}$ decrease in viable polio virus was detected after 30 minutes, compared with a 150 minutes exposure time to achieve the same reduction of *E. coli*. The increased susceptibility of the polio virus to photoinactivation was postulated to be due to the low surface to volume ratio compared with bacteria, which provided a higher rate of hydroxyl radical reaction with the extracellular protein capsid of the virus (Watts et al., 1995).

1.3.3.3.2 Detecting changes in the bacterial cell architecture

The activity of the hydroxyl radical is limited by diffusion through the outer and cytoplasmic membranes (Watts et al., 1995; Sunada et al., 1998), therefore compromise of these barriers will allow greater activity of the reactive oxygen species. Potassium ion (K^+) leakage was used to demonstrate increased cell membrane permeability as an indicator of damage to the integrity of the cell membrane. An increase in the extracellular K^+ concentration was detected after light irradiation with TiO_2 present as a powder, which occurred in parallel with the loss in cell viability (Saito et al., 1992; Lu et al., 2003). The leakage of larger molecules such as RNA and protein has also been detected accompanied by a loss in cell viability (Saito et al., 1992).

Using transmission electron microscopy (TEM), the internal changes associated with photocatalysis could be visualised and the destruction of the cytoplasmic membrane and intracellular contents was observed after 60 – 120 minutes light irradiation (Saito et al., 1992). The reactive oxygen species generated initially damaged the bacterial peptidoglycan layer before attacking the cytoplasmic membrane, causing irreversible damage. Changes in the outer membrane structure of *E. coli* inoculated onto TiO_2 thin films has been demonstrated by atomic force microscopy (AFM) (Lu et al., 2003; Sunada et al., 2003). After 10 minutes, cell viability had decreased and a complete loss in integrity was seen after 60 minutes. When bacterial spheroplasts (which lack a cell wall) were inoculated onto TiO_2 thin films, the rate of bactericidal activity was greater than that observed for the intact cells, suggesting that the cell wall has a protective effect on *E. coli* and is the initial site of photocatalytic attack (Sunada et al., 2003). Quantum dots (QD) have also been used as a marker of changes in the permeability of

the cell membrane. QD are light emitting colloidal nanocrystalline semiconductors and after 20 minutes irradiation, QD were shown to enter *E. coli* cells, demonstrating a change in cell membrane permeability (Lu et al., 2003).

Lipid peroxidation has been demonstrated to occur at the surface of *E. coli* during photoinactivation in the presence of TiO_2 (Maness et al., 1999; Sökmen et al., 2001). Lipid peroxidation is a process in which free radicals remove electrons from lipids such as those within the bacterial cell membranes, which results in a reduction in the integrity of the membrane and thus cell viability. Malondialdehyde (MDA), a product of lipid peroxidation, was used as a marker and an accumulation of MDA was detected with an accompanying decrease in cellular respiratory activity. The authors proposed that reactive oxygen species were generated on the TiO_2 surface and attacked the polyunsaturated phospholipids present in the outer membrane (Maness et al., 1999).

TiO_2 particles also interact with the outer membrane causing reversible damage which does not affect the viability of the cells (Huang et al., 2000). Oxidative damage follows, which increases the permeability of the cell, causing efflux of intracellular components. Once the cytoplasmic membrane has been severely compromised, TiO_2 particles can enter the cell and directly attack intracellular components. Intracellular components are then able to leak out of the cell and the o-nitrophenol (ONP) assay can be used to detect this. An increase in ONP levels was observed in *E. coli* which signified increased permeability of the cell membranes (Huang et al., 2000). Bacterial endotoxin is also degraded in the photocatalytic process and occurs simultaneously with *E. coli* cell death (Sunada et al., 1998).

1.3.3.3.3 Photoinduced oxidative bacterial decomposition

Interestingly, bacteria can undergo oxidative decomposition upon the surface of TiO_2 thin films upon exposure to 356 nm light (Jacoby et al., 1998). A suspension of *E. coli* was inoculated onto irradiated TiO_2 thin films and SEM and carbon dioxide evolution was used to monitor photocatalytic oxidation. After 75 hours exposure to UV light, decomposition of the bacterial cells was evident in stark contrast to the uncoated glass slides used as controls. A concomitant increase in the concentration of carbon dioxide (CO_2) was also detected. Photocatalytic oxidation of *Bacillus subtilis* vegetative cells, *B. subtilis* spores and *Aspergillus niger* spores was also demonstrated, and increased CO_2 concentrations were used as markers of microbial decomposition (Wolfrum et al., 2002). The rate of oxidation was slower for *A. niger* cells compared with the other tested organisms. This has important translational implications as it provides evidence that the coatings are self-cleaning and do not require a physical removal step after photoinactivation; organic matter present on the surface of the catalyst can be mineralised if exposed to the light source for an adequate time period providing more space for photocatalytic reactions to take place.

1.3.3.4 Enhancing the properties of titanium dioxide thin films

Additional elements can be added to TiO_2 to alter the chemistry of the material. TiO_2 can be doped with substances such as nitrogen or sulfur to cause a batho-chromic shift, which alters the band onset energy (Section 1.3.3.1.4) so that photons of light with a lower frequency are absorbed and are able to excite the electrons to a higher energy state (Asahi et al., 2001; Carp et al., 2004). Transition metal ions such as iron, lead and copper can also be used as dopants to enhance the photocatalytic properties

of TiO_2 (Thompson and Yates, 2006). The aim of this doping is to generate a material that can be activated by visible light, such as indoor lighting conditions, which broadens the commercial applications of the material. A ten-fold increase in the number of photons available for photocatalysis would be generated by a shift in the TiO_2 band onset of just 40 – 50 nm (Dunnill and Parkin, 2009).

The exact mechanisms governing visible light photocatalysis are poorly understood, although it is generally agreed that nitrogen doping causes increased photocatalysis at lower photon energies and localised nitrogen 2p states above the valence band are generated by the addition of nitrogen (Thompson and Yates, 2006). It is not yet agreed whether substitutional or interstitial nitrogen binding provides the most favourable visible light driven photocatalytic properties.

1.4 Relevance of surfaces in ventilator-associated pneumonia

Ventilator-associated pneumonia (VAP) is a serious healthcare-associated infection that affects patients on ventilators, predominantly in the intensive care unit. The intubated patient usually has serious co-morbidities such that they require assistance with their breathing, and the physical presence of the endotracheal tube (ETT) both compromises the normal action of the respiratory tract and allows micro-aspiration of contaminated subglottic secretions.

A number of clinical measures can be applied to prevent VAP as prevention requires a multifactorial approach and research into the subject includes the use of alternative ETT materials (Balk, 2002; Pneumatikos et al., 2009; Torres et al., 2009; Bouadma et al., 2010; Berra et al., 2011; Blot et al., 2011; Coppadoro et al., 2011; Rewa and

Muscedere, 2011). Bacteria originating from the oropharynx colonise the ETT and produce a biofilm on the lumen of the tube which is difficult to remove and provides a potential source of colonisation and infection of the lower airways (Sottile et al., 1986). Therefore, the prevention of bacterial adhesion to the surface of the ETT and the destruction and removal of bound organisms is of clinical interest (Berra et al., 2003).

Polyurethane cuffed ETTs are being used in preference to the traditional polyvinylchloride ETTs as they are more flexible and a better seal is produced at the base of the tube which prevents leakage of oropharngeal contents into the lower airways (Berra et al., 2008b; Miller et al., 2010). An alternative novel way to decontaminate the ETT is by using the Mucus Shaver which physically removes both mucus and bacterial biofilms from the inner lumen of the tubing (Kolobow et al., 2005).

ETTs can also be impregnated with antibiotics or other antibacterial compounds to prevent the initial biofilm formation stage or to kill the adherent organisms. Silver ions have been added to polyurethane ETTs and a series of *in vitro* studies have demonstrated reduced adherence of MRSA, *P. aeruginosa, Enterobacter aerogenes* and *A. baumannii* to the silver-coated materials (Berra et al., 2008a; Rello et al., 2010). Colonisation of silver-coated ETTs by *P. aeruginosa* was shown to be lower and take longer than on uncoated control ETTs, with lower levels of lung colonisation observed in ventilated dogs as a consequence (Olson et al., 2002; Rello et al., 2010). A similar study used silver-sulfadiazine and chlorhexidine coated ETTs in ventilated dogs and demonstrated a reduction in tracheal colonisation and an absence of lung colonisation (Berra et al., 2004).

When silver-coated ETTs were used in a study involving nine patients, none of the ETTs were colonised with pathogens, there was less colonisation of commensal organisms and there was a decrease in biofilm formation compared with the non-coated control ETTs (Rello et al., 2010). A delayed ETT colonisation time and positive tracheal aspirate culture time was demonstrated in an earlier study using the same coated material (Rello et al., 2006) and no bacterial growth or biofilm production was detected on a silver sulfadiazine coated polyurethane ETT used in a cohort of 46 intubated patients (Berra et al., 2008b). A reduced incidence of VAP within 10 days of intubation was observed in the NASCENT trial which recruited over 2,000 patients; silver-coated ETTs were used in the test group and were compared with non-coated equivalents that were used in the control group (Kollef et al., 2008).

A number of silver-coated ETTs are now commercially available but widespread use has been hindered by the price, which is up to 45 times more than uncoated ETTs; however, a theoretical cost-analysis model showed silver-coated ETTs were actually associated with financial savings of over $12,000 per averted case of VAP (Shorr et al., 2009; Torres et al., 2009).

Chlorhexidine has been combined with the dye brilliant green or gentian violet to form the novel compounds gardine and gendine, respectively. These compounds have displayed significant antibacterial activity *in vitro* and in an elegant biofilm disruption assay, demonstrated superiority to silver coated ETTs. These compounds are relatively cheap to produce and the authors propose clinical use after thorough *in vivo* assessment (Chaiban et al., 2005; Hanna et al., 2006; Hachem et al., 2009; Reitzel et al., 2009; Raad et al., 2011). These studies illustrate the benefits of antibacterial and

novel ETT materials and to further improve the incidence of VAP and other device-related infections, further research should be conducted.

1.4.1 Photodynamic therapy

A different method of generating an antibacterial effect on the surface of the ETTs is via a process called photodynamic inactivation (PDI). Phototherapy was first used by the Nobel Prize winner Niels Finsen to treat a tuberculosis skin condition called lupus vulgaris in the 1890's by applying light directly onto the lesions (Bonnett, 1995; Dolmans et al., 2003). Photodynamic therapy (PDT) evolved from this initial work and involves the use of a photosensitising agent and a light source to generate toxic reactive oxygen species (Wainwright, 1998). The procedure can be used in the targeted treatment of cancerous tumours (Marcus and McIntyre, 2002; Dolmans et al., 2003), in ophthalmology to treat age-related macular degeneration (Bressler and Bressler, 2000), atherosclerosis (Rockson et al., 2000) and in the localised treatment of bacterial infections, particularly in dentistry (Wainwright, 2003). When PDT is used to kill bacteria, it is termed photodynamic inactivation (PDI) (Hamblin and Hasan, 2004).

There are two types of photosensitisation reactions, type I and type II and the pathways involved in generating these reactions are illustrated in Figure 1.11. When a photosensitiser molecule is irradiated with light of an appropriate wavelength, it can undergo an electronic transition, to form the singlet excited state with paired electron spins. The molecule then either undergoes electronic decay and returns to the ground state or the energy can be transferred so that the molecule undergoes an electronic transition to the triplet excited state. The electron spins at this point are unpaired. The

molecule could once again lose the energy, depending on the environmental conditions and the structure of the molecule itself and return to the ground state. Alternatively, if oxygen is present, the energy could be transferred and used to drive redox reactions and generate radical ions (type I) or to generate singlet oxygen (type II reaction). The major pathway involved in generating the bactericidal effect in PDI is the production of singlet oxygen (Wakayama et al., 1980). To be an efficient photosensitiser, a molecule must be efficient at producing singlet oxygen and that in turn is dependent on the generation of a large population of long-lived molecules in the triplet state (Wainwright, 1998).

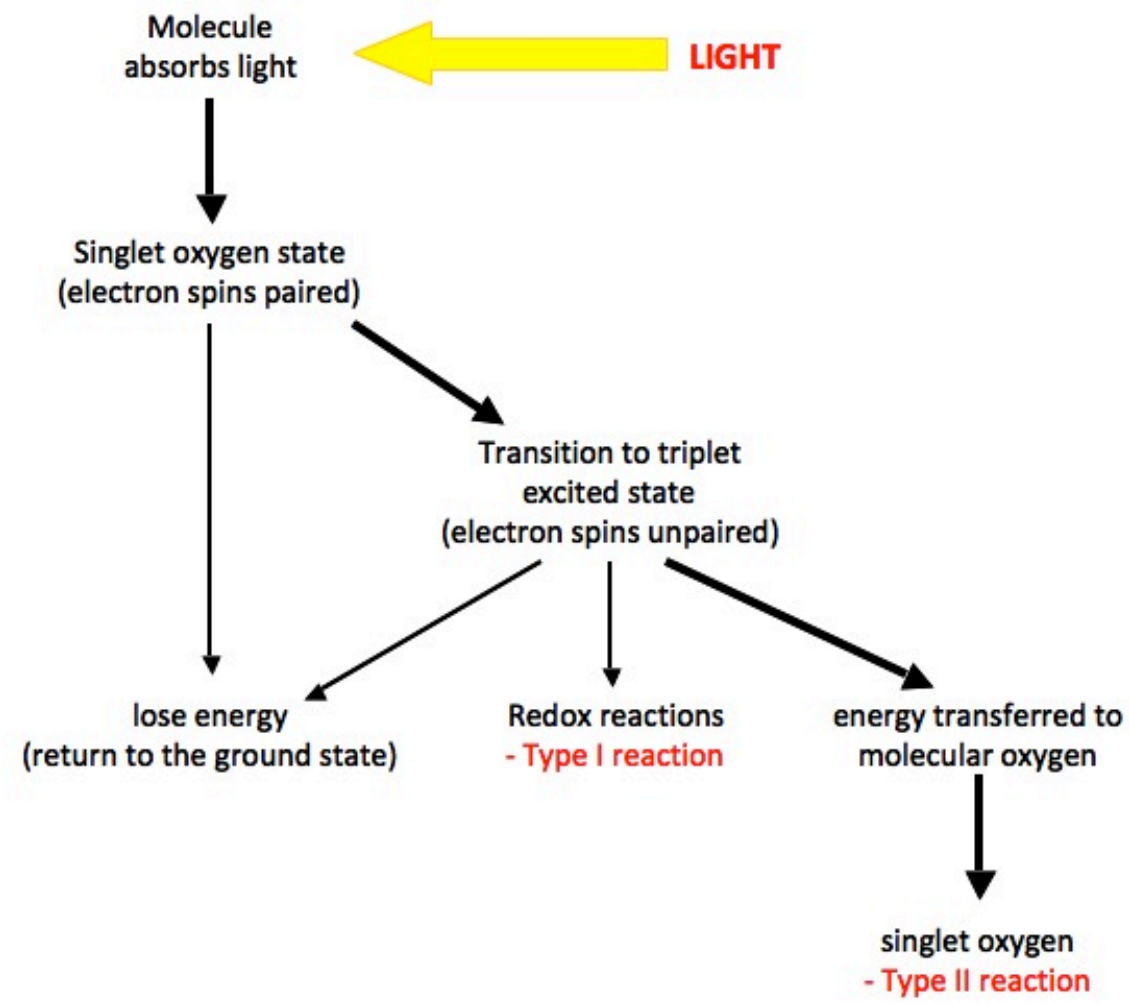

Figure 1.11 Flow diagram to demonstrate the generation of singlet oxygen. The bold arrows indicate the pathway to the Type II reaction (Bonnett, 1995; Wainwright, 1998).

The reactive oxygen species-driven bactericidal effect is similar to that generated by TiO_2 thin films upon irradiation with suitable wavelengths of light. Singlet oxygen species exert a direct effect on microbial cells by oxidising cell constituents such as the cell wall, cell membrane or intracellular components such as nucleic acids, with the cytoplasmic membrane as the primary target. PDI causes a loss of membrane integrity, such that the intracellular contents leak out of the cell, controlled transport of solutes across the membrane is compromised and the cell loses viability due to the lack of essential constituents needed for anabolic and catabolic pathways (Jori et al., 2006).

The reactive oxygen species are then able to access the intracellular DNA and cause further damage (Dunipace et al., 1992; Salmon-Divon et al., 2004; Chi et al., 2010). Singlet oxygen has a diffusion distance of approximately 20 nm; therefore if the bacterial species are in contact with the light-activated material then the generated singlet oxygen should be active against both the bacterial cell wall and underlying membrane.

An advantageous feature of PDI is that multi-drug resistant strains of bacteria which are resistant to a number of different antibiotic classes do not show enhanced resistance to PDI compared with the equivalent antibiotic sensitive strains (Malik et al., 1990). The susceptibility of 60 multi-drug resistant strains of *P. aeruginosa* to the photosensitiser toluidine blue and red laser light were compared with 19 antibiotic sensitive strains and no difference in susceptibility was observed (Tseng et al., 2009). In addition, the growth phase of *P. aeruginosa* does not impact on its susceptibility to TBO-mediated photosensitisation (Komerik and Wilson, 2002), unlike some classes of antibiotics which have selective activity for bacteria in the exponential phase of growth (Tuomanen et al., 1986). Due to the multi-site activity of the reactive oxygen species generated during light irradiation, it is unlikely that resistant phenotypes will be selected (Hamblin and Hasan, 2004).

1.4.1.1 Types of photosensitisers

There are a number of different aromatic compounds which can act as photosensitisers when irradiated by specific wavelengths of light. The compounds are usually coloured as they reflect light in the visible part of the electromagnetic spectrum. An ideal photosensitiser would contain an overall cationic charge as

bacterial cells carry an overall anionic charge because of the presence of the cytoplasmic membrane (Hamblin and Hasan, 2004). Examples of photosensitisers which have been used for PDI are the phenothiazines toluidine blue (Wakayama et al., 1980; Paardekooper et al., 1992; Wainwright et al., 1997; Perni et al., 2009b; Ragas et al., 2010) and methylene blue (Decraene et al., 2009; Perni et al., 2009a), the halogenated xanthene rose bengal (Decraene et al., 2006) and acridines such as acridine orange (Wainwright et al., 1997).

Photosensitisers can be used in solution and applied to the treatment area, or can be impregnated into a polymer which can be used in a variety of settings. For example, a solution of photosensitiser can be injected into a periodontal pocket before the application of laser light to exert PDI on the pathogens present (Wilson, 1993, 1996). Alternatively, the photosensitiser could be immobilised in a polymer used in as a catheter material, so that any bacteria present in the lumen or exterior of the tubing would be exposed to the reactive oxygen species generated during PDI upon application of the light source (Perni et al., 2011).

1.5 Methods of producing light-activated antimicrobial materials

1.5.1 Chemical vapour deposition

Thin films of TiO_2 are commonly synthesised using the chemical vapour deposition (CVD) technique, indeed it is the method used industrially by Pilkington to synthesise their Pilkington Activ™ self-cleaning glasses (Mills et al., 2003). The deposition process requires heating to a high temperature (> 500°C), therefore the choice of substrate is limited as the substrate has to withstand the rise in temperature; this constraint

makes glass an ideal choice. Precursor molecules containing titanium and oxygen are heated into a gaseous phase and transported via the nitrogen carrier gas into the reaction chamber. The precursor molecules are adsorbed onto the heated substrate and decompose; the elements of choice remain adhered to the substrate and waste products are removed from the system by the nitrogen carrier gas (West, 1999; Carp et al., 2004; Page, 2009). A schematic of a typical CVD rig is displayed in Figure 1.12.

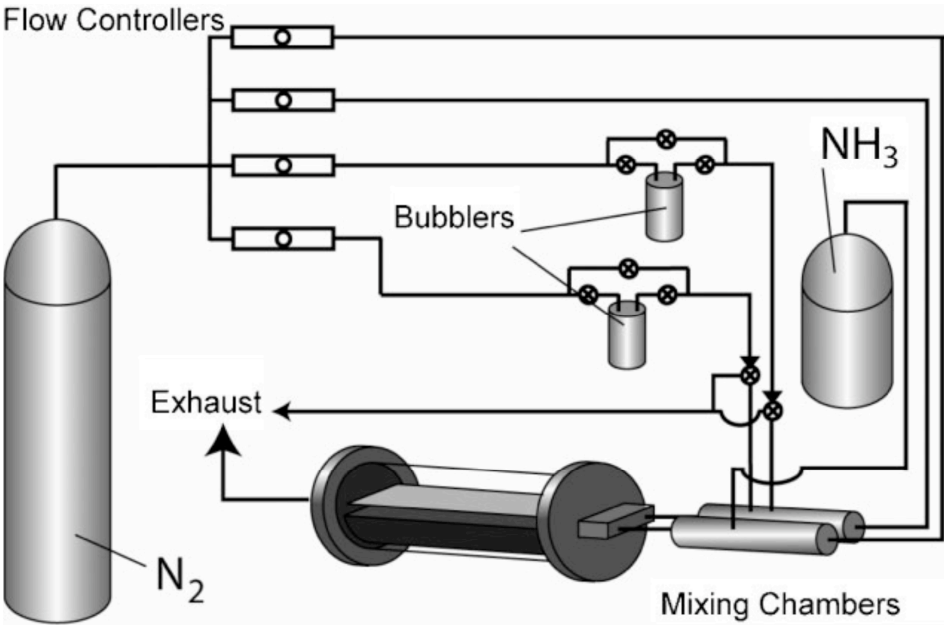

Figure 1.12 Schematic representation of a CVD apparatus. The setup shown in this diagram was used to deposit thin films of titanium oxynitride, as discussed in Chapter 4 (Aiken et al., 2010).

1.5.2 Sol-gel

The sol-gel technique is considered to be more reproducible than CVD and the production of a uniform film is possible on a small scale (Carp et al., 2004). To synthesise TiO_2 thin films by the sol-gel method, a homogenous solution is prepared containing the cationic reactants required for the synthesis; an alkoxide is used as a

source of TiO_2, water is required to hydrolyse the alkoxide and an alcohol is added to catalyse the reaction (West, 1999; Rampaul et al., 2003; Page, 2009). A viscous gel develops containing colloidal particles, which grows further as the solution is left to age. During this time, the water and alcohol trapped in the matrix of the polymer evaporate, and so the resultant aged sol is transparent and homogenous with no crystalline phases or precipitates. The glass substrate can then be dipped into the sol and the sol adheres to the surface of the glass; it is removed at a constant rate so that the thin film produced is of a consistent thickness along the length of the material. The sol dries readily, but is mechanically weak, so is sintered at a high temperature to remove any organic matter and a dense, crystalline oxide coating is produced.

1.5.3 Swell encapsulation

Swell encapsulation is a chemical method used to impregnate polymers with an organic compound, and can be modified to add a photosensitiser molecule to a polymer in order to generate a light-activated antibacterial material. When an elastomer is immersed in an organic solution containing a photosensitiser, the photosensitiser is able to penetrate the polymer as the elastomeric matrix swells. The elastomer is removed from the photosensitiser-containing solution after a defined period and the polymer reverts back to its original size as the solvent evaporates. The photosensitiser remains embedded in the elastomeric matrix during evaporation, and the final concentration of photosensitiser can be adjusted by varying the concentration in the organic solution (Perni et al., 2009a; Perni et al., 2011).

1.6 Measuring environmental contamination

Accurate methods are required to monitor microbial contamination of environmental surfaces to assess cleaning regimens and to detect any bacteria present (Manheimer and Ybanez, 1917; Salo and Wirtanen, 1999; Moore and Griffith, 2002; Verran et al., 2002; Hedin et al., 2010; Verran et al., 2010a).

1.6.1 Swabbing

Bacterial culture is a widely used method, as any viable bacteria present can be detected, quantified and identified at a relatively low cost. The test surface can be sampled using a swab or spatula, which can be made from a variety of materials including cotton, viscose, nylon or man-made substances such as the brush-textured nylon flock. Samples can then either be streaked directly onto an agar plate or re-suspended into a growth enhancing broth before subculture onto solid media (Moore and Griffith, 2007). If the bacterial inoculum is high, the sample can be serial diluted before plating out to allow enumeration of the single colonies on the culture plate, ensuring a more accurate estimation of the original bacterial inoculum. Pathogenic yeasts and fungi can also be detected in this way. However, the technique relies upon the ability of the swab to collect all microbial contamination on the surface and the release of the organisms from the swab head during processing (Favero et al., 1968).

1.6.2 Dipslides

Environmental surfaces can alternatively be directly sampled by placing a section of agar directly onto the surface by use of a RODAC (replicate organism detection and counting) plate or a similar sampling device and enumeration of the colonies after an

incubation period. Dipslides have a greater sensitivity and reproducibility compared with swabbing without enrichment culture when sampling surfaces, especially if the surface is dry (Moore et al., 2001; Moore and Griffith, 2002; Food Standards Agency, 2004; Obee et al., 2007). However, quantification can be difficult if the surface level of contamination is too high, as the microbial load on the surface cannot be diluted, resulting in confluent growth on the agar, which makes colony counting impractical. Growth is instead classified instead as moderate or heavy based on the surface coverage of the slide and comparison with visual images of controls.

1.6.3 Air sampling

Air sampling devices are used to sample the microbial contamination of the surrounding air. A defined volume of air is drawn into the device and is passed over an agar plate, so that microorganisms found in the air are inoculated onto the plate surface. Airborne spores are also inoculated onto the plates and growth occurs after germination. These units have been employed in the healthcare environment to monitor efficiency of cleaning schedules and terminal decontamination regimens (Jeanes et al., 2005; Wong et al., 2011), the fungal contamination of air during building work (Goodley et al., 1994) and the quality of air in operating theatres (Whyte et al., 1982; Hambraeus, 1988; Landrin et al., 2005). A risk factor for surgical site infections is microbial contamination of the air in operating theatres, so knowledge of the air quality is essential to ensure air handling units are functioning correctly and prevent these infections occurring (Whyte et al., 1982; Hambraeus, 1988; Whyte et al., 1992). Microbial contamination of the air can also be monitored using settle plates, which are large agar plates that are placed in the test environment. Airborne micro-organisms

which fall onto the plates are then detected by colony counting after incubation. However, droplet nuclei stay suspended in the air so cannot be detected using this method and the plates require longer periods of sampling (circa 24 hours) compared with a mechanical device that takes minutes to obtain a sample.

1.6.4 ATP bioluminescence

All of the methods described above have the disadvantage that they are dependent upon the ability of organisms to grow on solid media, so bacteria in the viable but non-cultivable (VBNC) state would not be cultured. Alternative sampling methods that overcome these limitations would therefore be useful (Moore and Griffith, 2007). ATP bioluminescence is a process based upon a naturally occurring light-generating reaction found in the North American firefly, *Photinus pyralis* (Hawronskyj and Holah, 1997). Both the male and female fireflies use the generation of light to locate one another and as mating signals (Encyclopedia Britannica, 2011). The luciferase enzyme isolated from *P. pyralis* can be used in the laboratory to catalyse the oxidation of luciferin using ATP as the energy source and the reaction is as follows:

$$\text{ATP + D-luciferin + } O_2 \xrightarrow{\text{luciferase}} \text{AMP +} PP_i \text{ + oxyluciferin + } CO_2 \text{ + light}$$

The light produced during the reaction can be quantified by a luminometer and the output is given in relative light units (RLU) (Lundin, 2000). The generated light is directly proportional to the amount of ATP present in the initial sample as one photon of light is emitted per molecule of ATP.

ATP is found in all living organisms and is also present as free ATP (Hawronskyj and Holah, 1997). Luminometers can be used to provide data on the level of organic debris and microbial contamination on a surface (Davidson et al., 1999). Eukaryotic ATP and ATP from extracellular sources can be degraded prior to the lysis of the bacterial cells with certain models (Hawronskyj and Holah, 1997), enabling the number of bacterial cells to be calculated from the amount of light emitted. Results can be available from five to thirty minutes, eliminating the time-consuming overnight incubation of culture plates.

ATP bioluminescence has been used for the last decade in the food industry and is especially useful in complying with specific food regulations, which serve to reduce the risk of food spoilage and contamination (Hawronskyj and Holah, 1997; Davidson et al., 1999; Wagenvoort et al., 2000). Qualitative measurements are usually taken so that a surface will either pass if an acceptable number of bacteria are present or fail if the number of bacteria is above a predetermined level (Cooper et al., 2007). The use of ATP bioluminescence in these situations is advantageous as the results are available in minutes, so if the surface contamination was deemed too high then it could be re-cleaned, re-tested and food production could continue if it subsequently passed.

There are a number of commercially available luminometers including the Clean-Trace (BioTrace, Bridgend, UK), a portable luminometer, which detects ATP bioluminescence of both microbial and non-microbial origin. This system is commonly used to assess the effectiveness of cleaning regimens as organic debris is also detected. The easily transportable BioProbe (Hughes Whitlock, Gwent, UK) and the Junior (Berthold Technologies GmbH, Bad Badwild, Germany) luminometers require additional reagents

to generate RLU readings, as does the Lumat luminometer (Berthold Technologies GmbH). The Microbial ATP Kit (BioThema AB, Sweden) can be used to degrade exogenous ATP before the bacterial cells are lysed, so a more accurate indication of the actual number of bacteria present on the test surface can be obtained (BioThema AB, 2006). These methodologies are not commonly used in the healthcare or a food environment, as they require a sample preparation step and take slightly longer (up to 30 minutes). These methodologies can be used for molecular experiments such as reporter gene assays where a higher sensitivity is required (Dyer et al., 2000; McKeating et al., 2004; BioThema AB, 2006).

1.6.5 Staining techniques

Staining techniques could alternatively be used to estimate the level of bacterial contamination on a surface. Acridine orange is a commonly used dye, used to perform direct counts on test surfaces, although no indication of bacterial viability is given. Fluorescent probes such as cyanoditolyl tetrazolium chloride (CTC) and rhodamine 123 can be used as indicators of cell viability; CTC is reduced to crystalline CTC-formazan, present as red crystals within bacterial cells and rhodamine 123 is concentrated in functioning mitochondria and cells fluoresce green (Yu and McFeters, 1994; Pyle et al., 1995). Visualisation requires the use of appropriate excitation and emission filters on a fluorescent microscope (Yu and McFeters, 1994). The Live / Dead BacLight™ Bacterial Viability stain (Molecular Probes Inc) is a fluorescent dye which can differentiate between viable and non-viable bacterial cells. The kit contains two dyes, SYTO 9 and propidium iodide. SYTO 9 emits at 500 nm and stains all cells green whereas propidium iodide is a red stain that emits at 635 nm and penetrates cells with a damaged cell

membrane (Boulos et al., 1999; Airey and Verran, 2007). All generated images can be captured on a camera attached to a fluorescent microscope to enable enumeration of the organisms present using computer software such as ImageJ (http://rsbweb.nih.gov/ij/index.html). Direct visualisation techniques can also detect the presence of non-microbial contamination, such as organic soil that could provide sustenance for bacterial growth (Verran et al., 2002).

1.6.6 Summary of environmental sampling techniques

There is currently no standardised technique for sampling environmental surfaces in a hospital environment, so a variety of methods are used (Hedin et al., 2010). ATP bioluminescence provides a snapshot of bacterial contamination and can detect the presence of organic soil. Viable bacteria can be enumerated by performing viable counts, which is cheap and easy to perform and improvements in the swab head material and sampling diluent have been shown to increase sampling efficiency, although the improvements observed were minimal (Hedin et al., 2010). Visualisation techniques require more specialised equipment and stains, but intact biofilms can be observed without disruption and non-viable bacteria included in the bacterial count. These techniques all possess inherent advantages and disadvantages so are best used with clear knowledge of these limitations, especially when interpreting any data generated (Verran et al., 2010a).

1.7 Methods of characterising and assessing the functionality of light-activated antimicrobial materials

1.7.1 UV-visible-IR spectroscopy

UV-visible-IR spectroscopy can be used to predict the likely photocatalytic activity of a potential antibacterial material by calculating the band onset (Section 1.3.3.1.3). When incident light with a wavelength between 200 nm and 700 nm is applied to a candidate material, three readings can be taken: (i) the transmission of light through the sample; (ii) the absorption of light by the sample and (iii) the reflectance of light from the sample. These readings can be used to estimate the band gap. A plot of $(\alpha h\nu)^{1/2}$ against $h\nu$ is then generated, where $h\nu$ equals the incident light and a equals the absorbance coefficient ($a = -\log T/T_0$, where T equals the transmission reading of the sample and T_0 equals the transmission of the substrate). When the curve is extrapolated along the linear portion of the curve, the band gap can be read from the *x* axis (Tauc, 1968, 1970; Sharma et al., 2009). This is called a Tauc plot. The transmission data can also be used to calculate the thickness of the thin films using the Swanepoel method (Swanepoel, 1983).

1.7.2 Photooxidation of stearic acid

The photodegradation of the organic molecule stearic acid (Figure 1.13) can be used to quantify the photocatalytic self-cleaning ability of candidate antibacterial materials and is based on the following equation (Mills et al., 2002):

$$CH_3(CH_2)_{16}CO_2H + 26O_2 \xrightarrow{h\nu \geq \text{band gap energy of semiconductor}} 18CO_2 + 18H_2O$$

Carbon dioxide and water is generated from organic molecules in a cold combustion reaction (Parkin and Palgrave, 2005). The process is relatively simple to perform and so a large number of thin films can be screened for potential photocatalytic activity. Infrared (IR) spectroscopy is used to monitor the degradation of the stearic acid molecules. The thin films that show the greatest activity by this method can then selected for antibacterial testing.

Figure 1.13 Chemical structure of stearic acid $C_{18}H_{36}O_2$

Infrared spectroscopy is an analytical method used to observe the vibrational energies of molecular bonds. Photons of light from the IR portion of the electromagnetic spectrum interact with molecular bonds within the sample. The incident light has a lower frequency than UV or visible light and causes molecular bonds to bend and stretch as they absorb light. Absorption of the photon of IR light causes an increase in the vibrational energy of the bond raising it to a higher vibrational energy level. The mode of vibration varies depending upon the constituent atoms in the bond and these chemical stretches and bends are identifiable on the IR spectra generated (McCarthy, 1997).

The IR measurements are plotted on a graph of wavenumber against transmittance or absorption. The changes in the vibrational energies of the molecular bonds are detected as inverted peaks on the resultant IR spectra as the transmittance of the incident light decreases because of the absorbance of the light by the molecular

bonds. These inverted peaks are termed absorption bands and are characteristic of the IR vibrations of specific molecular bonds. Stearic acid has three modes which are visible in the IR spectrum: the symmetric C – H stretch (CH_2) has an absorbance band of 2923 cm^{-1}; the C – H stretch (CH_3) has an absorbance band of 2958 cm^{-1} and the asymmetric C – H stretch (CH_2) has an absorbance band of 2853 cm^{-1}. The concentration of stearic acid can be approximated by integrating the area of the latter two peaks; the first peak is of low intensity and is generally not used. An integrated area of 1 cm^{-1} equates to approximately 9.7 x 10^{15} molecules (Mills and Wang, 2006) and so the destruction of stearic acid can be monitored over time by normalising the concentration of stearic acid molecules on the test surface as C_x / C_0 readings, where C_0 is the initial concentration and C_x is the concentration of stearic acid at a given time point.

1.7.3 Contact angle measurements

Photo-induced superhydrophilicity can be induced on photocatalytic thin films such as TiO_2, after irradiation with light possessing band gap energy (Mills et al., 2002). The hydrophilicity or indeed, hydrophobicity of a substrate can be calculated by determining the contact angle of a droplet of water inoculated onto the surface of the material. A hydrophilic material will possess a low water contact angle, as the droplet will spread flat on the 'water-loving' hydroxylated surface, with an accompanying increase in the diameter of the droplet. Conversely, a hydrophobic material will not have an affinity for the droplet of water, so the diameter of the droplet will be reduced, resulting in a high water contact angle (Page, 2009). Hydrophobic surfaces

have water contact angles above 90°, hydrophobic surfaces have water contact angles below 90° and superhydrophilic surfaces have water contact angles approaching 0°.

During photo-induced superhydrophilicity on a TiO_2 semiconductor, light exposure causes the trapping of holes at lattice sites near the surface of the material, and a concomitant reduction of Ti^{4+} to Ti^{3+} (Carp et al., 2004). The bonds between the titanium and oxygen within the lattice are weakened by the trapped holes, which enable the release of oxygen atoms, which in turn creates oxygen vacancies and an increase in the hydroxylation state of the surface. Hydroxyl groups are adsorbed onto the surface, which bind with the water inoculated onto the surface due to an increase in the van der Waals forces and hydrogen bonding (Carp et al., 2004).

1.7.4 Standard methods of assessment

International standards have been developed to assess the activity of novel antimicrobial products, such as the Japanese Industrial Standard JIS Z 2801, which measures antibacterial activity and efficiency and numerous ISO standards developed by the International Organisation for Standardisation (International Organisation for Standardisation, 2011). Antibacterial activity can be calculated using the following formula $R = \log(B/C)$, where R is a measure of the antibacterial activity, B is the average number of viable cells of bacteria on an untreated sample after 24 hours and C is the average number of viable bacteria on the antibacterial sample after 24 hours. If a test sample has a value of greater than 2.0, then it is denoted an antibacterial material, according to JIS Z 2801:2006.

The methylene blue reduction test can also be used for the assessment of photocatalytic surfaces and has recently been adopted as an ISO standard (ISO 10678:2010). When methylene blue is inoculated onto a test surface, photogenerated electrons reduce atmospheric oxygen to produce superoxide, which degrades the dye, or photogenerated holes either directly oxidise methylene blue or generate reactive oxygen species that directly attack the dye (Atherton and Newlander, 1977; Zita et al., 2009). These reactions result in a decrease in the intensity of the colouration of the dye, and this colour change can be monitored on a spectrophotometer over time, compared with an untreated control sample, to determine the ability of UV-activated surfaces to photodegrade dissolved organic molecules. Therefore, this would be a useful tool to screen a large number of different photocatalysts before focusing on a smaller number of samples to test against bacterial suspensions. However, the assay is not validated to use on surfaces activated by visible light or against bacterial targets. Acid Orange 7 is another dye that is oxidised during photocatalysis and degradation of the molecule can be monitored as a method of determining photocatalytic activity. A more recent development is the use of an ink, Resazurin, which is described as a faster and simpler method (Mills and McGrady, 2008). During photocatalysis, the positive holes generated are trapped by glucose, which is contained within the preparation, and the photogenerated electrons reduce Resazurin (Zita et al., 2009). The colour of the ink changes from blue to pink, which occurs in seconds, compared with the hours required for the former methods and the colour change can be detected by eye, which provides an inexpensive semi-quantitative measure of photocatalytic activity.

1.8 Overview and project aims

A multi-disciplinary approach is required to prevent HCAIs, as the acquisition and transmission of infection is rarely caused by an isolated event, but as a consequence of a number of failures in procedure (Dettenkofer et al., 2011). Hand hygiene is viewed as the most important and effective method for preventing the transmission of HCAIs. Adequate isolation facilities need to be available, and high-risk patients need to be transferred into these areas promptly. This requires sensitive, specific and rapid detection of the infective organisms so that these scarce resources are used appropriately (Cheng et al., 2011). Prudent antibiotic prescribing is important to prevent the emergence of resistant organisms and has been shown to reduce the rates of *C. difficile* infection (Mears et al., 2009). The patient environment should be kept free of pathogens by methods as basic as regular scheduled cleaning and hand decontamination after each patient contact. This has been shown to significantly reduce the transmission of microorganisms and prevents the transfer of organisms from patient-to-patient and from the environment-to-patient (Devine et al., 2001; Rampling et al., 2001; Dancer, 2004; Johnston et al., 2006; Department of Health, 2008; Dancer et al., 2009). Novel technologies could also be employed as part of the armoury of interventions used to prevent the transmission of infectious microorganisms within hospitals as currently employed methods such as cleaning and hand hygiene alone, are not proving to be sufficient (Rampling et al., 2001; French et al., 2004). Recontamination of surfaces occurs readily after disinfection of areas surrounding an infected patient, which allows further transmission of the organisms (Collins, 1988; Weber and Rutala, 1997; Brady et al., 2003). Self-cleaning surfaces could potentially lower the bacterial load in the near-patient environment, and reduce re-

colonisation rates, as organisms shed in-between cleaning events would be killed, breaking the cycle of re-colonisation. Antimicrobial polymers could be used to produce ETTs and catheters to reduce the adherence of bacteria within the lumen of tubing, and potentially decrease the incidence of device-related HCAIs.

The purpose of this project was to generate and assess the antibacterial activity of a range of light-activated materials with the potential to be used in a healthcare setting to reduce the transmission and acquisition of HCAIs.

2 Materials and methods

2.1 Target organisms

Bacterial type strains used in these studies are listed in Table 2.1. All of the bacterial strains were stored at -80°C in brain heart infusion broth (BHI) containing 10% glycerol and maintained by weekly subculture onto 5% Columbia blood agar plates (all media from Oxoid Ltd., Basingstoke, UK). A clinical isolate of *C. albicans* was also used (Table 2.1) and was stored on a Sabouraud dextrose agar slope at 22°C and maintained by weekly subculture onto Sabouraud dextrose agar plates.

Table 2.1 Bacterial and fungal strains used in these studies.

Bacterial / fungal strain	Reference number
Escherichia coli	ATCC 25922
Staphylococcus aureus	NCTC 6571
Staphylococcus aureus	ATCC 8325-4
Epidemic meticillin resistant-*Staphylococcus aureus* 16	Clinical isolate
Epidemic meticillin resistant-*Staphylococcus aureus* 15	Clinical isolate
Meticillin resistant-*Staphylococcus aureus*	ATCC 43300
Streptococcus pyogenes	ATCC 12202
Enterococcus faecalis	Clinical isolate
Pseudomonas aeruginosa	PAO1
Pseudomonas aeruginosa	Clinical isolate
Acinetobacter baumannii	Clinical isolate
Stenotrophomonas maltophilia	Clinical isolate
Candida albicans	Clinical isolate

2.2 Growth conditions

Bacteria were grown aerobically in either nutrient broth (*P. aeruginosa, E. coli, S. maltophilia* and *A. baumannii*) or BHI broth (*S. aureus, S. pyogenes, S. epidermidis* and *E. faecalis)* and incubated for 18 hours at 37°C in an orbital incubator (Sanyo BV, Loughborough, UK) at a speed of 200 rpm. *C. albicans* was grown aerobically in Sabouraud dextrose liquid media for 18 hours at 37°C in an orbital incubator.

2.3 Preparation of the bacterial inoculum

A 1 mL aliquot of the overnight culture was centrifuged at 12,000 rpm, and the pellet was re-suspended in 1 mL phosphate buffered saline (PBS) (Oxoid Ltd.). An optical density of 0.05A at a wavelength of 600 nm was achieved by adding an aliquot of the re-suspended solution to 10 mL PBS which equates to approximately 10^7 cfu / mL. For *C. albicans* experiments, the entire re-suspended pellet was added to 10 mL PBS to achieve an optical density of 1.100 A, which corresponded to approximately 10^7 cfu / mL.

For experiments involving an alginate swab, the PBS was substituted with 3 mL Calgon ringer's solution and for those using Live/Dead stains, 1 mL buffered peptone water (BPW) was used.

2.4 Light sources

2.4.1 White light source

For white light photocatalysis experiments, a General Electric 28W Biax 2D compact fluorescent lamp (GE Lighting Ltd., Enfield, UK) was used. This lamp is commonly found

in UK hospitals and emits light across the visible spectrum; the spectral distribution chart is shown in Figure 2.1. For experimental purposes the lamp was affixed inside a cooled incubator to maintain a constant temperature of 22°C (LMS Series 1 Cooled Incubator Model 303; LMS Ltd., Sevenoaks, Kent). The intensity of the light was measured using a lux meter (LX101 Lux meter; Lutron Electronic Enterprise Co. Ltd, Taiwan) and readings were recorded in lux units. The term visible light indicates wavelengths of light in the visible portion of the electromagnetic spectrum, namely between 400 – 700nm, however the terms white light and visible light are used interchangeably in this thesis and indicate use of this fluorescent light source.

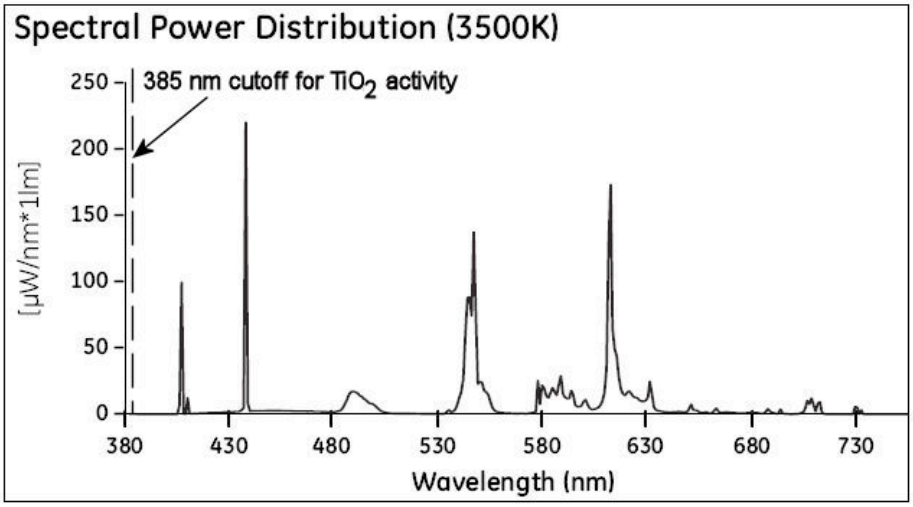

Figure 2.1. Spectral power distribution graph for the light source used in the visible light photocatalysis experiments (Technical publication for the 2D series lamp, 2005).

2.4.2 Ultraviolet (UV) light sources

2.4.2.1 365 nm light source

For the UV light photocatalysis experiments a UV fluorescent lamp was used (Vilber Lourmat VL-208BLB, Leicestershire, UK). The light source emitted light primarily at a

wavelength of 365 nm and the intensity of the light was measured using a UV light meter, Solarmeter Model 5.0 (Solartech Inc., Harrison Township, Michigan, USA), with the readings recorded in mW cm^{-2}. Experiments were conducted in a cabinet (Philip Harris Ltd., Shenstone, UK) fitted with a UV safety screen.

2.4.2.2 254 nm light source

A second UV light source was used (Vilber Lourmat VL-208G, VWR Ltd, Leicestershire, UK), either as a method for decontaminating the used samples or to activate the TiO_2 slides before exposure to the 365 nm light source. This germicidal UV fluorescent lamp emitted light primarily at a wavelength of 254 nm. Experiments were conducted in a cabinet (Philip Harris Ltd., Shenstone, UK) fitted with a UV safety screen.

2.4.3 Laser light source

A HeNe laser light source (Changchun New Industries Optoelectronics Tech. Co., Ltd., Changchun, China) was used for the photodynamic therapy experiments. The light source emitted light primarily at a wavelength of 660 nm and a light intensity of 230 mW.

2.5 General sampling methodology

A suspension of bacteria containing 10^7 cfu / mL bacteria, as described in Section 2.3, was diluted tenfold in PBS to produce a series of bacterial concentrations ranging from 10^7 - 10^4 cfu / mL. The standard volume of bacterial suspension used in these experiments was 25 µL which occupied an area of approximately 1 cm^2 upon the test samples; therefore the final bacterial population ranged from $2.5x10^5$ – $2.5x10^2$ cfu cm^-

^{2}. A standard volume (25 µL) of bacterial suspension was inoculated onto a clean microscope slide of dimensions 76 x 26 x 0.8 – 1.0 mm (length x width x thickness) (VWR International Ltd., Lutterworth, UK) and was sampled using a cotton-tipped swab. The surface was swabbed for 20 seconds in three directions with continual rotation of the swab head in a standardised manner, before inoculation into a bijou containing 1 mL of PBS. The bijou was vortexed for 2 minutes to remove the adherent bacterial cells and prior to preparation of tenfold serial dilutions. Twenty microlitres of each dilution was plated out onto either MacConkey agar for *E. coli* or mannitol salt agar for *S. aureus* and the plates were incubated at 37°C for up to 48 hours. The aerobic colony count (ACC) was calculated by counting the resultant colonies to determine the number of colony forming units per square centimetre (cfu / cm^2).

2.6 ATP bioluminescence

A series of luminometers were used to measure ATP bioluminescence as an alternative method of detecting and quantifying bacteria from the test surfaces. All luminometers were programmed to capture luminescence readings every 1 second and the mean reading in relative light units (RLU) was reported after 10 seconds. Test tubes were required for the detection of ATP using certain models of luminometer and to destroy any exogenous ATP before use, they were placed under the 254 nm germicidal UV lamp (Section 2.4.2.2) for 30 minutes within sealed plastic bags. The bag was inverted at the halfway point to provide even exposure to the light source.

2.6.1 Luminometer-specific methodologies

2.6.1.1 Junior luminometer

The cotton-tipped swab was added to a test tube containing 50 µL ATP Eliminating Reagent from the Microbial ATP Kit (BioThema AB, Handen, Sweden) post sampling. The tube was incubated for 10 minutes at room temperature according to the reagent kit instructions before 50 µL Extractant BS was added, and the covered tube was vortexed for 5 seconds to thoroughly mix the solution. Four hundred microlitres of ATP Reagent HS was finally added and the light generated was quantified by placing the tube into the Junior LB9509 luminometer (Berthold Technologies GmbH & Co KG; Bad Wildbad, Germany). An ATP standard was used on each run and 10 µL of the premixed 100 nmol / L ATP standard was added to the final solution, so that the equivalent of 1 pmol ATP was added to the test solution. The ATP bioluminescence of the test sample plus the ATP standard was then quantified by the Junior luminometer.

For each bacterial concentration on a surface, three independent swabs were used to generate an ATP bioluminescence reading and one swab was used for ACC measurements, with each dilution plated out in duplicate. Each experiment was performed at least in triplicate, to demonstrate reproducibility.

2.6.1.2 Lumat luminometer

The Lumat LB9507 luminometer (Berthold Technologies GmbH & Co KG) is a more sensitive but less portable model than the Junior luminometer. The methodology used to measure ATP bioluminescence emitted from test samples in combination with the Lumat luminometer was as described for the Junior luminometer in Section 2.6.1.1,

with the exception that the test tube was placed in the Lumat luminometer for the bioluminescence readings.

2.6.1.3 BioProbe luminometer

The BioProbe luminometer (Hughes Whitlock Ltd; Gwent, UK) was used in combination with the Microbial ATP Kit as in the previously described methodologies. However, the ATP bioluminescence generated from the bacterial suspension could be measured directly from the test surface so the reagents were applied directly to the test surfaces and the unnecessary swabbing stage was omitted. Instead, the BioProbe luminometer was placed above the test surface creating a seal between the inoculated laboratory bench and the luminometer. The luminescence generated was then quantified by the BioProbe luminometer.

2.6.1.4 Clean-Trace NG luminometer

The Microbial ATP Kit was not required for the detection assay utilising the Clean-Trace NG luminometer (3M; Bracknell, UK). This luminometer was designed for use with custom-made, pre-moistened swabs which, after sampling in the standard manner, were returned to the casing and immersed in a reagent solution located at its base. The entire swab casing was placed in the luminometer for quantification after vortexing for 5 seconds. A positive control was used on every run. This was a freeze-dried powder containing 5 pmol ATP which was sampled with the pre-moistened swab, and handled using the same methodology as the test samples.

2.7 Direct visualisation of bacteria – Live/Dead staining

Slides were examined under the fluorescent light microscope post-sampling, using the Live/Dead BacLight Bacterial Viability Kit (Invitrogen Ltd., Paisley, UK) to visualise any remaining bacterial cells and to determine their viability. The kit consisted of two stains; SYTO 9™ which penetrated the membranes of all cells, and propidium iodide which penetrated bacterial cells with damaged membranes (Boulos et al., 1999). Viable cells appeared green under the fluorescent microscope, whereas non-viable cells generated a red fluorescence. Images were captured on a camera attached to the microscope and bacterial cells were enumerated and the proportion of viable and non-viable cells was noted. The final bacterial population was compared to the starting inoculum value to evaluate the efficiency of the sampling process.

2.8 Effect of white light on bacterial survival

Glass microscope slides were placed in a moisture chamber which was custom-designed to prevent evaporation of the bacterial inoculum during exposure to white light (Figure 2.2). Filter paper, 150 mm in diameter (Whatman plc, Maidstone, UK) soaked in sterile distilled water was used to line the base of a square 24 cm x 24 cm petri dish. Wooden sticks were placed on top of the filter paper to rest the slides on. An additional moisture chamber was covered in foil to prevent light penetration, and slides which were to be incubated in the absence of light were placed in this moisture chamber for the exposure period, as a dark control. The moisture chambers were placed in the cooled incubator and the uncovered chamber was placed on a shelf, 20 cm from the light source, with the foil covered chamber on the shelf directly below.

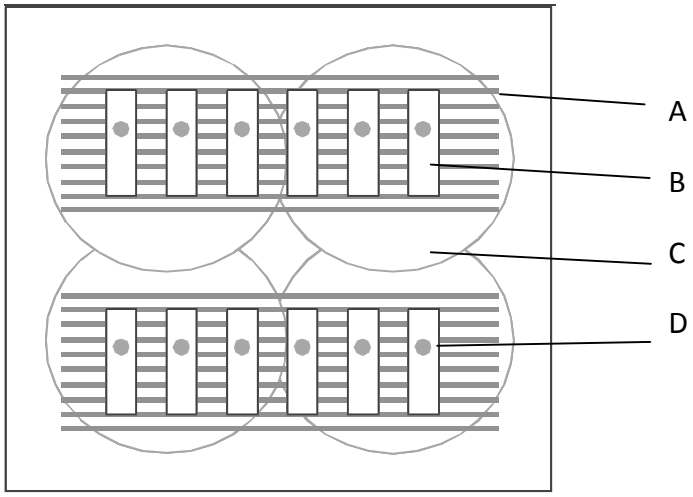

Figure 2.2. Experimental set up of the moisture chamber used during white light experiments, where A = wooden swabs; B = glass slides; C = moistened filter paper; D = bacterial inoculum.

The effect of the white light source on the viability of a number of bacterial species was investigated. A suspension of bacteria was inoculated onto a microscope slide prior to incubation under the white light source for 24 hours. Any decrease in the ACC after the irradiation period was calculated as a percentage and log reduction.

2.9 Optimisation of the sampling technique

To increase the proportion of bacteria that were recovered from the test surfaces, a series of experiments were performed and a single variable was changed. Uncoated, clean microscope slides were inoculated with a suspension of 25 µL of a Gram-negative bacterium *(E. coli)* or a Gram-positive bacterium *(E. faecalis)* and then either:

(i) sampled using a range of different swab types

(ii) sampled with a cotton swab and either vortexed or sonicated to remove adherent bacteria

(iii) sampled with up to three different cotton swabs which were re-suspended into the same bijou

(iv) sampled with up to three different cotton swabs which were re-suspended into separate bijoux.

Total bacterial numbers were calculated by serially diluting the bacterial suspension within the bijou and inoculating duplicate 20 µL aliquots onto 5% blood agar plates. The ACC was calculated after up to 48 hours growth at 37°C to determine the cfu / mL and this value was compared with the ACC recovered from the starting inoculum.

2.10 Preparation of light-activated antibacterial materials

2.10.1 Thin films generated by chemical vapour deposition

Novel antibacterial thin films were generated by one of two post-doctoral researchers based at the UCL Department of Chemistry. The thin films were prepared by atmospheric pressure chemical vapour deposition (APCVD) (Section 1.5.1). The depositions were carried out on the SiO_2 surface of slides of standard float glass from Pilkington of dimensions 220 x 85 x 4 mm (length x width x thickness) coated on one side with a barrier layer of SiO_2 to prevent ion diffusion from the glass to the film. The glass was washed prior to insertion into the APCVD reactor using sequential washings of water, acetone, petroleum ether (60-80) and propan-2-ol giving a clean and smear free finish.

2.10.1.1 Nitrogen-containing titania thin films TiON-1 and TiON-2

The nitrogen containing thin films TiON-1 and TiON-2 were prepared by Dr. Geoff Hyett with anhydrous ammonia (BOC Ltd.) as the nitrogen source, titanium (IV) chloride ($TiCl_4$; 99.9%; Sigma-Aldrich Ltd.) as the titanium source, and ethylacetate (EtAc; 99.0%; BOC Ltd., Guildford, UK) as the oxygen source (Hyett et al., 2007; Aiken et al., 2010). Depositions were carried out at 550°C for 60 seconds and the resulting films were cut into seven equally sized sections of 32 mm x 89 mm once cooled.

A nitrogen carrier gas was used for the $TiCl_4$ and EtAc at a flow rate of 2 L / min. The $TiCl_4$ bubbler was heated to 61°C and the EtAc bubbler to 44°C at a flow rate of 0.5 L / min which produced a molar mass flow ratio of 1:2. The $TiCl_4$ and EtAc were carried to a single mixing chamber through gas delivery lines which were maintained at 200°C and heated to 250°C, with an additional flow of nitrogen carrier gas at a rate of 12 L / min. The glass substrate was doped with nitrogen by flowing ammonia without the carrier gas through the reservoir at a flow rate of 0.26 L / min. The $TiCl_4$ and EtAc mixture and the ammonia gas were introduced just before contact with the glass substrate, and the $TiCl_4$: EtAc : ammonia mass flow ratio of the resultant thin film was 2.85 : 4 : 1. The resultant thin film was TiON-1, the titanium oxynitride. Thin film TiON-2 was prepared using the same methodology, except the deposition was carried out at 450°C instead of 550°C.

2.10.1.2 Nitrogen-doped titanium dioxide thin films N1, N2 and N3

The nitrogen containing thin films N1, N2 and N3 were prepared by Dr. Charles Dunnill with t-butylamine (99.5%; Fisher Scientific UK Ltd., Loughborough, UK) as the nitrogen

source, titanium (IV) chloride ($TiCl_4$; 99.9%; Sigma-Aldrich Ltd.) as the titanium source, and ethylacetate (EtAc; 99.0%; BOC Ltd., Guildford, UK) as the oxygen source (Dunnill et al., 2009b; Dunnill et al., 2009c; Dunnill and Parkin, 2009). The resultant coatings were nitrogen-doped titanium dioxide (N-doped TiO_2) thin films and depositions were carried out at 500°C for 30 seconds.

A nitrogen carrier gas was used for the $TiCl_4$ and EtAc, which was preheated to 150°C at a flow rate of 0.5 L / min. The $TiCl_4$ bubbler was heated to 70°C and the EtAc bubbler to 40°C, which produced a molar mass flow ratio of 1:2. The $TiCl_4$ and EtAc were carried to a single mixing chamber and heated to 250°C, with an additional flow of nitrogen carrier gas preheated to 150°C at a rate of 6 L / min. The glass substrate was doped with nitrogen by flowing the carrier gas, preheated to 60°C, through the t-butylamine reservoir, set at 5°C; the temperature of the t-butylamine reservoir was controlled using a water bath containing water and ethylene glycol in equal parts. The $TiCl_4$ and EtAc mixture and the t-butylamine gas were introduced just before contact with the glass substrate, at 100°C, with an additional flow of carrier gas at 1 L / min. The $TiCl_4$: EtAc : t-butylamine mass flow ratio of the resultant thin film was 1 : 2.5 : 0.3. Sections of the same sheet of the generated film were divided into 2.5 x 2.5 cm samples once cooled and divided into three groups, representing thin films N1, N2 and N3.

2.10.1.3 Sulfur-doped titanium dioxide thin films

Three sets of sulfur containing thin films (S-doped TiO_2) were prepared by Dr. Charles Dunnill, using titanium tetrachloride ($TiCl_4$; Sigma-Aldrich Ltd.) as the titanium source, ethyl acetate (EtAc; 99.0%; BOC Ltd.) as the oxygen source and carbon disulfide (CS_2;

99.9%; Alfa Aesar, Heysham, UK) as the sulfur source (Dunnill et al., 2009a). A nitrogen carrier gas was used for the $TiCl_4$ and EtAc, which was preheated to 150°C at a flow rate of 0.5 L / min. The $TiCl_4$ bubbler was heated to 70°C and the EtAc bubbler to 40°C, which produced a molar mass flow ratio of 1:2. The $TiCl_4$ and EtAc were carried to a single mixing chamber and heated to 250°C, with an additional flow of nitrogen carrier gas preheated to 150°C at a rate of 6 L / min. The glass substrate was doped with sulfur by flowing the carrier gas, preheated to 60°C, through the CS_2 reservoir, set at a temperature between 0 and 10°C; the temperature of the CS_2 reservoir was controlled using a water bath containing water and ethylene glycol in equal parts. The $TiCl_4$ and EtAc mixture and the CS_2 gas were introduced just before contact with the glass substrate, at 100°C, with an additional flow of carrier gas at 1 L / min. Depositions were carried out at 500°C for 30 seconds and three thin films were produced with different $TiCl_4$: EtAc : CS_2 mass flow ratios, which varied dependent upon the temperature of the CS_2 reservoir during synthesis:

(i) during synthesis of sample S1, the reservoir was set at 0°C, generating a mass flow ratio of 1 : 2.5 : 0.9

(ii) during synthesis of sample S2, the reservoir was set at 5°C, generating a mass flow ratio of 1 : 2.5 : 1.2

(iii) during synthesis of sample S3, the reservoir was set at 10°C generating a mass flow ratio of 1 : 2.5 : 1.6.

The resulting films were cut into seven equally sized sections of 32 mm x 89 mm once cooled.

2.10.1.4 Control thin films

Thin films of TiO_2 were synthesised using APCVD with the same synthetic conditions as that described above but omitting the addition of the dopant (i.e. ammonia, t-butylamine or carbon disulfide). Uncoated glass of the same size was used as an additional control.

2.10.2 Thin films generated by sol-gel deposition

The silver-titania thin films were generated in a two-step process (Dunnill et al., 2011); glass slides were initially coated with titanium dioxide and annealed, before a coating of silver nitrate was added.

2.10.2.1 Titanium dioxide sol preparation and thin film synthesis

The TiO_2 sol was prepared by adding 2.5246 g of acetylacetone (0.02526 mol, 99+%, Sigma-Aldrich Ltd.) to a 250 mL glass beaker containing 32 cm^3 butan-1-ol (0.35 mol, 99.4%, Sigma-Aldrich Ltd.). This produced a clear and colourless solution, to which 17.50 g titanium n-butoxide (0.05 mol, 97.0%, Fluka) was added. The solution was vigorously stirred for 1 hour before 3.64 mL distilled water dissolved in 9.05 g isopropanol (0.15 mol, analytical grade, Fisher Scientific) was added to the stirring titanium n-butoxide solution. The yellow colouration of the sol deepened, but remained clear and it was stirred for a further hour. Lastly, 1.66 g acetonitrile (0.04 mol, 99% min; Fisons Scientific UK Ltd.) was added to the solution and it was stirred for an hour. The deep yellow coloured sol was covered with parafilm and left to age overnight in the dark.

2.10.2.2 Titanium dioxide thin film synthesis

On the following day, clean single cavity ground glass slides (Jencons Scientific Ltd., East Grinstead, UK) of dimensions 76 x 26 x 1 mm (length x width x thickness) were attached to the dip coating apparatus in batches of 4 (Figure 2.3).

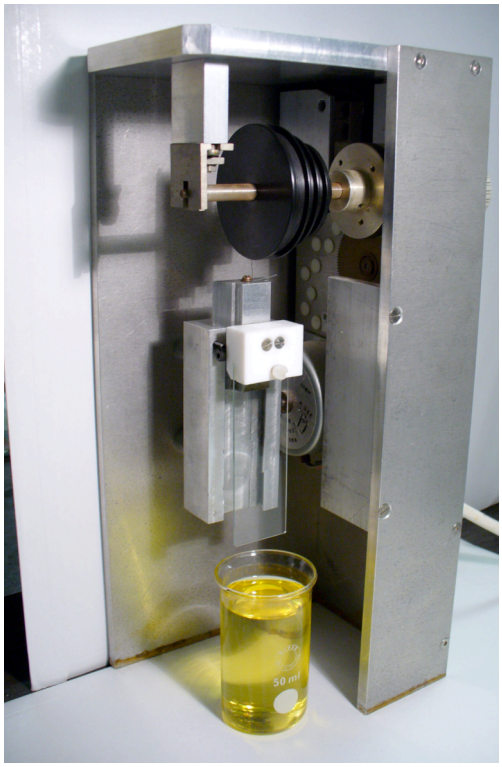

Figure 2.3 The dipping apparatus used to produce a xerogel on the microscope slides. Photograph reproduced with permission from Dr. Kristopher Page.

The cavity slides were lowered into a glass beaker containing the aged sol and after 20 seconds, the cavity slides were withdrawn by the apparatus at a steady rate of 120 cm / min. The first coat was allowed to dry before the process was repeated. The deposited xerogel films required calcination in order to adhere the coating to the cavity slide and to become crystalline. Therefore, the coated cavity slides were placed inside a muffle furnace and fired at 500°C for 1 hour, with a heating rate of 10°C / min

and a cooling rate of 60°C / min. The thin films were then left in the furnace overnight to cool and stored in a dark container until required. The resultant coatings are referred to as TiO_2 thin films.

2.10.2.3 Silver-titanium dioxide thin film synthesis

A solution of silver nitrate was prepared by adding 0.42 g silver nitrate to 500 mL of methanol (both Fisher Scientific UK Ltd.) to produce a final concentration of $5x10^{-3}$ mol / dm^3. The TiO_2 thin films were attached to the dip coating apparatus, dipped in the silver nitrate solution and withdrawn at a rate of 120 cm / min. The thin films were then exposed to the 254 nm UV lamp for 5 hours, within a custom made light box and were stored in the dark for at least 72 hours before bacteriological testing. Photodeposition occurs quickly (<30 min), but an excess of time was used to remove the time of irradiation as a variable and ensure that the films were fully clean and activated prior to initial characterization. The resultant coatings are referred to Ag-TiO_2 thin films.

2.10.3 Toluidine Blue O-containing polymers generated by swell encapsulation

Toluidine Blue O (TBO) was incorporated into polyurethane polymers by swell encapsulation. To achieve this, 125 mg of TBO was added to 25 mL distilled water, before the addition of 225 mL acetone, forming a 9:1 ratio of acetone to distilled water (H_2O 10% v/v). The solution was placed in a sonicating water bath for 15 minutes to ensure the TBO was evenly distributed throughout the suspension. To prevent interaction of the solution with light, the container was covered in foil during sonication. Ten millilitre aliquots of the TBO solution was dispensed into glass screw

capped bottles and a 1 cm^2 square of polyurethane was added. The bottles were stored horizontally in the dark for 24 hours. The polyurethane squares were then removed and laid to dry on a paper towel and covered for 1 hour. After this time they were rinsed with sterile distilled water until the excess TBO adhered to the surface of the polymers had detached and the water remained clear. The polymers were then dried and stored in the dark for a further 24 hours before use. Batches of 24 polymers were made and control polymers were also prepared without the addition of TBO (Perni et al., 2009b).

2.11 Characterisation and functional assessment of light-activated antibacterial materials

2.11.1 UV-visible-IR spectroscopy

UV-visible-IR spectroscopy was employed to determine the band onset of the thin films and assess the likely photocatalytic activity of the material. The thin films were decontaminated by exposure to the 254 nm germicidal UV lamp for 12 hours and stored in the dark for 72 hours. The thin film was then placed inside the UV-Visible-IR spectrophotometer (Perkin Elmer λ950, Massachusetts, USA) and percentage transmission readings were measured, which were converted to absorption and absorbance using the reflectance to gauge the thickness of the films by the Swanepoel method (Swanepoel, 1983). Data were transformed and a Tauc Plot was generated to determine the optical band gap of the thin films, by extrapolating the linear curve to the abscissa. A Tauc plot can be calculated using the formula $(a \times hv)^{1/2}$ against energy, where a denotes the absorbance of the material and hv denotes the energy of the

photon of light (Tauc, 1968, 1970). Measurements were also taken of the titanium dioxide thin film and uncoated glass slide, so that the readings could be compared.

2.11.2 Contact angle measurements

Water droplet contact angles were measured to determine the potential photo-induced hydrophilicity of the thin films. The thin films were decontaminated by exposure to the 254 nm germicidal UV lamp for 12 hours and stored in the dark for 72 hours. A FTA 1000 droplet analyser was used to measure the diameter of a 8.6 µL droplet of deionised water inoculated onto the thin film, using a side mounted camera. The drop was formed and dispensed by gravity from the tip of a gauge 27 needle. Readings were taken before and after irradiation with UV light (Section 2.4.2.1) or filtered white light (Section 2.4.1) between 200 and 2500 nm. An uncoated glass slide and titanium dioxide thin film were used as controls. Results were entered into a computer programme to calculate the contact angles based upon the volume-diameter data. An average of 5 readings were taken at each exposure time so that the results obtained were reproducible.

2.11.3 Photooxidation of stearic acid

The stearic acid test was used to quantify the photocatalytic activity of the thin films as a preliminary indicator of their potential antibacterial activity. The destruction of stearic acid was measured by Fourier Transform Infrared Spectroscopy (FTIR) using a Perkin Elmer Spectrum RX1 FTIR spectrometer.

The thin films were decontaminated by exposure to the 254 nm germicidal UV lamp for 12 hours and stored in the dark for 72 hours. The thin films were then attached to

an IR sample holder, comprised of a sheet of aluminium with a circular hole in the centre, before a 10 µL drop of a 0.01 M solution of stearic acid in methanol (Fisher Scientific UK Ltd) was applied to the exposed portion of the thin film. A characteristic white smear was observed once the droplet had evaporated and the samples were then stored once again in the dark for at 72 hours, prior to the baseline reading at 0 hours. FTIR spectra were obtained for the stearic acid layer between 2800 and 3000 cm^{-1} and an uncoated glass slide was used as a control for the background readings. Baseline readings (C_0) were taken of the thin films and blank controls, then all samples were placed in the custom-made light box and were exposed to the light source. Readings (C_x) were taken at 24 hour intervals and the samples were returned to the light box after each reading. For each time point, the area of the peaks were integrated and the values combined to give an approximate concentration of stearic acid on the surface, where 1 cm^{-1} in the integrated area between 2700 and 3000cm^{-1} corresponds to approximately 9.7×10^{15} molecules / cm^2 (Mills and Wang, 2006). A graph was plotted of the normalised concentration of stearic acid detected on the surface (C_x/C_0) against time, which allowed the destruction of stearic acid to be observed.

The light sources were attached to the lids of the custom-made light boxes, which were suspended 25 cm from the surface of the thin films. Three lighting conditions were examined: a UV light source (Section 2.4.2.2); a white light source (Section 2.4.1) and the white light source fitted with a UV filter. The UV filter used was a 3 mm thick sheet of Optivex™ glass, which is described to cut off all radiation below 400nm (Instrument Glasses, 2000). The filter was positioned 1 cm above the samples and was setup such that all light arriving at the samples had passed through the filter.

2.12 Microbiological assessment of light-activated antimicrobial materials

2.12.1 Decontamination of the thin films

Prior to microbiological assessment, coated samples were soaked in 70% isopropanol for 30 minutes to kill and remove any adherent contaminants, rinsed with fresh isopropanol and air-dried. The samples were then incubated in a hot air oven (Weiss Gellenkamp oven BS, Leicestershire, UK) for 1 hour at 160°C to kill any residual organisms and stored in the dark until required. This process was repeated after microbiological assessment in preparation for further testing.

The decontamination procedure was later amended and after microbiological assessment, the slides were rinsed with sterile distilled water and air-dried before exposure to the 254 nm germicidal UV lamp (Section 2.4.2.2) for 18 hours to kill any remaining adherent organisms. The slides were then placed in the dark to reverse the activating effect of the UV light. Samples were then ready for re-use after 72 hours dark storage. Thin films were re-used due to the lack in reproducibility of the deposition method.

2.12.2 Measuring the effect of light on the thin films generated by APCVD or sol-gel

The thin films were placed in a 24 x 24 cm petri dish lid, 20 cm from the light source for the activation step (designated A+) for the desired time period. The thin films were not covered during this light exposure period. As a control, duplicate thin films were also

placed in the cabinet, but within a foil-encased 24 x 24 cm petri dish to prevent light penetration (designated A-).

The thin films were then positioned within the moisture chamber (Figure 2.4), before a 25 µL droplet of bacterial suspension was added. The lid was added to prevent droplet evaporation and the moisture chamber was placed under the light source, at a distance of 20 cm for the irradiation step (designated L+) and exposed for the desired period of time before sampling. Control duplicate thin films were incubated within a foil-encased moisture chamber during the white light exposure period (designated L-). The nomenclature used for the light exposure experiments is summarised in Table 2.2.

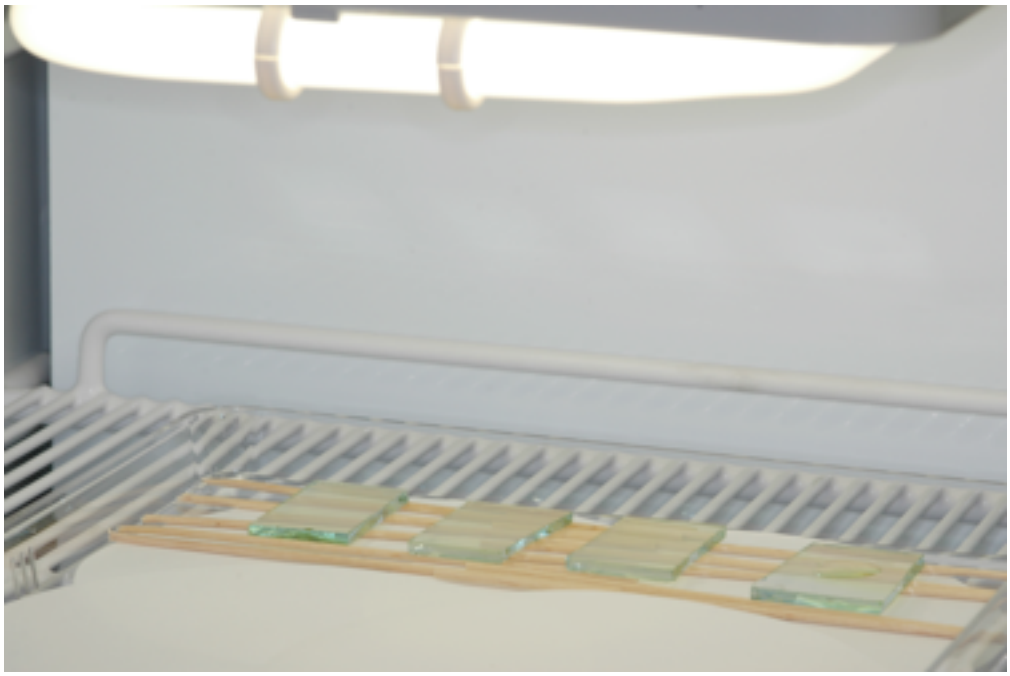

Figure 2.4 Irradiation of the nitrogen-doped thin films to white light, with the samples placed within the custom designed moisture chamber.

Table 2.2. Nomenclature used during microbiological assessment of the thin films.

Nomenclature	Description
A+L+	Sample exposed to first light dose, bacterial droplet added, then sample exposed to second light dose
A-L+	Sample stored in the dark, bacterial droplet added, then sample exposed to second light dose
A+L-	Sample exposed to first light dose, bacterial droplet added, then sample stored in the dark
A-L-	Sample stored in the dark, bacterial droplet added, then sample stored in the dark

Bacteria were recovered by sampling the thin films, as described in Section 2.5. Experiments were performed in at least duplicate and repeated on a minimum of three separate occasions for each type of thin film and exposure time.

2.12.3 Measuring the effect of light on Toluidine Blue O-impregnated polymers generated by swell encapsulation

Newly synthesised polymers (described in Section 2.10.3) were used for each experiment and were discarded after each use. A polymer was placed in a well within a 6-well microtitre plate before a 25 µL droplet of the microbial suspension was added. A glass cover slip was carefully placed on top to spread the droplet evenly across the surface of the polymer and the plate was transferred to a raised platform, 24 cm from the laser light source. The light emitted from the laser passed through a beam diffuser to spread the light beam so that the entire polymer was exposed to the laser light and the polymer was exposed to the laser light for the required period of time.

Once the exposure time had ended the coverslip was aseptically removed and placed inside a 50 mL tube, containing 135 µL PBS. A 10 µL aliquot of the microbial droplet was removed from the polymer and inoculated directly onto an appropriate agar plate and spread using an L-shaped spreader. The remaining 15 µL of microbial suspension was recovered, placed in the 50 mL tube and briefly vortexed before tenfold serial dilutions were prepared. Twenty microlitres of each dilution was inoculated and spread onto an appropriate agar plate in duplicate. As controls, TBO-containing polymers were inoculated with the microbial suspension for the same length of time in the absence of laser light (L-S+), or polymers prepared without the addition of TBO were inoculated with the microbial suspension and exposed to identical periods of laser light (L+S-) or not exposed to the laser light (L-S-). The sampling process was repeated three times for each polymer type and exposure time and the entire experiment was repeated on at least three separate occasions for each organism and exposure time (Perni et al., 2009b).

2.13 Statistical analysis

In order to determine the significance of any decreases in the cfu observed between the light-activated antibacterial materials exposed to different conditions, the Mann Whitney U test was used. The number of survivors recovered from the test group (i.e. the light-activated material exposed to light) was compared to the number of survivors from the control groups (i.e. the light-activated materials not exposed to light or the uncoated samples). Median values were taken because the data were not normally distributed and the values were transformed to $\log_{10}$ for normalisation. A p value of less than 0.05 was considered statistically significant. Statistical significance is

diagrammatically represented on the box and whisker plots in the results sections as asterisks; one asterisk denotes a p value < 0.05, two asterisks denotes a p value < 0.01 and three asterisks denotes a p value < 0.001. All statistical analyses were performed using the SPSS statistical package (version 16.0, SPSS Inc., Chicago, IL, USA).

3 Development of protocols used to assess the activity of the photocatalytic thin films

3.1 Introduction

The purpose of the work described in this chapter was to develop a reproducible method of testing the antibacterial photocatalytic activity of thin films. Initially the sampling technique was examined to determine the sampling efficiency and an optimised regimen was developed. Researchers from our laboratory had previously used swabs (Page et al., 2007) to remove bacteria from the test surface in order to detect changes in the bacterial concentration post-exposure to antibacterial coatings. Other groups have used dipslides as a direct detection method, but this is unsuitable for accurately quantifying high concentrations of bacteria as it results in confluent growth, which only generates an estimate of the bacterial load. The recovery of bacteria from glass surfaces was initially compared using a range of swabs with swab heads comprised of different materials; using a differing number of swabs per sample and using sonication as a method of releasing bacterial cells from the swab head. There are however, inherent problems with swabbing, as bacteria are either left behind on the surface after swabbing, or get caught within the mesh of the swab head and are not released into the diluent after sampling (Davidson et al., 1999).

Antimicrobial coatings are generally assessed using the viable count technique and bacterial survival is determined by counting colonies originating from (i) serial dilutions of the bacterial suspension on the coating (Wilson, 2003; Decraene et al., 2006; Page et al., 2007), (ii) those grown on an agar overlay, applied to the entire coating (Decraene et al., 2008b), (iii) serial dilutions of the bacterial suspension after the entire

coating has been immersed in a sterile fluid and agitated to remove adherent organisms (Decraene et al., 2008a) or (iv) a combination of these (Perni et al., 2009a). These techniques have proven to be effective at determining the activity of novel antimicrobial coatings, but the turnaround time for results is around 48 hours so an alternative, faster method is still desirable.

ATP bioluminescence has been used as a rapid diagnostic test to detect bacteria from urine samples (Selan et al., 1992) and more recently, has been applied in the hospital environment to rapidly assess the efficiency of cleaning regimens in hospitals, as described in Section 1.6.4 (Griffith et al., 2000; Malik et al., 2003; Dancer, 2004; Aycicek et al., 2006; Griffith et al., 2007; Willis et al., 2007; Lewis et al., 2008; Boyce et al., 2009; Mulvey et al., 2011), following on from the successful use of this method in the food industry for the monitoring of surface cleanliness (Poulis et al., 1993; Hawronskyj and Holah, 1997; Aycicek et al., 2006). The cleanliness of a surface can be rapidly assessed and if the level of ATP is above an acceptable level then the surface can be re-cleaned and retested.

ATP bioluminescence utilises the firefly luciferase enzyme, to catalyse the conversion of ATP into AMP resulting in the emission of light (Lundin, 2000). The amount of light emitted is quantified by a luminometer and is directly proportional to the initial amount of ATP in the sample. If the eukaryotic ATP is removed from the surface before sampling then this value is in turn proportional to the amount of bacteria in the starting sample as one photon of light is generated per molecule of ATP. For this study, the method was evaluated for its potential use as a tool to assess the effectiveness of novel antibacterial coatings by quantifying bacteria present on a surface before and

after light exposure. The generation of quantitative data, especially at low bacterial concentrations, would be useful and it was postulated that ATP bioluminescence could supersede swabbing as the first choice for bacterial detection from surfaces in this project.

Also assessed in this chapter was the effect of the incident light source on the survival of bacteria. Certain specific wavelengths of white light are known to inactivate some Gram-positive strains of bacteria (Maclean et al., 2008, 2009) so it was important to be aware of the effect of the light source used to activate the novel thin films. Any decrease in the bacterial concentration could then be attributed to the activity of the thin films and not to incident light source.

3.2 Materials and methods

3.2.1 Optimisation of the sampling technique

Bacterial strains were maintained as described in Section 2.1 and bacterial suspensions of *E. coli* and *E. faecalis* were prepared as detailed in Section 2.3, resulting in a starting inoculum of approximately 10^7 cfu / ml. A number of strategies were employed in an attempt to improve bacterial recovery from the surface of uncoated microscope slides as described in Section 2.9. Three different cotton swabs were used (all Fisher Scientific UK Ltd): woodstick cotton tipped swabs - Cotton A; cotton swabs sterilised by ethylene oxide - Cotton B; and cotton swabs sterilised by UV light - Cotton C. Alginate and viscose swabs were also used in the comparison.

3.2.2 ATP bioluminescence

Bacterial strains were maintained as described in Section 2.1 and bacterial suspensions of *E. coli* and *S. aureus* were prepared as detailed in Section 2.3, resulting in a starting inoculum of approximately 10^7 cfu / ml. ATP bioluminescence was used to detect bacteria inoculated onto the surface of uncoated microscope slides as described in Section 2.6.1. A number of commercial luminometers were used with output given in relative light units (RLU) and the amount of ATP present in the samples was calculated using the following formula (Hughes Whitlock Ltd., 1995):

$$ATP_{sample} = RLU_{sample} / (RLU_{sample + standard} - RLU_{sample})$$

The number of bacteria present in each sample was then calculated based on previously documented studies which estimate that each bacterial cell contains approximately $2x10^{-18}$ mol ATP (Lundin, 2000; BioThema AB, 2006). It was important to determine the initial amounts of ATP present as otherwise the RLU readings obtained from different luminometers could not be directly compared (Hawronskyj and Holah, 1997). To assess the sensitivity of the assay using each instrument, one-tailed t-tests were performed where the sensitivity was the lowest concentration that was significantly different from the negative control, with 95% confidence. The coefficient of variation (CV) was calculated as a percentage for each dilution to demonstrate the reproducibility of each luminometer, where greater reproducibility is represented by lower CV values, particularly below 100% (Griffith et al., 1994). The luminometer-specific methodologies were assessed to determine the precision, accuracy and sensitivity of each assay using the definitions described in Table 3.1.

Table 3.1 Definitions of the terms used to compare the luminometer-specific methodologies.

Parameter	Definition
Precision	A measure of the reproducibility of the luminometer-specific method. Assessed by calculating the coefficient of variation (CV)
Sensitivity	The lowest concentration of bacteria that is significantly different to the negative control. Assessed by performing one-tailed t-tests.
Accuracy	How close the value generated by the luminometer-specific method is to the true value. Assessed by comparison with the inoculum level, estimated by viable colony count

3.2.3 Measuring the effect of white light on bacterial survival

Bacterial strains were maintained as described in Section 2.1 and bacterial suspensions of *S. aureus* NCTC 6571, *E. coli* ATCC 25922, *E. faecalis, S. pyogenes* ATCC 12202, EMRSA-16, EMRSA-15, MRSA 43300, *S. aureus* NCTC 8325-4 and *S. epidermidis* 01 were prepared as detailed in Section 2.3, resulting in a starting inoculum of approximately 10^7 cfu / ml, equating to approximately 2.5 x 10^5 cfu / sample. The effect of the white light on the viability of bacterial strains was determined using the methodology described in Section 2.8 and Figure 2.2. The Mann Whitney test was used to determine the statistical significance of any differences observed, as described in Section2.13.

3.3 Results

3.3.1 Optimisation of the sampling technique

The use of different swabs during sampling did not result in a notable increase in bacterial recovery (Figure 3.1); the greatest recovery of *E. coli* and *E. faecalis* was observed using the alginate swab but there remained a 97.3% and 99.2% respective loss compared with the starting inoculum. Recovery of *E. coli* and *E. faecalis* using cotton swab C resulted in a 98.9% and 99.6% loss of bacteria respectively and the use of cotton swab A resulted in a 98.9% and 99.7% loss of bacteria, respectively. Overall, recovery of *E. coli* was better than recovery of *E. faecalis*.

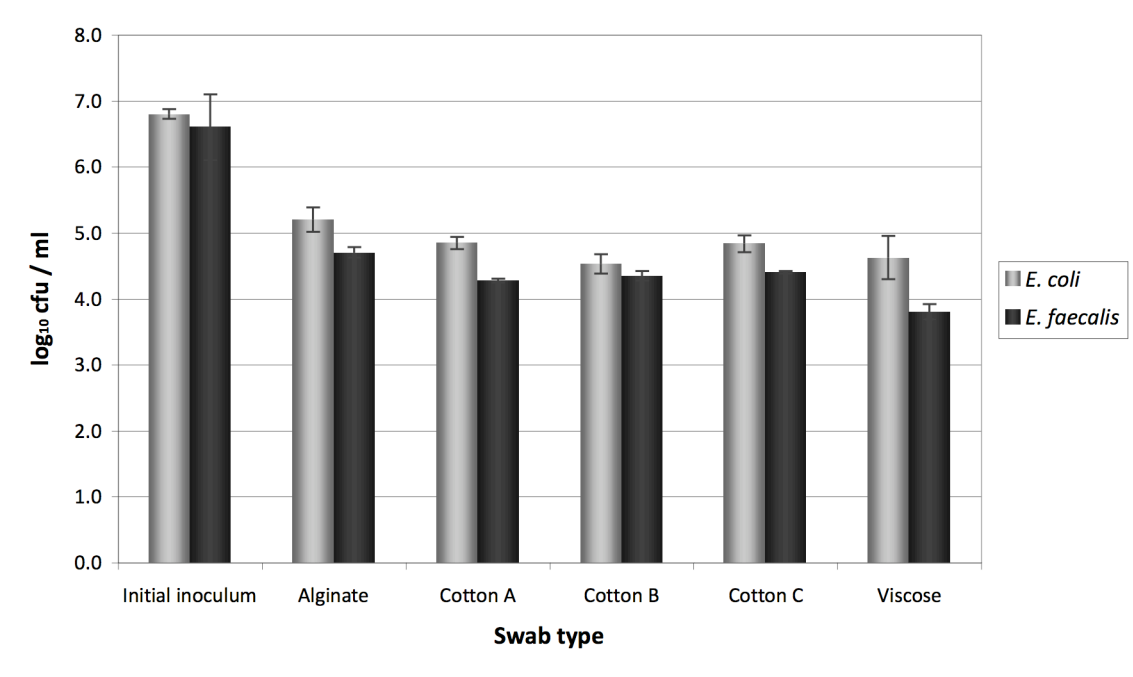

Figure 3.1 Comparison of different swab types to increase the recovery of E. coli *and E. faecalis*. The use of any of the swab types resulted in a loss of more than 97% of bacteria during the swabbing process. Bars indicate mean values (n=8) and error bars represent standard deviations.

Therefore, *E. coli* was used to assess further improvements in the sampling technique, with cotton swab A. Sonicating the swabs after sampling the surface did not result in a greater recovery of *E. coli*, nor did the use of more than one swab (Figure 3.2). The method which resulted in the greatest recovery of bacteria was the 2-swab in 1 bijou method, but there was still a 98% difference between the starting concentration of *E. coli* and the concentration recovered. All nine methods tested resulted in losses of more than 98% of *E. coli*. Therefore the 1-swab technique, with cotton swab A and a 120 second vortex was used for all subsequent experiments. The difference in recovery between the various techniques was not substantial and the chosen method was the least labour intensive and most cost effective.

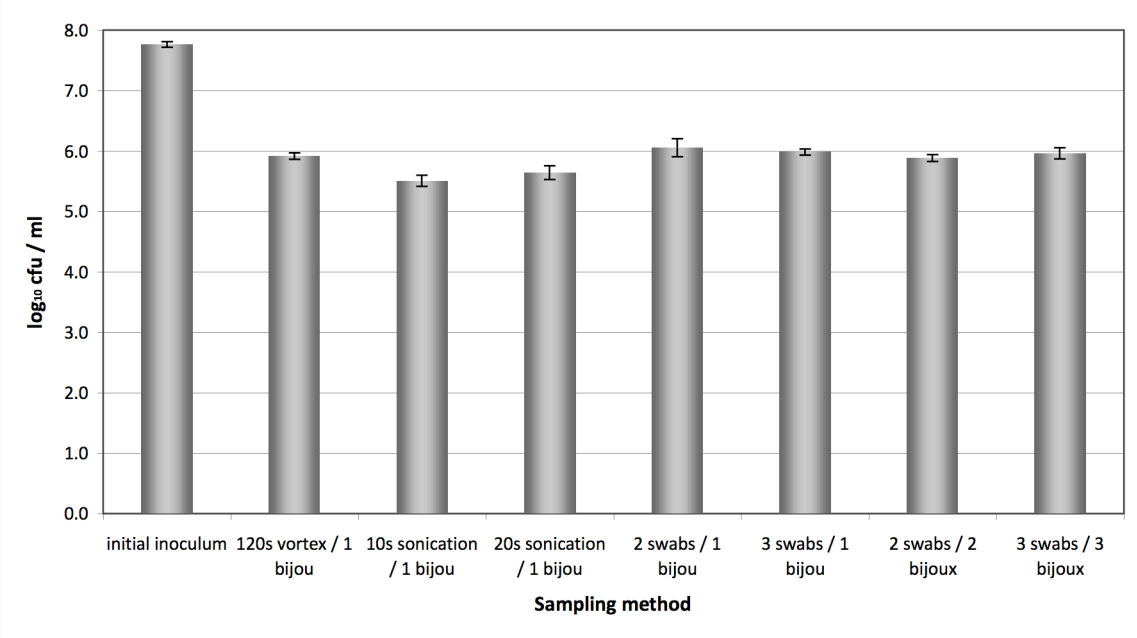

Figure 3.2 Comparison of different sampling methods used to increase the recovery of *E. coli*. All sampling methods trialled resulted in losses of more than 98% of *E. coli*. Bars indicate mean values (n=8) and error bars represent standard deviations.

3.3.2 ATP bioluminescence

3.3.2.1 S. aureus

The most accurate prediction of the concentration of *S. aureus* was produced when the BioProbe luminometer was used to detect ATP bioluminescence; a starting inoculum of $2.5x10^5$ / cm^2 was reported as $6.7x10^5$ / cm^2 (Figure 3.3). However, the highest dilutions of bacteria were not always detected and were falsely reported as negative, which resulted in large standard deviations and a coefficient of variation (CV) of over 100% for the lowest concentration of bacteria (Table 3.2). Furthermore, the methodology was not the most sensitive; the calculated sensitivity of the BioProbe assay was $2.5x10^4$ / cm^2 (p <0.05), which meant that lower bacterial concentrations could not be differentiated from the negative control. An accurate estimate of the *S. aureus* concentration was also produced when the Junior luminometer was used to detect ATP bioluminescence. However, at the lowest test concentration, the variance of the data was very large, which similarly resulted in a CV value above 100%.

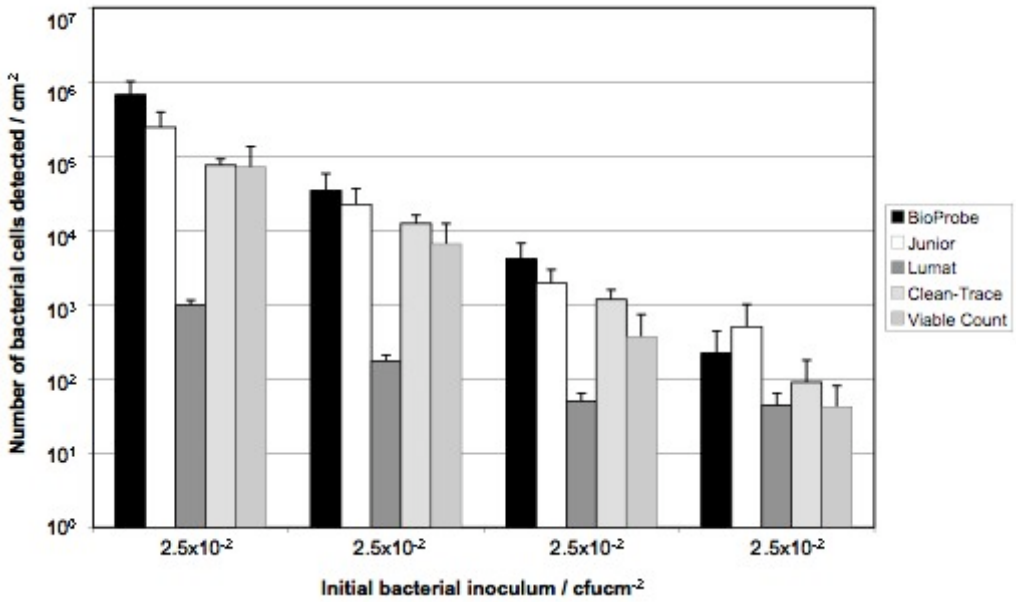

Figure 3.3 Comparison of the five different methods employed for the detection of surface-associated *S. aureus*. Data points represent mean values and error bars represent standard deviations (Aiken et al., 2011).

Table 3.2 Reproducibility of the ATP bioluminescence assay using the four luminometers to detect *S. aureus*, displayed as coefficients of variation (CV) where a lower CV represents a greater reproducibility. All values are expressed as percentages. The sensitivity of each assay is marked with an asterisk.

cfu / cm^2 *S. aureus*	Lumat	Junior	BioProbe	Clean-Trace
$2.5x10^5$	16	62	52	21
$2.5x10^4$	20	64	70*	29
$2.5x10^3$	27	51	62	35*
$2.5x10^2$	44*	158*	137	133

The most precise estimate of the bacterial load on the test surface was generated when the Lumat luminometer was used to detect ATP bioluminescence (p <0.01), where precision is an indication of the reproducibility of the method. The presence of

$2.5x10^2$ / cm^2 (the lowest dilution factor tested) of *S. aureus* was consistently detected (Figure 3.3) and low levels of bacteria were not misreported as negative, which was confirmed by the low CV values obtained (Table 3.2) for all dilution factors. However, the accuracy of the device was poor as the detected concentration of bacteria was at least a factor of 10 lower than the inoculum added to the test surface.

When the Clean-Trace luminometer was used to detect ATP bioluminescence, an inaccurate result was always generated although the data produced was always reproducible. The concentration of *S. aureus* was underestimated by almost a factor of 10 at each dilution factor. At low bacterial concentrations, an absence of ATP was commonly reported, resulting in large standard deviations and a CV value over 100% at the lowest bacterial concentration.

Reproducible estimates were obtained using the viable count method; however the bacterial load was underestimated by up to a factor of 10 and was lower than those values generated by the ATP bioluminescence assays using the BioProbe or Junior luminometers. A large variation in the values obtained at higher concentrations was also seen although the presence of bacteria was never misreported.

3.3.2.2 E. coli

The most accurate prediction of the concentration of *E. coli* was produced when the BioProbe luminometer was used to detect ATP bioluminescence and a starting inoculum of $2.5x10^5$ / cm^2 was reported as $2.2x10^5$ / cm^2 (Figure 3.4). However, the highest dilutions of bacteria were not always detected and were falsely reported as negative, which resulted in large standard deviations and CV values of over 100%. A

less accurate prediction of the concentration of *E. coli* present on the test surface was provided when the Junior luminometer was used to detect ATP bioluminescence. For example, when the starting inoculum was $2.5x10^5$ / cm^2 the bacterial concentration was underestimated by a factor of 10 and at the lowest bacterial concentration no bacteria were detected on any of the six replicates performed (Figure 3.4). The reproducibility of the assay was poor which was reflected by the high CV values; a CV value of 0 was obtained when the starting inoculum was $2.5x10^2$ / cm^2, but this was only because of the inability of the assay to detect the presence of *E. coli.*

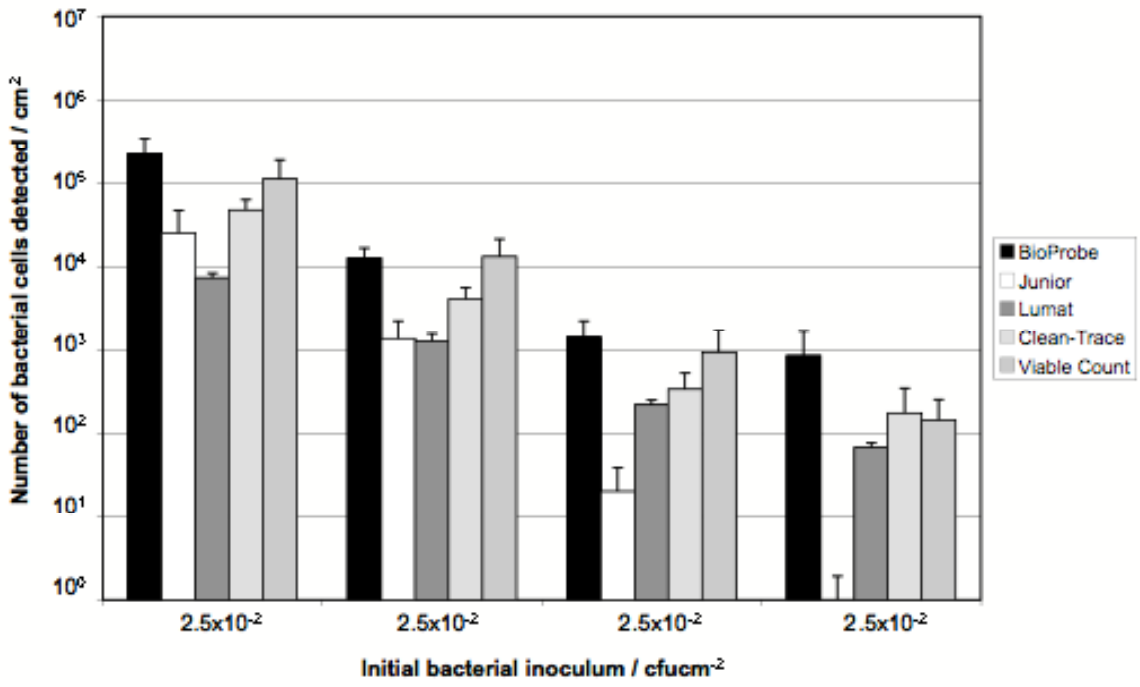

Figure 3.4 Comparison of the five different methods employed for the detection of surface-associated *E. coli*. Data points represent mean values and error bars represent standard deviations (Aiken et al., 2011).

Table 3.3 Reproducibility of the ATP bioluminescence assay using the four luminometers to detect *E. coli*, displayed as coefficients of variation (CV) where a lower CV represents a greater reproducibility. All values are expressed as percentages. The sensitivity of each assay is marked with an asterisk.

cfu / cm^2 *E. coli*	Lumat	Junior	BioProbe	Clean-Trace
$2.5x10^5$	14	85	52	32*
$2.5x10^4$	23	67*	32	36
$2.5x10^3$	15	254	58*	54
$2.5x10^2$	13*	0	98	104

The most sensitive and reproducible estimate of the number of *E. coli* present on the test surface was generated when the Lumat luminometer was used to detect ATP bioluminescence (Figure 3.4). Low levels of bacteria were always detected and not misreported as negative and there was very little variation observed in the readings generated which was confirmed by the low CV values obtained for all concentrations of bacteria tested (Table 3.3). However the accuracy of the estimate was poor as was also seen in the *S. aureus* assay and the detected concentration of bacteria was at least a factor of 10 lower than the inoculum level. For example, just $7.4x10^3$ / cm^2 of *E. coli* was detected by this method when the starting inoculum was $2.5x10^5$ / cm^2.

When the Clean-Trace luminometer was used to detect ATP bioluminescence an accurate prediction of the concentration of *E. coli* at the lowest dilutions was provided (Figure 3.4). However, there was little differentiation between the highest two dilutions of bacteria tested. For example, a starting concentration of *E. coli* of $2.5x10^3$ / cm^2 was reported as $3.4x10^2$ / cm^2 and a starting concentration of $2.5x10^2$ / cm^2,

reported as $1.7x10^2$ / cm^2 and this problem was compounded by the fact that the highest dilutions of either bacteria were not always detected and thus falsely reported as negative, resulting in large standard deviations and CV values of over 100%.

The viable count method was superior to all other methods for *E. coli* detection. For example, when the starting inoculum of *E. coli* was either $2.5x10^5$ / cm^2 or $2.5x10^2$ / cm^2 respective concentrations of $1.1x10^5$ / cm^2 and $1.4x10^2$ / cm^2 were obtained (Figure 3.4). The presence of bacteria was always reported, even at low concentrations, which was not shown for all the luminometer-based methods.

3.3.3 Measuring the effect of white light on bacterial survival

3.3.3.1 Comparison of 4 bacterial strains on a glass substrate

White light was observed to have an antibacterial effect on the survival of *S. aureus* NCTC 6571 on a glass surface (Figure 3.5). After 24 hours exposure to white light, a statistically significant reduction in viable organisms was seen (5.6 $\log_{10}$ cfu / sample), compared with the control conditions without white light exposure. The median count was below the detection limit of the assay but there was a wide range in counts and values between 0 and 4.7 $\log_{10}$ cfu / sample were obtained (p <0.001).

White light did not have an effect on the survival of *E. coli* ATCC 25922 on a glass surface (Figure 3.6). After 24 hours exposure to white light, a negligible reduction in viable organisms was seen (0.2 $\log_{10}$ cfu / sample), compared with the control sample, which was not exposed to white light. Although, when the data were statistically analysed, a highly significant difference in counts was observed; this was due to the

very small error bars in this series of experiments attributed to the little variation in counts obtained on each experimental repeat. Such small differences would not be considered microbiologically different.

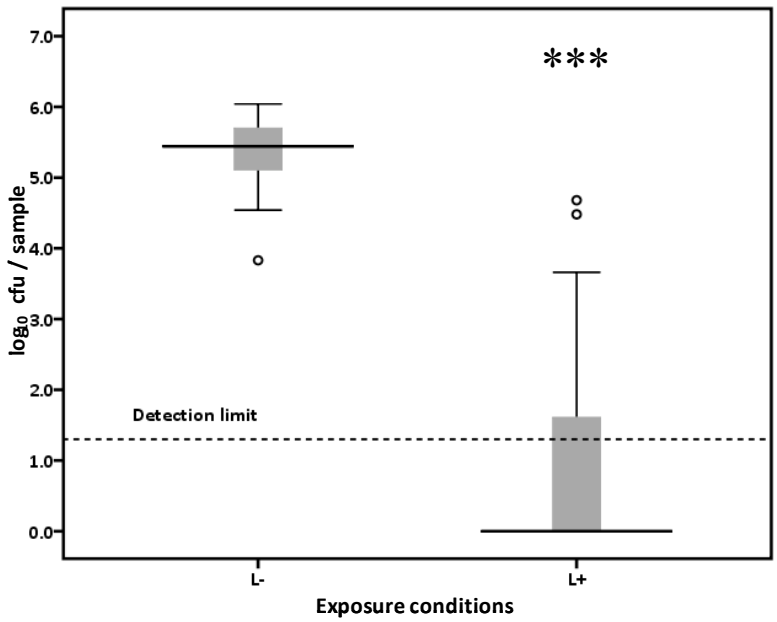

Figure 3.5 Effect of the white light source on the survival of *S. aureus* NCTC 6571 on a glass surface. A 25 µl bacterial suspension was inoculated onto a glass slide before expose to white light for 24 hours (L+; n = 29). As a control, inoculated glass slides were also incubated in the dark for 24 hours (L-). The thick horizontal lines indicate median values, the base and top of each box represents the 25% and 75% quartiles respectively, and the error bars, the 10% and 90% percentiles and the small circles are outliers. The dotted horizontal line indicates the detection limit of the sampling method, 1.4 $\log_{10}$ cfu / sample.

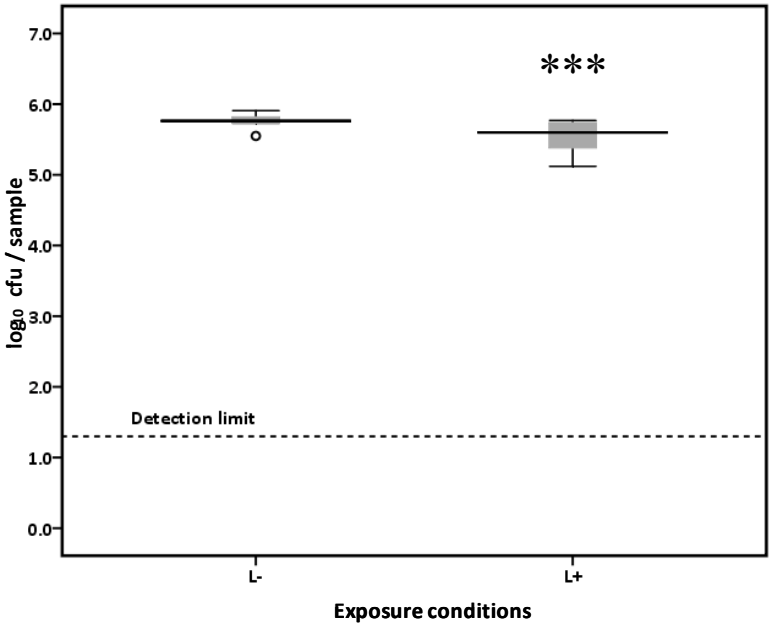

Figure 3.6 Effect of the white light source on the survival of *E. coli* ATCC 25922 on a glass surface. Samples were exposed to white light for 24 hours after addition of 25 µl of a bacterial inoculum (n = 10).

The effect of white light on the survival of *E. faecalis* on a glass surface can be seen in Figure 3.7. After 24 hours exposure to white light, a small but statistically significant reduction in viable organisms was seen (0.1 $\log_{10}$ cfu / sample), compared with the control sample that was not exposed to white light (p <0.05). A wide range in counts was obtained with values between 2.2 and 5.4 $\log_{10}$ cfu / sample observed on the surface exposed to light.

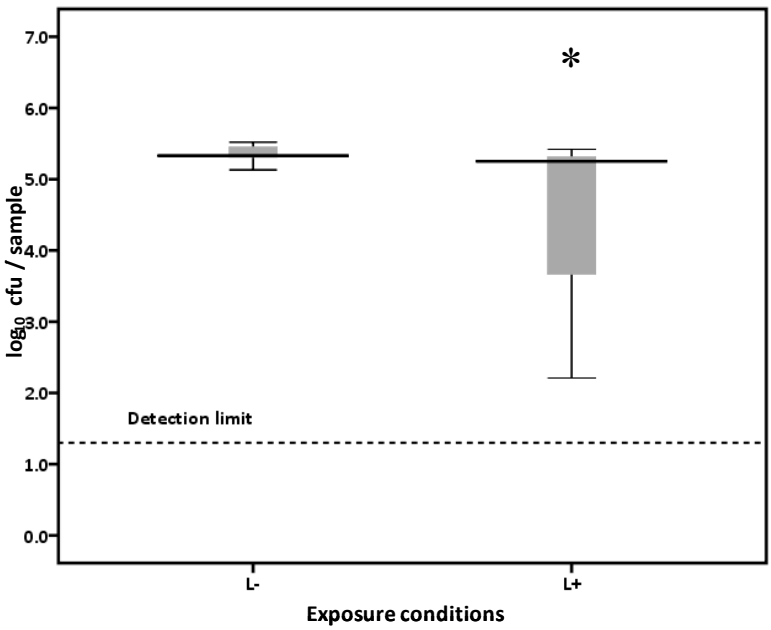

Figure 3.7 Effect of the white light source on the survival of *E. faecalis* on a glass surface. Samples were exposed to white light for 24 hours after addition of 25 µl of a bacterial inoculum (n = 6).

White light was also observed to have an effect on the survival of *S. pyogenes* ATCC 12202 inoculated onto a glass surface (Figure 3.8). After 24 hours exposure to white light, a 1.3 $\log_{10}$ cfu / sample reduction in viable organisms was seen compared with the control conditions without white light exposure, which was statistically significant (p <0.05). There was a wide range in counts and values between 0 and 4.5 $\log_{10}$ cfu / sample were obtained.

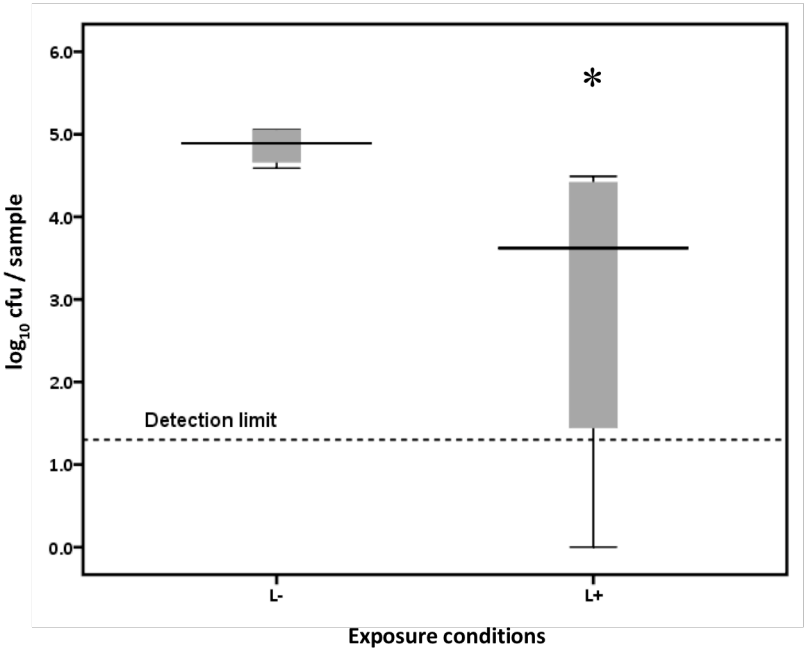

Figure 3.8 Effect of the white light source on the survival of *S. pyogenes* ATCC 12202 on a glass surface. Samples were exposed to white light for 24 hours after addition of 25 µl of a bacterial inoculum (n = 4).

3.3.3.2 Comparison of *S. aureus* strains on a glass substrate

The data collected in the previous sections suggested that *S. aureus* NCTC 6571 was particularly susceptible to the white light used for this series of experiments, so it was decided to examine other *S. aureus* strains to see whether they share this increased sensitivity to white light inactivation. This was particularly important as it would be useful to assess the activity of the light-activated antimicrobial coatings against strains of *S. aureus*, especially the epidemic strains EMRSA-15 and EMRSA-16, because they are a common cause of HCAIs, they have been the predominant circulating strains of MRSA in the UK, and are cited as the cause of more than 95% of MRSA bacteraemias (Johnson et al., 2001; Ellington et al., 2010).

A reduction in the recovery of both EMRSA-16 (Figure 3.9) and EMRSA-15 (Figure 3.10) was seen from the glass surfaces exposed to the white light source, compared to that

recovered from the surfaces not exposed to white light. The observed reductions were statistically significant and were 0.9 $\log_{10}$ cfu / sample and 1.5 $\log_{10}$ cfu / sample for EMRSA-16 (p <0.01) and EMRSA-15 (p <0.01) respectively, indicating that EMRSA-16 was less susceptible to the white light, compared with EMRSA-15.

White light was observed to have a much greater effect on the survival of MRSA 43300 inoculated onto a glass substrate (Figure 3.11). After 24 hours exposure to white light, a statistically significant reduction in viable organisms was seen (4.6 $\log_{10}$ cfu / sample), compared with the control conditions without white light exposure. The median count was below the detection limit of the assay but there was a wide range in counts and values between 0 and 4.6 $\log_{10}$ cfu / sample were obtained. These results were similar to those observed after *S. aureus* NCTC 6571 was exposed to the same light conditions (Figure 3.5).

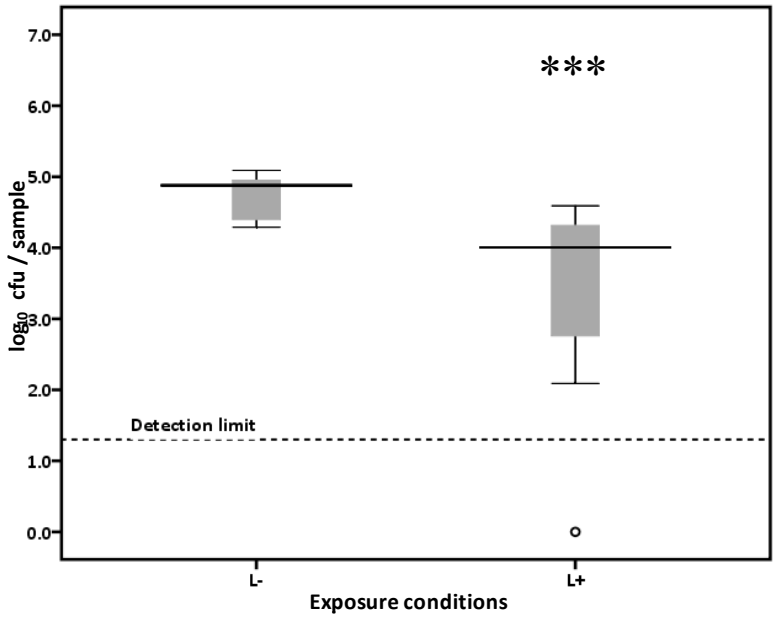

Figure 3.9 Effect of the white light source on the survival of EMRSA-16 on a glass surface. Samples were exposed to white light for 24 hours after addition of 25 µl of a bacterial inoculum (n = 8).

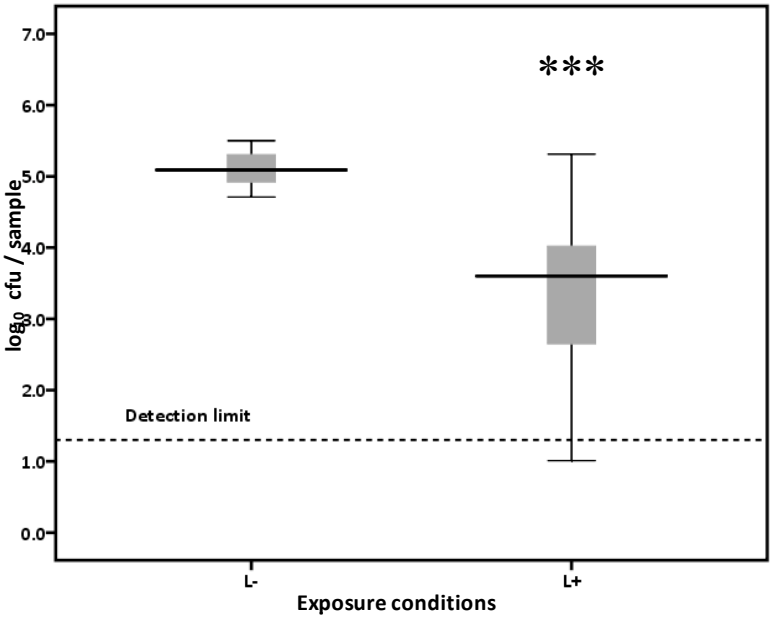

Figure 3.10 Effect of the white light source on the survival of EMRSA-15 on a glass surface. Samples were exposed to white light for 24 hours after addition of 25 µl of a bacterial inoculum (n = 12).

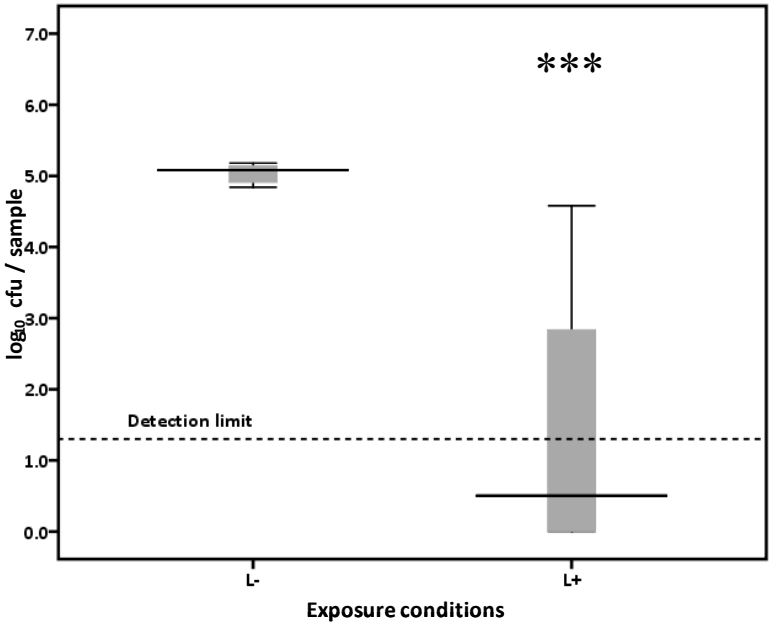

Figure 3.11 Effect of the white light source on the survival of MRSA 43300 on a glass surface. Samples were exposed to white light for 24 hours after addition of 25 µl of a bacterial inoculum (L-, n = 10 / L+, n = 12).

The effect of white light on the survival of *S. aureus* NCTC 8325-4 is shown in Figure 3.12. A 3.3 $\log_{10}$ cfu / sample reduction in bacterial count was observed compared with the control group which was not exposed to white light and this reduction was highly statistically significant. The survival of *S. aureus* NCTC 8325-4 also appeared to be affected by the experimental set up as a reduction in the recovery of bacteria from the control group was seen, which was also statistically significant at the 0.1% level. *S. aureus* NCTC 8325-4 appeared to be slightly more tolerant to the effects of the white light compared with *S. aureus* NCTC 6571 (Figure 3.5).

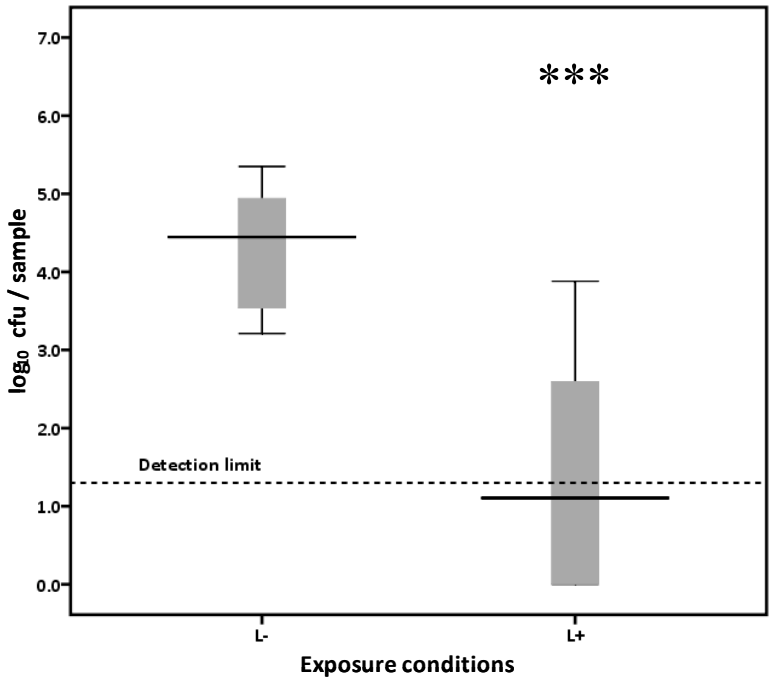

Figure 3.12 Effect of the white light source on the survival of ***S. aureus*** NCTC 8325-4 on a glass surface. Samples were exposed to white light for 24 hours after addition of 25 µl of a bacterial inoculum (n = 8).

Table 3.4 Summary of results from the series of experiments examining the effect of white light on bacterial survival. Data are expressed as median values.

Bacterial strain	Reduction in bacterial recovery (log_{10} cfu / sample)
S. aureus NCTC 6571	5.6
E. coli ATCC 25922	0.2
E. faecalis	0.1
S. pyogenes ATCC 12202	1.3
EMRSA-16	0.9
EMRSA-15	1.5
MRSA 43300	4.6
S. aureus NCTC 8325-4	3.3

3.4 Discussion

3.4.1 Optimisation of the sampling technique

Accurate assessment of the activity of the light activated coatings is dependent upon a reliable and reproducible method of detecting bacteria found on the surface of the coatings both before and after light exposure (Verran et al., 2010a). Therefore, the sampling technique used previously in this laboratory was examined to determine whether it could be further improved. Different techniques were used to measure the level of microbial contamination on uncoated surfaces. Swabs are the most commonly used technique for measuring surface contamination but it has been well reported that the rate of bacterial recovery using this method is poor (Davidson et al., 1999; Moore and Griffith, 2007). Cotton-tipped swabs are often used because they absorb a large volume of the bacterial suspension on the surface, so the surface appears dry after sampling. However, bacteria become entangled within the meshwork of the

cellulose fibres of the swab head, and are not readily released during vortexing, resulting in a low count during enumeration (Favero et al., 1968). Viscose is a derivative of cotton so would be likely to absorb liquid to the same degree. Alginate swabs have been reported to improve the recovery of bacteria from surfaces (Page et al., 2007), but these data show that this improvement was not substantial and that the bacterial recovery was comparable to the other swab head materials. Swab heads comprised of man-made fibres such as nylon do not retain liquid to the same degree and so any organisms taken up by the swab are readily released. However, fewer bacteria are taken up by the initial sampling event, so a similarly low count is generated (Davidson et al., 1999). Detergent based sampling solutions have been used to increase sampling efficiency and could have been used instead of PBS in these studies to improve bacterial recovery (Salo and Wirtanen, 1999).

Other factors to consider when interpreting data generated from viable counts are that each colony forming unit counted on a plate does not necessarily correspond to one bacterial cell, as a clump of numerous cells will form one colony, as will one bacterial cell. Light exposure causes bacterial stress, which in turn causes bacterial clumping and a concomitant reduction in the number of organisms recovered. Furthermore, both the swabbing and vortexing processes, used to remove adherent organisms from the surface and swab head respectively, can damage the integrity of the bacterial cell wall, which would also result in a smaller number of viable cells and a lower viable count (Obee et al., 2007). To detect the presence of residual microorganisms remaining on the surface, post-sampling microscopic examination

could be employed and any remaining bacteria could be stained with a differential viability stain (Verran, 2010; Verran et al., 2010a).

3.4.2 ATP bioluminescence

Sampling a surface with a swab can give a good indication of the presence of bacteria, but does not provide an exact concentration of the bacteria present on the surface (Moore and Griffith, 2007; Verran et al., 2010a). Luminometers are used frequently in the food industry (Davidson et al., 1999; Storgards et al., 1999) and increasingly in the healthcare profession (Griffith et al., 2000; Dancer, 2004; Lewis et al., 2008) to detect the presence of microbial contamination and organic soil. Four different luminometers were tested as alternative sampling methods to swabbing and performing viable counts.

Previous studies have shown that it is not possible to detect low numbers of bacteria from a test surface using ATP bioluminescence (Salo et al., 1999), specifically $<10^3$ cfu / cm^2 (Davidson et al., 1999; Moore et al., 2001; Moore and Griffith, 2002). Improved, more sensitive luminometers, such as the Lumat and the Junior, were used in this chapter, in addition to an improved detection reagent that eliminated non-microbial ATP and claimed to be able to detect as few as five bacterial cells (BioThema AB, 2006), so an increased sensitivity was expected.

However, this study supports previous findings and has demonstrated that ATP bioluminescence was not suitable for accurately detecting the number of bacteria on a test surface over a range of concentrations (Aiken et al., 2011). The methodology utilising the BioProbe was able to detect higher concentrations of both *E. coli* or *S.*

aureus, but no one method was able to reproducibly detect both organisms at all bacterial concentrations. At lower concentrations of bacteria, the BioProbe-based assay either did not detect the presence of bacteria, or made no distinction between the suspensions containing $2.5x10^3$ / cm^2 and $2.5x10^2$ / cm^2. The BioProbe methodology was likely to have produced the best results because the instrument was specifically designed for detecting bacteria directly from a flat surface. However, the BioProbe is no longer commercially available, so the use of this instrument was unsuitable for future studies. The methods employing the Junior, Clean-Trace and Lumat luminometers and indeed viable counts all incorporate a swabbing step. For the organisms to be detected by these methods they therefore needed to be both captured by the swab from the test surface and released from the swab head into the diluent prior to quantification (Moore and Griffith, 2002), which limits the recovery of bacteria from the surface.

The Lumat luminometer was statistically the most sensitive model tested (p <0.01 at $2.5x10^2$ / cm^2 for both *E. coli* and *S. aureus*) and produced consistent data at every dilution tested. However, the estimate, although reproducible, was not always accurate and was up to ten fold lower than both the known concentration of bacteria inoculated onto the test surface and the estimates made using alternative luminometers. This was disappointing as under optimum conditions, the instrument is able to detect 1 amol ATP, which corresponds to less than one bacterial cell (BioThema AB, 2006; Berthold Technologies GmbH & Co. KG, 2007). The instrument is designed for experiments such as gene reporter assays and luminescent immunoassays (Dyer et

al., 2000; McKeating et al., 2004) and this work suggests that the published sensitivity cannot be transferred to the quantification of bacteria from surfaces.

In the present laboratory study, a correlation between colony forming units and RLU was made but it has previously been difficult to demonstrate a high, direct correlation between these parameters outside of laboratory conditions because ATP bioluminescence detects all ATP present on the sampled surface, including organic material of bacterial origin, food residues, human secretions and dirt (Poulis et al., 1993). Generally, of the total ATP isolated from a hand touch surface, 33% is microbial in origin, therefore, it is likely that the RLU values obtained will be higher than that expected if only microbial ATP was detected (Griffith et al., 2000). However, a number of groups have demonstrated a correlation between these parameters.

Selan et al., (1992) used ATP bioluminescence to detect urinary pathogens from either bacterial culture or patient samples and employed the NRB / Lumit PM kit. At high bacterial concentrations (>10^5 cfu / ml), a correlation between cfu / ml and RLU was observed, where 10^5 cfu / ml *E. coli* corresponded to 10 – 500 RLU and 10^9 cfu / ml *E. coli* corresponded to an RLU of around 87,000. A statistically significant but low correlation between cfu / ml and RLU values was demonstrated when the 3M Clean-Trace ATP system was used to monitor the effectiveness of cleaning in a hospital (Boyce et al., 2009). Other groups have demonstrated a weak correlation between the ATP score and microbial growth when different ATP systems were used to assess the cleanliness of hospital wards (Aycicek et al., 2006; Mulvey et al., 2011). In a separate cleaning study, sites which were considered unsatisfactory by ATP bioluminescence were also shown to be unsatisfactory by microbiological swabbing (Willis et al., 2007).

Articles in the literature have questioned the value in correlating the aerobic colony count and ATP bioluminescence RLU values because they measure different parameters; the former measures the number of viable microorganisms and the latter measures the residual organic soil, which could be of microbial or non-microbial origin (Lewis et al., 2008). In this chapter, a relationship between the viable count and ATP bioluminescence readings was sought and this was valid because the test surfaces were decontaminated before use so it was assumed that no residual ATP remained. Additionally, the reagent kit that was used contained an initial step which eliminated non-microbial ATP which further increases the likelihood that any ATP detected on the surfaces was of bacterial origin and not from another exogenous source. However, this question is perhaps invalid within the context of assessing the cleanliness of a hospital environment.

An important limitation of ATP bioluminescence is that no information about the bacterial species is given (Hawronskyj and Holah, 1997). Within a hospital environment it would be advantageous to differentiate between bacterial species, for example the presence of MRSA on a patient's bed-rail would be of much greater interest clinically than the presence of coagulase-negative staphylococci on the same surface. Molecular techniques such as the polymerase chain reaction (PCR) or culture-based methods would be required to speciate the bacteria present.

3.4.3 The effect of white light on bacterial survival

Finally, the effect of white light on the viability of a range of microorganisms was investigated to ensure that any reduction in bacterial counts observed on the novel

light activated thin films to be tested was attributed directly to the intrinsic activity of the coatings and not due to the light exposure itself. When *E. coli* and *E. faecalis* were inoculated onto uncoated glass surfaces and then exposed to white light, an insubstantial reduction in cell number was observed. A reduction in the recovery of *E. coli* has previously been observed after irradiation with 458 and 488 nm light (Vermeulen et al., 2008), although a zenon arc lamp was used which generates light of a much greater intensity. Interestingly, this was not the case with *S. aureus* NCTC 6571. An average reduction of 5.6 $\log_{10}$ cfu / sample was observed on an uncoated glass surface. This effect was also seen to a lesser extent in a different strain of *S. aureus,* ATCC 8325-4 and an average reduction of 3.3 $\log_{10}$ cfu / sample was observed. *S. aureus* NCTC 6571 has previously been shown to be unaffected by 6 hours exposure to the same white light source (Decraene et al., 2006, 2008b), implying that the killing occurs after a prolonged irradiation time. Indeed, Maclean et al (2009) demonstrated that longer exposure times were required for photoinactivation of certain bacterial species, such as *E. coli* and *E. faecalis*. This group and others have used light with a wavelength of between 400 – 420 nm to photoinactivate a range of bacterial species (Guffey and Wilborn, 2006; Maclean et al., 2008, 2009; 2010).

The mechanism of action is proposed to be due to photo-excitation of endogenous intracellular porphyrins, resulting in the generation of cytotoxic singlet oxygen species (Hamblin and Hasan, 2004; Lipovsky et al., 2009). It is proposed that the observed reductions in bacterial viability described in these studies are likely to be caused by the same mechanism but this has not been investigated further. The variation in bacterial counts observed in some of the experiments could also be due to differences in the

intracellular concentration of porphyrins, but the reason for this variation is unclear (Hamblin et al., 2005).

Interestingly, the epidemic strains of MRSA did not show the same level of sensitivity to the effect of the white light source. EMRSA-16 appears to show an increased tolerance to the inhibitory effect of the white light source compared to other tested *S. aureus* strains, as a 0.9 $\log_{10}$ cfu / sample decrease in the recovery of EMRSA-16 was seen after 24 hours exposure to the white light, compared with a 1.5 $\log_{10}$ cfu / sample decrease when EMRSA-15 was used and much greater reductions for meticillin-sensitive strains. Variations in the sensitivity of *S. aureus* to the effects of white light has been described previously and was proposed that the differences in susceptibility were due to increased production of porphryns, increased generation of reactive oxygen species, and decreased production of carotenoids in the light-sensitive strains (Lipovsky et al., 2009). A mutation could be present in epidemic strains, which confers increased tolerance to white light by overproduction of the carotenoids, antioxidants or decreased production of porphyrins. Amplification of the genes flanking either the *S. aureus*-specific porphyrin coproporphyrin or golden pigment carotenoid, and sequencing of the PCR product could confirm this hypothesis.

The observed decreased susceptibility to white light could contribute towards the persistence of epidemic strains such as EMRSA-16 in the hospital environment. Therefore, when choosing an epidemic MRSA strain to use for assessment of the light-activated antimicrobial coatings, it would be logical to select the strain that is less light sensitive and these studies show this to be EMRSA-16.

3.5 Conclusions

Sampling the test surfaces by swabbing and subsequently performing viable counts has been shown to provide an adequate estimate of concentration of bacteria on a test surface. Data generated in this chapter suggest that a method incorporating the use of ATP bioluminescence for testing novel antimicrobial coatings would not be appropriate. The superiority of the viable count technique was especially apparent at low bacterial concentrations, when the ATP bioluminescence based techniques were unable to consistently confirm the presence of small numbers of bacteria. Two meticillin-sensitive strains of *S. aureus* were shown to be susceptible to photoinactivation by white light alone, whereas the meticillin-resistant strains of *S. aureus* tested showed increased tolerance, indicating a possible virulence factor found in EMRSA-16. *E. coli* and *E. faecalis* also displayed tolerance to the inhibitory effects of the white light source, so *E. coli* will be initially used to assess the antibacterial activity of the light-activated coatings.

4 Assessment of novel APCVD-synthesised light-activated antibacterial materials for use in the hospital environment

4.1 Introduction

Presented in this chapter are the findings from a series of novel antimicrobial coatings that were activated by either visible or ultraviolet light. The films were generated using a process called APCVD (Section 1.5.1) where dopants were added during the synthesis of the TiO_2 thin films in order to alter the photochemical properties. TiO_2 is a well-described photocatalyst, both as a powder and when immobilised within thin films (Matsunaga et al., 1985) and is normally activated by ultraviolet (UV) light. The aim of the current work was to shift the band width of novel TiO_2 films so that light of a lower frequency was able to initiate photocatalysis (Section 1.3.3). *E. coli* was used as the test organism for the initial screening as it has been demonstrated that it is not affected by the white light used for activation, unlike some of the staphylococcal species tested (Section 3.3.3) which have previously been shown to have an increased resistance to the activity of photocatalysis (Decraene et al., 2006; Page et al., 2007). Pure TiO_2 thin films were also tested to demonstrate the difference between the doped and un-doped materials. The antibacterial activity of the materials was assessed using a swab-based methodology and not an ATP bioluminescence based technique, as viable counts produced the most reproducible results in Chapter 3; the presence of *E. coli* was always reported even at low concentrations.

4.2 Materials and methods

4.2.1 Synthesis of the thin films

The titanium (IV) oxynitride films ($Ti_{2.85}O_4N$) (TiON-1) were produced by APCVD using ammonia as the nitrogen source, as described in Section 2.10.1.1. A nitrogen-doped thin film (TiON-2) was also synthesised using ammonia as the nitrogen source as described in Section 2.10.1.1. The nitrogen-doped TiO_2 films N1, N2 and N3 were produced by APCVD using t-butylamine as the nitrogen source as described in Section 2.10.1.2 and were cut from different areas of a single sheet of coated glass. The sulfur containing thin films S1, S2 and S3 were prepared with carbon disulfide as the sulfur source and titanium tetrachloride ($TiCl_4$) as the titanium source, as described in Section 2.10.1.3. TiO_2 thin films were prepared as controls as described in Section 2.10.1.4.

The conditions chosen for all experiments allowed for the rapid deposition of a thin film, which remained defect- and pinhole-free by eye. The films were all well adhered to the substrate and resistant to abrasion. The thin films were characterised and the functional activity assessed as described previously (Dunnill et al., 2009a; 2009b; Aiken et al., 2010).

4.2.2 Measuring the antibacterial effect of the thin films

Bacterial strains were maintained as described in Section 2.1 and bacterial suspensions of *E. coli* ATCC 25922 were prepared as detailed in Section 2.3, resulting in a starting inoculum of approximately 10^7 cfu / ml, equating to approximately 2.5 x 10^5 cfu / sample. The effect of the photocatalytic thin films on the viability of bacterial strains was determined using the swab-based methodology described in Section 2.12.2 and

Figure 2.2. Samples were denoted C for the nitrogen or sulfur-containing samples, T for the TiO_2 thin films and G for the uncoated glass. The Mann Whitney test was used to determine the statistical significance of any differences observed, as described in Section 2.13.

4.2.3 Assessment of the decontamination regimen

Prior to microbiological assessment, the thin films were decontaminated, as described in Section 2.12.1. The decontamination procedure was later amended and stored in the dark to deactivate, and used only after a period of 72 hours.

4.2.4 Effect of the covering material on thin film activity

To prevent dehydration of the bacterial inocula, the effect of the materials used to cover the moisture chamber was investigated. The thin films were incubated under the white light for 24 hours with a range of coverings, which still allowed light penetration onto the bacterial suspension inoculated onto the thin film. The following covers were used: (i) glass cover slips; (ii) quartz cover slips; (iii) the petri dish lid (iv) clingfilm. A UV-visible light trace was also generated to measure the transmission of light through the petri dish lid and the clingfilm. The intensity of light generated by the lamp was quantified using a light meter (LX101 Lux meter, Lutron Electronic Enterprise Co. Ltd, Taiwan).

4.3 Results

4.3.1 Photocatalytic activity of titanium dioxide thin films

The activity of the TiO_2 films was initially examined to check whether any photocatalytic activity was observed using white light as the source of incident light. TiO_2 thin films prepared in-house were assessed alongside commercially produced thin films. When the TiO_2 thin films were assessed for photocatalytic antibacterial activity against *E. coli* (Figure 4.1), no statistical difference in bacterial recovery was observed from the thin films after a 24 hour exposure period compared with the bacterial recovery from the glass slides (p >0.05); therefore these TiO_2 thin films were used as controls for the remaining experiments, where necessary.

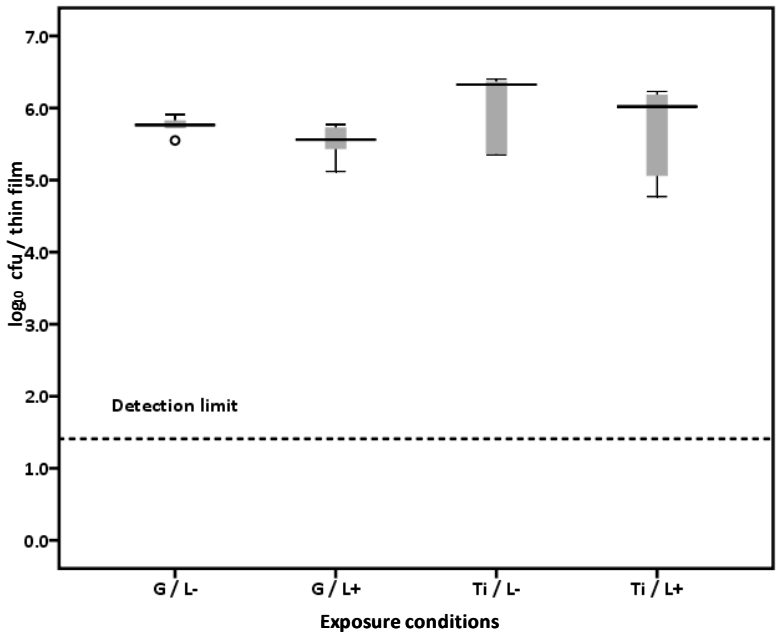

Figure 4.1 Activity of the TiO_2 thin films prepared in-house. An aliquot of *E. coli* was added to the thin films before exposure to the white light source for 24 hours (L+). Alternatively, thin films were incubated in the dark throughout (L-). Uncoated glass sides and TiO_2 thin films are denoted by G and Ti, respectively. The thick horizontal lines indicate median values, the base and top of each box represents the 25% and 75% quartiles respectively, and the error bars, the 10% and 90% percentiles and the small circles are outliers. The dotted horizontal line indicates the detection limit of the sampling method, 1.4 log_{10} cfu / sample.

The commercially produced TiO_2 thin film Pilkington Activ^{TM} was also assessed for any photocatalytic activity using the white light source and a 0.3 log_{10} cfu / sample reduction in the recovery of *E. coli* was observed compared with the thin film incubated in the absence of light (Figure 4.2). This small decrease was statistically significant ($p < 0.001$) which is likely to be due to the small level of variance in the viable count recovered from the thin films in the control group, rather than to a difference from the number of bacterial colonies observed in the test group and such small differences would not be considered microbiologically different.

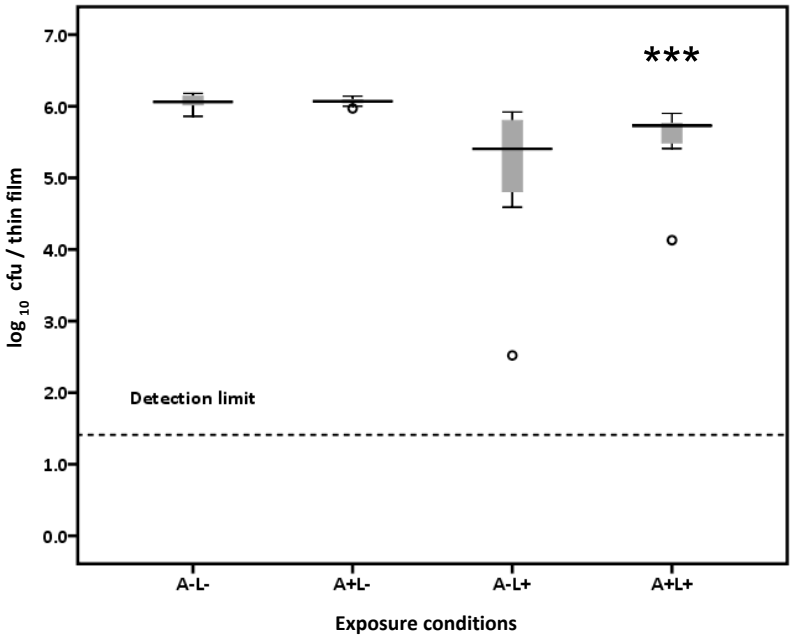

Figure 4.2 Effect of the commercially produced TiO_2 thin film Pilkington Activ^{TM} on the survival of *E. coli.* Thin films were exposed to white light for 24 hours (A+), the bacterial droplet was added then the sample was exposed a second light exposure period of 24 hours (L+). Alternatively, thin films were exposed to just the latter light dose (A-L+), the first light dose only (A+L-) or incubated in the dark throughout (A-L-). The asterisk denotes statistical significance compared with an uncoated control incubated under the same lighting conditions, as described in Section 2.13.

4.3.2 Photocatalytic antibacterial activity of nitrogen-containing titanium dioxide thin films TiON-1 and TiON-2

4.3.2.1 Photocatalytic activity after exposure to ultraviolet light

The activity of the nitrogen-doped thin films TiON-2 were assessed initially using two UV lamps (254 nm, 365 nm) as the light sources. When the thin film TiON-2 was pre-exposed to 1 hour of 254 nm light, inoculated with *E. coli* and then subjected to 4 hours of 365 nm light, (C A+L+), a 1.4 $\log_{10}$ cfu / sample (95.5%) reduction in bacteria was observed, compared with the uncoated control exposed to the same light conditions (G A+L+). This difference is statistically significant ($p < 0.01$) and is shown graphically, along with the bacterial counts for a number of the other conditions in Figure 4.3.

Exposing the uncoated slides to both light incubation steps (G A+L+) or just the latter light incubation step (G A-L+) resulted in a 0.5 $\log_{10}$ cfu / sample reduction of *E. coli* compared with the slides incubated in the absence of light (G A-L-); as this difference was statistically significant ($p < 0.01$) the G A+L+ slide was used as the negative control throughout.

The pre-inoculation, activation step did not substantially enhance the activity of the thin films when they were subsequently exposed to the 365 nm light. A similar decrease in bacterial recovery was observed whether the thin films were pre-activated (1.4 $\log_{10}$ cfu / sample reduction) or not (1.1 $\log_{10}$ cfu / sample reduction) and these values were not statistically different ($p >0.05$). There was no significant decrease in the number of bacteria recovered from thin films which were exposed to just the activation step (C A+L-) and no significant decrease in the number of recoverable *E. coli*

was observed from the thin films which were incubated in the absence of light throughout (C A-L-), in fact the bacterial recovery was greater from these thin films than from the negative control.

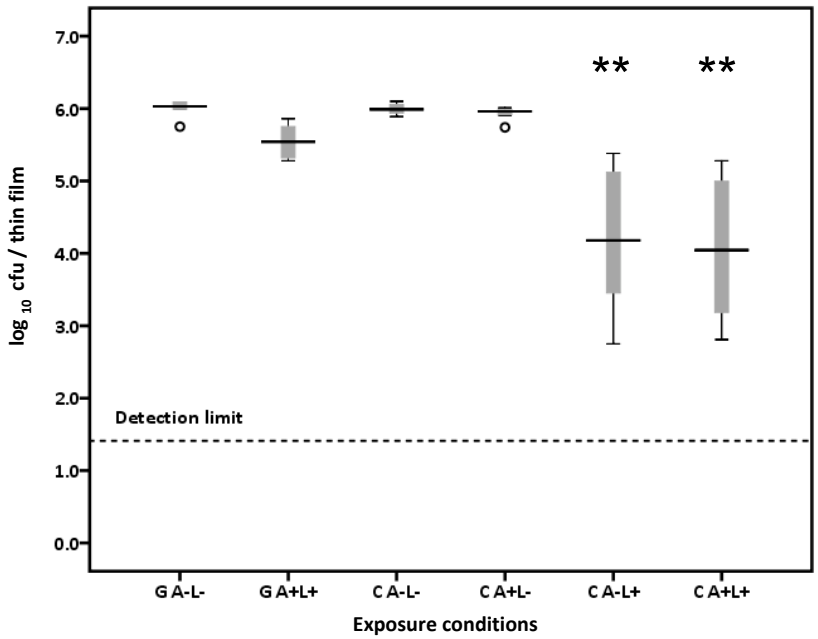

Figure 4.3 Concentration of *E. coli* remaining on the thin film TiON-2 after exposure to 1 hour 254 nm light and 4 hours 365 nm light (C A+L+) or just the latter light dose (C A-L+). Thin films were also exposed to the activation step only (C A+L-) or incubated in the dark throughout (C A-L-). Uncoated glass slides were exposed to both light conditions (G A+L+) or neither (G A-L-).

When the titanium (IV) oxynitride film TiON-1 was pre-exposed to 1 hour of 254 nm light, inoculated with *E. coli*, and then exposed to 4 hours of 365 nm light (C A+L+), a 4.1 $\log_{10}$ cfu / sample (99.99%) reduction in bacterial count was observed, compared with the uncoated control exposed to the same light conditions (G A+L+) (Figure 4.4). This difference was highly statistically significant ($p < 0.01$).

The pre-inoculation, activation step was found to enhance the activity of the thin films. The recovery of *E. coli* from the oxynitride thin films which were exposed to the 365 nm light for four hours without prior activation was not significantly different from the

recovery from the uncoated control slides (p >0.05). Similarly, no significant decrease in the number of bacteria recovered from the thin films was observed when they were just activated (C A+L-) or when the thin films were incubated in the absence of light (C A-L-).

In comparison, when the TiO_2 thin films were exposed to 365 nm light with a 254 nm activation step there was a 4.1 $\log_{10}$ cfu / sample reduction in bacterial count. It was conversely found that for the TiO_2 thin films the activation step was unnecessary and exposure to 365 nm light alone led to a 4.1 $\log_{10}$ cfu / sample reduction after four hours of light exposure (data not presented).

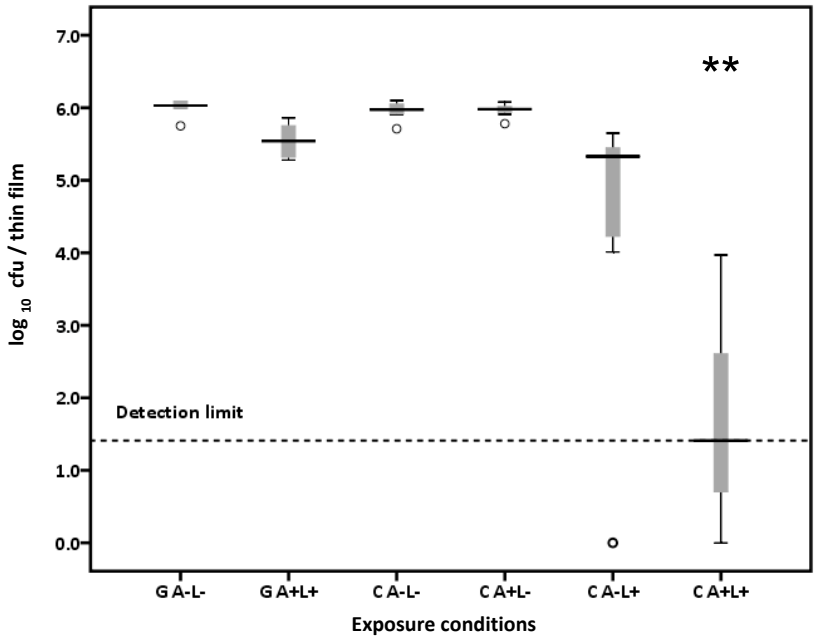

Figure 4.4 Concentration of *E. coli* remaining on the thin film TiON-1 after exposure to 1 hour 254 nm light and 4 hours 365 nm light (C A+L+) or just the latter light dose (C A-L+). Thin films were also exposed to the activation step only (C A+L-) or incubated in the dark throughout (C A-L-). Uncoated glass slides were exposed to both light conditions (G A+L+) or neither (G A-L-).

4.3.2.2 Photocatalytic activity after exposure to white light

The photoactivity of these thin films was subsequently assessed using visible light as the activating light source. As white light has a lower frequency than ultraviolet light, the samples had to be exposed to the white light for a longer time period. The thin films were exposed to the white light for 24 hours as an 'activating' step, then inoculated with *E. coli* and exposed to the white light for either 6, 18 or 24 hours. The thin film TiON-2 did not display any significant photoactivity after 6, 18 or 24 hours exposure to the white light (Figure 4.5). The greatest decrease in bacterial recovery was exhibited after 24 hours, where just a 0.5 $\log_{10}$ cfu / sample reduction was observed compared with the thin films incubated in the absence of light throughout the duration of the experiment (A-L-). However, the effect of the light source alone should be incorporated into this reduction to show that any reduction in bacterial recovery was due to the photoactivity of the thin films and not an artefact caused by the light source.

It was demonstrated in Section 3.3.3.1 and Figure 3.6 that 24 hours exposure to the white light resulted in a 0.2 $\log_{10}$ cfu / sample decrease in the recovery of *E. coli.* This figure was subtracted from the reductions seen in this section, and this value was used as the overall negative control (G A+L+). Therefore, the greatest decrease in bacterial recovery for the nitrogen-doped thin film was just 0.2 $\log_{10}$ cfu / sample after exposure to both 24 hour light incubation steps, which was not statistically significant.

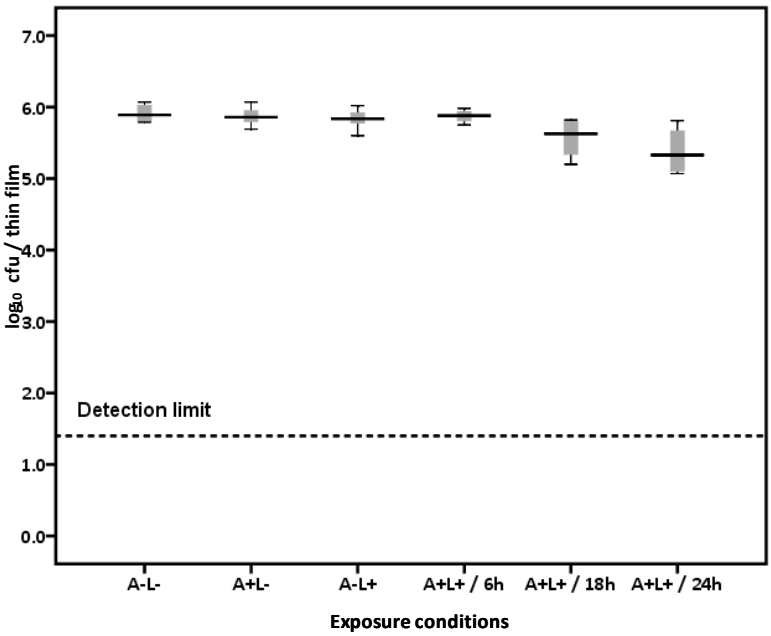

Figure 4.5 Effect of the thin film TiON-2 on the survival of *E. coli.* Thin films were exposed to white light for 24 hours (A+), the bacterial droplet was added then the sample was exposed a second light exposure period of either 6, 18 or 24 hours (L+). Alternatively, thin films were exposed to just the latter light dose (A-L+), the first light dose only (A+L-) or incubated in the dark throughout (A-L-).

When the titanium (IV) oxynitride film TiON-1 was exposed to the white light for either 6 or 18 hours there was no significant reduction in the recovery of *E. coli*. However, after 24 hours irradiation a reductive effect was seen and the average recovery of *E. coli* from the thin film (A+L+) was 0.6 $\log_{10}$ cfu / sample lower than the recovery from the uncoated glass slides exposed to the same light conditions (G A+L+) as displayed in Figure 4.6. This result was statistically significant ($p < 0.01$). However, the observed effect was not consistent, demonstrated by the variability of the A+L+ / 24h data shown in Figure 4.6. Even after five experimental repeats, a consistent result could not be achieved and reductions in the bacterial count ranged from 4.9 $\log_{10}$ cfu / sample to 0.5 $\log_{10}$ cfu / sample with an average reduction of just 0.6 $\log_{10}$ cfu / sample.

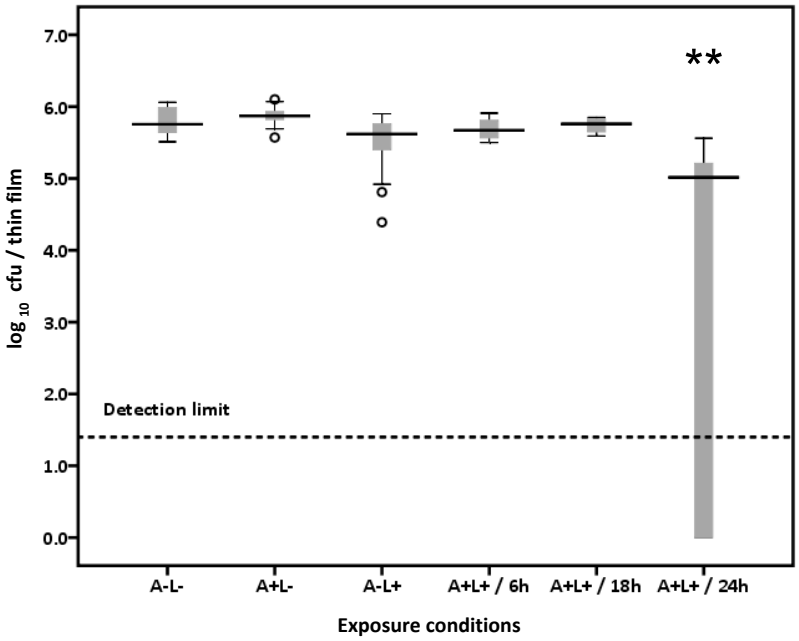

Figure 4.6 Effect of the thin film TiON-1 on the survival of *E. coli.* Thin films were exposed to white light for 24 hours (A+), the bacterial droplet was added then the sample was exposed a second light exposure period of either 6, 18 or 24 hours (L+). Alternatively, thin films were exposed to just the latter light dose (A-L+), the first light dose only (A+L-) or incubated in the dark throughout (A-L-).

The anti-*E. coli* effect of titanium (IV) oxynitride thin film TiON-1 was greater than the nitrogen-doped thin film TiON-2 under both lighting conditions, which demonstrates that the former thin film was a more effective photocatalyst under the test conditions.

4.3.3 Photocatalytic antibacterial activity of nitrogen-doped titanium dioxide thin films N1, N2 and N3

4.3.3.1 Photocatalytic activity after exposure to white light

The activity of a second set of novel nitrogen-containing thin films was assessed, using white light as the activating source of irradiation. The thin films were exposed to the white light for 24 hours, then inoculated with *E. coli* and re-exposed to the white light for 24 hours. The greatest reduction in bacterial recovery was seen when *E. coli* was

inoculated onto thin film N1 and a 2.8 $\log_{10}$ cfu / sample (99.9%) reduction was observed (Figure 4.7) compared with the thin films incubated in the absence of light throughout the duration of the experiment (A-L-). When the uncoated glass sample exposed to both light conditions was used as a control (G A+L+), the overall reduction in *E. coli* caused directly by the activity of the N-doped thin film N1 was approximately 2.5 $\log_{10}$ cfu / sample (99.7%), which was highly statistically significant ($p < 0.001$).

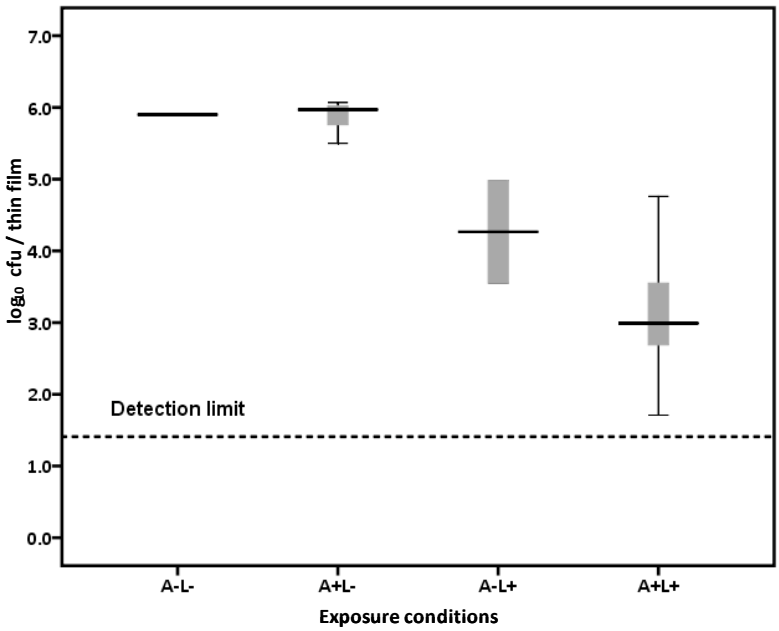

Figure 4.7 Effect of the thin film N1 on the survival of *E. coli.* Thin films were exposed to white light for 24 hours (A+), the bacterial droplet was added then the sample was exposed a second light exposure period of 24 hours (L+). Alternatively, thin films were exposed to just the latter light dose (A-L+), the first light dose only (A+L-) or incubated in the dark throughout (A-L-).

Exposing the thin films to just the second light condition (A-L+) resulted in a 0.9 $\log_{10}$ cfu / sample reduction in the recovery of *E. coli* ($p < 0.05$), compared with the uncoated control incubated under the same conditions (G A+L+). Exposing the thin films to the initial activating light dose only (A+L-) did not have a significant effect on

the recovery of *E. coli*, nor did exposure to the thin films in the absence of light, in fact a higher recovery of *E. coli* was observed in this control group. Hence, an additive effect was observed whereby exposure to either the second light dose or both light doses resulted in a significant reduction in bacterial recovery, with the greatest decrease observed after both light exposure periods.

When the thin film N2 was exposed to white light for both 24 hour periods, a 1.6 $\log_{10}$ cfu / sample reduction was observed (Figure 4.8), compared with the thin films incubated in the dark throughout. When the uncoated glass slide exposed to the same light conditions was used as the control, then the recovery of *E. coli* was reduced to 1.1 $\log_{10}$ cfu / sample. No statistical significant difference was seen between the test and control groups, as the data sets were small. No decrease in bacterial recovery was observed when the thin films were exposed to the white light for 24 hours without pre-activation (A-L+), when the thin films were just pre-activated (A+L-), or when the thin films were incubated in the absence of light (A-L-), compared with the uncoated control exposed to both light doses.

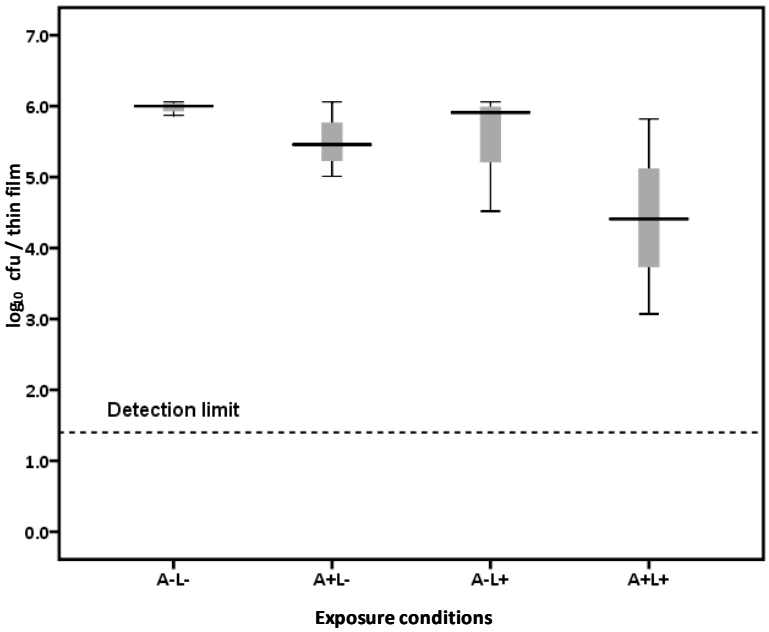

Figure 4.8 Effect of the thin film N2 on the survival of *E. coli.* Thin films were exposed to white light for 24 hours (A+), the bacterial droplet was added then the sample was exposed a second light exposure period of 24 hours (L+). Alternatively, thin films were exposed to just the latter light dose (A-L+), the first light dose only (A+L-) or incubated in the dark throughout (A-L-).

A large variation in the recovery of *E. coli* was observed from the set of thin films (N3) displayed in Figure 4.9. On average, the reduction in bacterial recovery from the pre-activated thin films incubated under white light for 24 hours was 0.9 $\log_{10}$ cfu / sample when compared with the thin films incubated in the dark throughout the duration of the experiment. The reduction drops to a 0.5 $\log_{10}$ cfu / sample reduction when compared with the uncoated control incubated exposed to both light doses. These reductions were not statistically different. The recovery of *E. coli* from these films ranged from 5.8 $\log_{10}$ cfu / sample to below the limit of detection, demonstrating the wide spectrum of activity that these thin films displayed under the experimental conditions. Whether the thin film N3 was exposed to just the second light dose whilst inoculated with *E. coli,* just the pre-activating white light dose or neither, there was no

significant reduction in bacterial recovery compared with the uncoated control exposed to both periods of light.

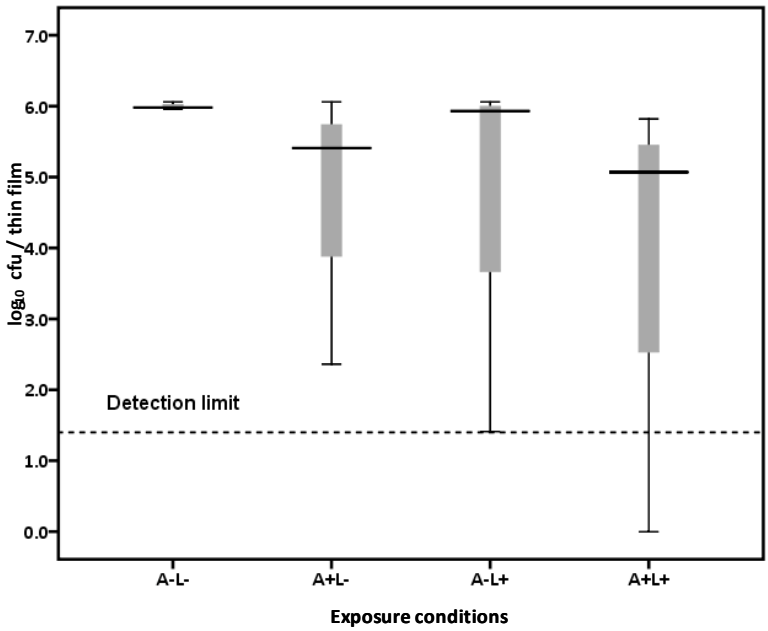

Figure 4.9 Effect of the thin film N3 on the survival of *E. coli.* Thin films were exposed to white light for 24 hours (A+), the bacterial droplet was added then the sample was exposed a second light exposure period of 24 hours (L+). Alternatively, thin films were exposed to just the latter light dose (A-L+), the first light dose only (A+L-) or incubated in the dark throughout (A-L-).

4.3.4 Effect of changing the decontamination regimen on thin film N1

The effect of the modified decontamination regime was evaluated by repeating the white light exposure experiments on the thin film designated N1. However, the thin films could not be reproduced to the same specifications and had therefore already been exposed to the original decontamination regime before the new method was used. The activity of the thin film was maintained for the first four replicates when the new decontamination regimen was used (Figure 4.10a); a statistically significant reduction in bacterial recovery was observed ($p < 0.01$) and the new regime was thought to be successful. However, the photocatalytic activity of the thin films was

then lost when the experiment was repeated on a subsequent three occasions (Figure 4.10b) and no statistically significant reduction in the recovery of *E. coli* was observed. When the thin films were stained using the Live/Dead differential stain, a fluorescent green smear was seen on surface of the films but no viable or non-viable bacterial cells were present.

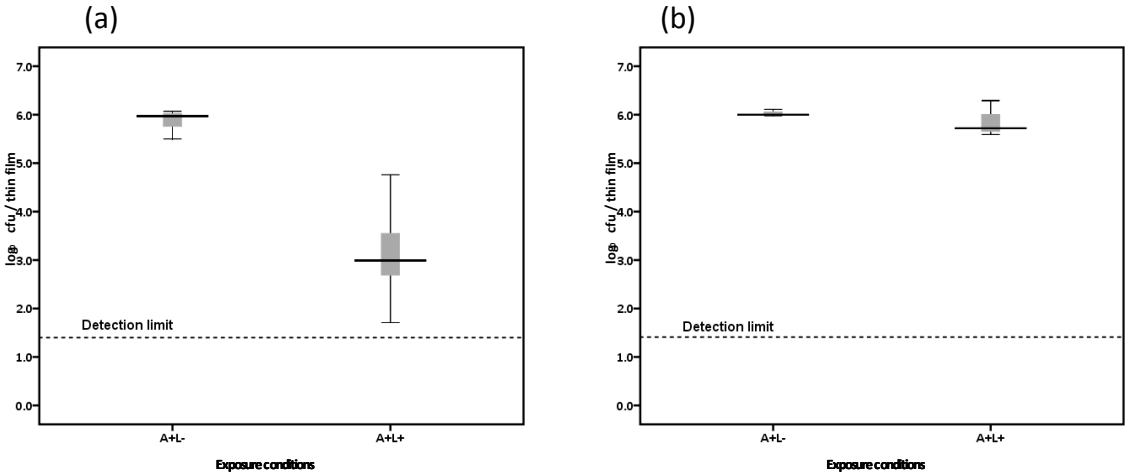

Figure 4.10 Light-activated antimicrobial killing of *E. coli* on thin film N1 (a) and after inactivation (b). The thin film was exposed to first light dose (A+), the bacterial droplet was added, and then the thin film was exposed to second light dose (L+). Alternatively, thin films were exposed to just the latter light dose (A-L+), the first light dose only (A+L-) or incubated in the dark throughout (A-L-).

4.3.5 Effect of covering material on thin film activity

The effect of the material used to cover the moisture chamber was investigated with regard to bacterial viability. Glass or quartz cover slips were used to cover the bacterial inoculum during exposure to the white light source but after 24 hours incubation the droplets had evaporated, it was not possible to culture the organisms onto solid agar using the viable count technique and the cells had become non-viable. This was confirmed by visualisation using the Live/Dead stain (data not included), which showed 100% of cells were dead. A bath of water was placed at the base of the incubator to

saturate the environment with moisture to prevent evaporation, but the bacterial inoculum had once again dried out after the 24 hour incubation period.

When the moisture chamber was covered with a plastic petri dish lid or clingfilm, the bacterial droplets did not dry out; therefore the effectiveness of these coverings was assessed. *E. coli* inoculated onto thin film TiON-2 showed a greater susceptibility to killing by UV light when the moisture chamber was covered with clingfilm (Figure 4.11) compared to when it was covered with the petri dish lid (Figure 4.3). A 4.9 $\log_{10}$ cfu / sample reduction in viable organisms was seen with the clingfilm covering, compared with a 1.4 $\log_{10}$ cfu / sample reduction when the plastic petri dish cover was used.

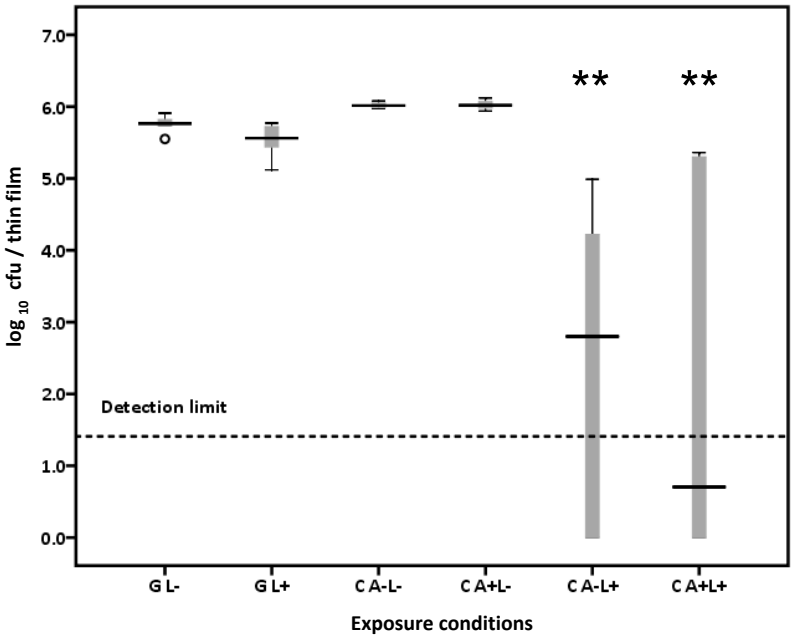

Figure 4.11 Concentration of *E. coli* remaining on the thin film TiON-1 using a clingfilm covering. The thin films were exposed to 1 hour 254 nm light and 4 hours 365 nm light (C A+L+) or just the latter light dose (C A-L+). Thin films were also exposed to the activation step only (C A+L-) or incubated in the dark throughout (C A-L-). Uncoated glass slides were exposed to both light conditions (G A+L+) or neither (G A-L-).

A UV-visible light transmission trace was produced to highlight any differences in the transmission of light through, and the reflectance from the two covering materials. The UV-visible light transmission trace (Figure 4.12) showed that around 90% of light from the visible portion of spectrum (with a wavelength between 400 and 700 nm) penetrated through both the petri dish and the clingfilm coverings. Less than 2% of light with a wavelength below 280 nm was able to penetrate through the petri dish lid. However, more than 80% of light of this wavelength could penetrate through the clingfilm covering. This finding indicates that this covering would not be suitable for the series of experiments evaluating the effect of the light activated antimicrobial coatings, as bacteria are inactivated by light of this wavelength and below (Saito et al., 1992). The greater reduction in bacterial recovery shown when the clingfilm was used to cover the moisture chamber suggests that wavelengths of light with a higher frequency were able to pass through the clingfilm resulting in the greater susceptibility of *E. coli* observed when inoculated onto the thin film TiON-2, which suggests there could be some leakage of sub-365nm UV light from the light source that caused the observed increase in photoactivity. Therefore, the petri dish lid was used to cover the moisture chamber in all light-activation experiments.

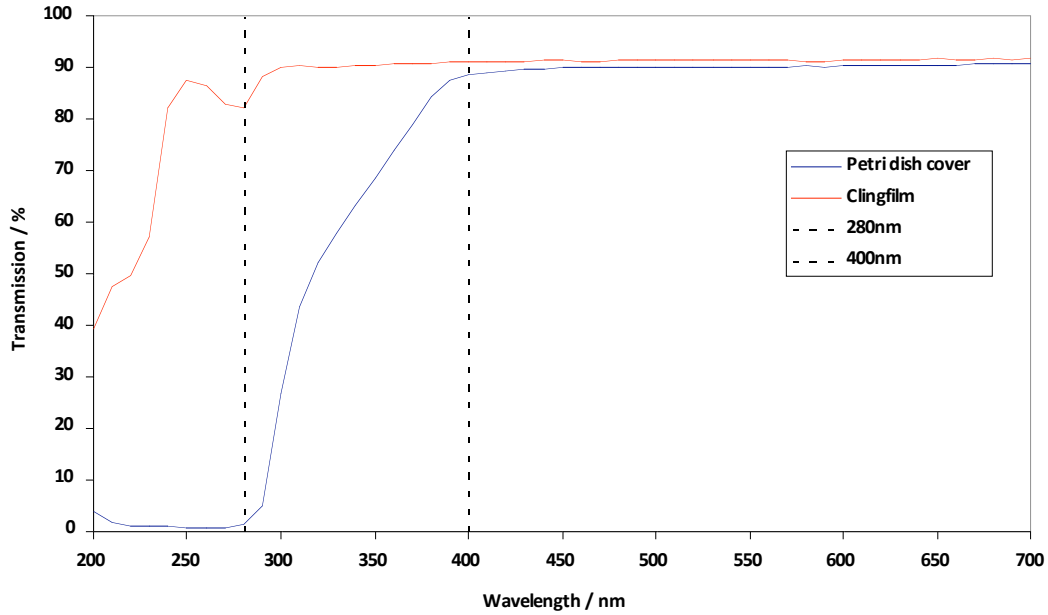

Figure 4.12 UV-visible light transmission trace of the petri dish lid and the clingfilm covers. The wavelengths 280 nm and 400 nm are indicated by vertical dotted lines.

4.3.6 Photocatalytic antibacterial activity of sulfur-based titanium dioxide thin films

The photocatalytic activity of a series of novel sulfur-doped thin films was assessed. The thin films were exposed to white light for 72 hours before a suspension of *E. coli* was added. The thin films were then re-incubated under the white light for a further 24 hours before sampling. The photocatalytic activity of thin film S2 is shown in Figure 4.13 where a significant decrease in bacterial recovery was observed ($p < 0.01$). A 2.5 $\log_{10}$ cfu / sample decrease was observed compared with the sulfur-doped thin film incubated in the dark throughout the duration of the experiment. The overall decrease in bacterial recovery when compared to a TiO_2 thin film exposed to the same light conditions was 2.2 $\log_{10}$ cfu / sample, which remains statistically significant ($p = 0.01$).

A large variation in bacterial recovery was observed when the thin film S2 was exposed to the white light for 24 hours without prior activation, ranging from 6.2 log_{10} cfu / sample to below the limit of detection, with an average recovery of 4.1 log_{10} cfu / sample, indicating that the activation step did not have a significant effect on the photoactivity of the S-doped thin film. No statistically significant decrease in the recovery of *E. coli* was observed under these conditions, when the thin film was exposed to the activating light dose alone or when incubated in the absence of light entirely.

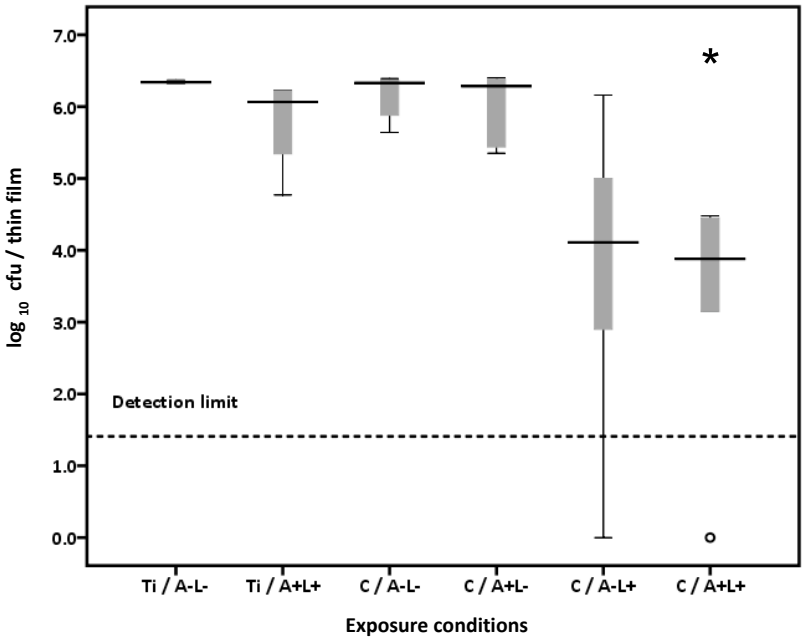

Figure 4.13 Effect of the thin film S2 on the survival of *E. coli.* Thin films were exposed to white light for 72 hours (A+), the bacterial droplet was added then the sample was exposed a second light exposure period of 24 hours (L+). Alternatively, thin films were exposed to just the latter light dose (A-L+), the first light dose only (A+L-) or incubated in the dark throughout (A-L-). TiO_2 controls were exposed to either both light doses (Ti / A+L+) or neither (Ti / A-L-).

The thin films S1 and S3 were less effective at reducing the *E. coli* bacterial load after exposure to the white light. There was no significant decrease in the recovery of *E. coli* from the surface of pre-activated thin film S1 after the 24 hour exposure period (Figure

4.14), compared with either the TiO_2 control exposed to the same lighting conditions or the sulfur-doped thin film incubated in the absence of light. Similarly, the pre-activated thin film S3 did not produce a significant reductive effect in the recovery of *E. coli* from the surface of the thin films after the 24 hour exposure period, when compared with either the TiO_2 control exposed to both light doses or the sulfur-doped thin film not exposed to white light (Figure 4.15). However, an inconsistent effect was seen on the S3 thin films which were not pre-exposed to the white light for 72 hours but incubated under the white light for 24 hours after addition of the bacterial suspension. This result was not reproducible, demonstrated in the box and whisker plot by the large size of both the box and error bars. A 0.9 $\log_{10}$ cfu / sample reduction was seen compared with the thin film incubated in the absence of light ($p < 0.05$). However, the median reduction was lower when compared with the TiO_2 thin film (0.6 $\log_{10}$ cfu / sample) or the uncoated glass control (0.1 $\log_{10}$ cfu / sample), and these reductions were not statistically significant.

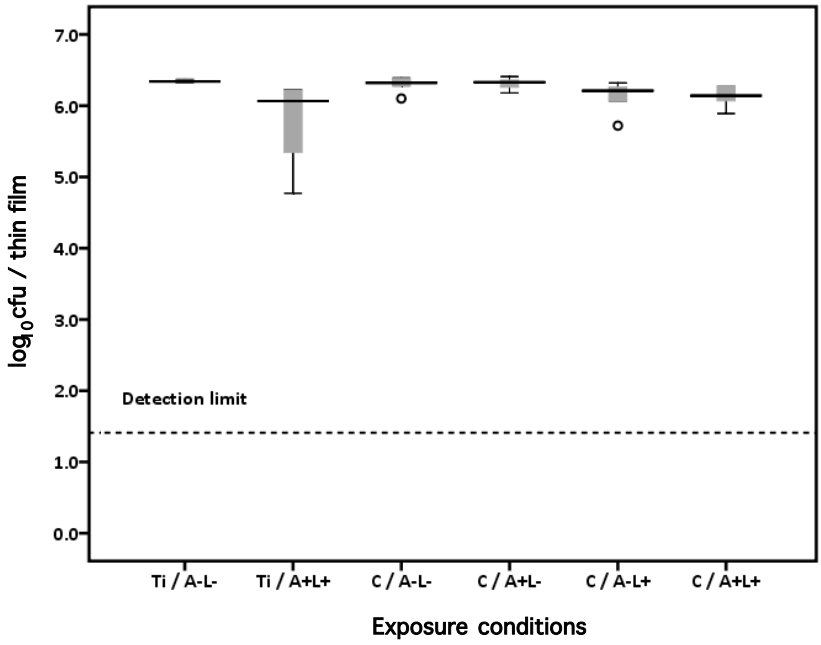

Figure 4.14 Effect of the thin film S1 on the survival of *E. coli.* Thin films were exposed to white light for 72 hours (A+), the bacterial droplet was added then the sample was exposed a second light exposure period of 24 hours (L+). Alternatively, thin films were exposed to just the latter light dose (A-L+), the first light dose only (A+L-) or incubated in the dark throughout (A-L-). TiO_2 controls were exposed to either both light doses (Ti / A+L+) or neither (Ti / A-L-).

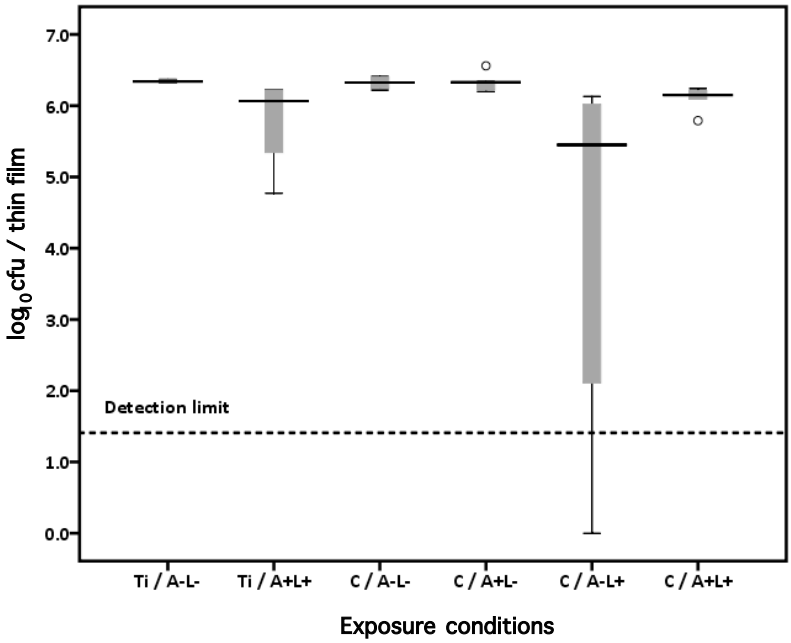

Figure 4.15 Effect of the thin film S3 on the survival of *E. coli.* Thin films were exposed to white light for 72 hours (A+), the bacterial droplet was added then the sample was exposed a second light exposure period of 24 hours (L+). Alternatively, thin films were exposed to just the latter light dose (A-L+), the first light dose only (A+L-) or incubated in the dark throughout (A-L-). TiO_2 controls were exposed to either both light doses (Ti / A+L+) or neither (Ti / A-L-).

Table 4.1 Summary of the photocatalytic activity of the nitrogen and sulfur doped thin films assessed in this chapter. Thin films were exposed to white light for 24 or 72 hours, for N-doped and S-doped samples, respectively. The bacterial droplet was added before the sample was exposed a second white light exposure period of 24 hours. Bacterial counts obtained were compared with uncoated glass slides exposed to the same lighting conditions.

Sample name	White light-induced photocatalytic activity / log_{10} cfu per sample	Statistical significance
TiON1	0.6	p <0.01
TiON-2	0.2	Nil (p >0.05)
N1	2.5	p <0.001
N2	1.1	Nil (p >0.05)
N3	0.5	Nil (p >0.05)
S1	No decrease	Nil (p >0.05)
S2	1.7	p >0.001
S3	No decrease	Nil (p >0.05)

4.4 Discussion

4.4.1 UV light-induced photocatalytic activity

The data presented in this chapter has demonstrated the antibacterial photoactivity of a number of novel doped TiO_2 thin films, generated by APCVD. The thin films that were initially assessed were doped with nitrogen and exposed to UV light in order to demonstrate equivalence with pure titania. The titanium (IV) oxynitride thin film TiON-1 demonstrated greater photoactivity than the N-doped thin film TiON-2, and a 4.1 log_{10} cfu / sample reduction was achieved on the pre-activated titanium (IV) oxynitride sample after just 4 hours exposure to the light source. These results also show that the

titanium (IV) oxynitride thin films demonstrated no anti-bacterial activity without UV exposure after the inoculation of the bacterial suspension; therefore the mode of action is unlikely to be related to the diffusion of ions onto the surface and is genuinely photo-activated.

4.4.2 White light-induced photocatalytic activity

The photocatalytic activity of the thin films was then assessed using white light as the activating light source. White light was used as an activating source light source as UV light is known to have a bactericidal effect (Vermeulen et al., 2008) and the applications of the resultant thin film would be wider using a lower energy light source. Any reduction in bacterial count observed under these conditions would indicate a shift in the band gap of the material, caused by the doping process, demonstrating that activation by light of a lower wavelength is possible (Dunnill and Parkin, 2009). A reduction of up to 4.9 $\log_{10}$ cfu / sample of *E. coli* was observed on thin film TiON-1 ($Ti_{2.85}O_4N$), but this was not consistent and the average reduction was just 0.6 $\log_{10}$ cfu / sample. However, this does provide a promising basis for further doping experiments.

The photocatalytic activity of the N-doped thin films N1, N2 and N3 were assessed next, using white light as the activating light source. Thin film N1 displayed the greatest photocatalytic activity and a 2.5 $\log_{10}$ cfu / sample decrease in the recovery of *E. coli* was observed after exposure to both light incubation steps. These findings confirm the chemical characterisation tests performed on these samples such as photooxidation of stearic acid and contact angle measurements, and these data are

published elsewhere (Dunnill et al., 2009b; 2009c; 2010). A 0.9 $\log_{10}$ cfu / sample decrease was observed when the 24 hour activating step was omitted, which demonstrated that the activation step was required to increase the photoactivity of the thin films. This increase in activity is attributed to the pre-cleaning effect of the treatment. The lack of activity on the thin films that had been activated but then not exposed to the second light step indicated the short lifetime of the reactive species on the surface of the thin films that are responsible for killing the bacterial cells. It is unlikely that the oxygen radicals generated in the presence of light survive long enough to kill the bacteria that were applied after the activation step has ended, given that singlet oxygen has a half life of just 1 μs (Perni et al., 2009a). The variability in photocatalytic activity observed on the N1, N2 and N3 thin films, which were synthesised on the same sheet of float glass, demonstrates the inherent lack of reproducibility in the composition of coatings produced using this deposition technique.

The activity of the N-doped thin film N1 was greater than that seen for the titanium (IV) oxynitride thin film TiON-1. The two thin films were synthesised with different precursors; the N-doped thin films were synthesised using t-butylamine as the nitrogen source and ammonia was used for the titanium (IV) oxynitride thin films. The chosen nitrogen precursor was introduced into the titanium (IV) chloride and ethyl acetate vapours at the point of entry to the deposition chamber, resulting in thermal decomposition of the nitrogen precursor on the surface of the glass substrate during formation of TiO_2 (Dunnill and Parkin, 2009). Pre-reaction complexes were more likely to form when ammonia was used as the nitrogen source rather than t-butylamine, and

these complexes can cause control line blockages, which can affect the concentration of nitrogen deposited onto the surface of the glass. The activity of the thin films is dependent upon the concentration of nitrogen in the TiO_2 thin film (Irie et al., 2003), so perhaps the greater control of nitrogen deposition displayed when t-butylamine was used as the nitrogen precursor conferred the increased photocatalytic activity observed.

The S-doped thin film S2 also displayed significant white light driven, photocatalytic activity and a 2.2 $\log_{10}$ cfu /sample decrease in the recovery of *E. coli* was observed after a 24 hour exposure period. Once again, the microbiological findings confirmed the initial chemical characterisation screening tests and the thin film with the fastest rate of stearic acid photodegradation demonstrated the most significant antibacterial activity (Dunnill et al., 2009a; 2010). However, the N-doped thin films displayed greater photocatalytic activity than the S-doped thin films even when the initial white light activation time was extended from 24 to 72 hours.

Reports in the literature have described the antibacterial properties of white light activated N- and S-doped thin films, but direct comparison is difficult due to differences in the method of synthesis used (Asahi et al., 2001; Mills et al., 2002; Diwald et al., 2004; Thompson and Yates, 2006). Indeed, the thin films described in this chapter are the first published thin films with interstitial nitrogen- or sulphur-doping, possessing white light activated antibacterial properties. N-doped thin films have been shown to generate a greater photocatalytic effect against *E. coli* compared with carbon-doped thin films (Wong et al., 2006). However, the reduction in bacterial recovery was minimal (less than a 1 $\log_{10}$ reduction) and when these films were

characterised, the nitrogen doping was shown by XPS to be substitutional, with an ionisation peak at 396 eV (Yang et al., 2004), in contrast to the interstitial-doped nitrogen described in this chapter with an ionisation peak at 400 eV (Dunnill et al., 2009c). This does however demonstrate that nitrogen is a better choice of dopant than carbon if photocatalytic properties are desired. Titanium oxide doped with both nitrogen and carbon was shown to exhibit enhanced photocatalytic properties and reductions of more than 3 $\log_{10}$ cfu / mL were observed (Li et al., 2007), but a halogen bulb was used as the light source which has a higher intensity than the white light source used in this chapter and so a greater photocatalytic effect would be expected. Additionally, powders have a greater surface area per volume ratio than solids further boosting the predicted level of photocatalysis.

The quantity of nitrogen present in the thin film is of paramount importance and some groups show high levels of nitrogen doping can result in the production of poor photocatalysts (Irie et al., 2003), whereas other groups show increased levels of photocatalysis when the nitrogen concentration is higher (Li et al., 2007). When nitrogen concentrations are higher, less TiO_2 reduction occurs, and there are more oxygen vacancies that act as recombination sites for positive holes and electrons, thus reducing the overall photocatalytic activity. The concentration of nitrogen in the N-doped thin film N1 was 0.13 at.% and reports in the literature surmise that concentrations around 1 – 2 at.% is favourable, although the optimal level is still under debate (Irie et al., 2003; Dunnill et al., 2011). Conversely when TiO_2 powder was doped with sulfur, increased levels of the dopant led to a higher level of photocatalysis and an

increased bactericidal effect was observed against *Micrococcus lylae* (Yu et al., 2005). The optimal level of doping is therefore debatable.

4.4.3 Limitations of the experimental work

Problems were experienced in synthesising reproducible thin films using the APCVD apparatus. The precursor gases used, namely titanium (IV) chloride and ethyl acetate, were chosen as they are used industrially in the production of TiO_2-based self-cleaning glass, but the setup of the deposition chambers used in this project were different. In an industrial setting, general mass flow controllers would be used to deliver the reactants and the gas outlets would be stable with the glass sheets moving underneath the float at 500 - 600°C (Dunnill et al., 2009b). These conditions result in a more consistent reaction on the surface of the glass and a more homogenous coating which is essential for a commercial product. The flow rate of the precursor gases are also more tightly regulated which was more difficult to control using the in-house apparatus; overall this meant that the resultant thin films varied in their chemical composition, with differences observed between batches of samples, samples synthesised during the same run and even on different areas on the same piece of float glass. For example, the N-doped samples N1, N2 and N3 were all cut from the same piece of float glass and yet displayed a large variation in photocatalytic activity against *E. coli.* This inconsistency is an inherent disadvantage of the APCVD methodology and made it very difficult to assess the thin films microbiologically, as for accurate assessment, the samples should at least be identical and tested at least in triplicate, for each light exposure condition, on three separate occasions, for each bacterial species.

As a result, the thin films were decontaminated after each microbiological assessment to enable re-use. It was postulated that bacterial cells remaining on the surface of the thin films would be inactivated by the isopropanol and heat treatments, which would restore the thin films to their native state. It has been shown previously that there was no residual antimicrobial effect when isopropanol treatment was used to decontaminate thin films so any activity observed after decontamination can be attributed to the activity of the coatings alone (Page, 2009). However, the photoactivity of the thin films decreased after each round of microbiological testing, so the decontamination regimen was amended so that a stage including exposure to UV light was incorporated. Any remaining bacterial cells were postulated to undergo photoinduced oxidative decomposition (Section 1.3.3.3.3) and non-bacterial debris would also be degraded after the extended light exposure period. The thin films were then incubated in the dark for at least 48 hours so to allow oxygen in the air to react with the hydroxyl species to negate the activating effect of the UV light (O'Neill et al., 2003).

Amendment of the decontamination regimen did not prevent the decrease in antibacterial activity observed on the thin films after sequential use and the exact mechanism for this loss in photoactivity was not established. Bacterial cells were not present on the thin film after decontamination but a fluorescent smear was observed, which was not seen on the unused thin films. In-depth microbiological assessment of these thin films was therefore not possible and an alternative, reproducible method of synthesis was sought, which will be explored in the following chapter. However, re-use

of the thin films did demonstrate the durability of the coatings, and the integrity of the coating was not compromised after repeated use and decontamination cycles.

Another limitation of the test method was the choice of media used to recover the bacterial strains from the test surfaces. The selective medium, MacConkey, was used to culture *E. coli* because round, discrete colonies were formed, which made enumeration easier to perform than when the counts were performed on a non-selective solid medium such as blood agar. However, bacteria recovered were likely to be subletally damaged by exposure to the photocatalytic effects of the thin films, and cultivation on selective media has been shown to inhibit the repair of these damaged strains (Sandel and McKillip, 2004). A non-selective agar overlay could have been poured over the selective medium after inoculation to increase the recovery of damaged cells (Sandel and McKillip, 2004).

4.5 Conclusions

Two sets of nitrogen based thin films were synthesised by chemical vapour deposition, namely N-doped TiO_2 and titanium oxynitride. These coatings displayed significant photocatalytic activity against *E. coli* after exposure to UV light and importantly a white light source, which demonstrates a shift in the band gap from the UV to the visible region of the electromagnetic spectrum. The N-doped thin films displayed a greater photocatalytic activity compared with the titanium (IV) oxynitride thin films. A series of sulfur-doped thin films were synthesised using the same apparatus, which also displayed significant photocatalytic activity against *E. coli* after exposure to a white light source. The N-doped thin film N1 displayed the greatest photoactivity. The

reproducibility of the thin films synthesised using APCVD was poor and a decrease in the photocatalytic activity of the thin films was observed after repeated use. An alternative method of deposition will be explored in the next chapter.

5 Assessment of novel sol-gel synthesised, light-activated antibacterial materials for use in the hospital environment

5.1 Introduction

In the previous chapter, a series of TiO_2 based thin films were synthesised by chemical vapour deposition (APCVD), which displayed photocatalytic properties when exposed to visible light. The thin films were doped with either nitrogen or sulfur, which caused a shift in the band gap energy of the coating so that lower energy photons of light could cause excitation of electrons from the valence band to the conduction band, resulting in the production of reactive oxygen species that are toxic to bacteria. There were however, issues with the reproducibility of the thin films, which meant it was difficult to synthesise a large number of films with identical compositions. In addition, the activity of the thin films decreased over time, so microbiological assessment of the used thin films generated results with a large variation.

An alternative method of synthesis was therefore sought, and sol-gel deposition was chosen. A large number of samples could be synthesised from the same homogenous sol, and there is little variation in the constitution of different batches of prepared sols, so the composition of the resultant films are easier to control. However, sol-gel synthesised films are generally thicker, less mechanically robust and required sintering after coating to anneal the film to the substrate compared with APCVD generated thin films (Brook et al., 2007b). Therefore, the synthesis methodology included a post-coating annealing step and the thickness and robustness of the thin films was be examined to determine whether this was detrimental to the photocatalytic activity.

Silver ions were added to the titania base layer to improve the photocatalytic and photo-activated antibacterial properties of titania. Silver has been used extensively in antibacterial materials because of its intrinsic activity (Silver, 2003; Silver et al., 2006; Noimark et al., 2009); silver ions can move from the surface of the antibacterial material, through the cell membrane of bacteria where they are able to elicit a potent toxic effect (Kawashita et al., 2000; Page, 2009; Page et al., 2009).

5.2 Materials and methods

5.2.1 Thin film synthesis

The thin films were synthesised using sol-gel deposition in a two-step process described in Section 2.10.2. The silver coated TiO_2 thin films were denoted Ag-TiO_2 and TiO_2 thin films and uncoated glass microscope slides were used as controls. The adherence of the TiO_2 and Ag-TiO_2 thin films to the glass substrates was tested by scratching with: (i) finger nails; (ii) a HB pencil; (iii) a 2H pencil; (iv) a steel scalpel (v) a diamond tip pencil and application and removal of scotch tape. The stability of the thin films were assessed by immersion in the following liquids for 2 hours: (i) methanol; (ii) acetone; (iii) distilled water; (iv) 2M HCl (v) 2M NaOH.

5.2.2 Characterisation and functional assessment of the thin films

Thin films of TiO_2 and Ag-TiO_2 were prepared on both glass and quartz substrates before characterisation using UV-visible spectroscopy, as described in Section 2.11.1. The reflectance data was used to calculate the thickness of the thin films using the Swanepoel method and to estimate the band onset of the thin films using a Tauc plot.

Further methods employed to characterise the thin films included XRD, Raman spectroscopy, AFM and XPS, as described in Dunnill et al., (2011).

5.2.2.1 Contact angle measurements

Water droplet contact angle measurements were taken of a droplet of deionised water inoculated onto both the Ag-TiO_2 and TiO_2 thin films and uncoated glass control as described in Section 2.11.2. Measurements were taken after: (i) incubation in the dark for 72 hours; (ii) irradiation with the UV light source for 30 minutes (Section 2.4.2.1); (iii) irradiation with the filtered white light source for 30 minutes (Section 2.4.1) (Instrument Glasses, 2000).

5.2.2.2 Photo-oxidation of stearic acid

A solution of stearic acid was inoculated onto both the thin films and the uncoated glass control slides to assess the rate of photo-oxidisation, as described in Section 2.11.3. The rate of photo-activity was determined after exposure to three lighting conditions: (i) 254 nm UV light source for up to 72 hours (Section 2.4.2.2); (ii) white light source for 96 hours (Section 2.4.1); (iii) the same white light source with a filter attached that absorbed virtually all sub-400 nm radiation (Instrument Glasses, 2000).

5.2.3 Antibacterial assessment of the thin films

Bacterial strains were maintained as described in Section 2.1 and bacterial suspensions of *E. coli* ATCC 25922 and EMRSA-16 were prepared as detailed in Section 2.3, except a 50 µL bacterial droplet was inoculated onto the surface, resulting in a starting inoculum of approximately 5 x 10^5 cfu / sample. The effect of the photocatalytic thin films on the viability of bacterial strains was determined using the methodology

described in Section 2.12.2 and Figure 2.2, except the activation step was omitted. When required, a UV light filter was positioned 2.5 cm above the moisture chamber. The Mann Whitney test was used to determine the statistical significance of any differences observed, as described in Section 2.13.

5.3 Results

Thin films of Ag-TiO_2 and TiO_2 were successfully synthesised using the sol-gel method of deposition (Figure 5.1). Control thin films consisting of just silver nanoparticles were also produced, but these coatings were unstable, demonstrating the essential role of the TiO_2 under-layer for adherence of the silver nanoparticles to the glass substrate. The TiO_2 and Ag-TiO_2 thin films were well adhered to the glass substrates after application and removal of scotch tape and were resistant to scratching by finger nails, a HB pencil, a 2H pencil and a steel scalpel. Both thin films were easily scratched with a diamond tip pencil. The thin films were stable after immersion in methanol, acetone, distilled water, or 2M HCl for 2 hours, but were dissolved in 2M NaOH.

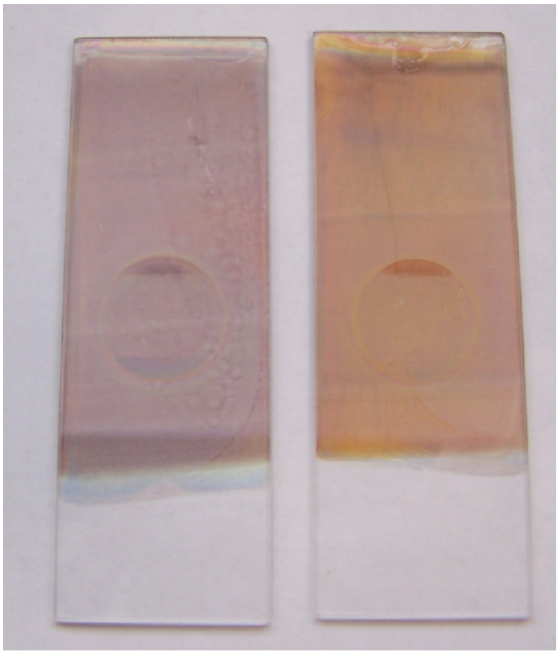

Figure 5.1 Photograph of the Ag-TiO_2 thin films. The purple coloured thin film (left) was stored in the dark and the orange coloured thin film (right) was irradiated with UV light to induce the colour change.

The thin films were uniformly adhered to the glass microscope slides and were orange in colour and transparent when synthesised. After storage in the dark for at least 72 hours, the thin films turned purple; reversion to the orange colour could be induced by irradiation with UV light for 10 minutes or standard indoor lighting conditions for 1 hour. The reversible photo-induced colour change can be described using the following formula:

$$\text{Silver oxide (purple)} \underset{\text{air}}{\overset{h\nu + TiO_2}{\rightleftharpoons}} \text{silver (orange)} + \text{oxygen}$$

To confirm this, orange and purple thin films were placed inside separate Schlenk flasks and the air was evacuated. The purple sample was irradiated with UV light in the created vacuum and turned orange. However, when the orange thin films were stored in the dark for 72 hours, the orange colour remained, indicating that oxygen was

required for the backward reaction and light exposure was needed for the forward reaction.

5.3.1 Characterisation and functional assessment of the thin films

5.3.1.1 UV-visible spectroscopy

Thin films of Ag-TiO_2 and TiO_2 were prepared using quartz as the underlying substrate in place of glass, as it allowed better measurement of the band onset using a Tauc plot, without the interference of the underlying glass band onset expected at about 3.3 eV. The UV-visible-IR spectroscopy results are displayed in Figure 5.2, and the Ag-TiO_2 and TiO_2 are very similar. The Ag-TiO_2 thin film showed a small decrease in transmission due to silver ions on the surface and a minimal red shift compared with TiO_2. The uncoated quartz slide showed no features above 300 nm.

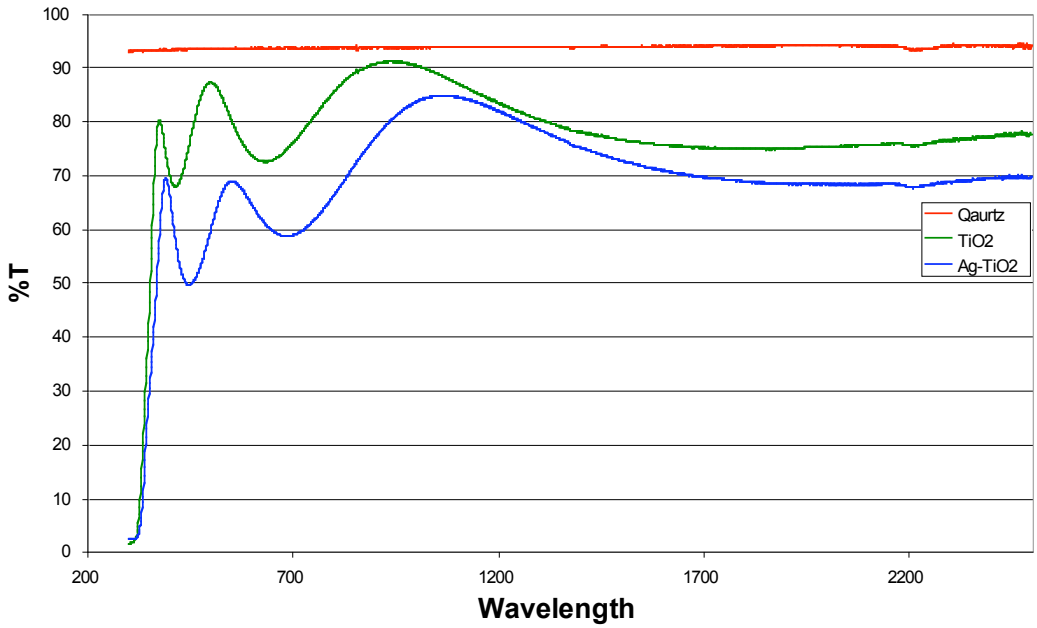

Figure 5.2 Transmission data of the Ag-TiO_2 and TiO_2 thin films deposited onto a quartz substrate, obtained by UV-visible-IR spectrometry

The thickness of the Ag-TiO_2 and TiO_2 thin films were estimated at 211 nm and 196 nm respectively, using the Swanpoel method, which indicated that addition of silver had little effect on the thickness of the thin films. The thickness of thin films synthesised from the same sol, can vary by 10 nm, suggesting that the difference observed between the Ag-TiO_2 and TiO_2 thin films was unsubstantial.

The band onset of the Ag-TiO_2 and TiO_2 thin films were estimated using the UV-visible-IR data to produce Tauc plots (Figure 5.3). The incorporation of silver onto the surface of the TiO_2 caused a shift in the band onset towards lower energy radiation, with a shift from 3.2 eV for titania to 2.9 eV for the silver-doped titania. This indicates an interaction between silver and the titania substrate causing a shift towards activation in the visible region of the spectrum.

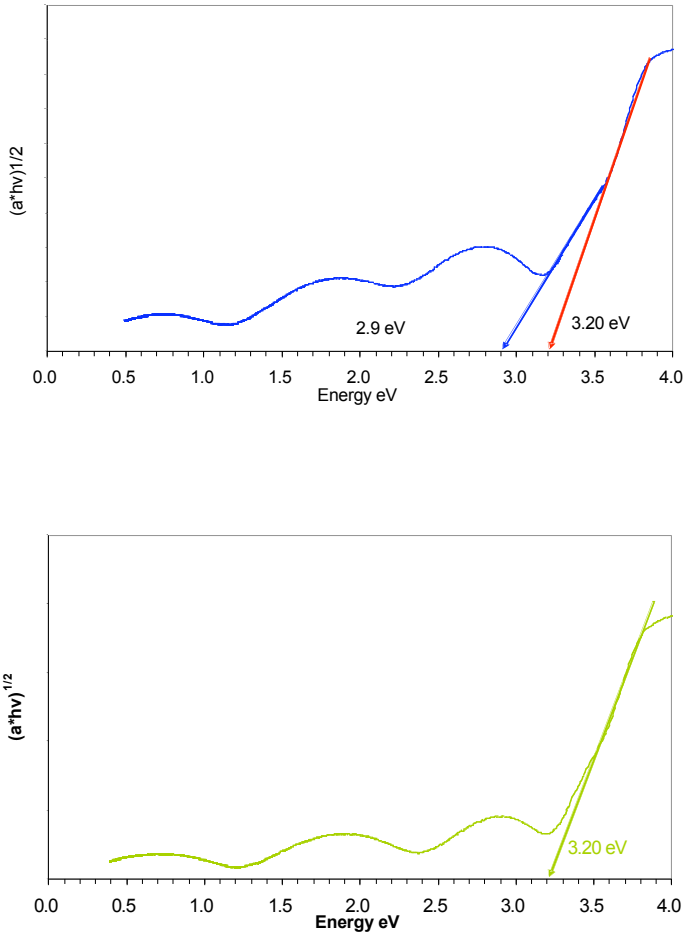

Figure 5.3 Tauc plots of the UV-visible-IR data taken for the (a) Ag-TiO_2 and (b) TiO_2 thin films prepared on quartz substrates.

5.3.1.2 Contact angle measurements

When the Ag-TiO_2 thin film was exposed to UV light, the water contact angle decreased from 60° to 8° as the surface became superhydrophilic (Table 5.1). A similar decrease in water contact angle was observed on the TiO_2 thin film after exposure to UV light (64° to 8°). The water contact angle on the uncoated glass slide did not change after irradiation with UV light, although the initial reading was comparatively low.

The samples were subsequently exposed to white light using the Optivex™ UV filter to eliminate any higher energy photons of light and the UV-visible IR spectrum of this

filter is displayed in Figure 5.4, which shows almost zero transmission of light below 400 nm. The decrease in water contact angle on the Ag-TiO_2 thin film was the same as that observed after UV irradiation (Table 5.1). The filtered white light source did not have an effect on the TiO_2 thin film and there was no substantial change in the water contact angle. These results clearly demonstrate the visible light-induced hydrophilicity of the Ag-TiO_2 thin films.

Table 5.1 The water contact angles of the Ag-TiO_2 thin films and the control samples. Measurements are accurate to ±2°

Sample name	Light source	Water contact angle
Uncoated glass slide	None	25(2)°
	UV	24(2)°
TiO_2	None	64(2)°
	UV	8(2)°
	Filtered white light	60(2)°
Ag-TiO_2	None	60(2)°
	UV	8(2)°
	Filtered white light	8(2)°

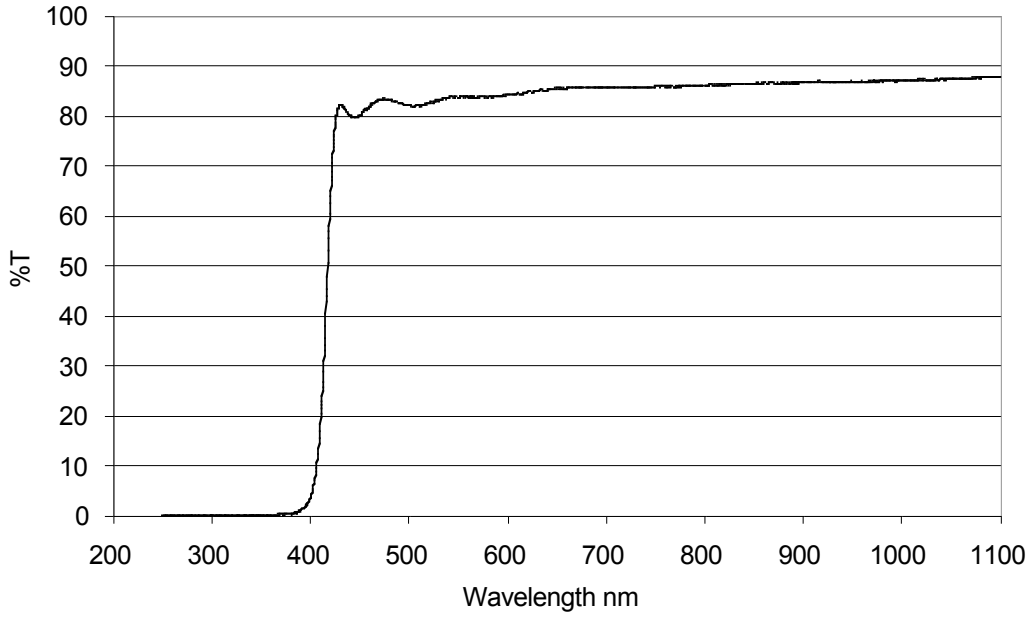

Figure 5.4 UV-Vis spectrum for the Optivex™ UV filter showing the cut-off for radiation below 400 nm in wavelength.

5.3.1.3 Photo-oxidation of stearic acid

The effect of the light sources on the concentration of stearic acid on the surface of the uncoated glass slide is illustrated in Figure 5.5a, Figure 5.6a and Figure 5.7a. The heights of the lines on the graph represent time with the highest peaks corresponding to the shortest irradiation time. The uncoated glass slides did not show any signs of photo-activity after exposure to any of the three lighting conditions and there was no appreciable decrease in the concentration of stearic acid detected on the surface of the samples after the exposure periods. Significant destruction of stearic acid was demonstrated on the TiO_2 and Ag-TiO_2 thin films after exposure to the 254 nm UV light source (Figure 5.5b and Figure 5.5c) and after 29 hours the peaks had disappeared. The rate of stearic acid destruction for both the TiO_2 and Ag-TiO_2 thin films was calculated to be approximately 1.1 x 10^{14} molecules / cm^2 per hour, based upon the assumption that 1 unit of integration between 2700 and 3000 / cm equated to approximately 9.7 x

10^{15} molecules / cm^2 (Mills and Wang, 2006). Therefore, silver doping did not have an effect on the photo-oxidisation of stearic acid after irradiation with UV light.

When the white light was used as the irradiation source, a significant decrease in the stearic acid concentration was demonstrated on the Ag-TiO_2 thin films (Figure 5.6c), whereas a minimal reduction was observed on the TiO_2 thin films (Figure 5.6b). The rate of stearic acid destruction for the TiO_2 and Ag-TiO_2 thin films were calculated to be approximately 1.6 x 10^{14} and 4.2 x 10^{14}, respectively (Table 5.2). However, TiO_2 should not display any photo-activity after irradiation with the white light source and activation should only occur after exposure to wavelengths of light below 385 nm, as the band onset of TiO_2 is 3.2 eV. Therefore, the Optivex™ UV filter was fitted to the light box to eliminate any higher energy photons of light. The photo-oxidation of stearic acid on the TiO_2 thin film was seriously compromised and only a negligible change in the concentration of the compound was observed (Figure 5.7b). In contrast, the photocatalytic activity was retained on the Ag-TiO_2 thin films (Figure 5.7c), which was shown to be 200 times more effective at destroying stearic acid than the TiO_2 control (Table 5.2). This is the first unequivocal evidence of visible light photocatalytic destruction of stearic acid (Dunnill et al., 2011).

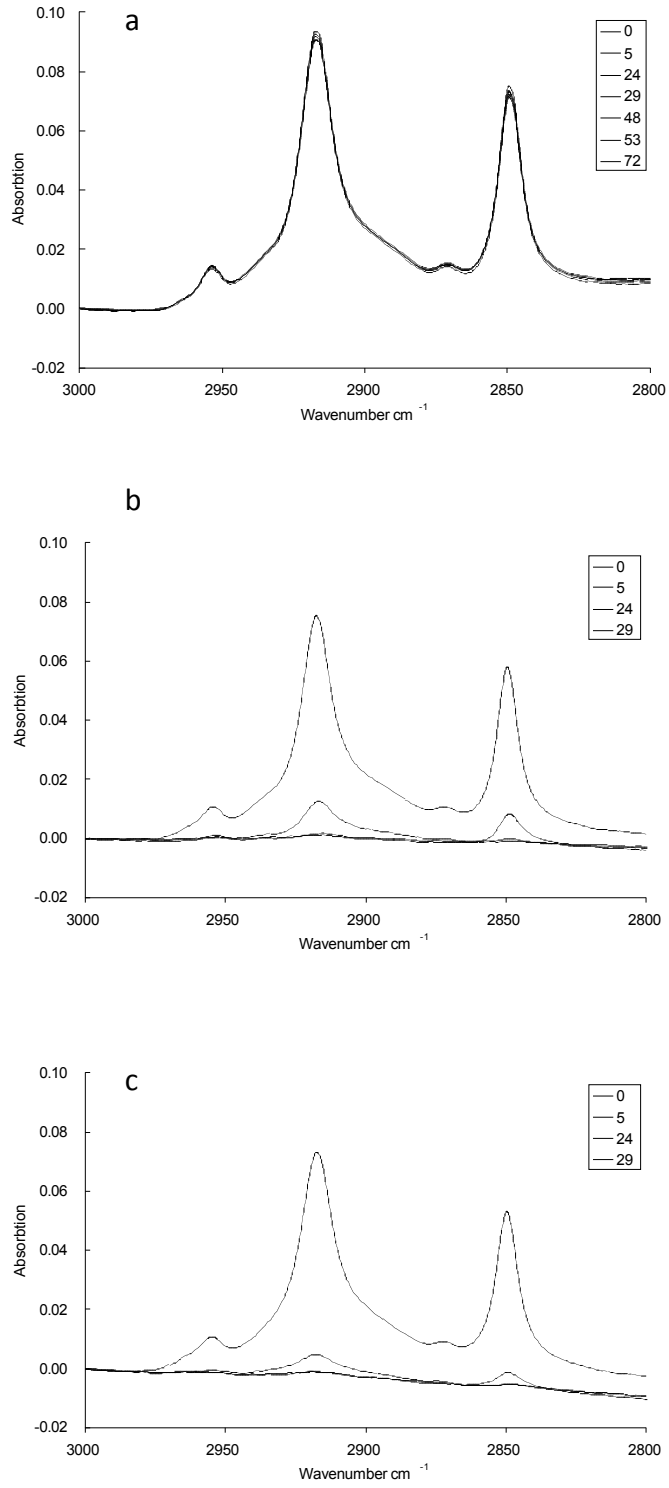

Figure 5.5 IR absorption data displaying the photo-oxidation of stearic acid molecules on the surface of the three materials over 72 hours using a 254 nm light source, where: a) uncoated glass slide; b) TiO_2 and c) Ag-TiO_2. Line times are shown in order of height on the graph and in all cases, the area under the curve indicates the amount of stearic acid remaining on the surface.

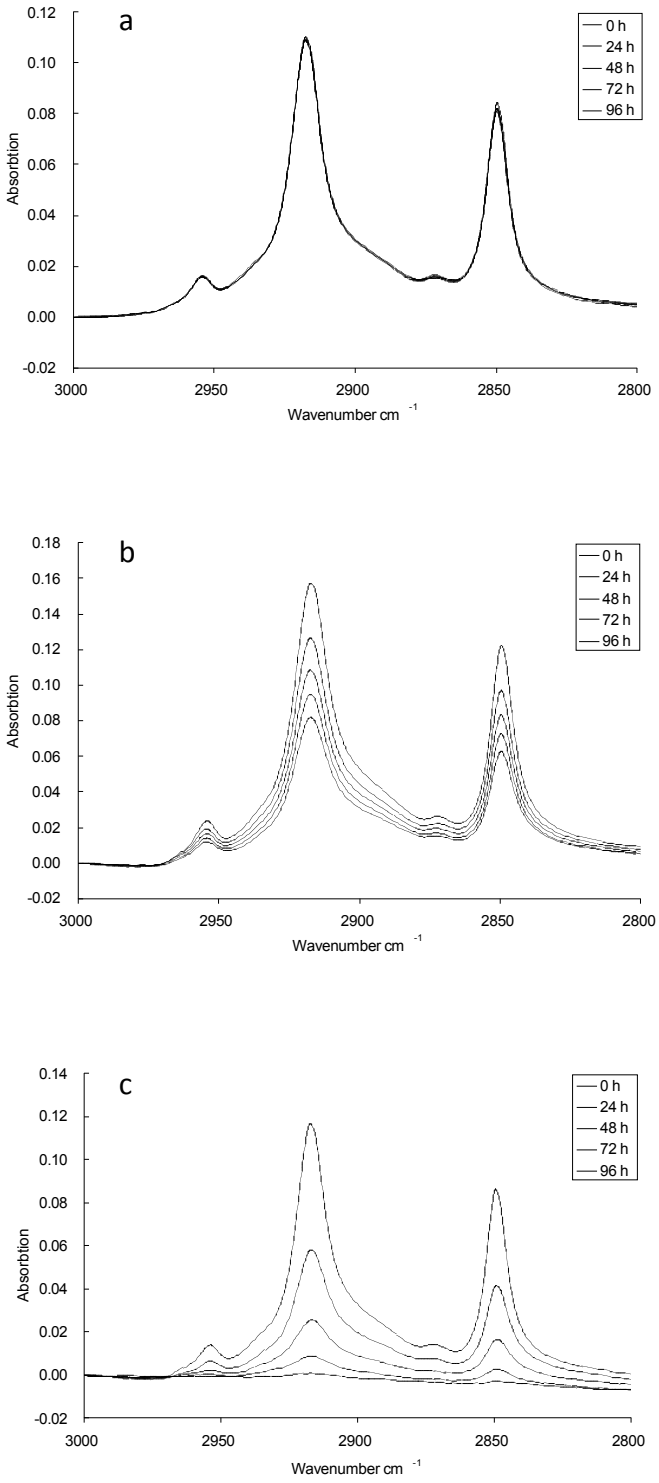

Figure 5.6 IR absorption data showing the photo-oxidation of stearic acid molecules on the surface of the three materials over 96 hours using a white light source where: a) uncoated glass slide; b) TiO_2 and c) Ag-TiO_2. Line times are shown in order of height on the graph and in all cases, the area under the curve indicates the amount of stearic acid remaining on the surface.

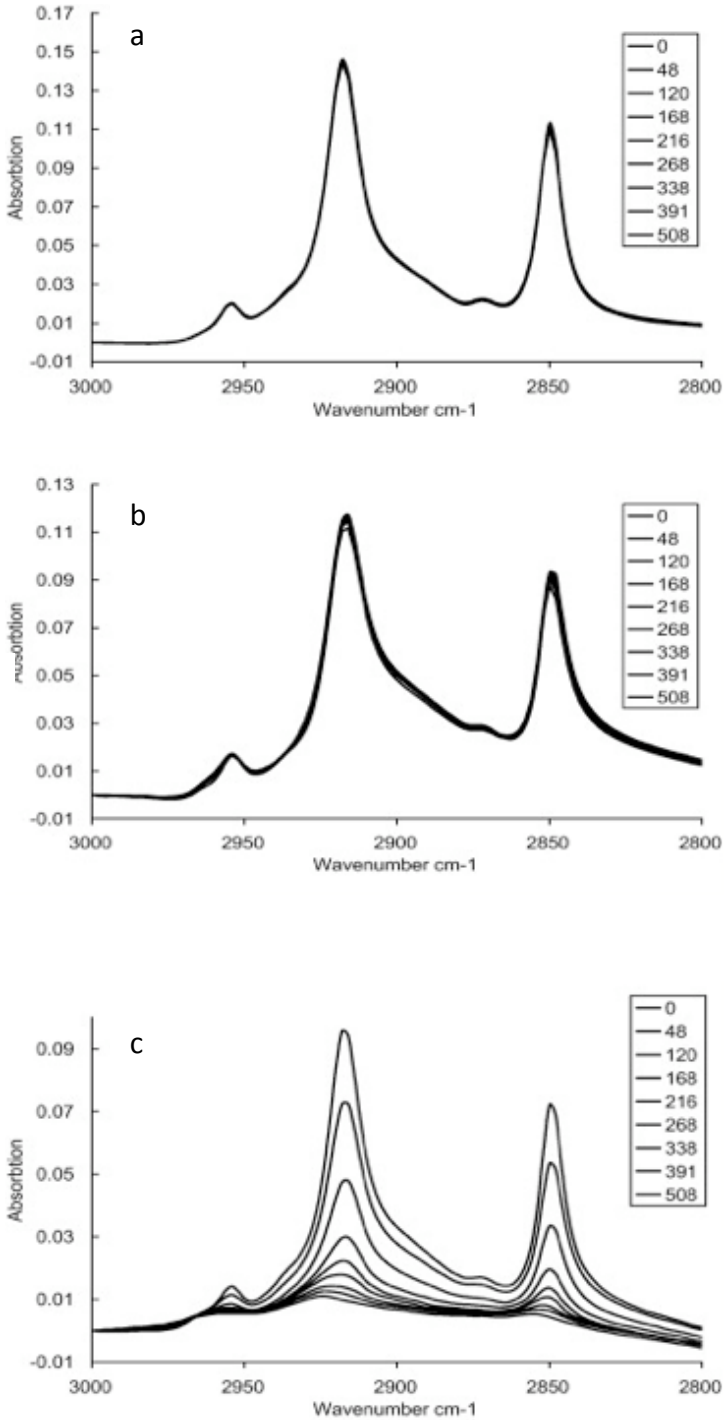

Figure 5.7 Raw data showing the photo-oxidation of stearic acid molecules on the surface of the three samples over 500 hours using a white light source and the Optivex™ UV filter where: (a) uncoated glass slide; (b) TiO_2 and (c) Ag-TiO_2. Line times are shown in order of height and in all cases, the area under the curve indicates the amount of stearic acid remaining on the surface.

Table 5.2 The number of molecules of stearic acid photo-oxidised during irradiation by the different light sources. Rates are given as molecules / cm^2 per hour. Exposure times to the UV, white light and filtered white light were 29 hours, 96 hours and 500 hours respectively.

Light source	TiO_2		Ag-TiO_2	
	Molecules oxidised	Rate	Molecules oxidised	Rate
UV – 254 nm	3.32×10^{16}	1.14×10^{15}	3.30×10^{16}	1.14×10^{15}
White light	1.49×10^{16}	1.55×10^{14}	4.05×10^{16}	4.22×10^{14}
Filtered white light	1.49×10^{16}	2.99×10^{11}	3.12×10^{16}	6.25×10^{13}

5.3.2 Antibacterial activity against *E. coli* ATCC 25922

The antibacterial activity of the thin films was assessed against *E. coli*. After 2 hours irradiation with white light, a 0.9 $\log_{10}$ cfu / sample decrease was observed, compared with both the uncoated controls and the TiO_2 controls exposed to the same lighting conditions (Figure 5.8). The decrease in bacterial recovery was much greater after 6 hours irradiation with the white light source; *E. coli* was not recovered from the Ag-TiO_2 thin films after the 6 hour exposure period on any of the experimental repeats. This reduction corresponds to a 4.8 $\log_{10}$ cfu / sample decrease in bacterial recovery, compared with the glass controls exposed to the same lighting conditions ($p < 0.001$). The decrease in recovery was slightly less when compared to the TiO_2 thin films, but a statistically significant 4.4 $\log_{10}$ cfu / sample decrease was still achieved ($p < 0.001$). However, *E. coli* could not be recovered from the Ag-TiO_2 thin films which were incubated in the dark for the 6 hour incubation period, indicating that the observed antibacterial activity observed was not light-dependent.

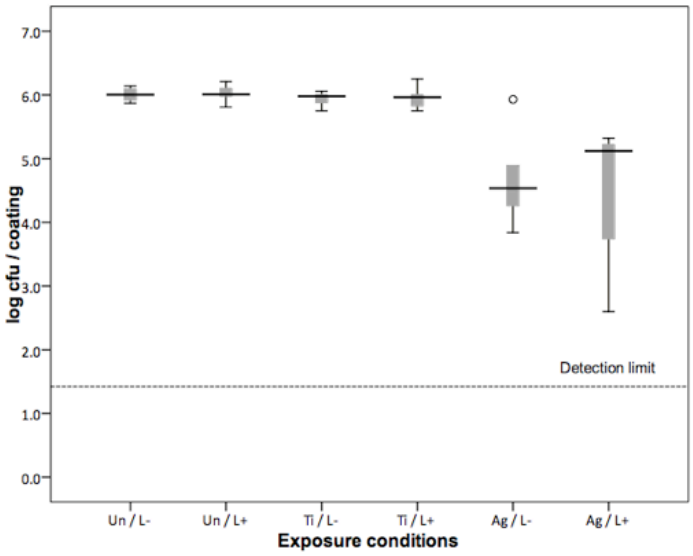

Figure 5.8 Effect of the thin film Ag-TiO_2 on the survival of *E. coli*. Thin films were irradiated with white light (L+) or incubated in the dark for 2 hours (L-). The uncoated glass slides, TiO_2 and Ag-TiO_2 are represented by 'Un', 'Ti' and 'Ag', respectively.

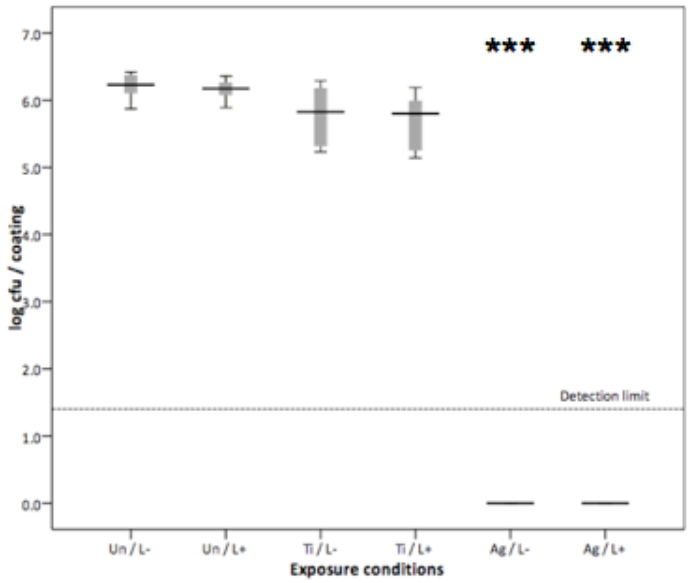

Figure 5.9 Effect of the thin film Ag-TiO_2 on the survival of *E. coli*. Thin films were irradiated with white light (L+) or incubated in the dark for 6 hours (L-). The uncoated glass slides, TiO_2 and Ag-TiO_2 are represented by 'Un', 'Ti' and 'Ag', respectively.

The antibacterial activity of the Ag-TiO_2 thin films was further assessed, the exposure period was extended to 12 hours and once again, it was not possible to recover *E. coli* from the Ag-TiO_2 thin films after the incubation time, and this effect was independent of light exposure (Figure 5.10). Interestingly, the activity of the TiO_2 thin films increased with extended exposure to white light and a 2.4 log_{10} cfu / sample decrease in bacterial recovery was observed, compared with the glass control exposed to the same lighting conditions. This finding supports the results from the functional testing, which demonstrated photo-oxidation of stearic acid after exposure to this white light source. Therefore, the Optivex™ UV filter was placed above the moisture chamber to eliminate the UV component of the white light source. The antibacterial activity of the TiO_2 thin films was eliminated (Figure 5.11); the reduction observed on the TiO_2 thin films was negligible (0.02 log_{10} cfu / sample decrease). The light-independent activity of the Ag-TiO_2 thin films was retained and the decrease in bacterial recovery was maintained at 4.9 log_{10} cfu / sample on the Ag-TiO_2 thin films, in the presence and absence of filtered light.

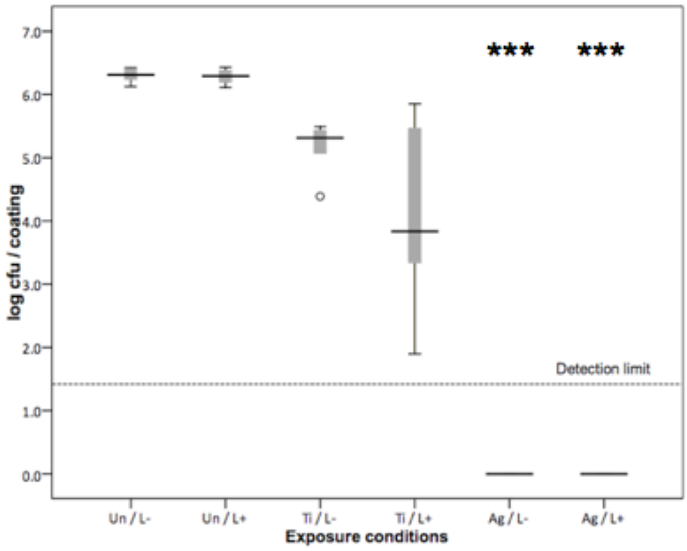

Figure 5.10 Effect of the thin film Ag-TiO_2 on the survival of *E. coli*. Thin films were irradiated with white light (L+) or incubated in the dark for 12 hours (L-). The uncoated glass slide, TiO_2 and Ag-TiO_2 are represented by 'Un', 'Ti' and 'Ag', respectively.

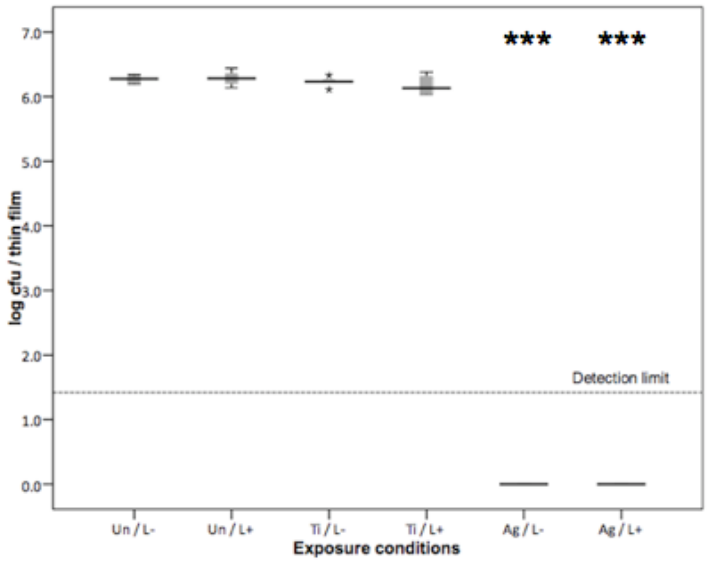

Figure 5.11 Effect of the thin film Ag-TiO_2 on the survival of *E. coli*. Thin films were irradiated with white light filtered with the Optivex™ glass (L+) or, incubated in the dark for 12 hours (L-). The uncoated glass slide, TiO_2 and Ag-TiO_2 are represented by 'Un', 'Ti' and 'Ag', respectively.

The antibacterial activity of the Ag-TiO_2 thin films were further determined after 18 hours exposure to the white light source. The light-independent activity of the thin films was maintained and a 4.6 $\log_{10}$ cfu / sample decrease in the recovery of *E. coli* was observed, compared with the glass controls exposed to the same lighting conditions ($p < 0.001$). No re-growth of *E. coli* was observed on either the thin films incubated in the presence or absence of light, indicating a sustained antibacterial effect. A minimal decrease in the recovery of *E. coli* was observed on the TiO_2 thin films after the 18 hour incubation period (0.3 $\log_{10}$ cfu / sample), which paradoxically was much less than that seen after 12 hours. This difference was however, statistically significant ($p < 0.01$). The white light alone did not have an effect on the survival of *E. coli* on the uncoated control slides, and no significant difference in bacterial recovery was observed on these samples, after incubation in the presence or absence of white light, which implies that the photo-activity observed on the TiO_2 thin films was not due to the effect of the white light source alone.

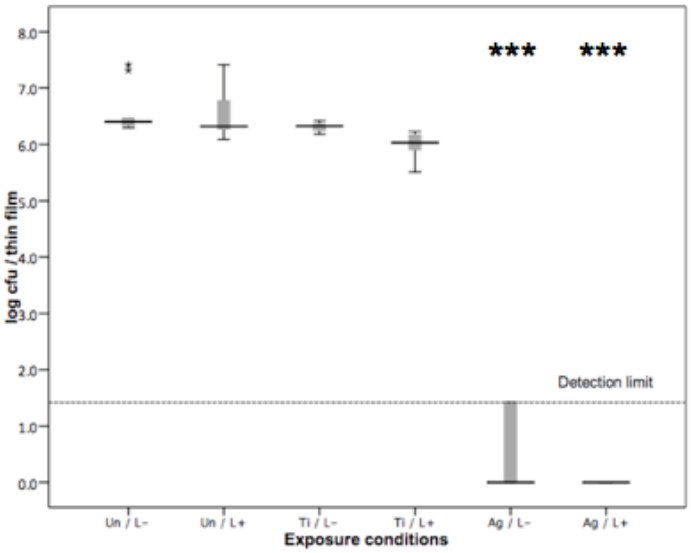

Figure 5.12 Effect of the thin film Ag-TiO_2 on the survival of *E. coli*. Thin films were irradiated with white light (L+) or incubated in the dark for 18 hours (L-). The uncoated glass slide, TiO_2 and Ag-TiO_2 are represented by 'Un', 'Ti' and 'Ag', respectively.

5.3.3 Antibacterial activity against EMRSA16

The antibacterial activity of the thin films was assessed against EMRSA-16. A 0.3 log_{10} cfu / sample decrease in the recovery of EMRSA-16 was observed after 6 hours irradiation with white light (Figure 5.13), compared with the uncoated glass slides exposed to the same lighting conditions, which did not reach statistical significance.

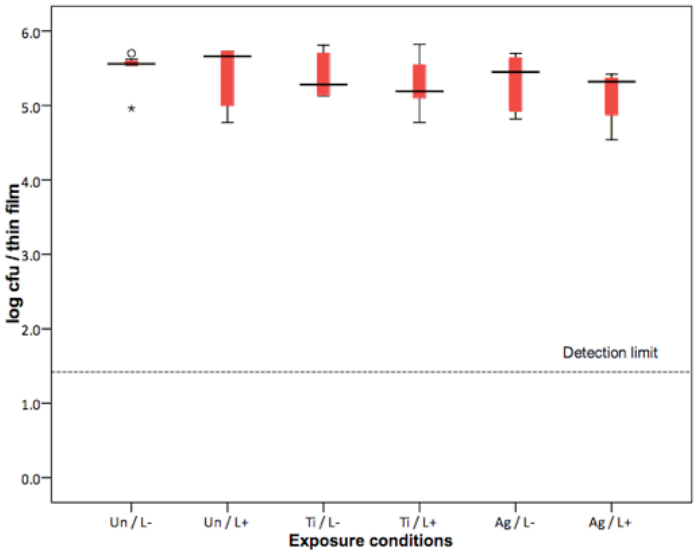

Figure 5.13 Effect of the thin film Ag-TiO_2 on the survival of EMRSA-16. Thin films were irradiated with white light (L+) or incubated in the dark for 6 hours (L-). The uncoated glass slide, TiO_2 and Ag-TiO_2 are represented by 'Un', 'Ti' and 'Ag', respectively.

The Ag-TiO_2 thin films were subsequently exposed to 12 hours white light, and a 2.6 log_{10} cfu / sample decrease in the recovery of EMRSA-16 was observed (p <0.01), compared with the uncoated glass slides (Figure 5.14). Negligible photo-activity was observed on the TiO_2 thin films and there was an insignificant difference observed in the recovery from the irradiated TiO_2 thin films compared to those incubated in the dark (0.2 log_{10} cfu / sample decrease). The antibacterial effect appeared to be light-dependent and there was a 2.3 log_{10} cfu / sample difference in the recovery of EMRSA-16 from the irradiated Ag-TiO_2 thin films compared with the non-irradiated Ag-TiO_2 thin films (p <0.01) and a 2.6 log_{10} cfu / sample difference in the recovery of EMRSA-16 from the uncoated irradiated samples (p <0.001).

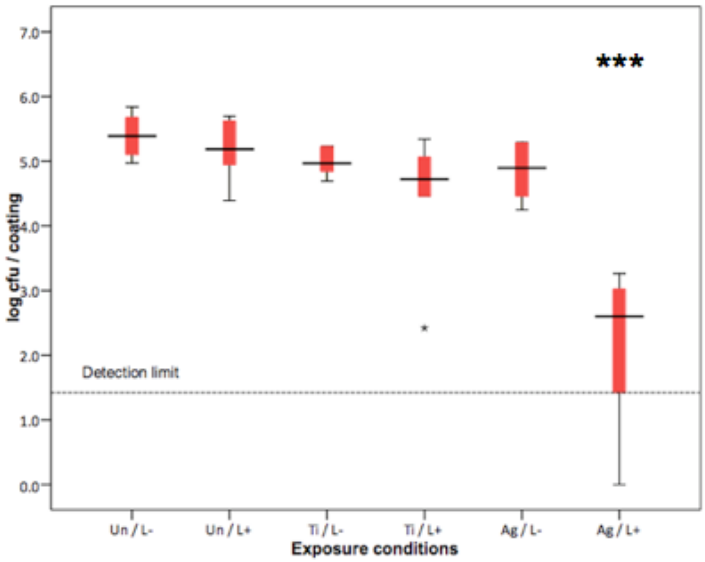

Figure 5.14 Effect of the thin film Ag-TiO_2 on the survival of EMRSA-16. Thin films were irradiated with white light (L+) or incubated in the dark for 12 hours (L-). The uncoated glass slide, TiO_2 and Ag-TiO_2 are represented by 'Un', 'Ti' and 'Ag', respectively.

The experiment was repeated with the Optivex™ UV filter *in situ* to eliminate any stray photons of sub 400 nm light, and the antibacterial activity of the Ag-TiO_2 thin films decreased (Figure 5.15). A 1.1 $\log_{10}$ cfu / sample reduction in the recovery of EMRSA-16 was observed, compared with the uncoated sample irradiated with the same filtered light source ($p < 0.001$). The minimal photo-activity observed on the TiO_2 thin films in the presence of unfiltered white light was maintained and a 0.2 $\log_{10}$ cfu / sample decrease was detected, compared with the uncoated samples irradiated with filtered white light. This difference was not statistically significant ($p > 0.05$).

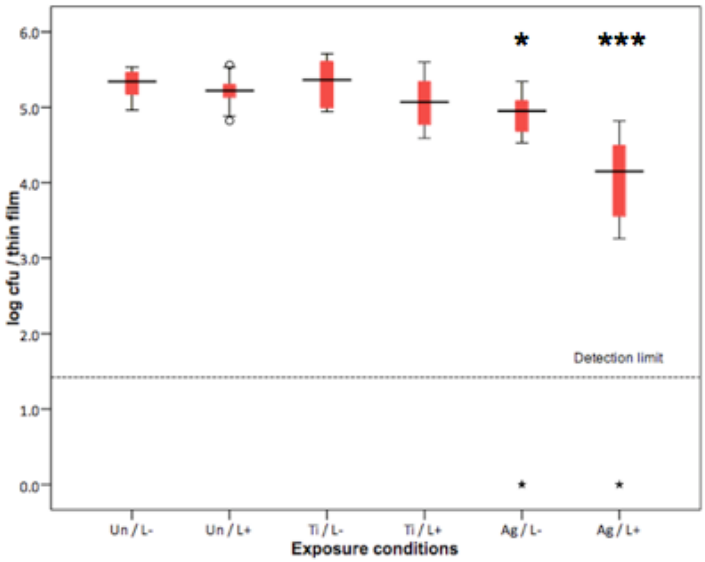

Figure 5.15 Effect of the thin film Ag-TiO_2 on the survival of EMRSA-16. Thin films were irradiated with white light filtered with the Optivex™ glass (L+) or incubated in the dark for 12 hours (L-). The uncoated glass slides, TiO_2 and Ag-TiO_2 are represented by 'Un', 'Ti' and 'Ag', respectively.

The Ag-TiO_2 thin films were subsequently irradiated with white light for 18 hours and the results are shown in Figure 5.16. A 3.4 $\log_{10}$ cfu / sample reduction in the recovery of EMRSA-16 was observed, compared with the glass controls exposed to the same lighting conditions ($p < 0.001$). The light-dependent activity of the thin films was sustained and a 2.9 $\log_{10}$ cfu / sample decrease in bacterial recovery was observed on the irradiated Ag-TiO_2 thin films compared with those incubated in the dark ($p < 0.001$). However, significant photo-activity was detected on the TiO_2 thin films, although this effect was extremely inconsistent, as indicated on the graph by the large error bars and was also less statistically significant ($p < 0.05$). A 3.4 $\log_{10}$ cfu / sample decrease in the recovery of EMRSA-16 was observed, compared with the uncoated glass controls exposed to the same lighting conditions. No activity was detected on the TiO_2 thin films incubated in the dark, indicating that the activity was light dependent and could once again be due to the UV component of the white light source.

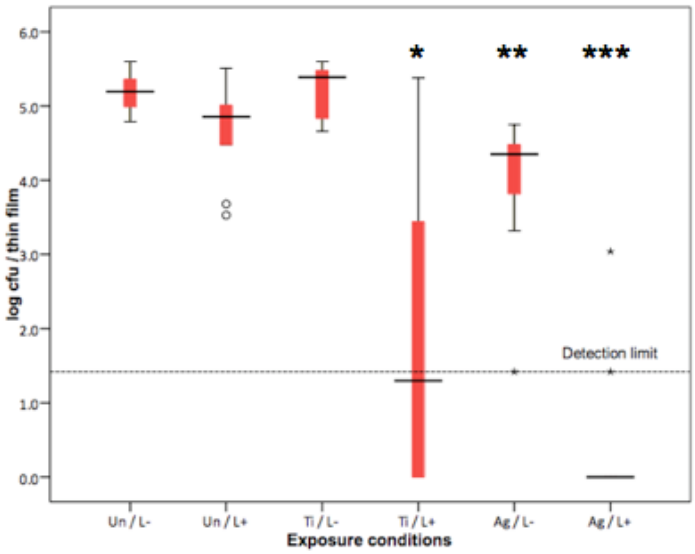

Figure 5.16 Effect of the thin film Ag-TiO_2 on the survival of EMRSA-16. Thin films were irradiated with white light (L+) or incubated in the dark for 18 hours (L-). The uncoated glass slides, TiO_2 and Ag-TiO_2 are represented by 'Un', 'Ti' and 'Ag', respectively.

Therefore, the Optivex™ filter added and the samples were irradiated with filtered white light (Figure 5.17). The antibacterial activity of the Ag-TiO_2 thin films was retained but at a reduced rate; the average decrease in bacterial recovery dropped from 3.4 $\log_{10}$ cfu / sample to 2.3 $\log_{10}$ cfu / sample using the unfiltered and filtered white light sources, respectively. This result mirrors that seen after 12 hours irradiation with the filtered light source and remained highly statistically significant ($p < 0.001$). The light dependent activity of the Ag-TiO_2 thin films was also replicated and 1.4 $\log_{10}$ cfu / sample decrease in bacteria was observed on the irradiated Ag-TiO_2 thin films compared with those incubated in the dark ($p < 0.05$), but again this reduction was less than that observed when the unfiltered light source was used.

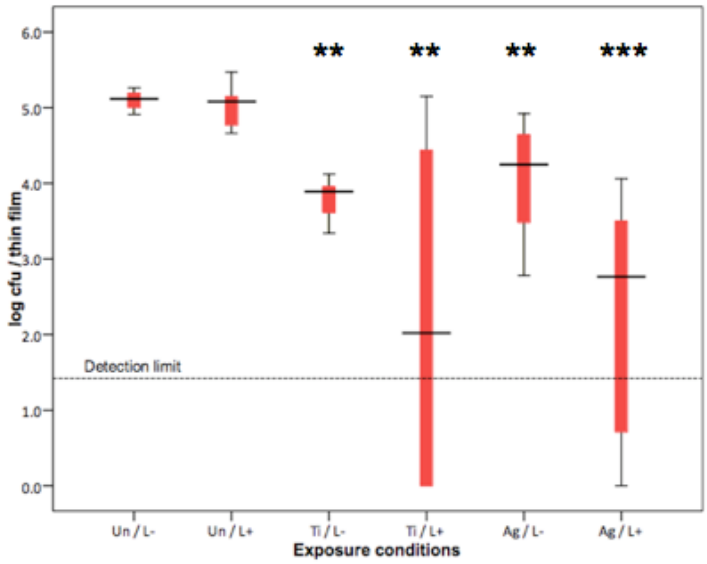

Figure 5.17 Effect of the thin film Ag-TiO_2 on the survival of EMRSA-16. Thin films were irradiated with white light filtered with the Optivex™ glass (L+) or incubated in the dark for 18 hours (L-). The uncoated glass slide, TiO_2 and Ag-TiO_2 are represented by 'Un', 'Ti' and 'Ag', respectively.

The most surprising result was the retained photo-activity of the TiO_2 thin films (Figure 5.17); the photo-activity was reduced when filtered white light was used as the irradiation source, but a statistically significant 3.1 $\log_{10}$ cfu / sample decrease in viable bacteria was still observed ($p < 0.01$), which was a greater decrease than that seen on the Ag-TiO_2 thin films. A wide range of bacterial recovery was observed, indicated by the large box on the graph; on occasion, no bacteria were recovered at all, and on other experimental replicates, the number of colonies present equalled that observed from the control samples incubated in the dark. The bacterial recovery from the control samples Ag-TiO_2 and TiO_2, which were incubated in the dark, was also significantly lower than the uncoated glass samples incubated in the dark ($p < 0.01$). Furthermore, the values obtained from the TiO_2 thin film incubated in the dark was significantly lower than that obtained in the previous 18 hour experiment (Figure 5.16).

5.4 Discussion

Silver has been shown both in this chapter and in the literature, to improve titanium dioxide photo-activity and this is achieved through three mechanisms. The first involves reduction of silver ions to silver by photo-excited electrons. The electrons are further attracted to silver particles in the following reaction, where the silver particles act as electron traps (Herrmann et al., 1997; He et al., 2002; Brook et al., 2007b):

$$(Ag) + e^- \longleftrightarrow e^-_{Ag}$$

The electrons move to the interior of the thin film and the holes move to the interfacial region, which enhances their separation and inhibits electron-hole recombination. The photo-generated holes then react with surface hydroxyl groups and water to form hydroxyl radicals and other reactive species, which possess antibacterial activity (Sclafani et al., 1991; Herrmann et al., 1997; Stathatos et al., 2001; He et al., 2002). Secondly, the electric field around the silver particles is increased by surface plasmon resonance effects, which further enhance photo-excitation of the electrons and electron-hole separation (Zhao et al., 1996). Finally, the surface roughness of the titanium dioxide thin film changes upon silver addition, so that the titanium dioxide particle size in the resultant thin films is smaller, which exposes a greater surface area available for photo-reaction, which further increases photo-activity (Herrmann et al., 1997; He et al., 2002; Martinez-Gutierrez et al., 2010). Therefore the properties of a photocatalyst can be adapted by reducing the particle size, to couple the intrinsic band onset properties to allow lower energy photocatalysis (Herrmann et al., 1997; He et al., 2002; Dunnill et al., 2011).

5.4.1 Synthesis of the silver-doped titania thin films

Analogous to nitrogen and sulfur doping of titania, the silver concentration is critical, and a decrease in the photo-activity of the thin films will occur if the silver concentration exceeds an optimum level (Sclafani et al., 1991; Dobosz and Sobczynski, 2003; Brook et al., 2007b). This is due to the 'screening effect' where the silver deposited on the surface of the thin film masks the photo-reactive sites so that they are inaccessible for interaction with photons (Dobosz and Sobczynski, 2003). In addition, the negatively charged silver particles on the thin film could attract the holes before any interaction with water, which would decrease the concentration of reactive oxygen species generated and the observed photo-activity (He et al., 2002).

Sol-gel deposition was used to synthesise the thin films in this chapter in contrast to APCVD, which was used to generate the thin films assessed in the previous chapter. APCVD was initially chosen as a deposition method, as the resultant coatings are transparent, robust and strongly adhered to the substrate. Sol-gel films are generally thicker, less mechanically robust and require sintering after coating to anneal the coating to the substrate (Brook et al., 2007b). A post-coating annealing step was included in the sol-gel method of synthesis so the thin films generated in this chapter were well adhered to the substrate and as mechanically stable as the APCVD generated thin films.

5.4.2 Characterisation and functional assessment of the silver-doped titania thin films

The silver-coated titania thin films exhibited photo-chromic behaviour, which was caused by a change in the oxidation state of the silver nanoparticles from silver oxide to metallic silver (Ohko et al., 2003; Paramasivam et al., 2007; Gunawan et al., 2009). Both UV and visible light were able to induce the more coloured orange metallic state, and the less coloured purple oxide state occurred after storage in the dark. Excited electrons generated during light exposure photo-reacted with the silver ions present within the purple film, and the films turned orange as the silver oxide was reduced to silver metal (Ohtani et al., 1987). When the films were subsequently stored in the dark in the presence of air, the photo-reduced silver was oxidised forming silver oxide and the films reverted to the purple colour due to a decrease in light absorbance (Paramasivam et al., 2007). These changes are caused by surface plasmon resonance effects, which in turn are influenced by the nanoparticle size, shape and the local refractive index (Jin et al., 2001; Mock et al., 2002; Ohko et al., 2003; Gunawan et al., 2009).

The band onset of the silver-coated titania thin films had shifted to 2.9 eV, towards the visible region of the electromagnetic spectrum, which in the absence of particle size modification, indicated doping of silver nanoparticles within the titanium dioxide structure. We had previously shown that doping titania thin films with either nitrogen or sulfur caused a shift in the band onset to 2.9 eV and 3.0 eV, respectively, indicating that these thin films would make better white light photocatalysts than titania alone. A lower band onset from silver-doped titania samples has been reported; a band onset

of 2.6 eV was estimated by Medina-Ramirez et al., (2011), although these were nanoparticulate composites and not thin films. The observed shift towards the visible spectrum could also be partly due to mixing of the band onsets silver oxide at approximately 1 eV for AgO and 1.4 eV for Ag_2O (Ida et al., 2008; Raju et al., 2009).

The water contact angle of the thin films was measured to determine any change in the hydrophilicity of the surface after irradiation with the different light sources. Superhydrophilicity occurs after photo-oxidation of hydrocarbons adsorbed onto the substrate, which results in the production of a hydroxylated surface (Zubkov et al., 2005). Predictably, the water contact angle of the titania thin films decreased after irradiation with the UV light source (Mills and LeHunte, 1997; Parkin and Palgrave, 2005) and the water contact angle of the silver coated titania thin films also decreased by a similar amount. The addition of silver nanoparticles to the surface of the titania thin film was predicted to result in an alteration of the hydrophilicity of the thin film prior to light exposure, as the surface roughness of the thin film had changed and larger contact angles are usually found on rougher surfaces, (Wenzel, 1936; Cassie and Baxter, 1944), but these data show this effect is insignificant even though silver coverage of the surface reached 64% (Dunnill et al., 2011). Irradiation with UV light did not have an effect on the water contact angle on the uncoated glass slide, although the water contact angle on the slide was initially low. The expected contact angle on a glass surface is approximately 70°, and the low reading observed in these experiments indicated that the glass substrate was in a very clean condition (Zubkov et al., 2005).

The visible light-induced hydrophilicity of the thin films was determined by irradiation with white light filtered with a sheet of Optivex™ glass, to eliminate any stray higher

energy photons of light with a wavelength of less than 400 nm. The water contact angle on the silver-coated titania thin film decreased to the same degree as that observed after UV irradiation. In contrast, no change in water contact angle was observed on the titania thin films. This clearly demonstrates the visible-light induced nature of the silver coated titania thin films.

The photo-oxidisation of stearic acid has been used extensively in the literature to indicate the photocatalytic activity of novel thin films and estimate their potential antibacterial activity (Mills et al., 2002; Mills and Wang, 2006; Brook et al., 2007a; 2007b; Page et al., 2007). The rate of stearic acid degradation was calculated for the N-doped and S-doped thin films assessed in the previous chapter after exposure to the white light source. The N-doped sample (N1) displayed a rate of destruction of approximately 1.4 x 10^{14} molecules / cm^2 per hour and the S-doped sample (S2) demonstrated a similar rate of 1.1 x 10^{14} molecules / cm^2 per hour (Dunnill et al., 2010). The silver-coated titania thin films generated in this chapter demonstrated rate of destruction of approximately 4.2 x 10^{14} molecules / cm^2 per hour, which is three times more efficient than the N-doped and S-doped thin films and twice as efficient as the titanium dioxide thin films. This implies that surface silver doping does not induce as much electron-hole recombination as that observed in the N-doped and S-doped titania, which results in improved photocatalysis.

The anatase titanium dioxide thin film should not exhibit any photo-activity after irradiation with the white light source, and activation should only occur after exposure to wavelengths of light below 385 nm as the band onset of titanium dioxide is 3.2 eV. The photo-activity observed suggests that there was light of an increased frequency

emitted from the white light source. The emission spectrum for the light source is shown in Figure 2.1 and no emission is detectable below 410 nm; however, the spectrum starts at 380 nm, so the profile at lower wavelengths is not known. White light sources, such as the fluorescent lamp used in these experiments, can leak very small amounts of higher energy photons of light as they age due to the release of phosphor from the inside of the fluorescent tubing, which could explain the photo-activity generated on the titanium dioxide thin film.

The Optivex™ UV filter was employed once more and the photo-activity of the silver-coated titania thin films was retained, and the photo-activity of the titania thin films was terminated. This demonstrated the true visible light driven photo-oxidation of stearic acid on the silver-coated titania thin films. The rate of stearic acid degradation was slower when the UV filter was employed, partly because the intensity of the white light was reduced, as only around 80% of emitted light was able to transmit through the glass shield and partly due to the loss of the UV part of the electromagnetic spectrum.

5.4.3 Antibacterial activity of the silver-doped titania thin films

The antibacterial properties of the silver-coated titania thin films were assessed using *E. coli* and EMRSA-16 as representative strains. Gram-negative strains such as *E. coli* have been demonstrated to be more difficult to kill using light-activated antimicrobial coatings than Gram-positive strains such as MRSA (Decraene et al., 2006; Page et al., 2009). However, in these experiments *E. coli* was eradicated from the silver-coated titania thin films at a quicker rate than EMRSA-16. A reduction in the recovery of *E. coli*

from the silver-coated titania thin films was observed after just 2 hours, and no viable bacteria could be recovered from the samples after 6 hours incubation. However, the observed antibacterial effect was independent of light exposure as a similar reduction in bacterial recovery was observed on the silver-coated titania incubated in the absence of light, which illustrates the activity was due to the toxicity of the silver ions rather than a light induced effect, which has been demonstrated in the literature (Feng et al., 2000; Kim et al., 2007; Jung et al., 2008). The increased susceptibility of Gram-negative bacteria to the silver containing thin film was postulated to be due to the thinner peptidoglycan layer in the cell membrane, which allows increased uptake into the interior of the bacterial cell (Schierholz et al., 1998). Conversely, Kowal et al., (2011) showed a greater susceptibility of MSSA and MRSA to silver-doped titania nanopowders compared with *E. coli*.

EMRSA-16 has been responsible for a significant proportion of the healthcare-associated cases of MRSA bacteraemia over the last decade and was shown in Chapter 3 to be a light tolerant strain of MRSA (Johnson et al., 2001; Ellington et al., 2010). The antibacterial activity of the silver-coated titania thin films increased with prolonged exposure to white light, with the largest reduction in bacterial recovery observed after 18 hours irradiation. Enhancement of the photocatalytic properties of the light-activated surface by the silver particles and the enhancement of the toxic properties of the silver by titania was observed on the silver-coated titania, which demonstrated a synergistic relationship between the two components of the thin film. This effect was much greater than that observed when the silver-coated titania films were incubated in the absence of light, or when either the titania or uncoated samples were irradiated

with white light. The silver ions alone appeared to have an effect on EMRSA-16, especially after a prolonged incubation time, but this was less significant than the effect seen after light exposure. The lack of activity observed on the uncoated glass slides demonstrated that the white light source did not have an inhibitory effect on the viability of EMRSA-16. The lack of activity observed on the titania thin film in the presence of 6 or 12 hours white light indicated that the UV component of the white light source was not sufficient to photo-activate the titania films. However, this pattern was not maintained and a significant difference in the recovery of EMRSA-16 from the irradiated TiO_2 thin films was observed, compared with the uncoated glass slides after 18 hours. This effect was not eliminated when the Optivex™ UV filter was applied. The significant decrease in recovery of EMRSA-16 observed on the TiO_2 thin film incubated in the dark suggests that a light-independent mechanism of action was involved.

It is possible to conclude that the photo-induced destruction was due to reactive oxygen produced by titania, driven by white light photocatalysis, induced by the silver. These effects did not occur in the absence of white light or silver. An alternative explanation could involve photo-assisted release of silver ions from the silver-coated titania, which in turn caused the antibacterial effect.

A major limitation of the experiments was that the test conditions were laboratory-controlled and did not take into account factors such as organic soil, which would be present on hand-touch surfaces. Substances such as sebaceous oils, blood and other human secretions would be likely to contaminate the thin films if they were used as antibacterial coatings in a patient environment, and the effect of these substances should be investigated as they are likely to cause an inhibition in the photocatalytic

activity of the thin films (Furno et al., 2004). Organic soiling of a surface is likely to precede bacterial contamination (Verran et al., 2002), so if the thin films were able to photo-degrade any organic soil present it would keep the surface hygienically clean and eliminate a potential nutrient source of any colonising bacteria.

5.5 Conclusion

This chapter has demonstrated that the antibacterial activity of titania thin films can be significantly enhanced by the addition of surface-bound silver/silver oxide nanoparticles. The thin films displayed photochromic behaviour and were found as either silver oxide or pure silver, depending on the storage conditions; oxidation of silver to silver oxide occurred after storage in the dark and a purple colouration whilst exposure to indoor lighting conditions caused photo-reduction of the silver oxide back to silver and an orange coloured film. White light induced photocatalysis was generated by a shift in the band onset of the thin films, caused by the addition of silver nanoparticles. Visible light photocatalysis was demonstrated when a UV filter was used to block out the minimal UV component of the white light source, and this was observed in the form of photo-oxidation of stearic acid, a reduction in the water contact angle and photocatalytic activity against EMRSA-16. This is the first example of unambiguous visible light photocatalysis and photo-induced superhydrophilicity alongside a titanium dioxide control that shows no activation.

6 Assessment of a novel antibacterial material for use in endotracheal tubes in intubated patients

6.1 Introduction

Ventilator-associated pneumonia (VAP) is a HCAI associated with significant morbidity and mortality. Intubated patients have an endotracheal tube (ETT) *in situ* to allow mechanically assisted breathing, which compromises the normal clearance of mucus and other upper airway secretions and allows micro-aspiration of contaminated subglottic secretions into the lungs. These secretions contain commensal bacteria that provide a source for pulmonary infection. In addition, the lumen of the ETT itself becomes colonised with bacteria, which provides a secondary source of infective organisms (Deem and Treggiari, 2010). A number of studies investigating the microbiology of VAP have shown that Gram-negative bacilli are isolated more commonly in patients with VAP compared with patients with hospital-acquired pneumonia (i.e. pneumonia acquired in hospital in the absence of mechanical ventilation). *P. aeruginosa, Acinetobacter* species and *S. maltophilia* are the most commonly observed Gram-negative pathogens causing VAP (Johanson et al., 1972; Richards et al., 1999; Weber et al., 2007; Bouadma et al., 2010). Both meticillin-sensitive and resistant *S. aureus* have also been isolated, but were observed more frequently in non-intubated patients (Weber et al., 2007).

It is advantageous to reduce microbial load and decrease biofilm formation in the lumen of the ETT as this would eliminate the bacterial reservoir and lower the risk of developing VAP. The use of antimicrobial silver ETTs has been recommended in combination with additional clinical measures in the prevention of VAP (Torres et al.,

2009; Coppadoro et al., 2011) and it would be desirable to expand on the pool of antimicrobial ETTs available. Photodynamic inactivation (PDI) of bacteria has proven to be an effective method of reducing the bacterial load on surfaces and this technology has the potential to be applied to an ETT. A laser light could be inserted along the length of the ETT and switched on periodically to activate the surface and kill any bacteria present. Figure 6.1 shows how this may be achieved in a catheter tube.

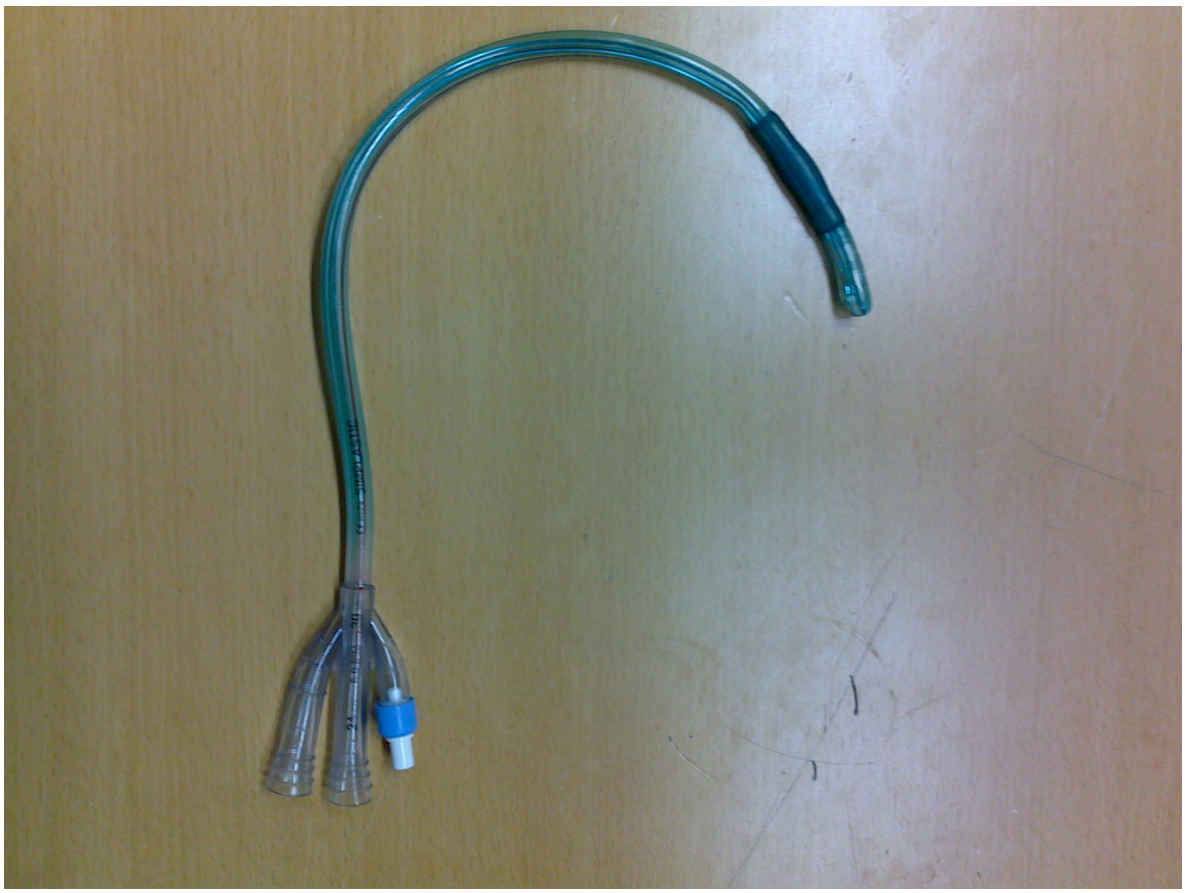

Figure 6.1 A catheter tube impregnated with the photosensitising agent methylene blue. It is suggested that light from a laser could be projected through the tube with the use of fibre optics. Photograph courtesy of Prof. Wilson (UCL).

This chapter describes the development of a polyurethane polymer which was impregnated with the photosensitising agent toluidine blue O (TBO). The antibacterial effect of the impregnated polymers after irradiation with laser light was observed

against a series of pathogens known to cause VAP. Both clinical and type strains were tested to assess any difference in susceptibility to PDI. The published literature described above was used to guide the choice of bacteria and material type assessed in this chapter.

6.2 Materials and methods

6.2.1 Material synthesis

The polyurethane polymers required for this series of experiments were synthesised as described in Section 2.10.3. Polymers were prepared containing TBO (S+) and control polymers were prepared in parallel without the addition of TBO (S-).

6.2.2 Measuring the antibacterial photo-activity of the TBO-impregnated polymers

Bacterial strains were maintained as described in Section 2.1 and bacterial suspensions of *P. aeruginosa* PAO1 and clinical strains of *P. aeruginosa, A. baumannii* and *S. maltophilia* were prepared as detailed in Section 2.3, resulting in a starting inoculum of approximately 10^7 cfu / ml, which equated to a concentration of approximately 10^6 cfu / polymer as described in Section 2.12.3. A suspension of *C. albicans* (10^7 cfu / ml) was also prepared as described in Section 2.3. The Mann Whitney U test was used for all statistical analyses to determine the statistical significance of any differences observed, as described in Section 2.13. The nomenclature used during this series of experiments is detailed in Table 6.1.

Table 6.1 Nomenclature used during microbiological assessment of the TBO-impregnated polymers

Nomenclature	Description
L+S+	TBO-impregnated sample exposed to laser light
L+S-	TBO-impregnated sample NOT exposed to laser light
L-S+	Non TBO-impregnated sample exposed to laser light
L-S-	Non TBO-impregnated sample NOT exposed to laser light

6.3 Results

6.3.1 Assessment of the antibacterial photo-activity of the TBO-impregnated polymers against *P. aeruginosa* PAO1, a type strain

The activity of the TBO-impregnated polyurethane polymers was first assessed against a type strain of *P. aeruginosa,* PAO1. The polymers were exposed to the laser light for time periods of between 30 seconds and 240 seconds and the results are illustrated in Figure 6.2 through to Figure 6.10.

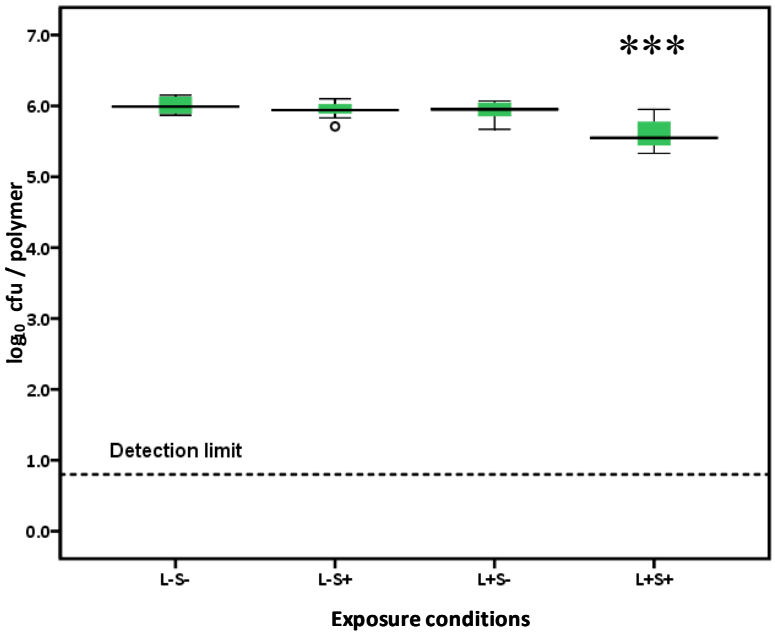

Figure 6.2 Antibacterial activity of TBO-impregnated polyurethane polymer against *P. aeruginosa* PAO1 after 30 seconds. The dotted horizontal line indicates the detection limit of the sampling method, 0.80 $\log_{10}$ cfu / polymer.

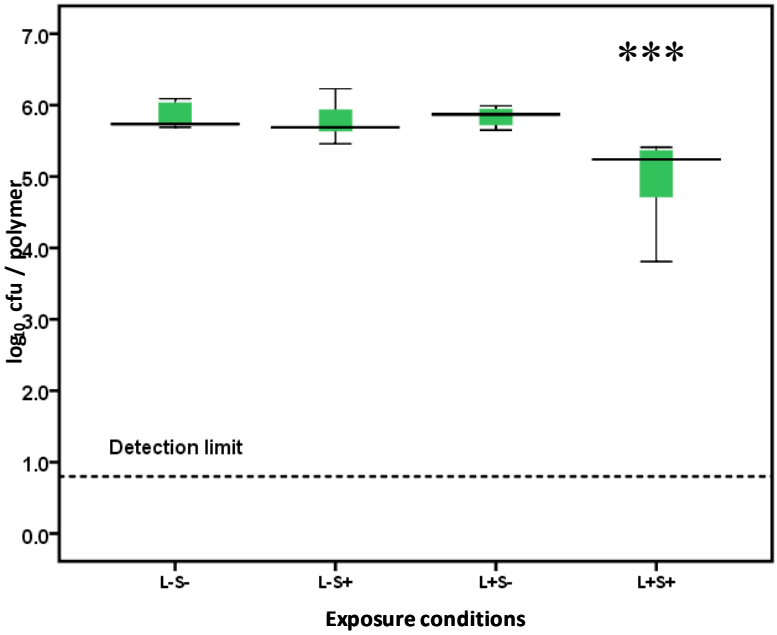

Figure 6.3 Antibacterial activity of TBO-impregnated polyurethane polymer against *P. aeruginosa* PAO1 after 60 seconds. The dotted horizontal line indicates the detection limit of the sampling method, 0.80 $\log_{10}$ cfu / polymer.

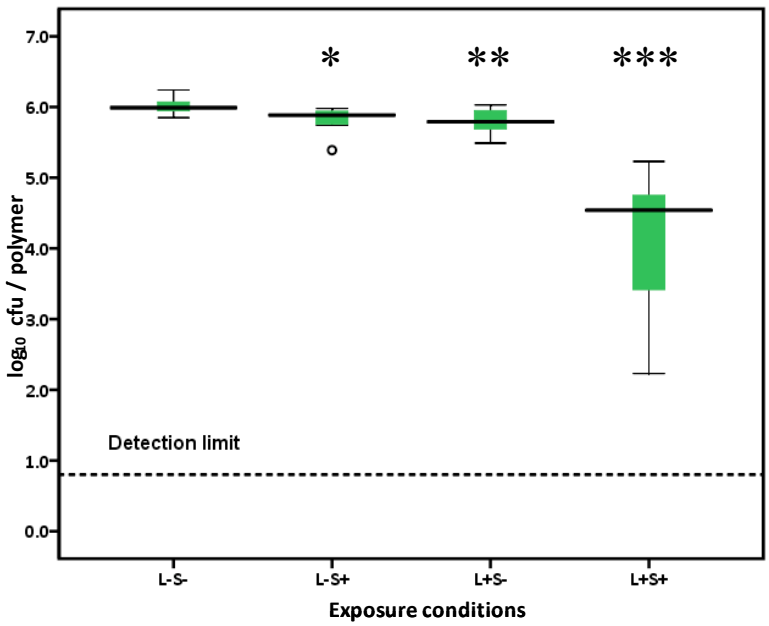

Figure 6.4 Antibacterial activity of TBO-impregnated polyurethane polymer against *P. aeruginosa* PAO1 after 90 seconds. The dotted horizontal line indicates the detection limit of the sampling method, 0.80 $\log_{10}$ cfu / polymer.

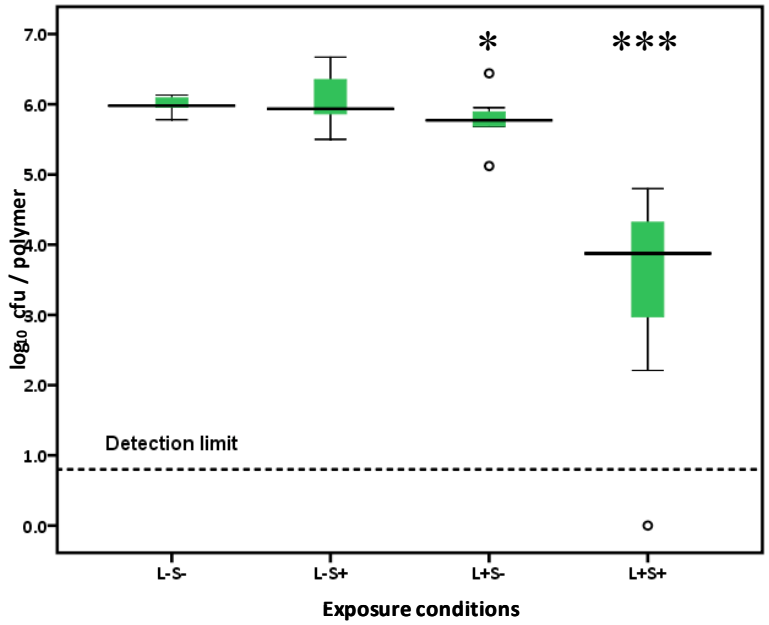

Figure 6.5 Antibacterial activity of TBO-impregnated polyurethane polymer against *P. aeruginosa* PAO1 after 120 seconds. The dotted horizontal line indicates the detection limit of the sampling method, 0.80 $\log_{10}$ cfu / polymer.

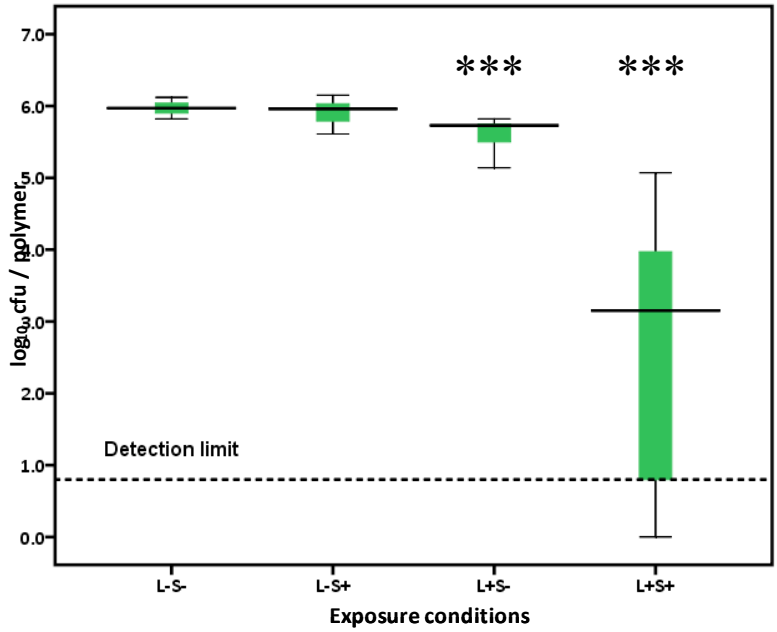

Figure 6.6 Antibacterial activity of TBO-impregnated polyurethane polymer against *P. aeruginosa* PAO1 after 150 seconds. The dotted horizontal line indicates the detection limit of the sampling method, 0.80 $\log_{10}$ cfu / polymer.

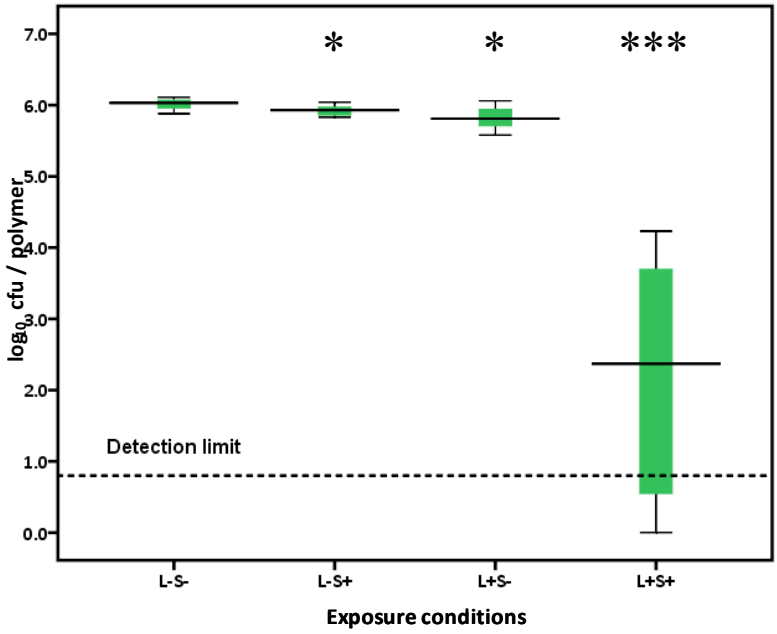

Figure 6.7 Antibacterial activity of TBO-impregnated polyurethane polymer against *P. aeruginosa* PAO1 after 180 seconds. The dotted horizontal line indicates the detection limit of the sampling method, 0.80 $\log_{10}$ cfu / polymer.

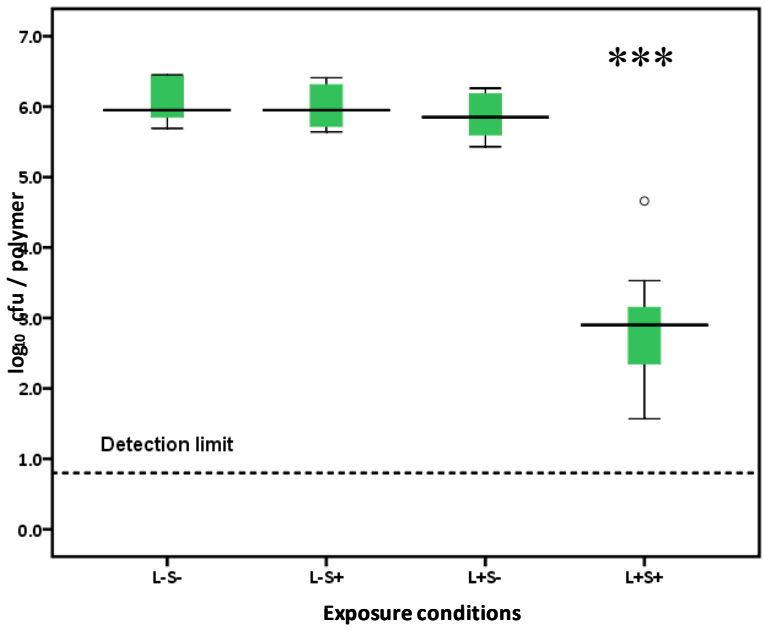

Figure 6.8 Antibacterial activity of TBO-impregnated polyurethane polymer against *P. aeruginosa* PAO1 after 210 seconds. The dotted horizontal line indicates the detection limit of the sampling method, 0.80 $\log_{10}$ cfu / polymer.

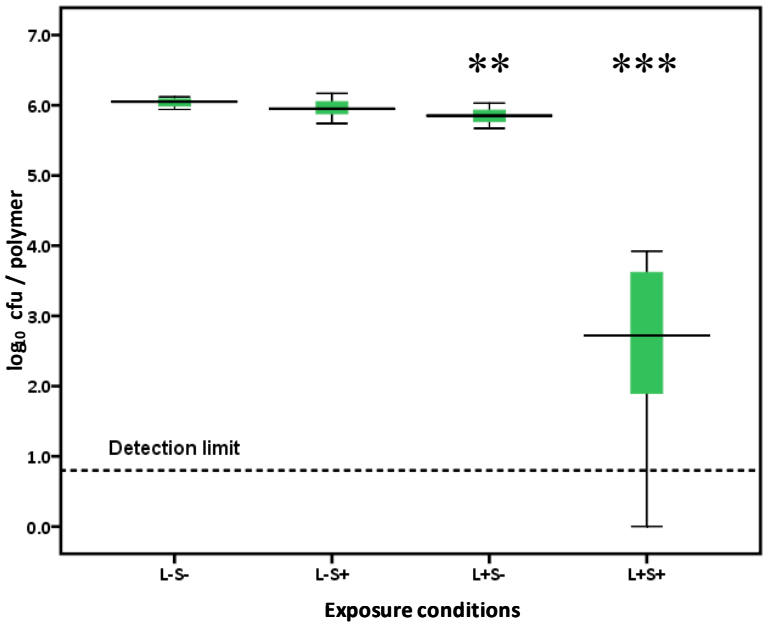

Figure 6.9 Antibacterial activity of TBO-impregnated polyurethane polymer against *P. aeruginosa* PAO1 after 240 seconds. The dotted horizontal line indicates the detection limit of the sampling method, 0.80 $\log_{10}$ cfu / polymer.

Highly statistically significant reductions in the number of viable *P. aeruginosa* PAO1 recovered from the TBO-impregnated polymers was observed at all time points tested

(all $p < 0.001$). The reduction in bacterial count followed a dose-dependent response, whereby as the dose of laser light was increased, the antibacterial activity of the impregnated polymers increased, which resulted in a lower recovery of bacteria. For example, a 1.41 $\log_{10}$ cfu / polymer decrease was observed after 90 seconds exposure to the laser light (Figure 6.5), rising to a 2.94 $\log_{10}$ cfu / polymer decrease after 180 seconds (Figure 6.7) and a 3.33 $\log_{10}$ cfu / polymer decrease after 240 seconds (Figure 6.9). The results from all of the experiments are summarised in Table 6.2.

Table 6.2 Summary of the data obtained from the *P. aeruginosa* PAO1 experiments. The stated reductions in bacteria are calculated by comparing the median bacterial recovery from the L-S- sample with the L+S+ sample.

Exposure time / seconds	Log reduction / cfu per polymer	Percentage reduction / cfu per polymer
30	0.44	63.9
60	0.49	67.9
90	1.41	96.1
120	2.09	99.2
150	2.82	99.85
180	2.94	99.89
210	3.05	99.91
240	3.33	99.95

The observed reductions in bacterial recovery were highly statistically significant ($p < 0.001$) at all time points (L-S- compared with L+S+), which demonstrates the potent light-dependent antibacterial activity of the TBO-impregnated polymers. When the two groups of TBO-impregnated polymers were compared and the effect of the laser

light was investigated (L-S+ and L+S+), the recovery of *P. aeruginosa* from the TBO-impregnated polymers exposed to light was significantly lower than recovery from the TBO-impregnated polymers incubated in the dark. This difference was highly statistically significant ($p < 0.001$) for all time points above 60 seconds; the difference was also statistically significant after 30 seconds with a p value of $p < 0.01$. These data further confirm the photocatalytic nature of the TBO-impregnated polymers. There was no statistical difference in the bacterial recovery obtained from the two sets of polymers incubated in the dark (L-S- compared with L-S+), which demonstrates the intrinsic lack of antibacterial activity of TBO in the absence of light of an appropriate wavelength.

6.3.2 Assessment of the antibacterial photo-activity of the TBO-impregnated polymers against a clinical strain of *P. aeruginosa*

The photo-activity of the TBO-impregnated polyurethane polymers was assessed against a clinical strain of *P. aeruginosa* to assess whether there were any differences in the susceptibility of the laboratory type strain compared with a strain recently isolated from a patient with clinically confirmed VAP. The polymers were exposed to the laser light for time periods of 90 seconds, 180 seconds and 240 seconds, using the same initial bacterial inoculum of approximately 10^6 cfu bacteria per polymer.

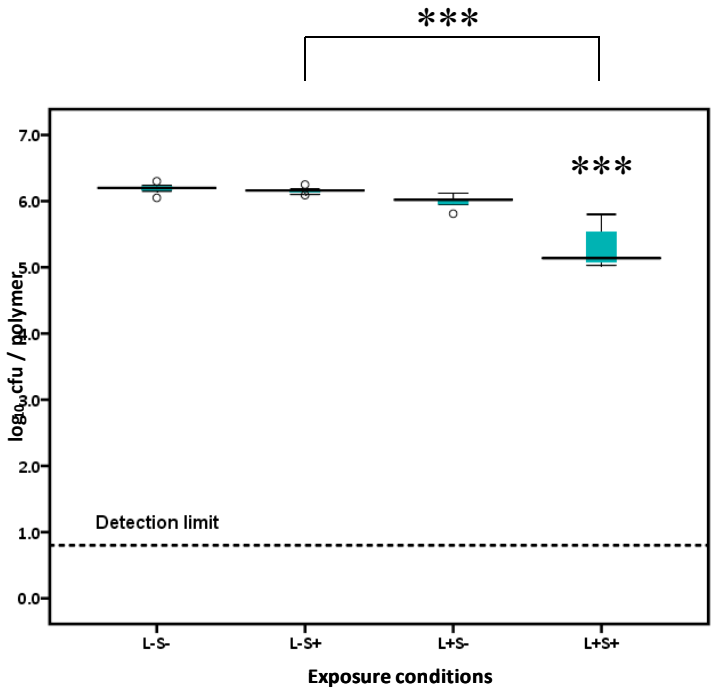

Figure 6.10 Antibacterial activity of TBO-impregnated polyurethane polymer against a clinical strain of *P. aeruginosa* after 90 seconds. The dotted horizontal line indicates the detection limit of the sampling method, 0.80 log_{10} cfu / polymer.

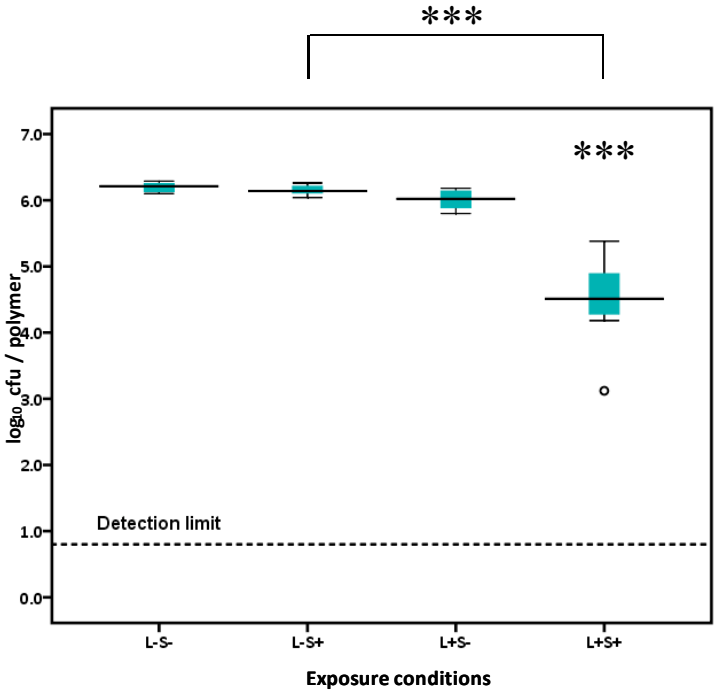

Figure 6.11 Antibacterial activity of TBO-impregnated polyurethane polymer against a clinical strain of *P. aeruginosa* after 180 seconds. The dotted horizontal line indicates the detection limit of the sampling method, 0.80 log_{10} cfu / polymer.

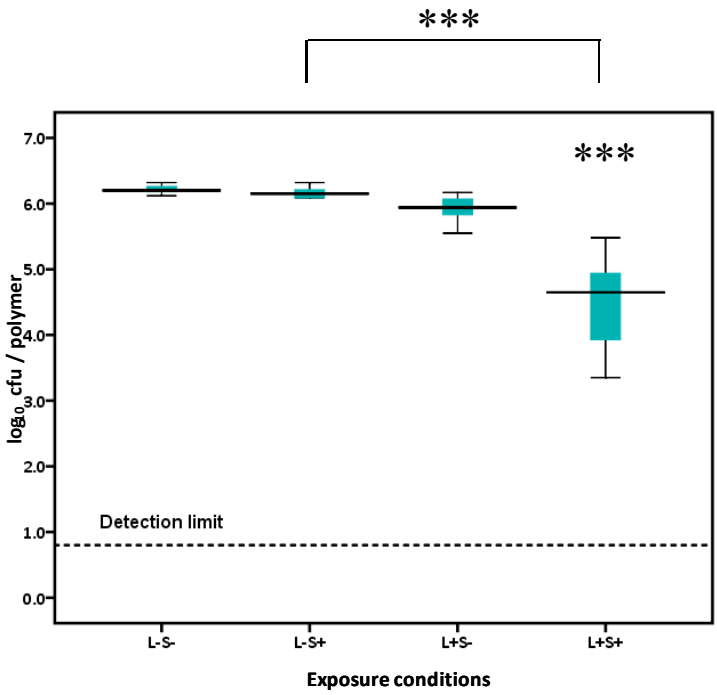

Figure 6.12 Antibacterial activity of TBO-impregnated polyurethane polymer against a clinical strain of *P. aeruginosa* after 240 seconds. The dotted horizontal line indicates the detection limit of the sampling method, 0.80 log_{10} cfu / polymer.

A highly significant reduction in the recovery of the clinical strain *P. aeruginosa* from the TBO-impregnated polymers after exposure to the laser light was achieved after 90 seconds (Figure 6.10), 180 seconds (Figure 6.11) and 240 seconds (Figure 6.12). This reduction was highly statistically significant for all time points tested ($p < 0.001$). A highly statistically significant decrease ($p < 0.001$) was observed on the TBO-impregnated polymers exposed to the laser light compared with those not exposed to the laser light. A lack of antibacterial activity was demonstrated in the absence of laser light; there was no statistical difference in the recovery of *P. aeruginosa* from the two sets of polymers, which were not exposed to the laser at any light exposure time. Combining these data illustrates the laser light-induced antibacterial nature of the polymers.

The direct effect of the laser light on the viability of *P. aeruginosa* was determined by comparing the bacterial counts from the non-impregnated polymers with the bacterial counts from the TBO-impregnated polymers irradiated with laser light. A small decrease can be observed on the box plots which was statistically significant ($p < 0.001$ at 90 s and 240 s; $p < 0.05$ at 180 s); however this reduction was not substantial (<0.5 log cfu / polymer reduction) and it is more likely that this is due to the small variation in the bacterial count rather than a genuine effect of the laser. To reinforce this statement, the bacterial count of *P. aeruginosa* from the non TBO-impregnated polymers exposed to the laser light (L+S-) was compared with that obtained from the TBO-impregnated polymers exposed to the laser light (L+S+), large reductions in bacterial counts were observed for all three time points tested (0.88, 1.51 and 1.29 $\log_{10}$ cfu / polymer decreases after 90, 180 and 240 seconds respectively), which were all highly statistically significant ($p < 0.001$).

The difference in the susceptibility of the two *P. aeruginosa* strains was investigated and summarised in Table 6.3. It was immediately evident that the laboratory type strain of *P. aeruginosa* PAO1 was more susceptible to the photodynamic effect of the TBO-impregnated polymers, compared with the clinical isolate. A greater recovery of bacteria was obtained during the experiments with the clinical *P. aeruginosa* isolate compared with the type strain, and this was demonstrated after 90, 180 and 240 seconds.

Table 6.3 Comparison of the data obtained from the two sets of *P. aeruginosa* experiments. The stated reductions in bacteria are calculated by comparing the median bacterial recovery from the L-S- sample with the L+S+ sample.

Exposure time / seconds	Clinical strain of *P. aeruginosa*		*P. aeruginosa* PAO1	
	Log reduction / cfu per polymer	Percentage reduction / cfu per polymer	Log reduction / cfu per polymer	Percentage reduction / cfu per polymer
90	1.06	91.3	1.41	96.1
180	1.70	98.0	2.94	99.89
240	1.55	97.2	3.33	99.95

6.3.3 Assessment of the antibacterial photo-activity of the TBO-impregnated polymers against a clinical strain of *A. baumannii*

The activity of the TBO-impregnated polyurethane polymers was subsequently assessed against a recently isolated clinical strain of *A. baumannii* and the results are displayed in the following three figures. The polymers were exposed to the laser light for time periods of 90 seconds, 180 seconds and 240 seconds, using the same concentration of approximately 10^6 cfu bacteria per polymer.

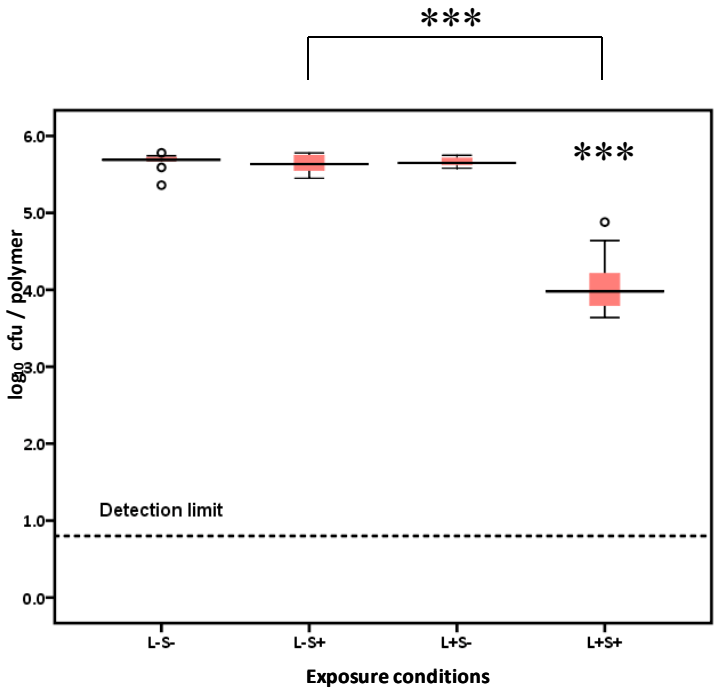

Figure 6.13 Antibacterial activity of TBO-impregnated polyurethane polymer against a clinical strain of *A. baumannii* after 90 seconds. The dotted horizontal line indicates the detection limit of the sampling method, 0.80 $\log_{10}$ cfu / polymer.

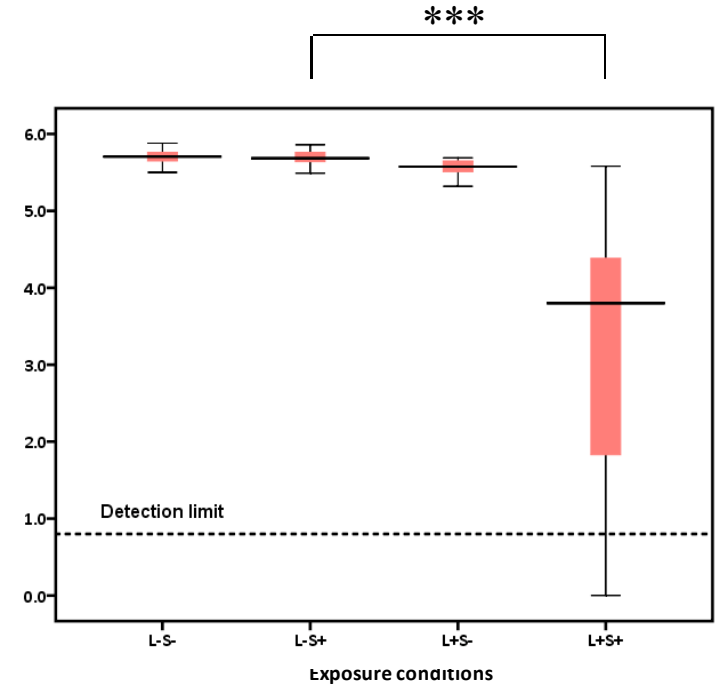

Figure 6.14 Antibacterial activity of TBO-impregnated polyurethane polymer against a clinical strain of *A. baumannii* after 180 seconds. The dotted horizontal line indicates the detection limit of the sampling method, 0.80 $\log_{10}$ cfu / polymer.

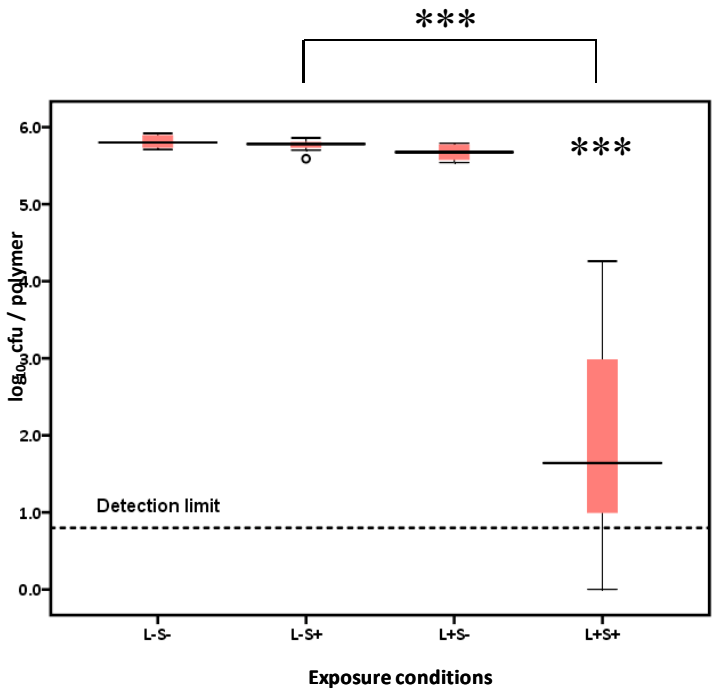

Figure 6.15 Antibacterial activity of TBO-impregnated polyurethane polymer against a clinical strain of *A. baumannii* after 240 seconds. The dotted horizontal line indicates the detection limit of the sampling method, 0.80 $\log_{10}$ cfu / polymer.

A reduction in the recovery of *A. baumannii* from the TBO-impregnated polymers was achieved after 90 seconds (Figure 6.13), 180 seconds (Figure 6.14) and 240 seconds (Figure 6.15) irradiation with the laser light, demonstrating the photocatalytic activity of the TBO-impregnated polymers. These reductions were all highly statistically significant ($p < 0.001$). There was no statistical difference in the recovery of *A. baumannii* from the two sets of polymers which were not exposed to the laser light (L-S- and L-S+), confirming the light dependent properties of the TBO-impregnated material. When the effect of the laser light alone was investigated (L-S- and L+S-), a statistically significant difference was observed at 180 seconds ($p < 0.001$) and 240 seconds ($p < 0.05$), and not at 90 seconds but the figures show that this reduction is minimal and this is likely to be a consequence of the small amount of variation in bacterial counts seen in these two groups. Furthermore, highly statistically significant

reductions ($p < 0.001$) were achieved when the recovery from the TBO-impregnated polymers exposed to the laser light were compared with the irradiated non-impregnated polymers, further emphasising the requirement for both the laser light and the photosensitiser to exert a highly significant, consistent antibacterial effect.

6.3.4 Assessment of the antibacterial photo-activity of the TBO-impregnated polymers against a clinical strain of *S. maltophilia*

The activity of the TBO-impregnated polyurethane polymers was assessed against a newly isolated clinical strain of *S. maltophilia* and the results are displayed in the following figures. The polymers were exposed to the laser light for time periods of 90 seconds, 180 seconds and 240 seconds, using the same concentration of approximately 10^6 cfu bacteria per polymer.

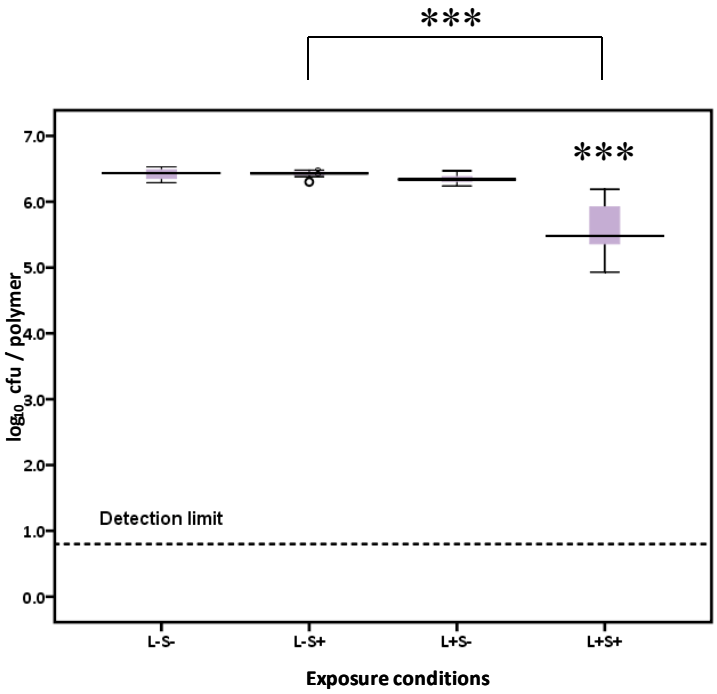

Figure 6.16 Antibacterial activity of TBO-impregnated polyurethane polymer against a clinical strain of *S. maltophilia* after 90 seconds. The dotted horizontal line indicates the detection limit of the sampling method, 0.80 log_{10} cfu / polymer.

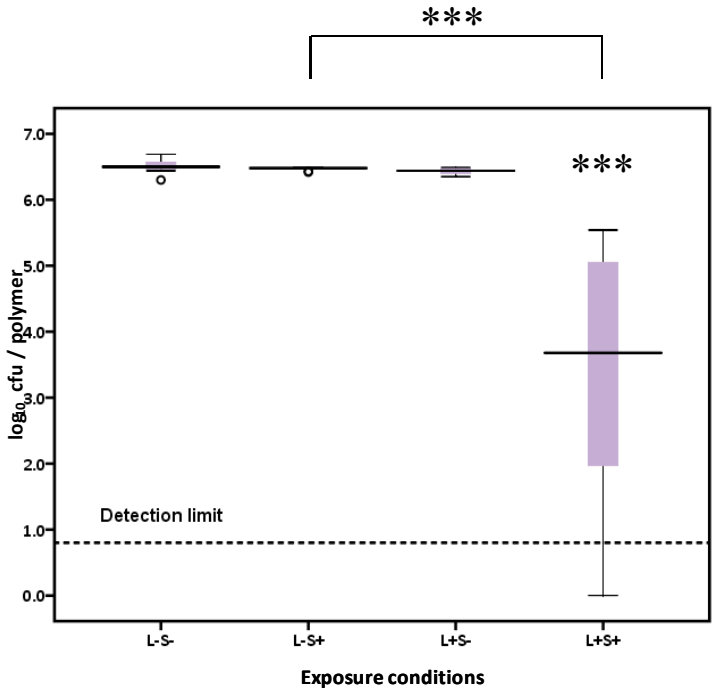

Figure 6.17 Antibacterial activity of TBO-impregnated polyurethane polymer against a clinical strain of *S. maltophilia* after 180 seconds. The dotted horizontal line indicates the detection limit of the sampling method, 0.80 log_{10} cfu / polymer.

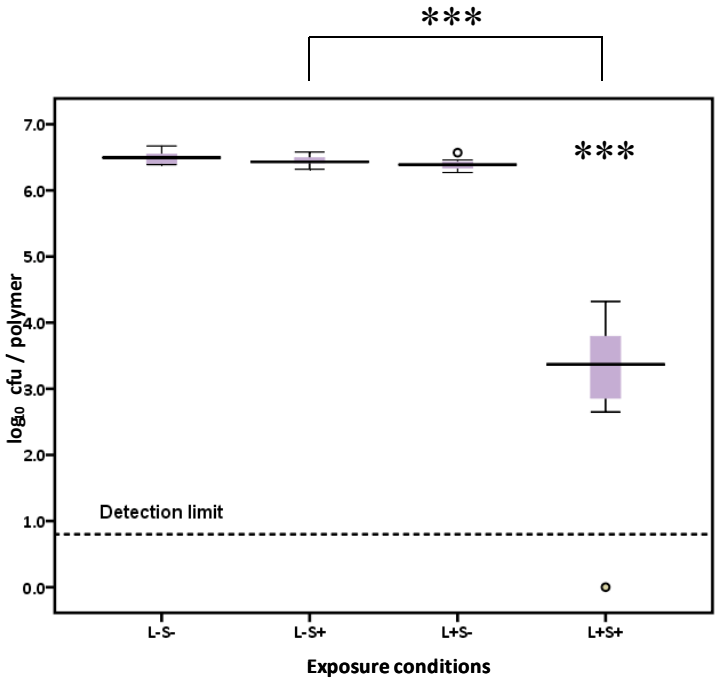

Figure 6.18 Antibacterial activity of TBO-impregnated polyurethane polymer against a clinical strain of *S. maltophilia* after 240 seconds. The dotted horizontal line indicates the detection limit of the sampling method, 0.80 $\log_{10}$ cfu / polymer.

The TBO-impregnated polymers exerted a significant antibacterial effect on *S. maltophilia* after exposure to the laser light for 90 seconds (Figure 6.16), 180 seconds (Figure 6.17) and 240 seconds (Figure 6.18). This reduction was highly statistically significant ($p < 0.001$) for all of the three exposure times. Comparison of the two groups of TBO-impregnated polymers showed a statistically significant decrease in the recovery of *S. maltophilia* from the polymers exposed to the laser light compared to that recovered from those polymers not exposed to the laser light. There was no statistical difference in the recovery of *S. maltophilia* from the two sets of polymers incubated in the absence of laser light (L-S- and L-S+), demonstrating the light dependent activity of the polymers. A small but statistically significant reduction in bacterial counts was observed when the direct effect of the laser light was investigated by comparing values obtained from recovery from the two groups of non-impregnated

polymers, but the effect of the laser light in combination with the impregnated photosensitiser was much larger. This finding mirrors the data obtained in the previous experimental sections assessing the activity of the TBO-impregnated polymers against *A. baumannii* (Section 6.3.3) and *P. aeruginosa* (Sections 0 and 6.3.2).

6.3.5 Assessment of the antibacterial photo-activity of the TBO-impregnated polymers against a clinical strain of *C. albicans*

The activity of the TBO-impregnated polyurethane polymers was assessed against a recently isolated clinical strain of *C. albicans* and the results are displayed in the following figures. The polymers were exposed to the laser light for time periods of 90 seconds, 180 seconds and 240 seconds, using the same concentration of approximately 10^6 cfu bacteria per polymer.

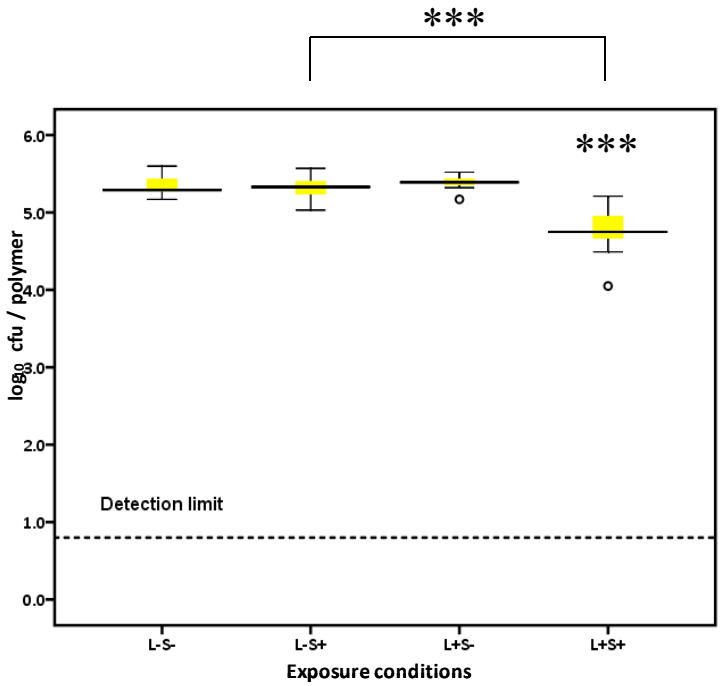

Figure 6.19 Antimicrobial activity of TBO-impregnated polyurethane polymer against a clinical strain of *C. albicans* after 90 seconds. The dotted horizontal line indicates the detection limit of the sampling method, 0.80 $\log_{10}$ cfu / polymer.

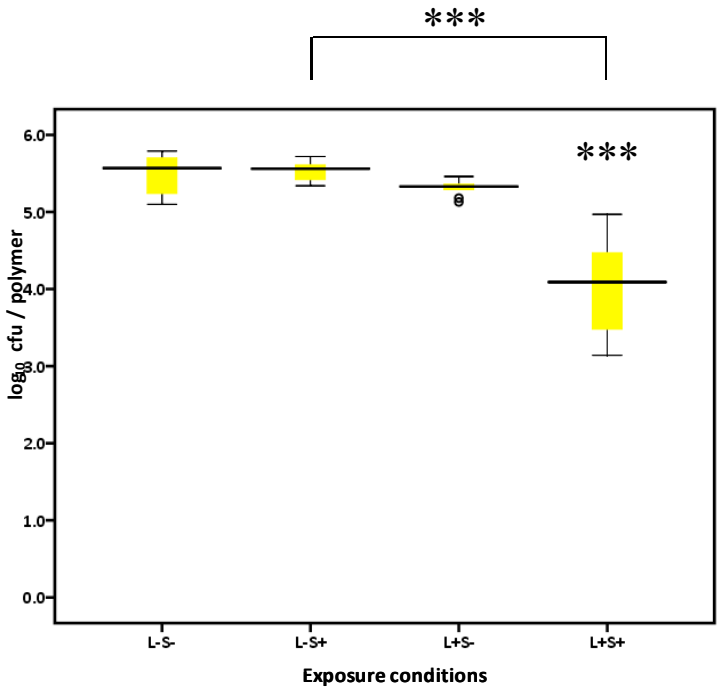

Figure 6.20 Antimicrobial activity of TBO-impregnated polyurethane polymer against a clinical strain of *C. albicans* after 180 seconds. The dotted horizontal line indicates the detection limit of the sampling method, 0.80 log_{10} cfu / polymer.

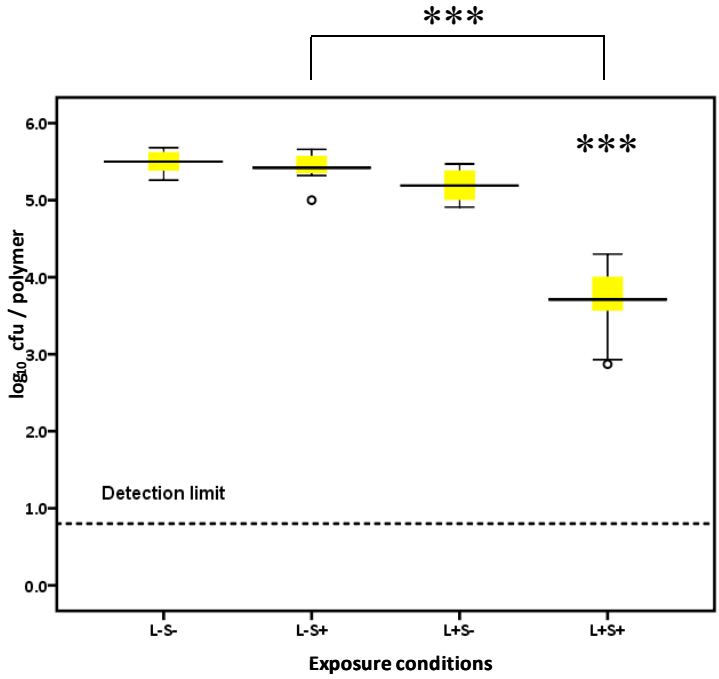

Figure 6.21 Antimicrobial activity of TBO-impregnated polyurethane polymer against a clinical strain of *C. albicans* after 240 seconds. The dotted horizontal line indicates the detection limit of the sampling method, 0.80 log_{10} cfu / polymer.

A decrease in the recovery of *C. albicans* from the TBO-impregnated polymers was noted after exposure to the laser light for 90 seconds (Figure 6.19), 180 seconds (Figure 6.20) and 240 seconds (Figure 6.21). The observed reduction was highly statistically significant ($p < 0.001$) for all of the three exposure times. The findings were similar to those obtained from the experiments involving bacterial causes of VAP, in that a decrease in the recovery of *C. albicans* was not detected from the TBO-impregnated polymers when incubated in the dark (L-S- compared with L-S+, $p>0.05$). Moreover, the laser light had no effect on the recovery of *C. albicans* after 90 seconds or 180 seconds irradiation and although a statistically significant decrease was observed after 240 seconds, the difference is rather small in absolute terms (0.31 $\log_{10}$ cfu / polymer). When the effect of the laser light in combination with TBO was compared with the TBO alone, a highly statistically significant decrease in count was observed, demonstrating the light-activated nature of the TBO-impregnated polymers.

The data from this chapter are summarised below in Table 6.4. It is immediately evident that the TBO-impregnated polymers in combination with the laser light exert an antimicrobial effect against all the organisms tested after 90 seconds, 180 seconds and 240 seconds. The TBO-impregnated polymers were most effective against *A. baumannii* where a reduction of over 4 $\log_{10}$ cfu / polymer was achieved after 240 seconds and was least effective against *C. albicans*, but a significant reduction approaching 2 $\log_{10}$ cfu / polymer was still observed after 240 seconds. As mentioned previously, the clinical isolate of *P. aeruginosa* was less susceptible to the photo-active nature of the TBO-impregnated polymers and a smaller reduction was observed compared with the laboratory type strain.

Table 6.4 Summary of the data obtained from the experiments investigating the activity of the TBO-impregnated polymers. The stated reductions in bacteria are calculated by comparing the bacterial recovery from the L-S- sample with the L+S+ sample.

Exposure time / seconds	Log reduction / cfu per polymer				
	P. aeruginosa PAO1	*P. aeruginosa*, clinical isolate	*A. baumannii*, clinical isolate	*S. maltophilia*, clinical isolate	*C. albicans*, clinical isolate
90	1.41	1.06	1.72	0.96	0.54
180	2.94	1.70	1.90	2.82	1.48
240	3.33	1.55	4.16	3.12	1.79

6.4 Discussion

6.4.1 TBO-mediated photodynamic bacterial inactivation

The assessment of novel antimicrobial materials for use in endotracheal tubes is a timely and pertinent task. Therefore, in this chapter, polyurethane polymers were impregnated with the photosensitiser TBO and exposed to wavelengths of light known to cause photoactivity. Polyurethane is a material commonly used in ETTs (Berra et al., 2008a; 2008b; Rello et al., 2010) and the polymers were impregnated with TBO rather than coated, as the process allows application of the antibacterial agent on both the inner and outer surfaces of the catheter, which can increase overall antibacterial activity (Furno et al., 2004). The TBO-impregnated polymers were assessed against a range of bacterial species commonly isolated from patients with VAP and the yeast *C. albicans* which has also been cultured from this patient group (Weber et al., 2007; Bouadma et al., 2010). Previous work in our laboratory has shown that the TBO-impregnated polymers produced photodynamic inactivation (PDI) of a meticillin-

resistant strain of *S. aureus* (EMRSA-16) and *E. coli* (Perni et al., 2009b). The current study expanded on these data to investigate the photoactivity of the polymers against the most common causes of VAP.

These experiments have shown that the TBO-impregnated polymers exerted a significant antimicrobial effect on all organisms tested after irradiation with laser light. The reductions followed a dose-dependent response, so that the greatest reductions in bacterial (or yeast) numbers were observed after the longest irradiation time. *A. baumannii* was shown to be most susceptible to photodynamic inactivation with the TBO-impregnated polymers, and a reduction of over 4 $\log_{10}$ cfu / polymer was achieved after a 4 minute irradiation time. Reductions of over 3 $\log_{10}$ cfu / polymer were also achieved in the recovery of *P. aeruginosa* PAO1 and *S. maltophilia* after the same irradiation time.

Many groups have reported photodynamic inactivation of a range of planktonic bacteria and yeasts in the presence of an aqueous solution of TBO and laser light. *E. coli* was first shown to be susceptible to a 2.5 μM solution of TBO in the presence of a tungsten lamp at a light intensity of 5400 lux. The generation of singlet oxygen during irradiation was confirmed as the addition of the singlet oxygen quencher, α-tocopherol reduced the photoactivity of the dye (Wakayama et al., 1980). A 2 - 3 $\log_{10}$ cfu / ml decrease in the recovery of *A. baumannii* was described after exposure to 635 nm light at a concentration of 2 μM and 22.5 J / cm^2 energy (Ragas et al., 2010) but a pre-sensitisation step of 30 minutes was required to achieve this level of photoinactivation. MRSA was shown to be susceptible to a suspension of TBO after exposure to a HeNe laser light for just 30 seconds (Wilson and Yianni, 1995) and the

susceptibility of *E. faecalis, B. cereus* and *P. aeruginosa* was demonstrated against a variety of phenothiazinium dyes including TBO after 60 minutes light exposure (Wainwright et al., 1997).

Gram-negative bacteria have been shown to be less susceptible than Gram-positive bacteria to the photoactivity of the TBO-impregnated polymers (Perni et al., 2009b) and to photodynamic therapy using other photosensitisers such as methylene blue and rose bengal (Phoenix et al., 2003; Decraene et al., 2006; Perni et al., 2009a). The cytoplasmic membrane is the primary target of the singlet oxygen generated during irradiation with the laser light (Wakayama et al., 1980; Jori et al., 2006), which has been demonstrated in *E. coli* and *S. cerevisiae* (Ito, 1977; Ito and Kobayashi, 1977). Gram-negative bacteria have a reduced rate of uptake of singlet oxygen due to the presence of the outer membrane (Jori et al., 2006), which prevents direct interaction of the singlet oxygen with the underlying cytoplasmic membrane. It also acts as a permeability barrier, preventing the diffusion of small molecules into the cytoplasm of the cell. Conversely, Gram-positive bacteria are surrounded by a relatively porous layer of peptidoglycan and are more likely to be susceptible to the action of the reactive oxygen species generated on the surface of the polymers. DNA damage occurs in Gram-positive and Gram-negative bacteria and in yeast cells once the permeability of the external membrane has been compromised and the reactive oxygen species are able to penetrate the interior of the cells (Dunipace et al., 1992; Chi et al., 2010). The susceptibility of Gram-negative bacteria to the effect of the TBO-impregnated polymers suggests that the mechanism of activity is the Type II pathway (Figure 1.11). The photosensitiser was immobilised in the polymer and was not able to interact

directly with the bacterial cell wall and so the phototoxic effect occurred via the generation of singlet oxygen which oxidised molecules in the outer membrane. It was hypothesised that reactive oxygen species generated by the Type I pathway wereunable to cause lethal damage to the outer membrane and required penetration of the membrane in order to exert lethal PDI (Jori et al., 2006).

It was hypothesised that the reductions observed for the Gram-negative organisms used in these experiments would be less than that observed for *S. aureus* (Perni et al., 2009b),. Although these results support the hypothesis, the data cannot be directly compared with the published work as a larger starting inoculum was used in this series of experiments, and cells are more susceptible to PDI when a lower inoculum is used (So et al., 2010). The initial bacterial concentration used in the Perni study equated to approximately 4 x 10^4 cfu / polymer and in preliminary experiments a 3.54 $\log_{10}$ cfu / polymer reduction in *P. aeruginosa* PAO1 was detected which was below the detection limit of the experiment (data not shown). Therefore, a higher initial bacterial load of 10^6 cfu / polymer was selected so that colonies were always detectable on the test (L+S+) plates and the values obtained were within the detectable limits of the experimental design. Alternatively, the exposure time to the laser could have been decreased to ensure the recovered bacteria were within the detection limits of the assay. For reference, the Perni et al., (2009a) study showed a >4 $\log_{10}$ cfu / ml reduction in EMRSA16 after a 1 minute irradiation time and a >4 $\log_{10}$ cfu / ml reduction in *E. coli* ATCC 25922 after a 2 minute irradiation.

These data also show that *C. albicans* was less susceptible to TBO-mediated photodynamic inactivation than the Gram-negative bacteria *S. maltophilia, A.*

baumannii and *P. aeruginosa* PAO1. It has previously been shown that *C. albicans* was susceptible to PDI using a solution of TBO and irradiation with red light (Wilson and Mia, 1993) and an increased tolerance to these conditions was displayed compared with the Gram-negative oral bacteria *Fusobacterium nucleatum, Actinobacillus actinomycetemeomitans* and *Porphyromonas gingivalis* (Wilson et al., 1993; Wilson and Mia, 1994). Yeast cells are much larger in size than bacterial cells; the diameter of a *C. albicans* cell is approximately 3 to 4 µm (Merz and Roberts, 1999) compared with *A. baumannii* which is approximately 1 to 1.5 by 1.5 to 2.5 µm in size (Schreckenberger and von Graevenitz, 1999) and *S. aureus* which is approximately 0.5 to 1.5 µm in diameter (Kloos and Bannerman, 1999; Sandel and McKillip, 2004). Therefore, the yeast cell is likely to require a larger dose of reactive oxygen species to exert a similar photodynamic effect (Jori et al., 2006). The structure of the yeast cell wall could also contribute towards increased tolerance to PDT (Bowman and Free, 2006).

6.4.2 Limitations of the experimental work

The clinical strain of *P. aeruginosa* was shown to be the least susceptible to the photoactivity of the TBO-impregnated polymers after a 4 minute irradiation time, and the reduction in bacteria observed was substantially less than that seen in for the laboratory strain of *P. aeruginosa,* PAO1. *P. aeruginosa* PAO1 was originally isolated from a wound in Melbourne, Australia in 1955 (Holloway, 1955). Since then it has been serially passaged for many years and shared with laboratories around the world, where further passages have taken place (Fux et al., 2005). The PAO1 strain was selected because it's ubiquitous use allows the data generated in these experiments to be compared with results generated by groups around the world on the sensitivity of

P. aeruginosa to the TBO-laser combination. However, it's limitations should be acknowledged and it is probable that the PAO1 strain in use today has lost characteristics found in the original strain as a result of serial passage (Fux et al., 2005).

The conditions that bacteria are exposed to during laboratory culture are substantially different from those experienced within the hostile environment of the human body. An abundance of nutrients are present in laboratory media to encourage bacterial growth and incubation conditions are optimal for rapid replication. Therefore, the genes that are required for colonisation and survival within the human host are surplus to requirement. For example, in *E. coli,* genes required for flagella production are inactivated after serial passage's (Edwards et al., 2002), which benefits the laboratory-adapted strain as flagella production is an energy-rich process that requires high levels of amino acid production. If these genes are inactivated, the replication time will be shorter, which will give the laboratory-adapted strain a fitness advantage over the wild type strain.

The ability of the laboratory adapted cells to adhere and form biofilms could also be reduced (Fux et al., 2005). Mucoid strains of *P. aeruginosa* are commonly isolated from patients with cystic fibrosis and this phenotype is often lost during laboratory culture due to a series of point mutations and a non-mucoid, rough colony morphology predominates (Govan, 1975; Drenkard and Ausubel, 2002). Mucoid strains produce a greater quantity of alginate (Simpson et al., 1989), a known scavenger of reactive oxygen species such as singlet oxygen, which is produced in abundance during the photodynamic reaction on the TBO-impregnated polymers (Wakayama et al., 1980). A possible reason for the decreased susceptibility of the clinical isolate to the

photoactivity of TBO-impregnated polymers could therefore be related to an increased production of alginate, which is a defence mechanism against the respiratory burst released by macrophages within the human host. Wong et al., (2006) showed that clinical isolates exposed to the visible-light driven photocatalytic effect of N-doped TiO_2 thin films displayed increased tolerance to killing compared with a laboratory strain of *E. coli* OP50 and it was suggested that the mechanism behind this was also linked to resistance to reactive oxygen species

The bacterial isolates used in this series of experiments were cultured in brain heart infusion (BHI) liquid media and subsequently re-suspended in PBS, which is a low protein saline solution. It has been shown that the PDI effect is reduced by the presence of proteins in the medium, and so it is possible that the inhibitory effect observed in these experiments would be reduced under *in vivo* conditions, as the tracheal secretions contain high levels of proteins (Wilson and Pratten, 1995; Nitzan et al., 1998). These proteins could absorb light, which would reduce the number of photons available, which would in turn decrease the concentration of reactive oxygen species generated (Komerik and Wilson, 2002). The proteins may also be used as alternative targets by the singlet oxygen species and shield bacteria from the cytotoxic effects generated.

6.4.3 Novel materials for potential use as antimicrobial endotracheal tubes

Numerous *in vitro* studies have been conducted on materials which could be used as novel antibacterial ETTs. Methylene blue was incorporated into silicone and the photodynamic effect with and without the addition of gold nanoparticles was

investigated (Perni et al., 2009a). A significant level of photoactivity was observed against *E. coli* and MRSA after 5 minutes irradiation with a red laser light, which was enhanced with the addition of gold nanoparticles. Berra et al., (2008a) coated polyurethane ETTs with silver sulfadiazine and challenged the tubes with *P. aeruginosa* PAO1. The silver coated ETT was examined by both scanning electron microscopy (SEM) and confocal laser scanning microscopy (CLSM) and sections of the tube were cultured after a period of 72 hours; adhesion of *P. aeruginosa* PAO1 to the substrate had been prevented and the growth rate was also reduced. The silver coated ETT was subsequently used in a ventilated sheep model. No bacteria were cultured from the coated ETTs after 24 hours, and a thinner layer of mucus was present on the lumen of the tube compared with the uncoated control, where bacterial colonisation was present (Berra et al., 2008a).

Rello et al., (2010) coated a proprietary hydrophilic polymer with silver ions and investigated the adherence of 18 organisms after an exposure time of 4 hours. A reduced level of bacterial attachment was observed for respiratory strains of MRSA, *P. aeruginosa* and *E. aerogenes,* but the attachment of a number of other organisms such as *C. albicans* and *K. pneumoniae* was not prevented. The antibacterial activity of the silver ion-coated ETT was then assessed in a rabbit model, which was challenged with a respiratory isolate of *P. aeruginosa.* After 16 hours, a reduced level of ETT colonisation was observed on the silver ion-coated tubes and *P. aeruginosa* was not isolated from the lungs of the rabbits. In comparison, *P. aeruginosa* was cultured from all non-coated ETTs and from the lungs of all rabbits intubated with the control tubes (Rello et al., 2010).

A large-scale randomised trial published in 2008 aimed to ascertain whether silver coated ETTs could reduce the incidence of VAP in humans (Kollef et al., 2008). Nearly 10,000 patients were screened for their eligibility into the study and suitable patients were assigned a silver-coated ETT or a non-coated tube. A reduction in the incidence of VAP was observed in patients with silver-coated tubes. These findings were extremely promising as they showed that by simply using a different ventilator tube, the incidence of VAP could be reduced, and it required no additional involvement from the medical team treating the patient. However, some authors have questioned the merit of reducing bacterial load on the ETT (Balk, 2002; Spronk et al., 2006) as there is no direct evidence to demonstrate that antibacterial ETTs can reduce length of hospital stay or mortality rates and the silver coated ETTs cost over $100 per tube, compared with less than $1 for a traditional uncoated tube (Deem and Treggiari, 2010).

6.5 Conclusions

The antibacterial photodynamic inactivation of *P. aeruginosa, S. maltophilia* and *A. baumannii* was assessed on TBO-impregnated polymers after irradiation with a HeNe laser light. A significant reduction in the recovery of all bacterial strains tested was observed after 90, 180 and 240 seconds. A recently isolated clinical strain of *P. aeruginosa* showed decreased susceptibility to the photo-activity of the TBO-impregnated polymers compared with a laboratory type strain. Significant photodynamic inactivation of *C. albicans* was also observed after exposure to the same light source, demonstrating that the light-induced effect is not restricted to bacteria.

7 Assessment of the disruptive and anti-adhesive properties of novel light-activated materials

7.1 Introduction

The anti-adhesive properties of two of the novel light-activated antibacterial materials generated in this thesis was explored in this chapter using a range of techniques. The silver-doped titanium dioxide thin films were examined to determine whether, in addition to the photo-activated bactericidal effects already demonstrated, initial bacterial adhesion to the surface could be prevented and whether the formation of an immature bacterial biofilm could be disrupted. The initial attachment of bacteria to the TBO-impregnated polyurethane polymers was assessed, after irradiation with the HeNe laser, which prompted the examination of the photo-bleaching effect of the laser on the antibacterial activity of the TBO-impregnated polymers.

Demonstrating a reduction in the recovery of viable bacteria inoculated onto the novel surfaces after light exposure is a useful initial method of establishing the antibacterial activity of the novel materials. However, it would also be advantageous to prevent the initial attachment of bacteria to the surface. During the initial adhesion events there will be a lower bacterial load so photoinactivation may occur at a faster rate. Also, in the clinical environment, the risk of onward transmission of bacteria from a hand-touch surface via the hands of patients or healthcare workers would be further reduced due to the smaller inoculum present. An additional measure which would prove beneficial in the clinical environment would be the detachment and inactivation of bacteria already bound to the surface before light exposure.

7.2 Materials and methods

7.2.1 Silver-doped titanium dioxide thin films

7.2.1.1 Assessment of initial attachment of EMRSA-16

Bacterial attachment to the Ag-TiO_2 thin films was measured using two single channel transmission FC 81-PC flow cells (BioSurface Technologies Corporation, Montana USA). Two flow cell chambers (50 x 13 x 2.35 mm) were joined together with tape before autoclaving and rinsing with water. The flask was prepared by constituting 500 mL PBS in a 1000 mL conical flask with a magnetic stirrer added; a rubber stopper was loosely placed on and covered with foil. The two female connectors were wrapped with foil and sealed with autoclave tape. Clamps were attached to the ends of both tubes, by the male connectors and on either side of the air filters and the entire unit was autoclaved for 15 minutes at 121°C.

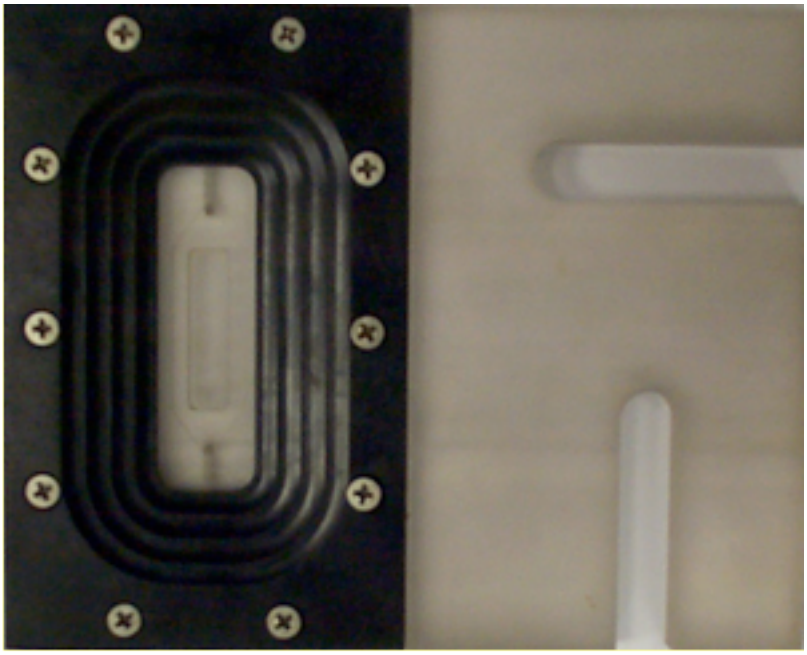

Figure 7.1 The flow cell chamber used to assess bacterial attachment. The Ag-TiO_2 thin film was placed within the chamber and adhesion was assessed by light microscopy as a bacterial suspension flowed across the material.

The flow cell chamber was assembled and a sealant was applied between each layer to prevent the leakage of liquid. A cover slip was placed on the clear plastic lid and the entry and exit points in the flow cell chamber were cleaned with an isopropanol-containing wipe to ensure there was no obstruction caused by sealant. The uncoated glass slide, denoted S-, was placed in the ridge on the clear plastic lid and screws were added to the top and not tightened. The Ag-TiO_2 thin films could not be autoclaved so these were not added at this point. The screws were loosely positioned on top and covered with tape. Foil was added to the top of the bubble trap and the ends of the two male connectors. Clamps were affixed to the ends of both tubes by the male connectors. The flow cell chamber was then laid flat in an autoclave bag and sealed, then placed into a second autoclave bag, sealed and labelled. The bag was sterilised by autoclaving at 121°C for 12 minutes.

After autoclaving, the rubber stopper on the top of the conical flask was secured and the clamps from either side of the air filter were removed. The flask of PBS and the flow cell chambers were allowed to cool before the Ag-TiO_2 slide, denoted S+, was placed into the flow cell chamber and all screws on the flow cell chamber were tightened to prevent any leakages. The clamps from the end of each tube were removed and the flow cell chamber was joined to the flask by placing the male and female connectors together. Finally, a 0.45 nm filter (Nalgene® Labware, Roskilde, Denmark) was added to the top of the bubble trap. A culture of EMRSA-16 was prepared in BHI, as described in Section 2.2.

After 24 hours growth, 5 mL of the overnight culture was dispensed directly into the flask containing 500 mL PBS, providing a dilution of approximately 1 in 100. The flow cell chamber and bubble trap was placed into a large white tray and the narrow section of tubing was passed through the peristaltic pump (Watson-Marlow Pumps Group, Falmouth, UK) to achieve a low flow rate. The whole system (peristaltic pump, flask and tubing) was transferred into the 22°C incubator containing the white light source, along with a magnetic stirrer. The peristaltic pump was then switched on and the speed set to 30, equating to a shear rate of 40 s^{-1}. The valve on the bubble trap was kept open until the liquid had reached the halfway mark, at which point the valve was closed and the liquid could pass through the system back to the conical flask.

After 0, 6 and 18 hours, the flow cell system was moved to the light microscope so that the attachment of bacteria on the surface of the thin films could be visualised. The x40 objective lens (Olympus ULWD CD Plan 40) was used and at least ten random fields of view were examined per sample and representative images were captured.

7.2.1.2 Disruption of an immature biofilm of EMRSA-16

Bacterial strains were maintained as described in Section 2.1 and bacterial suspensions of EMRSA-16 were prepared in PBS as detailed in Section 2.3. Alternatively, an aliquot of the re-suspended pellet of bacteria was added to a 10 mL of BHI and the optical density was measured on the spectrophotometer. In both cases, the resulting bacterial suspension contained approximately 10^7 cfu / mL. Silver-doped titanium dioxide thin films or uncoated controls were placed in the moisture chambers described in Figure 2.2, before 50 µL of the bacterial suspension was added and the moisture chambers were incubated in the dark for 24 hours to allow an immature biofilm to develop.

The moisture chambers were subsequently transferred to the cooled incubator and incubated at 22°C for 24 hours under the white light source. The Live / Dead stain (Molecular Probes) was prepared by adding 2.0 µL of both SYTO 9™ and propidium iodide to a foil-covered universal containing 40 mL PBS and was incubated in the dark for 30 minutes before use. The Live / Dead stain was poured into a petri dish, the samples were immersed in the petri dish and incubated in the dark for 5 minutes to allow the stain to penetrate the bacterial cells before viewing. Two slides were examined for each exposure condition as detailed in Table 7.1 and at least ten fields of view were examined per sample and representative images were captured. The samples were examined on the confocal laser scanning microscope (CLSM) using the x40 lens with a blue filter and later analysed using the ImageJ computer programme which can be accessed for free from http://rsbweb.nih.gov/ij/. The experiment was repeated to demonstrate reproducibility.

Table 7.1 Description of the samples examined under the confocal scanning laser microscope.

Sample reference	Sample type	Exposure conditions	Inoculum
K2 / K3	Ag-TiO_2	light	EMRSA in PBS
K4 / K5	Ag-TiO_2	dark	EMRSA in PBS
K6 / K7	Ag-TiO_2	light	EMRSA in BHI
K8 / K9	Ag-TiO_2	dark	EMRSA in BHI
K10 / K13	Ag-TiO_2	light	No bacteria
K14 / K17	Ag-TiO_2	dark	No bacteria
B1 / B2	Uncoated slide	light	No bacteria
B3 / B4	Uncoated slide	dark	No bacteria

7.2.2 TBO-impregnated polymers

7.2.2.1 Prevention of initial *P. aeruginosa* PAO1 attachment

Bacterial strains were maintained as described in Section 2.1 and bacterial suspensions of *P. aeruginosa* PAO1 were grown and prepared in PBS as detailed in Section 2.2 and Section 2.3, resulting in a bacterial suspension containing approximately 10^7 cfu / mL. The described method was adapted from a paper by Chrzanowski et al., (2010). The test samples were prepared and placed in a 24 well microtitre plate as illustrated in Figure 7.2. Empty wells were filled with foil to prevent laser light penetrating into adjacent wells. One millilitre of bacterial suspension was added to the test well ensuring the polymer did not float to the surface, and the remaining wells were covered with a sheet of black paper. The well was irradiated with the HeNe laser source described in Section 2.4.3 for the designated exposure time and the emitted light was passed through a beam diffuser to ensure that the entire polymer was

exposed to the laser light. The process was repeated for each appropriate sample before static incubation at 37°C for the designated time period, before re-exposure to the laser source. After three hours, each sample was placed into a separate bijou containing 3 mL PBS and incubated at 22°C for 5 min or prepared for scanning electron microscopy. The polymer was subsequently transferred to a bijou containing 1 mL PBS and 5 glass beads each with a diameter of 3 mm and vortexed for 1 min. Twenty microlitres of the bacterial suspension was then removed, serially diluted and spread onto MacConkey agar plates before incubation at 37°C for 48 hours. The resultant colonies were counted and compared with the controls to calculate the level of biofilm disruption.

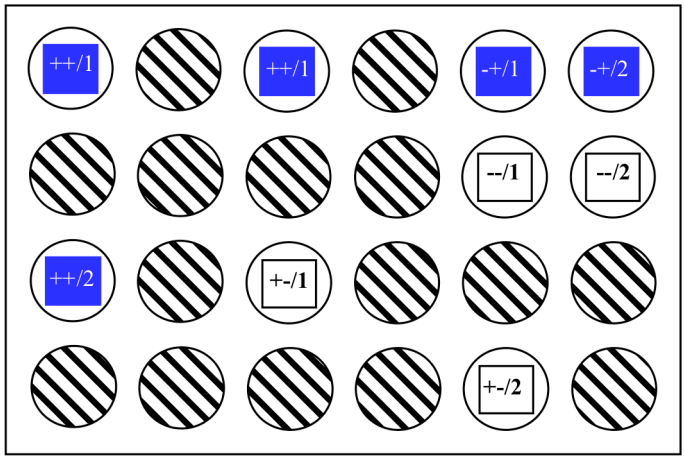

Figure 7.2 The layout of the microtitre plate during the biofilm disruption assays, where ++ corresponds to a TBO-impregnated polyurethane polymer exposed to the laser light; -+ corresponds to a TBO-impregnated polyurethane polymer not exposed to the laser light; +- corresponds to a polyurethane polymer exposed to the laser light and -- corresponds to a polyurethane polymer not exposed to the laser light. Shaded circles represent wells filled with foil.

7.2.2.2 Scanning electron microscopy

After three hours incubation at 37°C, the samples were prepared for SEM analysis by Dr. Nicky Mordan. The samples underwent a series of 10 minutes dehydration stages

in increasing concentrations of alcohol (20%, 50%, 70%, 90% and 3x 100%), before immersion in hexamethyldisilazane (HMDS) (TAAB Laboratories Ltd, Reading, UK) for 5 min followed by drying on filter paper for 2 -3 hours, to ensure that the HMDS had completely evaporated. The samples were then fixed onto alumininum SEM stubs (Agar Scientific), using carbon conducting cement (Neubauer Chemikalien, Munster, Germany) as an adhesive, before sputter-coating with gold/palladium in a Polaron E5000 Sputter Coater (Quorum Technologies Ltd, Newhaven, UK). A Cambridge Stereoscan 90B (LEO Electron Microscopy Ltd, Cambridge, UK) was used to view the specimens operating at 15 kV and at least ten fields of view were examined. The i-scan 2000software (ISS Group, Manchester, UK) was used to capture representative digital images for each sample.

7.2.2.3 Photo-bleaching effects

The TBO-impregnated polymers were irradiated with the HeNe laser source described in Section 2.4.3 for either 90, 180 or 240 seconds, before incubation in a sterile petri dish for 24 hours at 22°C. The polymers were then processed as described in Section 2.12.3; polymers which had been initially irradiated for 90 seconds were exposed to another 90 second laser dose, polymers irradiated for 180 seconds were re-exposed for 180 seconds and polymers irradiated for 240 seconds were treated with a further 240 second light dose. Naïve TBO-impregnated polymers were used as controls, i.e. TBO-impregnated polymers that had been stored in the dark during the initial irradiation step. Three TBO-impregnated polymers were tested for each exposure time and the experiment was repeated three times to demonstrate reproducibility.

7.3 Results

7.3.1 Silver-doped titanium dioxide thin films

7.3.1.1 Assessment of bacterial attachment

The attachment of EMRSA-16 to the surface of the Ag-TiO_2 thin films was assessed using the flow cell model. Bacteria were observed in the circulating broth after zero hours in low numbers in Figure 7.3(a) and Figure 7.3(b); the cocci were in constant motion, moving in the direction of the flow suggesting that attachment had not yet occurred. A similar number of bacteria were found on the Ag-TiO_2 thin films and the uncoated control slides. After 6 hours, the number of bacteria observed on both coating types had increased substantially and a near complete coverage of the slide was observed (Figure 7.4a and Figure 7.4b). Again there was no difference in the attachment of bacteria to the irradiated Ag-TiO_2 thin film and the uncoated control exposed to the same light conditions. After 18 hours exposure to the white light, no reduction in the number of bacteria was observed on the Ag-TiO_2 thin films exposed to the white light and there was no visual difference in the number of bacteria observed on the Ag-TiO_2 thin film compared with the uncoated control (Figure 7.5a and Figure 7.5b).

The shrink cracks which can be clearly seen on the Ag-TiO_2 thin films are a feature of the coating and are a result of the annealing process. There was no greater than bacterial attachment observed in these areas than on the non-cracked areas of the thin film.

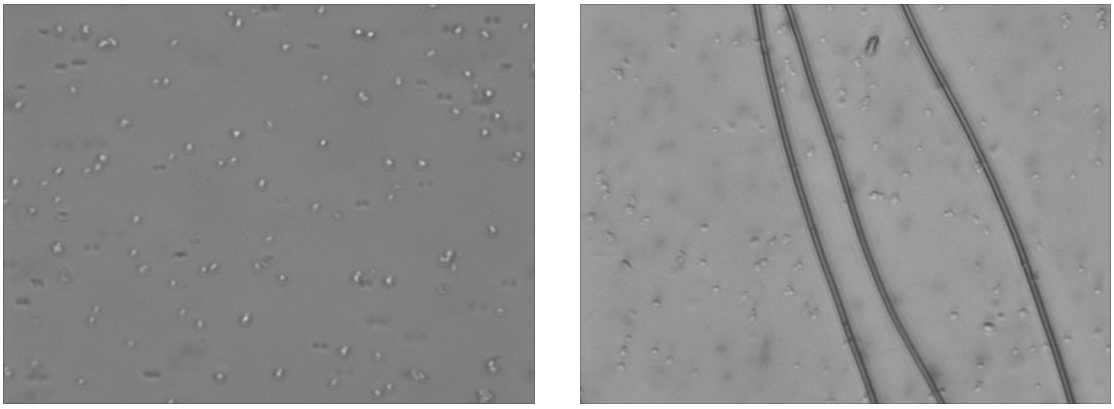

Figure 7.3 Attachment of EMRSA-16 to either an (a) uncoated slide or (b) Ag-TiO_2 thin film after 0h exposure to the white light source.

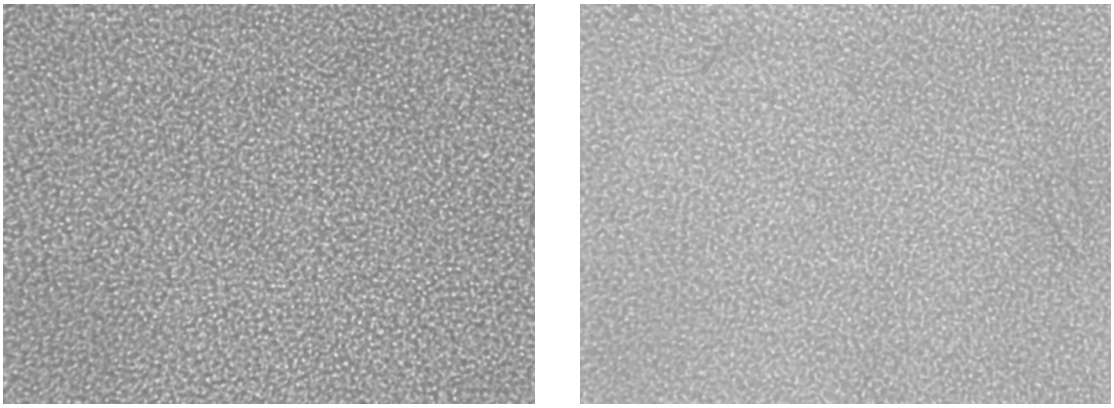

Figure 7.4 Attachment of EMRSA-16 to either an (a) uncoated slide or (b) Ag-TiO_2 thin film after 6h exposure to the white light source.

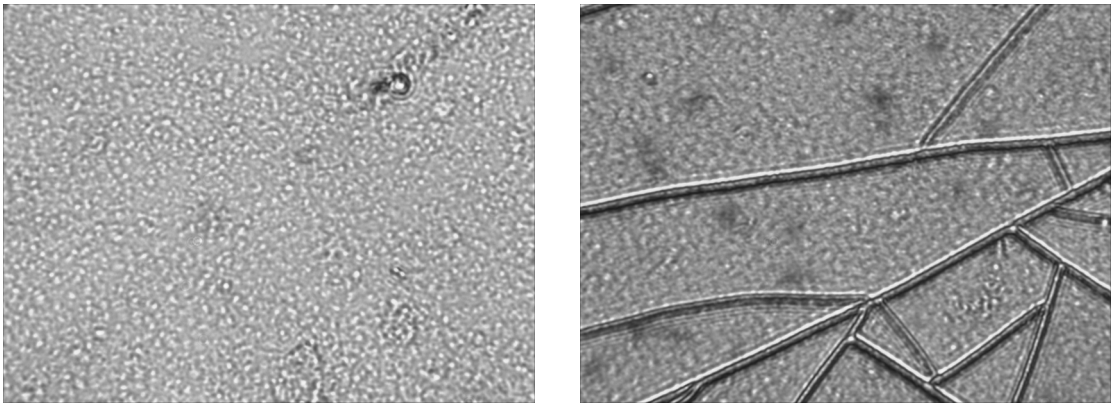

Figure 7.5 Attachment of EMRSA-16 to either an (a) uncoated slide or (b) Ag-TiO_2 thin film after 18h exposure to the white light source.

7.3.1.2 Disruption of an immature biofilm of EMRSA-16

As there was no difference in the attachment of EMRSA-16 to the Ag-TiO_2 thin films, the viability of EMRSA-16 was examined after irradiation with white light. It is possible that the photo-activated thin films were not preventing bacterial attachment but were inactivating the bacteria that did adhere. An immature biofilm of EMRSA-16 in PBS was grown on the surface of the Ag-TiO_2 thin films and exposed to white light for 24 hours; a reduction in the viability of the attached bacterial cells was observed. There were substantially more non-viable cells on the Ag-TiO_2 thin films exposed to white light (Figure 7.6) compared that observed on the surface of the Ag-TiO_2 thin films incubated in the dark (Figure 7.7). This demonstrates that white light irradiation of the Ag-TiO_2 thin films caused an increase in the permeability of the cell membrane to the propidium iodide stain and accompanying damage to the integrity of the bacterial cell membrane. No antibacterial activity was observed in the absence of light, which suggests that the damage to the bacterial cell membranes was not caused by the leakage of silver ions from the surface of the thin film.

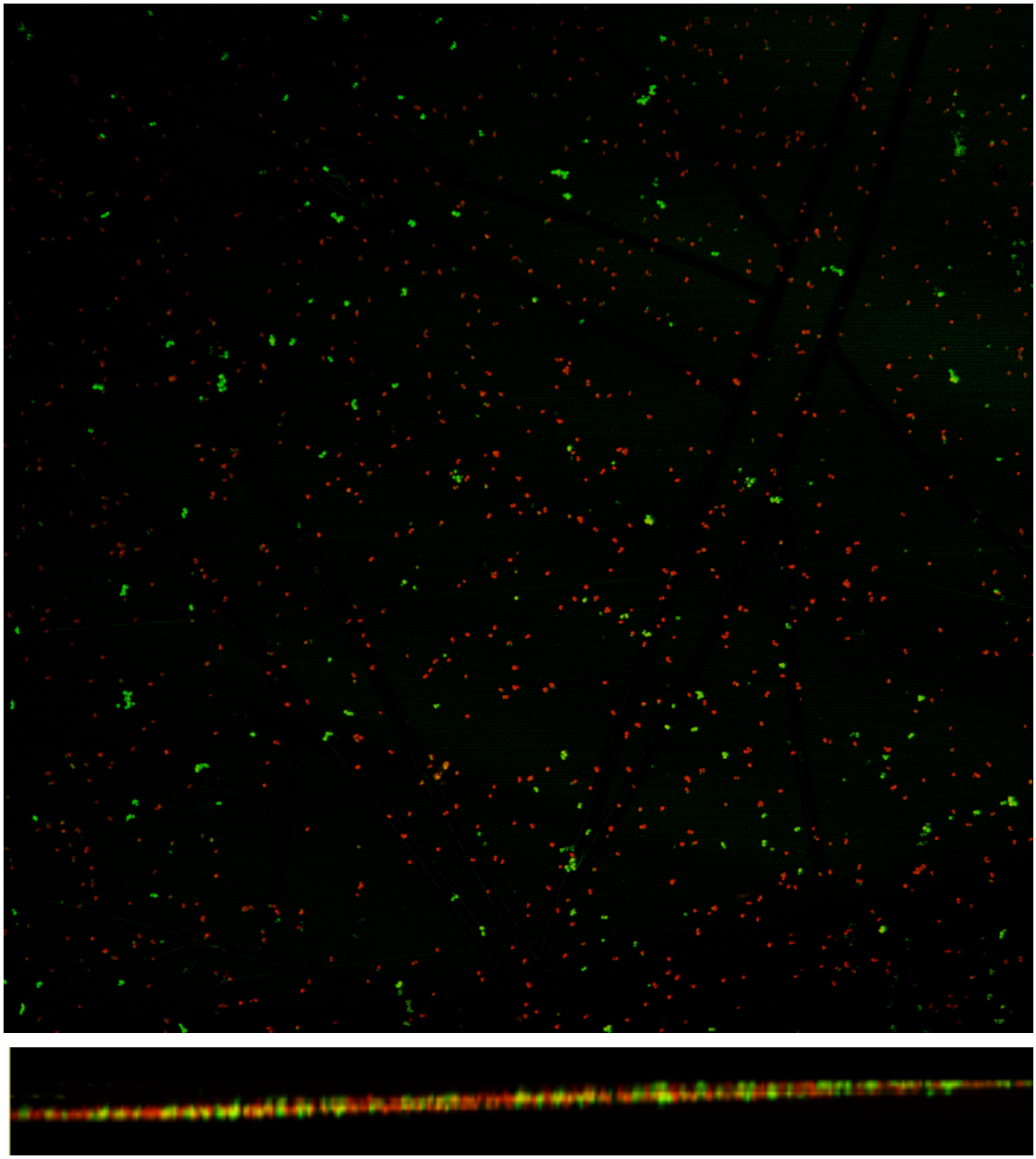

Figure 7.6 Confocal micrograph of EMRSA-16 in PBS on the Ag-TiO_2 thin film after 24 hours growth at 37°C in the dark and 24 hours exposure to white light at 22°C (xy projection, 300 x 300 µm). Viable bacterial cells are stained green and non-viable cells are stained red. The depth of the bacterial growth is displayed underneath the main image (xz projection).

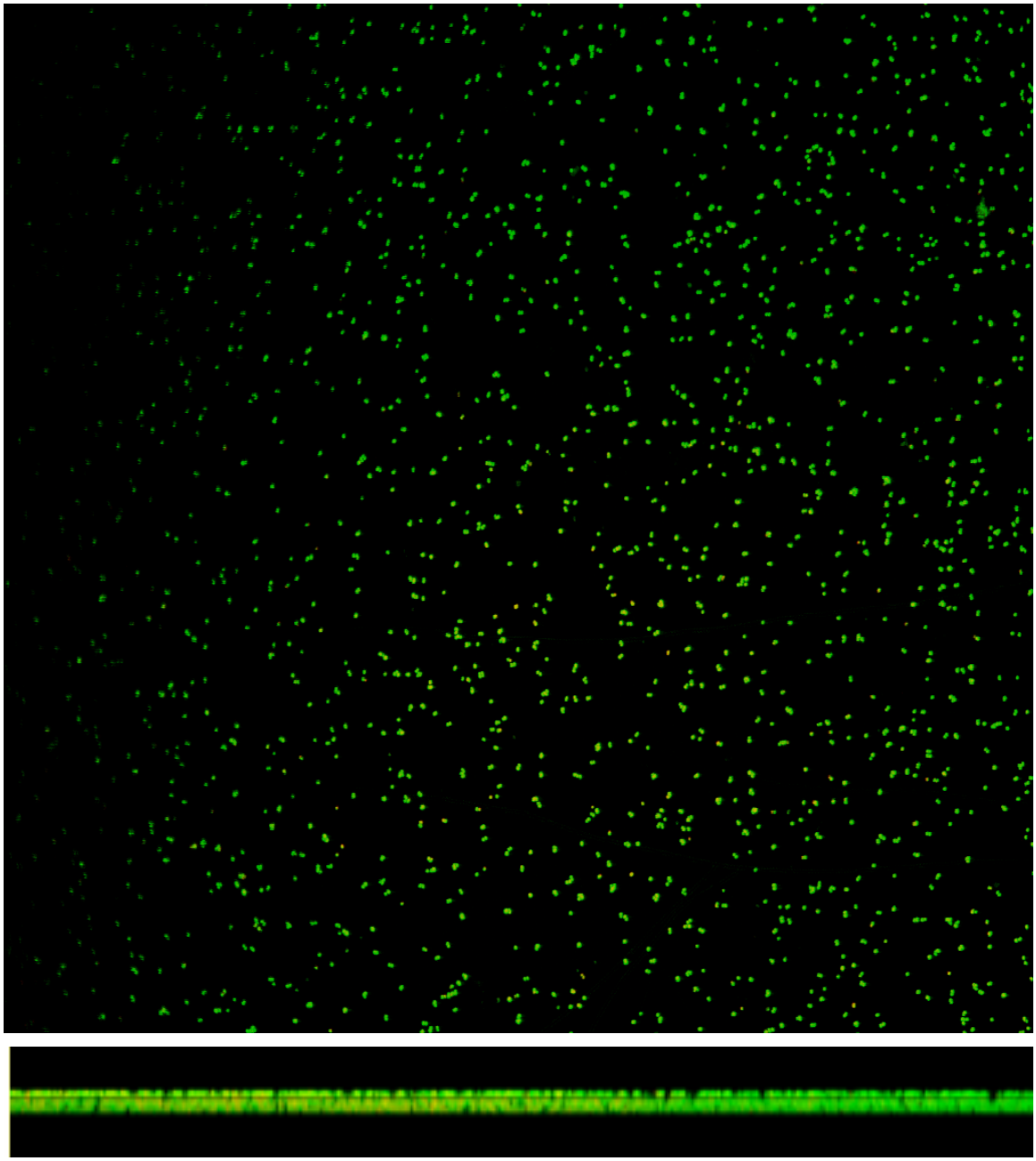

Figure 7.7 Confocal micrograph of EMRSA-16 in PBS on the Ag-TiO_2 thin film after 24 hours growth at 37°C in the dark and 24 hours incubation at 22°C in the dark (xy projection, 300 x 300 µm). Viable bacterial cells are stained green and non-viable cells are stained red. The depth of the bacterial growth is displayed underneath the main image (xz projection).

Figure 7.8 and Figure 7.9 show the attachment of EMRSA on the surface of the Ag-TiO_2 thin films after re-suspension in the nutrient-rich medium BHI with and without exposure to the white light source, respectively. The photocatalytic antibacterial activity of the Ag-TiO_2 thin films was not evident; only a small number of non-viable cells were observed after 24 hours exposure to white light and these were located in small defined areas whereas when EMRSA-16 was re-suspended in PBS and grown on the thin films, the non-viable cells were dispersed more evenly across the surface of the sample. The cells attached to these surfaces had begun to coalesce, the distinct single cells that were in abundance in the nutrient-poor conditions were seen less frequently and the initial stages of a biofilm were beginning to develop.

The continued viability of EMRSA-16 observed in the presence of white light also suggests that the damage to the cell membrane seen in Figure 7.6 was not a direct effect of the white light, but produced due to the photocatalytic activity of the Ag-TiO_2 thin film.

The thickness of the immature biofilms on the surface of the Ag-TiO_2 thin films are displayed at the bottom of each confocal micrograph. The immature biofilm formed from EMRSA-16 re-suspended in PBS and exposed to the white light (Figure 7.6) is less thick than the biofilms formed when EMRSA-16 was re-suspended in PBS and incubated for 24 hours at 22°C in the dark, or when EMRSA-16 was re-suspended in BHI and incubated for 24 hours at 22°C in the presence or absence of light (Figure 7.7, Figure 7.8 and Figure 7.9).

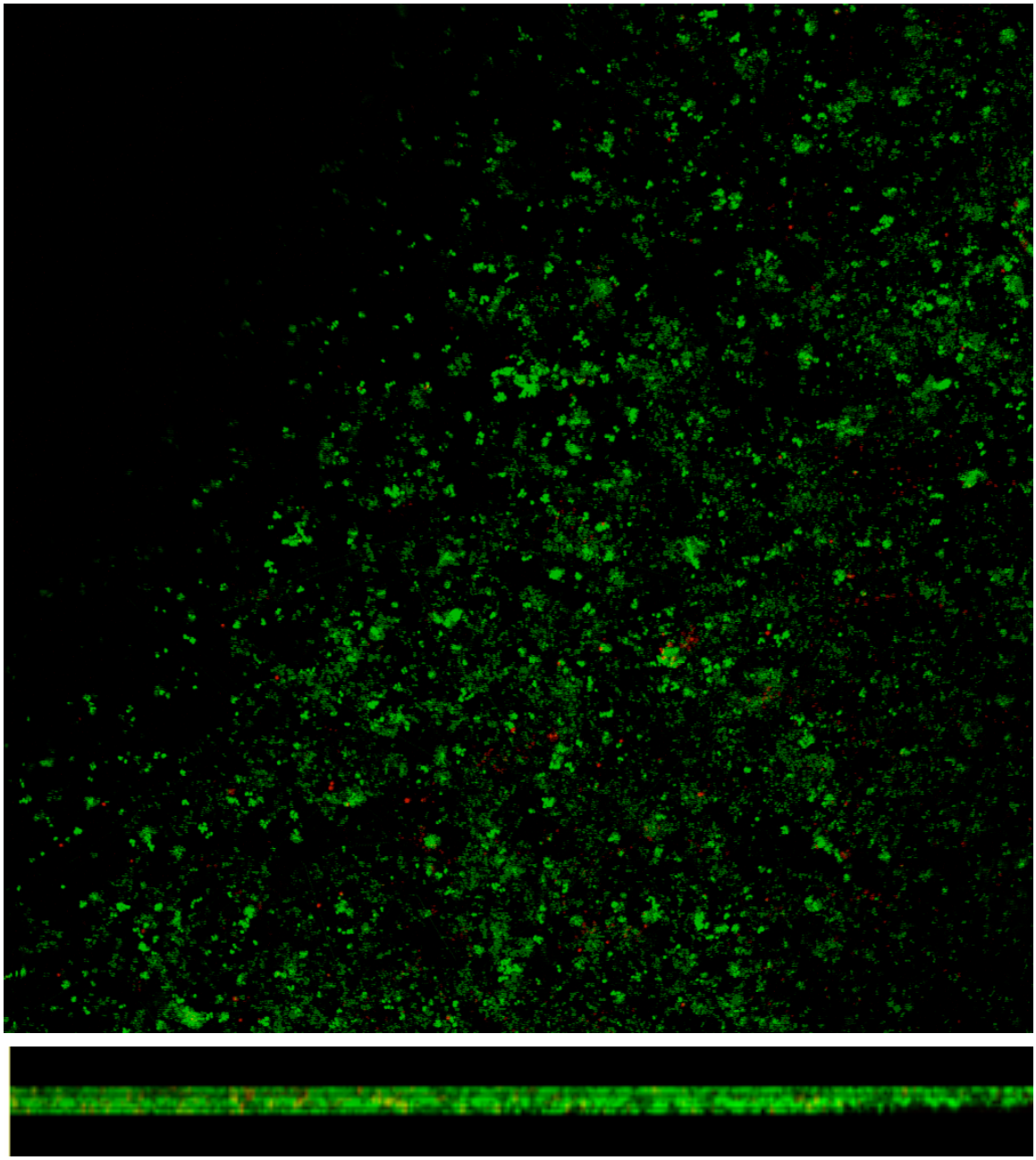

Figure 7.8 Confocal micrograph of EMRSA-16 in BHI on the Ag-TiO_2 thin film after 24 hours growth at 37°C in the dark and 24 hours exposure to white light at 22°C (xy projection, 300 x 300 µm). Viable bacterial cells are stained green and non-viable cells are stained red. The depth of the bacterial growth is displayed underneath the main image (xz projection).

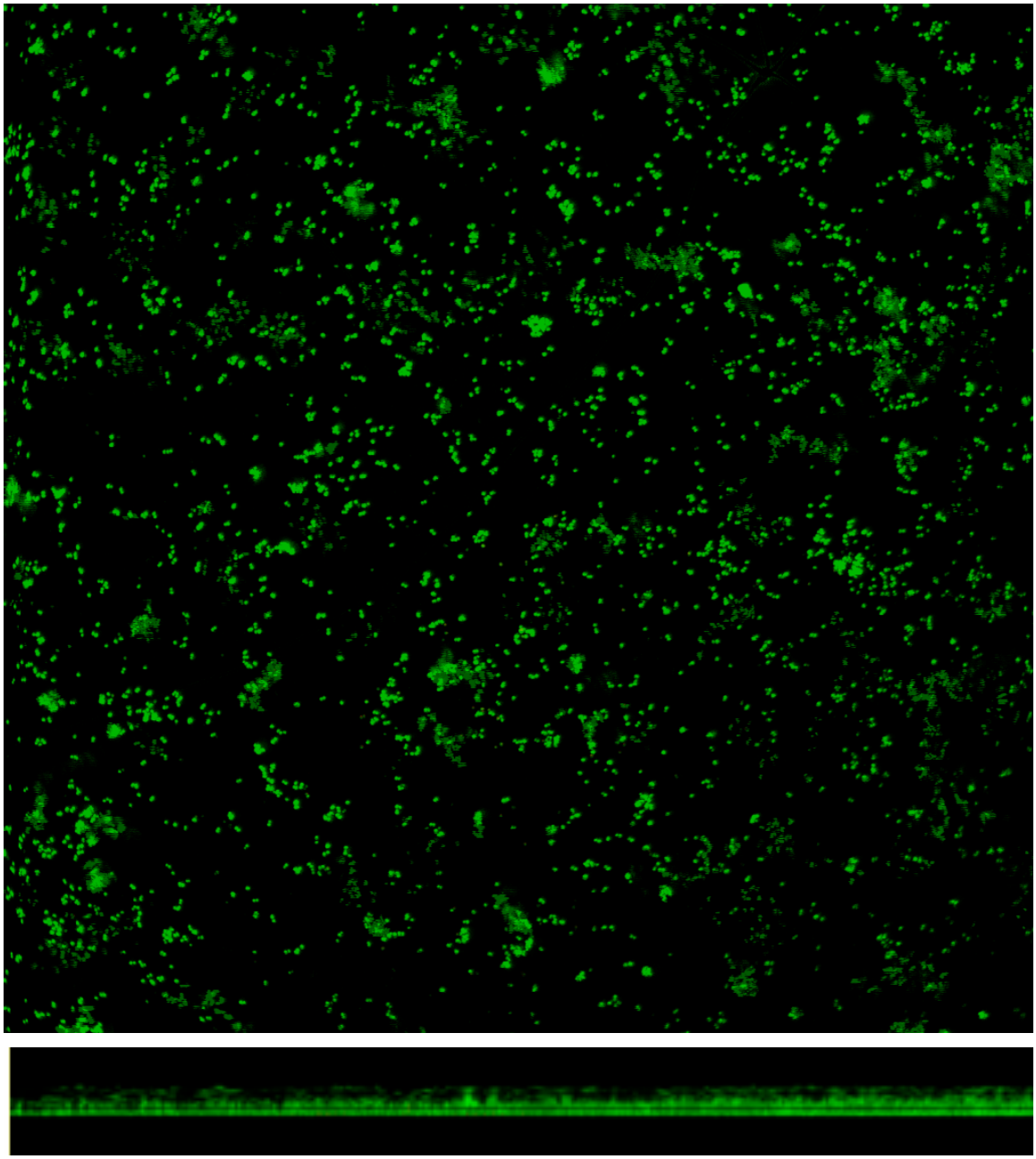

Figure 7.9 Confocal micrograph of EMRSA-16 in BHI on the Ag-TiO_2 thin film after 24 hours growth at 37°C in the dark and 24 hours incubation at 22°C in the dark (xy projection, 300 x 300 µm). Viable bacterial cells are stained green and non-viable cells are stained red. The depth of the bacterial growth is displayed underneath the main image (xz projection).

7.3.2 TBO-impregnated polymers

7.3.2.1 Prevention of initial *P. aeruginosa* PAO1 attachment

The TBO-impregnated polyurethane polymers were assessed for their ability to prevent the initial attachment of *P. aeruginosa* PAO1 after irradiation with the HeNe laser. The TBO-impregnated polymers were initially irradiated with the HeNe laser for 90 seconds and then incubated in a suspension of *P. aeruginosa* for 3 hours; there was no significant difference in bacterial attachment compared with the control polymers incubated in the dark. The irradiation period was doubled to 180 seconds and the anti-attachment properties of the polymer were not improved. Therefore the frequency of the irradiation dosing was increased, and the time of dosing altered (Table 7.1).

Table 7.2 Results of the bacterial attachment assays, where row 1 denotes that the samples were irradiated with the HeNe laser once, for 90 seconds at time point 0 minutes, which resulted in a 0.13 log cfu / ml reduction in viable bacteria.

Irradiation period / sec	Irradiation frequency	Irradiation dosing times / min	Log reduction / cfu ml^{-1}
90	1	0	0.13
180	1	0	0.00
180	2	0, 90	0.58
180	3	0, 60, 120	0.53
180	3	0, 90, 180	1.56

A significant decrease in bacterial attachment was demonstrated when the TBO-impregnated polymers were irradiated three times, for 180 seconds at time points 0, 60 and 180 minutes (Figure 7.10). A 97.3% reduction in bacterial attachment was

observed, which corresponded to a 1.56 log reduction ($p < 0.001$). This therefore demonstrates that increasing the dosing frequency improved the anti-adhesive properties of the TBO-impregnated polymer and frequent doses of the laser light were required to prevent the attachment of *P. aeruginosa* to the TBO-impregnated polymers. The laser light alone did not have a significant effect on *P. aeruginosa* attachment, but a significant decrease in attachment was observed on the TBO-impregnated polymer in the absence of the laser light ($p < 0.01$) suggesting that the presence of the photosensitiser alone did have an effect on bacterial attachment.

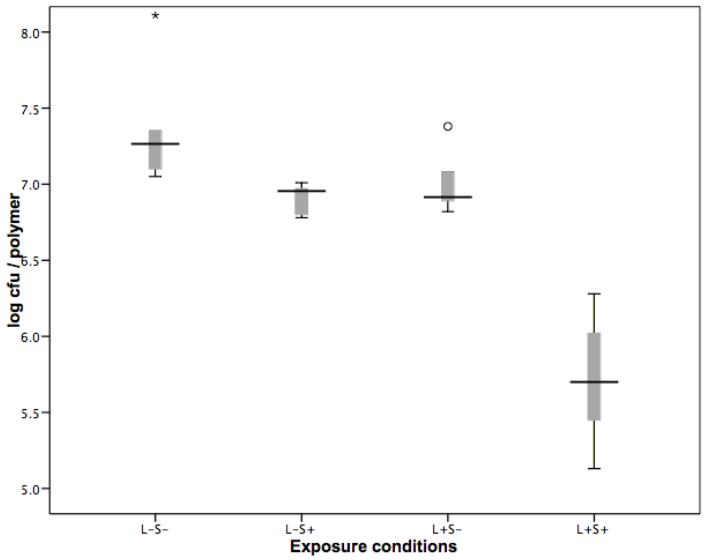

Figure 7.10 Ability of the TBO-impregnated polymers to prevent the initial attachment of *P. aeruginosa* PAO1. TBO-impregnated (S+) or non-impregnated control (S-) polymers were either irradiated with laser light (L+) or incubated in the dark (L-).

7.3.2.2 Scanning electron microscopy

The attachment of *P. aeruginosa* to the TBO-impregnated polymers was further investigated by visualisation of bacterial attachment by SEM after the biofilm disruption assay. The most effective irradiation schedule was used (180 seconds irradiation after 0, 90 and 180 minutes) and the decrease in bacterial recovery

observed in Section 7.3.1.2 was confirmed. There were substantially less bacteria adhered to the surface of the irradiated TBO-impregnated polymers (Figure 7.11) than the TBO-impregnated polymers that were not exposed to the laser light (Figure 7.12).

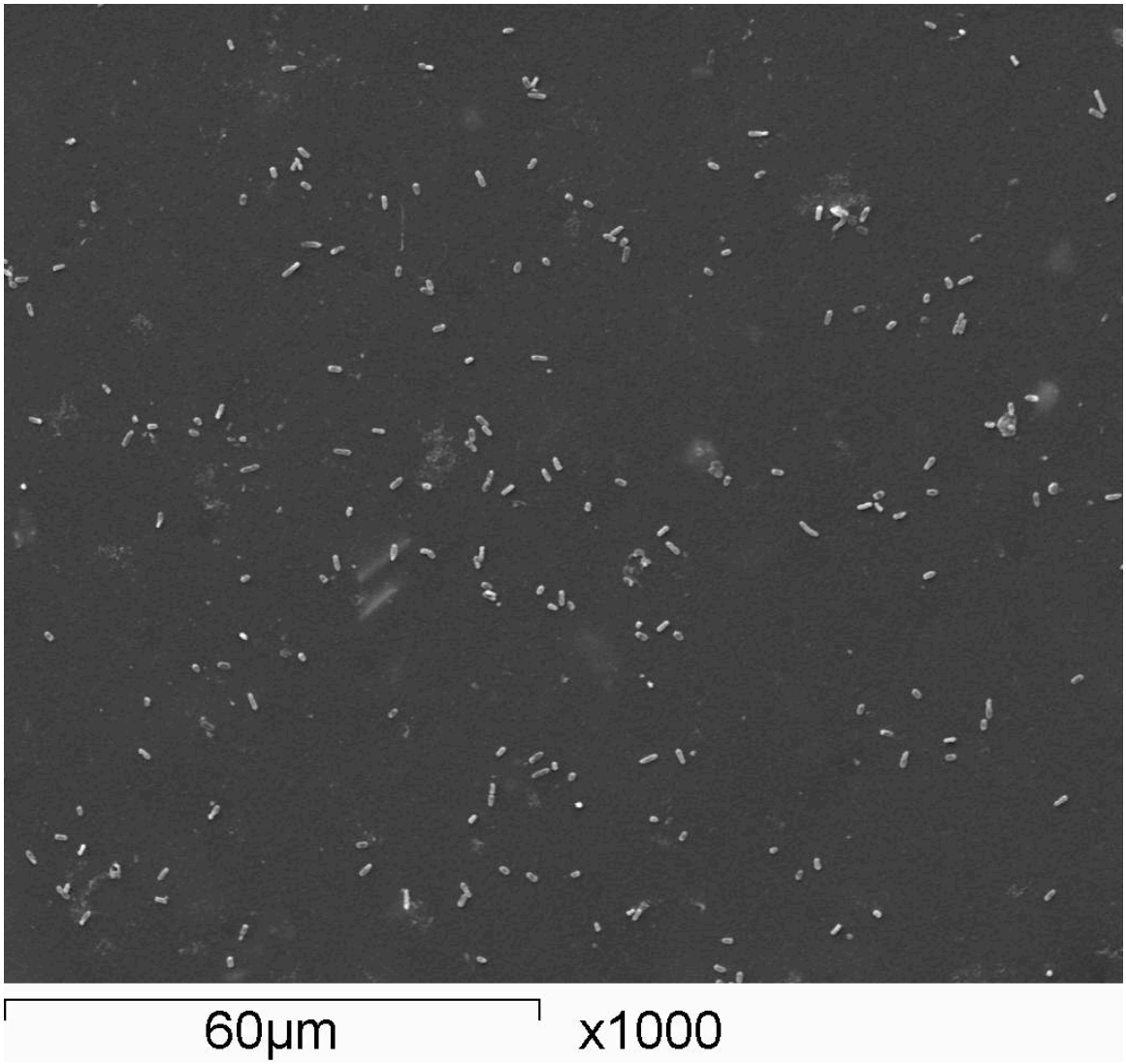

Figure 7.11 SEM image of *P. aeruginosa* PAO1 on the surface of a TBO-impregnated polymer after irradiation with the most effective irradiation schedule (180 seconds irradiation after 0, 90 and 180 minutes). The total incubation time was 3 hours.

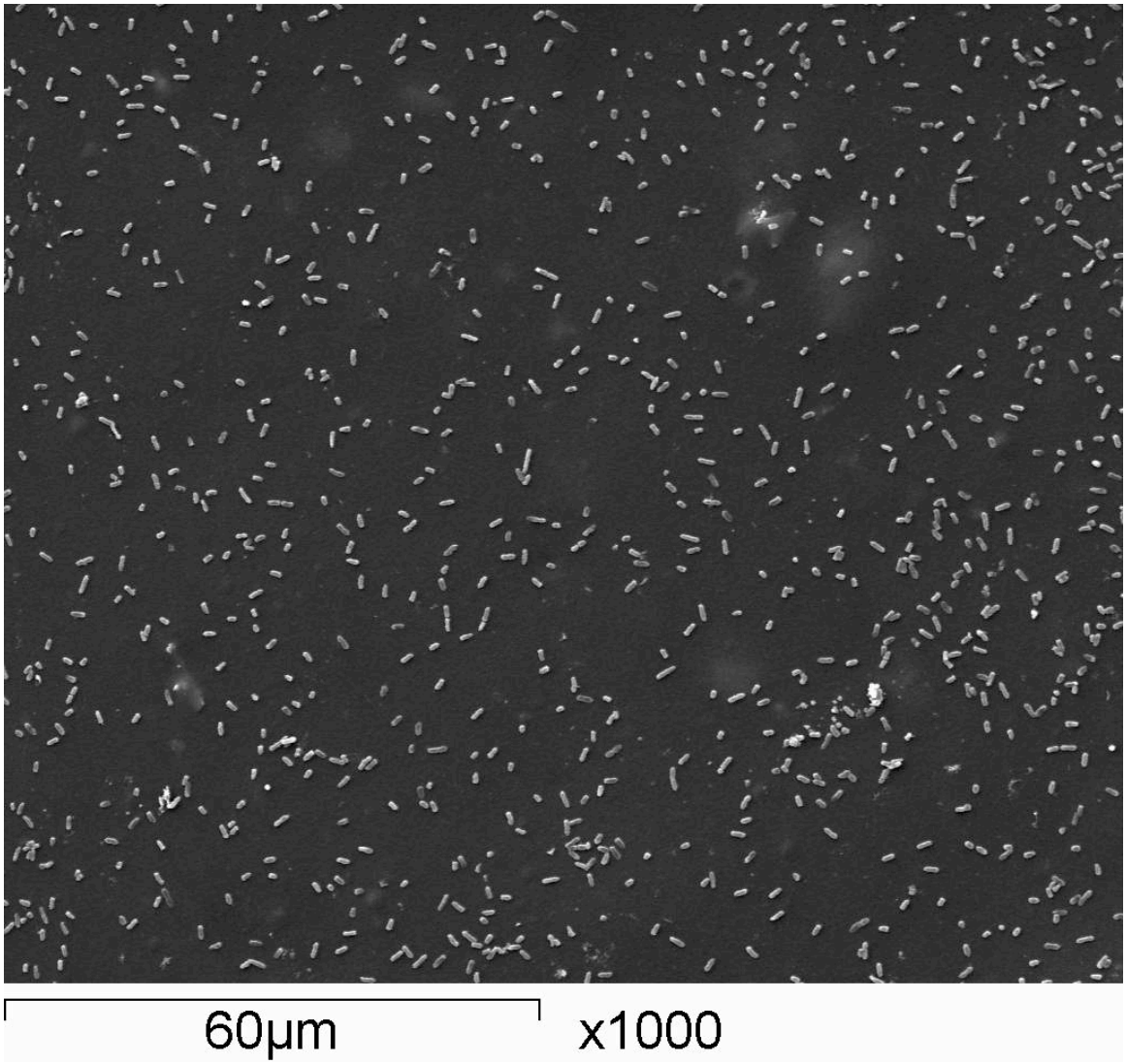

Figure 7.12 SEM image of *P. aeruginosa* PAO1 on the surface of a TBO-impregnated polymer after 3 hours incubation in the absence of laser light.

7.3.2.3 Photo-bleaching effects

During the bacterial attachment assay, the TBO-impregnated polymers were exposed to multiple doses of laser light, which caused the intensity of the blue colouration to decrease. The decrease in colouration was accompanied by a concomitant reduction in antibacterial activity (Figure 7.13). It was shown in Chapter 6 that the antibacterial activity of the TBO-impregnated polymers was proportional to the irradiation time and this was replicated in this experiment, as the greatest reduction in *P. aeruginosa*

recovery from the TBO-impregnated polymers was observed after 240 seconds; a 1.85 $\log_{10}$ cfu / polymer decrease was observed compared with the TBO-impregnated polymers incubated in the dark. However, this reduction was significantly less than that observed on the naïve TBO-impregnated polymers that were not pre-irradiated ($p < 0.001$). This reduction in antibacterial activity was observed for all time points tested and the differences in recovery were all statistically significant ($p < 0.001$).

The reduction in *P. aeruginosa* recovery observed on the naïve TBO-impregnated polymers after 180 seconds irradiation in Figure 7.13 was much greater than that seen when this experiment was first conducted in Chapter 6; a 2.94 $\log_{10}$ cfu / polymer was originally observed and a 3.56 $\log_{10}$ cfu / polymer was observed in this experiment. Moreover, the reduction in *P. aeruginosa* recovered from the TBO-impregnated polymers was greater after 180 seconds irradiation than 240 seconds. This demonstrates the intrinsic variation in activity of the TBO-impregnated polymers, which is also illustrated graphically by the large error bars on the bar chart.

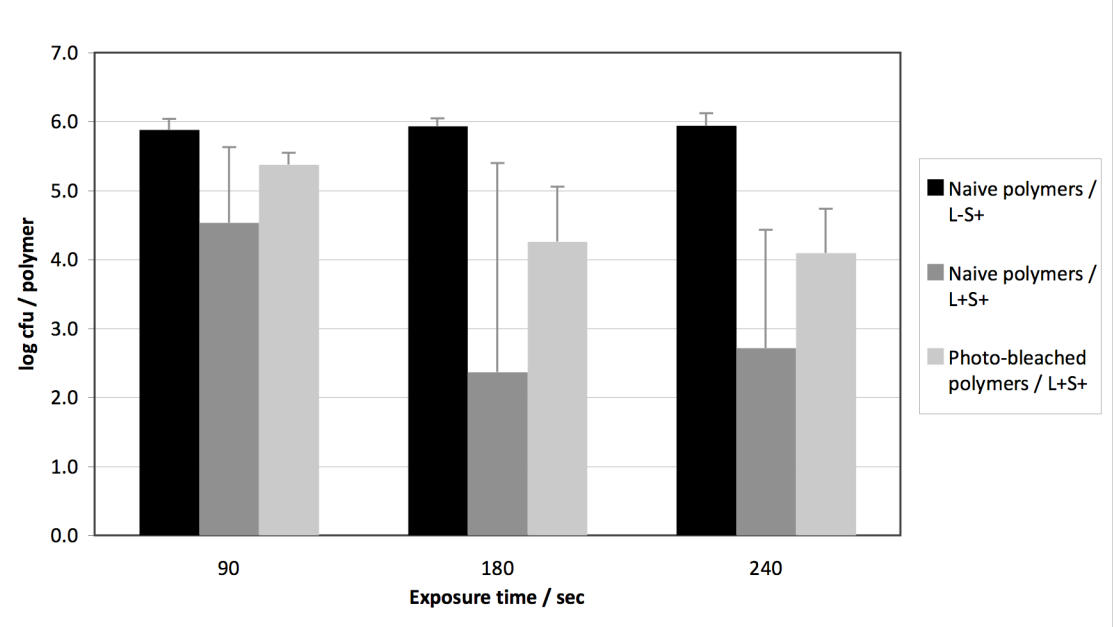

Figure 7.13 Effect of photo-bleaching on the anti-P. aeruginosa activity of the TBO-impregnated polymers

7.4 Discussion

7.4.1 Assessment of initial attachment of EMRSA-16

It was previously shown that the Ag-TiO_2 thin films and TBO-impregnated polymers caused a significant decrease in the recovery of various bacterial species after exposure to light of an appropriate wavelength. The viable colony count method was used to observe the photocatalytic activity of the materials, which was established by showing changes in bacterial recovery after exposure to the relevant light source. In this chapter, visualisation techniques were employed to observe the antibacterial effect of the light-activated materials. Initially, the photo-induced ability of the Ag-TiO_2 thin films to prevent the initial attachment event was investigated. It had previously been shown bacterial cells are more susceptible to the photo-induced effects when the inoculum is lower (Saito et al., 1992; So et al., 2010). Therefore, the hypothesis was

if the thin films were able to reduce adhesion of bacteria to the surface, then there may be fewer bacteria present on the surface to be targeted by the reactive oxygen species generated. The flow cell was used to monitor attachment of EMRSA-16 to the Ag-TiO_2 thin films and no difference in bacterial attachment was observed between the Ag-TiO_2 thin films and the uncoated controls after exposure to the white light source. This result was surprising as a 3.4 $\log_{10}$ cfu / cm^2 decrease in bacterial recovery was detected by aerobic colony count after 18 hours irradiation and the water contact angle significantly decreased after white light irradiation, so a reduction in bacterial attachment was expected.

Page et al., (2009; 2011) demonstrated increased attachment of *S. aureus* on irradiated titania-containing thin films that had demonstrated photo-induced antibacterial activity; however, the bacterial cells were more dispersed, which could prove beneficial for photoinactivation of bacteria. Liquid inoculated onto superhydrophilic materials like the Ag-TiO_2 thin films spread out as a thin layer, which means that more of the bacterial suspension is exposed to the thin film, resulting in faster bacterial photo-inactiavtion. The group also examined the roughness of the titania-containing thin films, and alterations in the surface roughness at the nanoscale did not affect adhesion. Increased surface roughness is commonly attributed to increased microbial adhesion, but this is on a microscale, not nanoscale (Verran et al., 1991; Morgan and Wilson, 2001; Gray et al., 2003). Li and Logan (2005) demonstrated decreased attachment of *B. subtilis, P. aeruginosa, E. coli* and *Burkholderia cepacia* on titania thin films after irradiation with UV light compared with uncoated glass, which was ascribed to photoinduced superhydrophilicity on the irradiated titania films. The

incident light source used in this chapter similarly used light with a band gap energy large enough to generate photocatalysis but a decrease in adhesion was not seen. More recent work by the same group used spectral force analysis to further investigate the adhesive properties of non-irradiated TiO_2 thin films and hypothesised that increased adhesion was not due to overall surface properties such as hydrophilicity or surface charge, but a small number of 'sticky sites' present on the highly heterogeneous surface (Ma et al., 2008). Application of this methodology to the Ag-TiO_2 thin films would determine whether the 'sticky sites' were also present, which could contribute towards the persistent adhesion of EMRSA-16.

7.4.2 Disruption of an immature biofilm of EMRSA-16

It was postulated that the bacterial cells had remained attached to the surface of the Ag-TiO_2 thin films, but had been photo-inactivated by the properties of the material and were non-viable. The Live / Dead BacLight™ Bacterial Viability kit was therefore used to stain bacterial cells in an immature 24 hour biofilm of EMRSA-16 and CLSM was used to visualise the cells. EMRSA-16 was initially inoculated in PBS, a nutrient-poor buffered solution, and incubated at 37°C for 24 hours to allow attachment to occur, before 24 hours irradiation with white light. There were substantially more red cells present on the irradiated thin films than the non-irradiated films, which indicated an increase in the permeability of EMRSA-16 cells to the propidium iodide stain, significant damage to bacterial cell membranes and a decrease in viability. This reduction in the viability of EMRSA-16 to the propidium iodide stain was not observed for EMRSA-16 inoculated onto the surface of Ag-TiO_2 thin films incubated in the absence of light, the irradiated uncoated samples or the uncoated samples incubated

in the dark. This suggests that the damage observed was dependent upon exposure to both the Ag-TiO_2 thin films and white light.

The presence of non-viable bacteria on the surface of the thin film increases further attachment of bacterial cells, as the forces attracting bacteria to a surface are greater when bacteria are already present on the surface compared with a bare surface (Emerson and Camesano, 2004). This would be a distinct disadvantage in a clinical setting. However, after continued white light irradiation, photoinduced oxidative decomposition of the remaining bacterial cells should render the surface sterile (Jacoby et al., 1998). Loss of cell membrane permeability is a well-described stage in the photo-degradation of bacteria on the surface of titanium dioxide based coatings after exposure to appropriate wavelengths of light and this phenomenon is also observed after bacterial exposure to silver ions or nanoparticles (Saito et al., 1992; Dibrov et al., 2002; Lu et al., 2003; Kim et al., 2007; Jung et al., 2008).

Interestingly, this effect was not replicated when the immature EMRSA-16 was grown in BHI, a nutrient-rich growth medium; low numbers of single non-viable cells were present after light exposure, but the majority of attached cells fluoresced green indicating viability. The cells present on the thin film had also begun to aggregate and form microcolonies, which is one of the initial stages of biofilm formation (Tolker-Nielsen et al., 2000). Overall, a greater number of cells were present after the incubation period and faster bacterial growth was encouraged because of the increased level of nutrients in the bacterial suspension, compared with the PBS-based experiment. The additional proteins present in the growth medium could have scavenged the reactive oxygen species generated, shielding EMRSA-16 from the

photocatalytic effects of the thin films (Blake et al., 1999; Komerik and Wilson, 2002). Furno et al., (2004) observed a similar effect on the viability of *S. epidermidis* inoculated onto silver-impregnated polymers after the addition of host-derived proteins. Conversely, Fuertes et al., (2011) showed decreased antibacterial activity of a suspension of silica-coated silver nanoparticles against *E. coli* in PBS compared with a standard growth media Luria-Bertani (LB) broth. The authors cited that the decreased activity was due to a larger zeta potential of *E. coli* and the silver nanoparticles in the PBS solution compared with the LB broth. This meant that the silver nanoparticles immersed in PBS were less likely to interact with *E. coli* compared with the LB broth, and the antibacterial activity was dependent upon the proximity to the nanoparticles. It is unlikely that the zeta potential had a large effect on the photocatalytic activity of the Ag-TiO_2 thin films described in this chapter, as the silver nanoparticles were immobilised on the thin film, rather than free in solution as a nanoparticulate powder, as described in the Fuertes paper.

7.4.3 Prevention of initial *P. aeruginosa* PAO1 attachment

The ability of the TBO-impregnated polymers to prevent initial attachment of *P. aeruginosa* PAO1 after irradiation with laser light was subsequently investigated. Repeated exposure to the laser light was needed to generate a significant reduction in bacterial attachment and the most effective regimen tested was 3 doses of laser light, for 180 seconds, in 90 minute intervals. A significant reduction in the viability of *P. aeruginosa* PAO1 was also observed on the irradiated TBO-impregnated polymers, compared with the TBO-impregnated polymers incubated in the absence of light and the non-impregnated polymers, regardless of the light exposure conditions. The

endpoint of the biofilm disruption assay was enumeration of bacterial colonies after inoculation onto agar plates, which only detects viable cells. Therefore, in order to visualise all bacteria remaining on the surface of the polymers after irradiation, the samples were examined by SEM. A reduction in the attachment of *P. aeruginosa* PAO1 to the surface of the irradiated TBO-impregnated polymers was observed when compared with the TBO-impregnated polymers incubated in the absence of laser light. These results combined, suggest that the photo-activity of the polymers inactivated *P. aeruginosa* PAO1, which resulted in a decrease in the number of viable organisms cultured and less bacteria remained adhered to the surface of the irradiated TBO-impregnated polymers, as demonstrated by SEM.

TBO-mediated PDI had been demonstrated to disrupt the architecture of *S. aureus* and *S. epidermidis* 16-hour biofilms, reducing the cell numbers and causing damage to the bacterial cell membranes (Sharma et al., 2008). This was observed after treatment with an aqueous solution of TBO, which should inactivate bacteria at a faster rate than TBO impregnated into a polymer, due to the increased surface area to volume ratio. Other research groups have described PDI of bacterial biofilms after treatment with a solution of TBO and irradiation (Dobson and Wilson, 1992; Seal et al., 2002; Zanin et al., 2006; Donnelly et al., 2007; Nastri et al., 2010), however, to the authors knowledge, biofilm disruption has not been demonstrated on an irradiated TBO-impregnated polymer, which makes this finding unique to this thesis. However, a photo-bleaching effect was noted on the TBO-impregnated polymers after exposure to the laser light, which resulted in a reduction in the photo-activity of the material. This

indicates that the lifespan of the photo-activity of the polymer could be limited, which would restrict the clinical application of the material.

7.4.4 Limitations of the experimental work

The anti-adhesive, photo-activity of each of the novel light-activated materials was assessed against only just bacterial strain and the adhesive properties of one isolate cannot always be used to predict the adhesive properties of another isolate of the same genus or even species. For example, the *bapL* gene was found to play a role in the attachment of *Listeria monocytogenes* 10403s to inanimate surfaces; however it was absent from a number of *L. monocytogenes* isolates from food sources, so the attachment mechanisms found in *L. monocytogenes* 10403s could not be extrapolated to other strains (Jordan et al., 2008).

The size and shape of bacterial cells can also affect the strength of the binding to surfaces; so attachment of the Gram-positive coccus EMRSA-16 is likely to differ from that of the Gram-negative bacillus *P. aeruginosa.* Microscopic cracks were observed on the surface of the Ag-TiO_2 thin films by light microscopy, and bacterial cells that are able to fit within these cracks could escape physical removal by cleaning (Verran et al., 2010b). However this problem would potentially be overcome by the photoactivity of the thin films, as silver nanoparticles were observed in these ridges and a photo-activated antibacterial effect would be exerted on these cells after irradiation with white light.

The flow cell model was used to investigate the adhesion of EMRSA-16 to the Ag-TiO_2 thin films, however it would be unlikely that the thin films would be exposed to the

shear forces experienced in the flow cell during the proposed use in a hospital environment. The flow cell was used as it enabled a constant bacterial inoculum to be passed over the thin film and provided the opportunity for attachment.

The bacterial growth atmosphere can also affect susceptibility to the photo-activity of the TBO-impregnated polymers. Bacteria colonising the oropharynx will be exposed to higher concentrations of carbon dioxide than that found in atmospheric conditions. Wilcox et al., (1991) found increased adherence to polyurethane and silicone catheters by some strains of coagulase-negative staphylococci after growth in 5% carbon dioxide, suggesting that carbon dioxide could be used by the cells as a trigger to up-regulate genes involved in adhesion. The isolates used in these experiments were grown in atmospheric conditions, so these candidate adhesion genes would not be expressed.

7.5 Conclusions

The anti-adhesive properties of the novel antibacterial Ag-TiO_2 thin films and TBO-impregnated polymers were investigated. A reduction in the viability of EMRSA-16 adhered onto the surface of the irradiated Ag-TiO_2 thin films was demonstrated using a differential viability stain and fluorescence microscopy. The reduction was observed when EMRSA-16 was prepared in a buffered saline suspension but it was not replicated when the bacterial inoculum was prepared in a nutrient-rich medium. Additionally, there was no difference in bacterial attachment on the irradiated Ag-TiO_2 thin films compared to those incubated in the dark, implying that the photo-inactivated cells remained adhered to the surface. A significant reduction in the

adhesion of *P. aeruginosa* on the TBO-impregnated polymers was observed after a 3-step irradiation schedule. This effect was determined using a biofilm disruption assay and confirmed by SEM. The irradiation source caused photo-bleaching of the TBO-impregnated polymers with a concomitant decrease in antibacterial activity which would limit the lifespan of the material.

8 Concluding remarks and future work

Healthcare associated infections (HCAIs) remain a significant problem in healthcare institutions and the near-patient environment is known to harbour bacteria. These microorganisms can be transferred from the environment to a patient and the most common vehicle of transmission is via unwashed hands. If the microbial load of the near-patient could be decreased, then the risk of bacterial transmission will be reduced, which may in turn reduce the acquisition and onwards transmission of HCAIs. Self-cleaning coatings could be applied to hand-touch surfaces in the vicinity of the patient, alongside other infection control measures, to achieve this aim.

A range of sampling methods was initially trialled to develop an optimal sampling regimen for assessing the antibacterial activity of novel light-activated coatings. Reports of the use of ATP bioluminescence to assess the efficiency of cleaning regimens within the healthcare environment are increasing, so this technology was applied to provide an accurate estimate of concentration of bacteria on the test surfaces. However, the viable count technique was shown to be superior, and this was especially apparent at low bacterial concentrations, when the ATP bioluminescence-based techniques were unable to consistently confirm the presence of small numbers of bacteria.

A series of light-activated, antibacterial materials were generated. Initially, two novel nitrogen-doped titanium dioxide (TiO_2) based thin films were synthesised by chemical vapour deposition (CVD); titanium oxynitride and nitrogen-doped titania. These thin films exhibited marked antibacterial activity against *E. coli* after irradiation with both

ultraviolet light (UV) and white light. Activation of the thin films with incident light of an increased wavelength demonstrated a shift in the band onset of the material, from the UV to the visible portion of the electromagnetic spectrum. The photocatalytic properties of the N-doped thin films were greater than that observed on the titanium oxynitride thin films. White-light activated sulfur-doped thin films were also synthesised, and a significant photocatalytic activity was observed against *E. coli.* The greatest antibacterial activity was generated on the N-doped thin films after 24 hours irradiation with white light and a 2.5 $\log_{10}$ cfu / sample decrease was observed. The durability of the thin films was assessed by exposure to successive cycles of use and decontamination, and the integrity of the coating remained intact. A longer-term evaluation of the effect on wear and successive cleaning cycles, in addition to an assessment of the toxicity against eukaryotic cells would be warranted, as these coatings would need to be extremely robust and non-toxic if applied onto hand-touch surfaces in a healthcare environment.

However, it was difficult to synthesise reproducible thin films using the CVD method of deposition, and so an alternative method was used to generate a second series of thin films. Silver-coated TiO_2 thin films were synthesised by the sol gel method of deposition, and the addition of the silver nanoparticles induced a shift in the band onset of the thin films, to enable white light activation. The thin films displayed photochromic behaviour, and a change in the oxidation state was induced by different storage conditions. After storage in the dark, silver was oxidised to silver oxide resulting in a purple coloured film; extended exposure to indoor lighting conditions or indeed UV light, induced photoreduction of the silver oxide back to silver, which

resulted in an orange coloured film. A UV filter was applied to the white light source to filter out the minimal UV component emitted during illumination, and true visible light photocatalysis was demonstrated by photo-oxidation of stearic acid, a reduction in the water contact angle and significant antibacterial activity against two microorganisms implicated in HCAIs; *E. coli* and EMRSA. *E. coli* was shown to display increased susceptibility to the antibacterial activity of the silver-coated TiO_2 thin films, via a light-independent mechanism. In contrast, the photo-induced destruction of EMRSA was due to reactive oxygen produced by TiO_2, driven by white light photocatalysis, in turn driven by silver. This is the first example of unambiguous visible light photocatalysis and photo-induced superhydrophilicity alongside a titanium dioxide control that showed no activation.

Assessment of the silver-coated TiO_2 thin films against non-vegetative cells such as bacterial spores and viruses would determine whether the activity observed was broad spectrum, which would further increase the potential use of the thin films. Introducing organic soil into the bacterial inoculum would establish whether the presence of non-bacterial contaminants affected the activity of the thin films, and altering the length and duration of the irradiation times would mimic the hospital lighting schedules and assess the effect of day-time activation and night-time deactivation. These further translational tests replicate conditions similar to that found within the hospital environment, which would provide more detailed information on the potential activity of the thin films in a healthcare setting.

The anti-adhesive properties of the silver-coated TiO_2 were also explored and the viability of an immature biofilm EMRSA on the surface of the thin film was reduced

after white light irradiation. This reduction was observed when EMRSA was prepared in a buffered saline solution, but was not repeated when the biofilm was grown in a nutrient rich medium. White light exposure did not reduce bacterial attachment to the thin films, which suggested that the photo-inactivated bacterial cells remained attached to the surface. This feature would be detrimental to the functionality of the thin film in a clinical setting, as further attachment of viable bacteria to the non-viable, attached cells would be greater than attachment to a naive surface, which would impact on reducing the bacterial load in the near patient environment.

Further investigation into the mechanism causing increased bacterial adhesion would be useful to increase understanding in this area. Spectral force analysis has demonstrated that the possession of numerous 'sticky sites' can contribute towards the adhesion of bacteria to titania thin films, rather than surface charge or hydrophilicity, which have previously been thought to be the main factors involved in attachment. Identification of the reactive oxygen species generated by the thin films would fully elucidate the mechanism of the observed antibacterial activity. This was attempted unsuccessfully with various specific fluorescent probes, and further analysis into this area would be of great interest.

Finally, a light-activated polyurethane polymer was synthesised by the swell encapsulation method, for potential use in endotracheal tubes (ETTs). The photosensitiser toluidine blue (TBO) was impregnated into the polymer, and the antibacterial activity of the material was assessed using a panel of pathogens known to cause ventilator-associated pneumonia. A type II photosensitisation reaction generated the significant dose-dependent antibacterial activity observed against all

tested bacterial strains. A clinical isolate of *P. aeruginosa* displayed decreased susceptibility to the photo-activity of the TBO-impregnated polymers compared with a laboratory strain, which suggests that the laboratory-adapted strain may have lost virulence factors necessary for withstanding attack from singlet oxygen. A significant reduction in the recovery of a clinical isolate of *C. albicans* was also observed, demonstrating that the light-induced effect was not restricted to bacteria. A significant reduction in the adhesion of *P. aeruginosa* was demonstrated on the irradiated TBO-impregnated polymers; however, a photo-bleaching effect was noted which reduced the antibacterial activity of the polymers. This would impact on the clinical application of the product, and reduce the lifespan of the material, so further modification of the polymer would be necessary to prevent this leaching effect and retain the photosensitiser within the polyurethane matrix.

9 Publications arising from this work

9.1 Peer-reviewed Publications

- **Aiken, Z. A.**, Wilson, M. & Pratten, J. (2011) *Evaluation of ATP bioluminescence assays for potential use in a hospital setting*. Infection Control and Hospital Epidemiology. 32:507-509.

- Dunnill, C. W., Page K., **Aiken, Z. A**., Noimark, S., Hyett G., Kafizas, A., Pratten, J., Wilson, M. & Parkin, I. P. (2011) *Nanoparticulate silver coated-titania thin films - Photo-oxidative destruction of stearic acid under different light sources and antimicrobial effects under hospital lighting conditions.* Journal of Photochemistry and Photobiology A: Chemistry. 220: 113-123.

- **Aiken, Z. A.**, Hyett, G., Dunnill, C. W., Wilson M., Pratten J. & Parkin I. P. (2010) *Antimicrobial activity in thin films of pseudobrookite-structured titanium oxynitride under UV irradiation observed for Escherichia coli.* Chemical Vapor Deposition. 16:19-22.

- Dunnill, C. W., **Aiken, Z. A.**, Pratten, J., Wilson, M. & Parkin, I. P. (2010) *Sulfur- and Nitrogen-doped titania biomaterials via APCVD*. Chemical Vapor Deposition. 16:50-4.

- Dunnill, C. W., **Aiken, Z. A.**, Pratten, J., Wilson, M., Morgan, D. J. & Parkin, I. P. (2009) *Enhanced photocatalytic activity under visible light in Nitrogen-doped TiO_2 thin films produced by APCVD preparations using t-butylamine as a nitrogen source and their potential for antibacterial films*. Journal of Photochemistry and Photobiology A: Chemistry.:207(2-3):244-53.

- Dunnill, C. W., **Aiken, Z. A.**, Kafizas, A., Pratten, J., Wilson, M., Morgan, D. J., & Parkin, I. P. (2009) *White light induced photocatalytic activity of sulfur-doped TiO_2 thin films and their potential for antibacterial application*. Journal of Materials Chemistry. 19:8747-54.

- Dunnill, C. W., **Aiken, Z. A.**, Pratten, J., Wilson, M. & Parkin, I. P. (2009) *Nitrogen doped titania thin films, prepared by atmospheric pressure chemical vapour deposition: Enhanced visible light photocatalytic activity and anti-microbial effects.* ECS Transactions. 25:65-72.

9.2 Poster presentations

- **Aiken, Z. A.**, Parkin, I. P., Dunnill, C. W., Pratten, J. & Wilson, M. (2009) *Evaluation of a novel antibacterial coating activated by white light.* Society of General Microbiology Conference, Harrogate, UK.

- **Aiken, Z. A.**, Wilson, M. & Pratten, J. (2008) *Evaluation of techniques to detect surface-associated pathogens.* Society of General Microbiology Conference, Dublin, Ireland.

9.3 Other publications

- **Aiken, Z. A.**, - Christine Philphot prize essay - 'The role of the environment in the acquisition of healthcare-associated infections.' 2010. ACM News.

- **Aiken, Z. A.**, – Press release on EurekAlert – 'Light-activated antibacterial coating is new weapon in fight against hospital-acquired infections.' 2009. http://www.eurekalert.org/pub_releases/2009-03/sfgm-lac032709.php [Accessed on 28/06/10]

10 References

Aiken, Z. A., Hyett, G., Dunnill, C. W., Wilson, M., Pratten, J. & Parkin, I. P., (2010). *Antimicrobial activity in thin films of pseudobrookite-structured titanium oxynitride under UV irradiation observed for Escherichia coli*. Chemical Vapor Deposition. **16:** 19-22.

Aiken, Z. A., Wilson, M. & Pratten, J., (2011). *Evaluation of ATP bioluminescence assays for potential use in a hospital setting*. Infection Control and Hospital Epidemiology. **32:** 507-9.

Airey, P. & Verran, J., (2007). *Potential use of copper as a hygienic surface; problems associated with cumulative soiling and cleaning*. Journal of Hospital Infection. **67:** 271-277.

Alekshun, M. N. & Levy, S. B., (2006). *Commensals upon us*. Biochemical Pharmacology. **71:** 893-900.

Allen, N. S., Edge, M., Sandoval, G., Verran, J., Stratton, J. & Maltby, J., (2005). *Photocatalytic coatings for environmental applications*. Photochemistry and Photobiology. **81:** 279-90.

Anderson, R. E., Young, V., Stewart, M., Robertson, C. & Dancer, S. J., (2011). *Cleanliness audit of clinical surfaces and equipment: who cleans what?* Journal of Hospital Infection. **78:** 178-81.

Asahi, R., Morikawa, T., Ohwaki, T., Aoki, K. & Taga, Y., (2001). *Visible-light photocatalysis in nitrogen-doped titanium oxides*. Science. **293:** 269-71.

Atherton, H. V. & Newlander, J. A. (1977). *Dye reduction tests: Methylene blue and resazurin*. *Chemistry and testing of dairy products.* 4th ed. Westport, USA: AVI Publishing.

Aycicek, H., Oguz, U. & Karci, K., (2006). *Comparison of results of ATP bioluminescence and traditional hygiene swabbing methods for the determination of surface cleanliness at a hospital kitchen*. International Journal of Hygiene and Environmental Health. **209:** 203-206.

Balk, R. A., (2002). *Is a silver coating a silver lining?* Chest. **121:** 682-3.

Bambauer, R., Mestres, P., Schiel, R., Klinkmann, J. & Sioshansi, P., (1997). *Surface-treated catheters with ion beam-based process evaluation in rats*. Artificial Organs. **21:** 1039-41.

BAPS. (1994). *Clostridium difficile Infection Prevention and Management*. Department of Health/Public Health Laboratory Service Joint Working Group.

Bartley, P. B., Schooneveldt, J. M., Looke, D. F., Morton, A., Johnson, D. W. & Nimmo, G. R., (2001). *The relationship of a clonal outbreak of Enterococcus faecium vanA to methicillin-resistant Staphylococcus aureus incidence in an Australian hospital*. Journal of Hospital Infection. **48:** 43-54.

Berra, L., Curto, F., Bassi, G. L., Laquerriere, P., Pitts, B., Baccarelli, A. & Kolobow, T., (2008a). *Antimicrobial-coated endotracheal tubes: an experimental study*. Intensive Care Medicine. **34:** 1020-1029.

Berra, L., De Marchi, L., Yu, Z. X., Laquerriere, P., Baccarelli, A. & Kolobow, T., (2004). *Endotracheal tubes coated with antiseptics decrease bacterial colonization of the ventilator circuits, lungs, and endotracheal tube*. Anesthesiology. **100:** 1446-56.

Berra, L., Kolobow, T., Laquerriere, P., Pitts, B., Bramati, S., Pohlmann, J., Marelli, C., Panzeri, M., Brambillasca, P., Villa, F., Baccarelli, A., Bouthors, S., Stelfox, H. T., Bigatello, L. M., Moss, J. & Pesenti, A., (2008b). *Internally coated endotracheal tubes with silver sulfadiazine in polyurethane to prevent bacterial colonization: a clinical trial*. Intensive Care Medicine. **34:** 1030-7.

Berra, L., Panigada, M., De Marchi, L., Greco, G., Y, Z. X., Baccarelli, A., Pohlmann, J., Costello, K. F., Appleton, J., Mahar, R., Lewandowski, R., Ravitz, L. & Kolobow, T., (2003). *New approaches for the prevention of airway infection in ventilated patients. Lessons learned from laboratory animal studies at the National Institutes of Health*. Minerva Anestesiologica. **69:** 342-7.

Berra, L., Sampson, J., Fumagalli, J., Panigada, M. & Kolobow, T., (2011). *Alternative approaches to ventilator-associated pneumonia prevention*. Minerva Anestesiologica. **77:** 323-33.

Berthold Technologies GmbH & Co. KG. (2007). *Lumat LB9507 ultra sensitive tube luminometer - Product information leaflet*.

Bhalla, A., Pultz, N. J., Gries, D. M., Ray, A. J., Eckstein, E. C., Aron, D. C. & Donskey, C. J., (2004). *Acquisition of nosocomial pathogens on hands after contact with environmental surfaces near hospitalized patients*. Infection Control and Hospital Epidemiology. **25:** 164-7.

BioThema AB. (2006). *Microbial ATP kit product information leaflet*.

Blake, D. M., Maness, P.-C., Huang, Z., Wolfrum, E. J., Huang, J. & Jacoby, W. A., (1999). *Application of the photocatalytic chemistry of titanium dioxide to disinfection and the killing of cancer cells*. Separation & Purification Reviews. **28:** 1-50.

Blot, S., Rello, J. & Vogelaers, D., (2011). *What is new in the prevention of ventilator-associated pneumonia?* Current Opinion in Pulmonary Medicine. **17:** 155-9.

Bonnett, R., (1995). *Photosensitizers of the porphyrin and phthalocyanine series for photodynamic therapy*. Chemical Society Reviews. **24:** 19-33.

Bouadma, L., Deslandes, E., Lolom, I., Le Corre, B., Mourvillier, B., Regnier, B., Porcher, R., Wolff, M. & Lucet, J. C., (2010). *Long-term impact of a multifaceted prevention program on ventilator-associated pneumonia in a medical intensive care unit*. Clinical Infectious Diseases. **51:** 1115-22.

Boulos, L., Prevost, M., Barbeau, B., Coallier, J. & Desjardins, R., (1999). *LIVE/DEAD(R) BacLight(TM): application of a new rapid staining method for direct enumeration of viable and total bacteria in drinking water*. Journal of Microbiological Methods. **37:** 77-86.

Bowman, S. M. & Free, S. J., (2006). *The structure and synthesis of the fungal cell wall*. Bioessays. **28:** 799-808.

Boyce, J. M., (2007). *Environmental contamination makes an important contribution to hospital infection*. Journal of Hospital Infection. **65:** 50-54.

Boyce, J. M., Havill, N. L., Dumigan, D. G., Golebiewski, M., Balogun, O. & Rizvani, R., (2009). *Monitoring the effectiveness of hospital cleaning practices by use of an adenosine triphosphate bioluminescence assay*. Infection Control and Hospital Epidemiology. **30:** 678-84.

Boyce, J. M., Havill, N. L., Otter, J. A. & Adams, N. M., (2007). *Widespread environmental contamination associated with patients with diarrhea and methicillin-resistant Staphylococcus aureus colonization of the gastrointestinal tract*. Infection Control and Hospital Epidemiology. **28:** 1142-1147.

Boyce, J. M., Havill, N. L., Otter, J. A., McDonald, L. C., Adams, N. M., Cooper, T., Thompson, A., Wiggs, L., Killgore, G., Tauman, A. & Noble-Wang, J., (2008). *Impact of hydrogen peroxide vapor room decontamination on Clostridium difficile environmental contamination and transmission in a healthcare setting*. Infection Control and Hospital Epidemiology. **29:** 723-9.

Boyce, J. M., Opal, S. M., Chow, J. W., Zervos, M. J., Potter-Bynoe, G., Sherman, C. B., Romulo, R. L., Fortna, S. & Medeiros, A. A., (1994). *Outbreak of multidrug-resistant Enterococcus faecium with transferable vanB class vancomycin resistance*. Journal of Clinical Microbiology. **32:** 1148-1153.

Boyce, J. M. & Pittet, D., (2002). *Guideline for Hand Hygiene in Health-Care Settings: recommendations of the Healthcare Infection Control Practices Advisory Committee*

and the HICPAC/SHEA/APIC/IDSA Hand Hygiene Task Force. Infection Control and Hospital Epidemiology. **23:** S3-40.

Boyce, J. M., Potter-Bynoe, G., Chenevert, C. & King, T., (1997). *Environmental contamination due to methicillin-resistant Staphylococcus aureus: possible infection control implications*. Infection Control and Hospital Epidemiology. **18:** 622-7.

Brady, M. J., Lisay, C. M., Yurkovetskiy, A. V. & Sawan, S. P., (2003). *Persistent silver disinfectant for the environmental control of pathogenic bacteria*. American Journal of Infection Control. **31:** 208-14.

Bragg, P. D. & Rainnie, D. J., (1974). *The effect of silver ions on the respiratory chain of Escherichia coli*. Canadian Journal of Microbiology. **20:** 883-889.

Bressler, N. M. & Bressler, S. B., (2000). *Photodynamic therapy with verteporfin (Visudyne): impact on ophthalmology and visual sciences*. Investigative Ophthalmology & Visual Science. **41:** 624-8.

Brook, L. A., Evans, P., Foster, H. A., Pemble, M. E., Sheel, D. W., Steele, A. & Yates, H. M., (2007a). *Novel multifunctional films*. Surface and Coatings Technology. **201:** 9373-9377.

Brook, L. A., Evans, P., Foster, H. A., Pemble, M. E., Steele, A., Sheel, D. W. & Yates, H. M., (2007b). *Highly bioactive silver and silver/titania composite films grown by chemical vapour deposition*. Journal of Photochemistry and Photobiology A: Chemistry. **187:** 53-63.

Carling, P. C. & Bartley, J. M., (2010). *Evaluating hygienic cleaning in health care settings: what you do not know can harm your patients*. American Journal of Infection Control. **38:** S41-50.

Carling, P. C., Parry, M. F. & Von Beheren, S. M., (2008). *Identifying opportunities to enhance environmental cleaning in 23 acute care hospitals*. Infection Control and Hospital Epidemiology. **29:** 1-7.

Carling, P. C., Po, J., Bartley, J. M. & Herwalt, L., (2010). *Identifying opportunities to improve environmental hygiene in multiple healthcare venues*. Journal of Hospital Infection. **76S1:** S33.

Carp, O., Huisman, C. L. & Reller, A., (2004). *Photoinduced reactivity of titanium dioxide*. Progress in Solid State Chemistry. **32:** 33-177.

Casewell, M. & Phillips, I., (1977). *Hands as route of transmission for Klebsiella species*. British Medical Journal. **2:** 1315-7.

Casey, A. L., Adams, D., Karpanen, T. J., Lambert, P. A., Cookson, B. D., Nightingale, P., Miruszenko, L., Shillam, R., Christian, P. & Elliott, T. S., (2010). *Role of copper in reducing hospital environment contamination*. Journal of Hospital Infection. **74:** 72-7.

Cassie, A. B. D. & Baxter, S., (1944). *Wettability of porous surfaces*. Transactions of the Faraday Society. **40:** 546-551.

Chaiban, G., Hanna, H., Dvorak, T. & Raad, I., (2005). *A rapid method of impregnating endotracheal tubes and urinary catheters with gendine: a novel antiseptic agent*. Journal of Antimicrobial Chemotherapy. **55:** 51-6.

Chaibenjawong, P. & Foster, S., (2011). *Desiccation tolerance in Staphylococcus aureus*. Archives of Microbiology. **193:** 125-135.

Cheng, V. C. C., Wong, L. M. W., Tai, J. W. M., Chan, J. F. W., To, K. K. W., Li, I. W. S., Hung, I. F. N., Chan, K. H., Ho, P. L. & Yuen, K. Y., (2011). *Prevention of nosocomial transmission of norovirus by strategic infection control measures*. Infection Control and Hospital Epidemiology. **32:** 229-237.

Chi, Z. X., Liu, R. T., Sun, Y. J., Wang, M. J., Zhang, P. J. & Gao, C. Z., (2010). *Investigation on the toxic interaction of toluidine blue with calf thymus DNA*. Journal of Hazardous Materials. **175:** 274-278.

Chrzanowski, W., Valappil, S. P., Dunnill, C. W., Abou Neel, E. A., Lee, K., Parkin, I. P., Wilson, M., Armitage, D. A. & Knowles, J. C., (2010). *Impaired bacterial attachment to light activated Ni-Ti alloy*. Materials Science & Engineering C-Materials for Biological Applications. **30:** 225-234.

Clement, J. L. & Jarrett, P. S., (1994). *Antibacterial silver*. Metal-Based Drugs. **1:** 467-82.

Collins, B. J., (1988). *The hospital environment: how clean should a hospital be?* Journal of Hospital Infection. **11:** 53-56.

Cooper, R. A., Griffith, C. J., Malik, R. E., Obee, P. & Looker, N., (2007). *Monitoring the effectiveness of cleaning in four British hospitals*. American Journal of Infection Control. **35:** 338-341.

Coppadoro, A., Berra, L. & Bigatello, L. M., (2011). *Modifying endotracheal tubes to prevent ventilator-associated pneumonia*. Current Opinion in Infectious Diseases. **24:** 157-62.

Dancer, S. J., (1999). *Mopping up hospital infection*. Journal of Hospital Infection. **43:** 85-100.

Dancer, S. J., (2002). *Hospital-acquired infection: is cleaning the answer?* CPD Infection. **3:** 40-46.

Dancer, S. J., (2004). *How do we assess hospital cleaning? A proposal for microbiological standards for surface hygiene in hospitals*. Journal of Hospital Infection. **56:** 10-15.

Dancer, S. J., (2008). *Importance of the environment in meticillin-resistant Staphylococcus aureus acquisition: the case for hospital cleaning*. The Lancet Infectious Diseases. **8:** 101-113.

Dancer, S. J., (2009). *The role of environmental cleaning in the control of hospital-acquired infection*. Journal of Hospital Infection. **73:** 378-85.

Dancer, S. J., (2010). *Control of transmission of infection in hospitals requires more than clean hands*. Infection Control and Hospital Epidemiology. **31:** 958-60.

Dancer, S. J., (2011). *Hospital cleaning in the 21st century*. European Journal of Clinical Microbiology & Infectious Diseases. **In Press**.

Dancer, S. J. & Carling, P. C., (2010). *All that glistens may be neither gold nor clean*. Journal of Hospital Infection. **76:** 177-8.

Dancer, S. J., White, L. & Robertson, C., (2008). *Monitoring environmental cleanliness on two surgical wards*. International Journal of Environmental Health Research. **18:** 357-64.

Dancer, S. J., White, L. F., Lamb, J., Girvan, E. K. & Robertson, C., (2009). *Measuring the effect of enhanced cleaning in a UK hospital: a prospective cross-over study*. BMC Medicine. **7:** 28.

Davidson, C. A., Griffith, C. J., Peters, A. C. & Fielding, L. M., (1999). *Evaluation of two methods for monitoring surface cleanliness-ATP bioluminescence and traditional hygiene swabbing*. Luminescence. **14:** 33-8.

Davies, R. L. & Etris, S. F., (1997). *The development and functions of silver in water purification and disease control*. Catalysis Today. **36:** 107-114.

Decraene, V., Pratten, J. & Wilson, M., (2006). *Cellulose acetate containing toluidine blue and rose bengal is an effective antimicrobial coating when exposed to white light*. Applied and Environmental Microbiology. **72:** 4436-9.

Decraene, V., Pratten, J. & Wilson, M., (2008a). *An assessment of the activity of a novel light-activated antimicrobial coating in a clinical environment*. Infection Control and Hospital Epidemiology. **29:** 1181-4.

Decraene, V., Pratten, J. & Wilson, M., (2008b). *Novel light-activated antimicrobial coatings are effective against surface-deposited Staphylococcus aureus*. Current Microbiology. **57:** 269-73.

Decraene, V., Rampaul, A., Parkin, I. P., Petrie, A. & Wilson, M., (2009). *Enhancement by nanogold of the efficacy of a light-activated antimicrobial coating*. Current Nanoscience. **5:** 257-261.

Deem, S. & Treggiari, M. M., (2010). *New endotracheal tubes designed to prevent ventilator-associated pneumonia: do they make a difference?* Respiratory Care. **55:** 1046-55.

Denton, M., Wilcox, M. H., Parnell, P., Green, D., Keer, V., Hawkey, P. M., Evans, I. & Murphy, P., (2004). *Role of environmental cleaning in controlling an outbreak of Acinetobacter baumannii on a neurosurgical intensive care unit*. Journal of Hospital Infection. **56:** 106-10.

Department of Health, (2001). *Standard principles for preventing hospital-acquired infections*. Journal of Hospital Infection. **47:** S21-S37.

Department of Health, (2008). *The Health Act 2006: Code of practice for the prevention and control of healthcare associated infections*.

Dettenkofer, M., Ammon, A., Astagneau, P., Dancer, S. J., Gastmeier, P., Harbarth, S., Humphreys, H., Kern, W. V., Lyytikainen, O., Sax, H., Voss, A. & Widmer, A. F., (2011). *Infection control - a European research perspective for the next decade*. Journal of Hospital Infection. **77:** 7-10.

Dettenkofer, M. & Spencer, R. C., (2007). *Importance of environmental decontamination - a critical view*. Journal of Hospital Infection. **65:** 55-57.

Devine, J., Cooke, R. P. & Wright, E. P., (2001). *Is methicillin-resistant Staphylococcus aureus (MRSA) contamination of ward-based computer terminals a surrogate marker for nosocomial MRSA transmission and handwashing compliance?* Journal of Hospital Infection. **48:** 72-5.

Dharan, S., Mourouga, P., Copin, P., Bessmer, G., Tschanz, B. & Pittet, D., (1999). *Routine disinfection of patients' environmental surfaces. Myth or reality?* Journal of Hospital Infection. **42:** 113-7.

Dibrov, P., Dzioba, J., Gosink, K. K. & Hase, C. C., (2002). *Chemiosmotic mechanism of antimicrobial activity of Ag+ in Vibrio cholerae*. Antimicrobial Agents and Chemotherapy. **46:** 2668-2670.

Diwald, O., Thompson, T. L., Zubkov, T., Walck, S. D. & Yates, J. T., (2004). *Photochemical activity of nitrogen-doped rutile TiO2(110) in visible light*. The Journal of Physical Chemistry B. **108:** 6004-6008.

Dobosz, A. & Sobczynski, A., (2003). *The influence of silver additives on titania photoactivity in the photooxidation of phenol*. Water Research. **37:** 1489-1496.

Dobson, J. & Wilson, M., (1992). *Sensitization of oral bacteria in biofilms to killing by light from a low-power laser*. Archives of Oral Biology. **37:** 883-7.

Dolmans, D. E., Fukumura, D. & Jain, R. K., (2003). *Photodynamic therapy for cancer*. Nature Reviews Cancer. **3:** 380-7.

Donnelly, R. F., McCarron, P. A., Cassidy, C. M., Elborn, J. S. & Tunney, M. M., (2007). *Delivery of photosensitisers and light through mucus: investigations into the potential use of photodynamic therapy for treatment of Pseudomonas aeruginosa cystic fibrosis pulmonary infection*. Journal of Controlled Release. **117:** 217-26.

Drees, M., Snydman, D. R., Schmid, C. H., Barefoot, L., Hansjosten, K., Vue, P. M., Cronin, M., Nasraway, S. A. & Golan, Y., (2008). *Prior environmental contamination increases the risk of acquisition of vancomycin-resistant enterococci*. Clinical Infectious Diseases. **46:** 678-85.

Drenkard, E. & Ausubel, F. M., (2002). *Pseudomonas biofilm formation and antibiotic resistance are linked to phenotypic variation*. Nature. **416:** 740-3.

Duckworth, G. J. & Jordens, J. Z., (1990). *Adherence and survival properties of an epidemic methicillin-resistant strain of Staphylococcus aureus compared with those of methicillin-sensitive strains*. Journal of Medical Microbiology. **32:** 195-200.

Dunipace, A. J., Beaven, R., Noblitt, T., Li, Y. M., Zunt, S. & Stookey, G., (1992). *Mutagenic potential of toluidine blue evaluated in the Ames test*. Mutation Research. **279:** 255-259.

Dunnill, C. W., Aiken, Z. A., Kafizas, A., Pratten, J., Wilson, M., Morgan, D. J. & Parkin, I. P., (2009a). *White light induced photocatalytic activity of sulfur-doped TiO_2 thin films and their potential for antibacterial application*. Journal of Materials Chemistry. **19:** 8747-8754.

Dunnill, C. W., Aiken, Z. A., Pratten, J., Wilson, M., Morgan, D. J. & Parkin, I. P., (2009b). *Enhanced photocatalytic activity under visible light in N-doped TiO_2 thin films produced by APCVD preparations using t-butylamine as a nitrogen source and their potential for antibacterial films*. Journal of Photochemistry and Photobiology A: Chemistry. **207:** 244-253.

Dunnill, C. W., Aiken, Z. A., Pratten, J., Wilson, M. & Parkin, I. P., (2009c). *N-doped titania thin films, prepared by Atmospheric Pressure Chemical Vapour Deposition: Enhanced visible light photocatalytic activity and antimicrobial effects*. ECS Transactions. **25:** 65-72.

Dunnill, C. W., Aiken, Z. A., Pratten, J., Wilson, M. & Parkin, I. P., (2010). *Sulfur- and nitrogen-doped titania biomaterials via APCVD*. Chemical Vapor Deposition. **16:** 50-54.

Dunnill, C. W., Page, K., Aiken, Z. A., Noimark, S., Hyett, G., Kafizas, A., Pratten, J., Wilson, M. & Parkin, I. P., (2011). *Nanoparticulate silver coated-titania thin films - Photo-oxidative destruction of stearic acid under different light sources and antimicrobial effects under hospital lighting conditions*. Journal of Photochemistry and Photobiology A: Chemistry. **220:** 113-123.

Dunnill, C. W. & Parkin, I. P., (2009). *N-doped titania thin films prepared by Atmospheric Pressure CVD using t-butylamine as the nitrogen source: Enhanced photocatalytic activity under visible light*. Chemical Vapor Deposition. **15:** 171-4.

Durucan, C. & Akkopru, B., (2010). *Effect of calcination on microstructure and antibacterial activity of silver-containing silica coatings*. Journal of Biomedical Materials Research Part B: Applied Biomaterials. **93:** 448-58.

Dyer, B. W., Ferrer, F. A., Klinedinst, D. K. & Rodriguez, R., (2000). *A noncommercial dual luciferase enzyme assay system for reporter gene analysis*. Analytical Biochemistry. **282:** 158-61.

Eby, D. M., Luckarift, H. R. & Johnson, G. R., (2009). *Hybrid antimicrobial enzyme and silver nanoparticle coatings for medical instruments*. ACS Applied Materials & Interfaces. **1:** 1553-60.

Edwards, R. J., Sockett, R. E. & Brookfield, J. F., (2002). *A simple method for genome-wide screening for advantageous insertions of mobile DNAs in Escherichia coli*. Current Biology. **12:** 863-7.

Ellington, M. J., Hope, R., Livermore, D. M., Kearns, A. M., Henderson, K., Cookson, B. D., Pearson, A. & Johnson, A. P., (2010). *Decline of EMRSA-16 amongst methicillin-resistant Staphylococcus aureus causing bacteraemias in the UK between 2001 and 2007*. Journal of Antimicrobial Chemotherapy. **65:** 446-8.

Emerson, R. J., IV & Camesano, T. A., (2004). *Nanoscale investigation of pathogenic microbial adhesion to a biomaterial*. Applied and Environmental Microbiology. **70:** 6012-6022.

Ena, J., Dick, R. W., Jones, R. N. & Wenzel, R. P., (1993). *The epidemiology of intravenous vancomycin usage in a university hospital*. JAMA: The Journal of the American Medical Association. **269:** 598-602.

Encyclopedia Britannica. (2011). *Bioluminescence* [Online]. Available: http://www.britannica.com/EBchecked/topic/66087/bioluminescence [Accessed 06/01/2011].

Erasmus, V., Daha, T. J., Brug, H., Richardus, J. H., Behrendt, M. D., Vos, M. C. & van Beeck, E. F., (2010). *Systematic review of studies on compliance with hand hygiene guidelines in hospital care*. Infection Control and Hospital Epidemiology. **31:** 283-94.

Farrington, M., Brenwald, N., Haines, D. & Walpole, E., (1992). *Resistance to desiccation and skin fatty acids in outbreak strains of methicillin-resistant Staphylococcus aureus*. Journal of Medical Microbiology. **36:** 56-60.

Favero, M. S., McDade, J. J., Robertsen, J. A., Hoffman, R. K. & Edwards, R. W., (1968). *Microbiological sampling of surfaces*. Journal of Applied Bacteriology. **31:** 336-43.

Feng, Q. L., Wu, J., Chen, G. Q., Cui, F. Z., Kim, T. N. & Kim, J. O., (2000). *A mechanistic study of the antibacterial effect of silver ions on Escherichia coli and Staphylococcus aureus*. Journal of Biomedical Materials Research. **52:** 662-8.

Flores, C. Y., Diaz, C., Rubert, A., Benitez, G. A., Moreno, M. S., Fernandez Lorenzo de Mele, M. A., Salvarezza, R. C., Schilardi, P. L. & Vericat, C., (2010). *Spontaneous adsorption of silver nanoparticles on Ti/TiO_2 surfaces. Antibacterial effect on Pseudomonas aeruginosa*. Journal of Colloid and Interface Science. **350:** 402-8.

Food Standards Agency. (2004). *Hazard Analyses Critical Control Point (HACCP) guidelines* [Online]. Available at http://www.food.gov.uk/foodindustry/meat/haccpmeatplants/, last accessed 29/10/08. Available: http://www.food.gov.uk/foodindustry/meat/haccpmeatplants/ [Accessed 29/10/08].

Fox, C. L., Jr., (1968). *Silver sulfadiazine--a new topical therapy for Pseudomonas in burns. Therapy of Pseudomonas infection in burns*. Archives of Surgery. **96:** 184-8.

Fox, C. L., Jr., Rappole, B. W. & Stanford, W., (1969). *Control of pseudomonas infection in burns by silver sulfadiazine*. Surgery Gynecology And Obstetrics **128:** 1021-6.

French, G. L., Otter, J. A., Shannon, K. P., Adams, N. M., Watling, D. & Parks, M. J., (2004). *Tackling contamination of the hospital environment by methicillin-resistant Staphylococcus aureus (MRSA): a comparison between conventional terminal cleaning and hydrogen peroxide vapour decontamination*. Journal of Hospital Infection. **57:** 31-7.

Fuertes, G., Sánchez-Muñoz, O. L., Pedrueza, E., Abderrafi, K., Salgado, J. & Jiménez, E., (2011). *Switchable bactericidal effects from novel silica-coated silver nanoparticles mediated by light irradiation*. Langmuir. **27:** 2826-2833.

Fujishima, A. & Honda, K., (1972). *Electrochemical photolysis of water at a semiconductor electrode*. Nature. **238:** 37-+.

Furno, F., Morley, K. S., Wong, B., Sharp, B. L., Arnold, P. L., Howdle, S. M., Bayston, R., Brown, P. D., Winship, P. D. & Reid, H. J., (2004). *Silver nanoparticles and polymeric medical devices: a new approach to prevention of infection?* Journal of Antimicrobial Chemotherapy. **54:** 1019-24.

Fux, C. A., Shirtliff, M., Stoodley, P. & Costerton, J. W., (2005). *Can laboratory reference strains mirror "real-world" pathogenesis?* Trends in Microbiology. **13:** 58-63.

Gaynes, R., Edwards, J. & System, N. N. I. S. N., (1996). *Nosocomial Vancomycin Resistant Enterococci (VRE) in the United States, 1989 - 1995: The first 1000 isolates*. Infection Control and Hospital Epidemiology. **17:** 1-60.

Gerasimchuk, N., Gamian, A., Glover, G. & Szponar, B., (2010). *Light insensitive silver(I) cyanoximates as antimicrobial agents for indwelling medical devices*. Inorganic Chemistry. **49:** 9863-74.

Goodley, J. M., Clayton, Y. M. & Hay, R. J., (1994). *Environmental sampling for aspergilli during building construction on a hospital site*. Journal of Hospital Infection. **26:** 27-35.

Gould, C. V., Umscheid, C. A., Agarwal, R. K., Kuntz, G. & Pegues, D. A., (2010). *Guideline for prevention of catheter-associated urinary tract infections 2009*. Infection Control and Hospital Epidemiology. **31:** 319-26.

Govan, J. R., (1975). *Mucoid strains of Pseudomonas aeruginosa: the influence of culture medium on the stability of mucus production*. Journal of Medical Microbiology. **8:** 513-22.

Grass, G., Rensing, C. & Solioz, M., (2010). *Metallic Copper as an Antimicrobial Surface*. Applied and Environmental Microbiology. **77:** 1541-7.

Gray, J. E., Norton, P. R., Alnouno, R., Marolda, C. L., Valvano, M. A. & Griffiths, K., (2003). *Biological efficacy of electroless-deposited silver on plasma activated polyurethane*. Biomaterials. **24:** 2759-2765.

Griffith, C. J., Blucher, A., Fleri, J. & Fielding, L., (1994). *An evaluation of luminometry as a technique in food microbiology and a comparison of 6 commercially available luminometers*. Food Science and Technology Today. **8:** 209-16.

Griffith, C. J., Cooper, R. A., Gilmore, J., Davies, C. & Lewis, M., (2000). *An evaluation of hospital cleaning regimes and standards*. Journal of Hospital Infection. **45:** 19-28.

Griffith, C. J., Obee, P., Cooper, R. A., Burton, N. F. & Lewis, M., (2007). *The effectiveness of existing and modified cleaning regimens in a Welsh hospital*. Journal of Hospital Infection. **66:** 352-359.

Guffey, J. S. & Wilborn, J., (2006). *Effects of combined 405-nm and 880-nm light on Staphylococcus aureus and Pseudomonas aeruginosa in vitro*. Photomedicine and Laser Surgery. **24:** 680-3.

Gunawan, C., Teoh, W. Y., Marquis, C. P., Lifia, J. & Amal, R., (2009). *Reversible antimicrobial photoswitching in nanosilver*. Small. **5:** 341-344.

Gupta, A., Matsui, K., Lo, J. F. & Silver, S., (1999). *Molecular basis for resistance to silver cations in Salmonella*. Nature Medicine. **5:** 183-8.

Hachem, R., Reitzel, R., Borne, A., Jiang, Y., Tinkey, P., Uthamanthil, R., Chandra, J., Ghannoum, M. & Raad, I., (2009). *Novel antiseptic urinary catheters for prevention of urinary tract infections: correlation of in vivo and in vitro test results*. Antimicrobial Agents and Chemotherapy. **53:** 5145-9.

Haenle, M., Fritsche, A., Zietz, C., Bader, R., Heidenau, F., Mittelmeier, W. & Gollwitzer, H., (2010). *An extended spectrum bactericidal titanium dioxide (TiO_2) coating for metallic implants: in vitro effectiveness against MRSA and mechanical properties*. Journal of Materials Science: Materials in Medicine. **22:** 381-7.

Hamblin, M. R. & Hasan, T., (2004). *Photodynamic therapy: a new antimicrobial approach to infectious disease?* Photochemical and Photobiological Sciences. **3:** 436-50.

Hamblin, M. R., Viveiros, J., Yang, C., Ahmadi, A., Ganz, R. A. & Tolkoff, M. J., (2005). *Helicobacter pylori accumulates photoactive porphyrins and is killed by visible light*. Antimicrobial Agents and Chemotherapy. **49:** 2822-7.

Hambraeus, A., (1988). *Aerobiology in the operating room - a review*. Journal of Hospital Infection. **11:** 68-76.

Han, S. H., Chin, B. S., Lee, H. S., Jeong, S. J., Choi, H. K., Kim, C. O., Yong, D., Choi, J. Y., Song, Y. G., Lee, K. & Kim, J. M., (2009). *Vancomycin-resistant enterococci bacteremia: risk factors for mortality and influence of antimicrobial therapy on clinical outcome*. Journal of Infection. **58:** 182-90.

Hanna, H., Bahna, P., Reitzel, R., Dvorak, T., Chaiban, G., Hachem, R. & Raad, I., (2006). *Comparative in vitro efficacies and antimicrobial durabilities of novel antimicrobial central venous catheters*. Antimicrobial Agents and Chemotherapy. **50:** 3283-8.

Hansen, D., Krude, J., Blahout, B., Leisebein, T., Dogru-Wiegand, S., Bartylla, T., Raffenberg, M., Benner, D., Biedler, A. & Popp, W., (2010). *Bed-making in the hospital setting - Does it pose infectious risks?* Healthcare Infection. **15:** 85-87.

Hawronskyj, J.-M. & Holah, J., (1997). *ATP: A universal hygiene monitor*. Trends in Food Science & Technology. **8:** 79-84.

Hayden, M. K., Bonten, M. J. M., Blom, D. W., Lyle, E. A., van de Vijver, D. & Weinstein, R. A., (2006). *Reduction in acquisition of vancomycin-resistant Enterococcus after enforcement of routine environmental cleaning measures*. Clinical Infectious Diseases. **42:** 1552-1560.

He, C., Yu, Y., Hu, X. & Larbot, A., (2002). *Influence of silver doping on the photocatalytic activity of titania films*. Applied Surface Science. **200:** 239-247.

Health Protection Agency. (2011a). *Escherichia coli bacteraemia: mandatory surveillance* [Online]. Available: http://www.hpa.org.uk/web/HPAweb&Page&HPAwebAutoListName/Page/1296687731211 [Accessed 28.06.2011].

Health Protection Agency. (2011b). *Glycopeptide-resistant enterococci (GRE) - frequently asked questions* [Online]. Available: http://www.hpa.org.uk/Topics/InfectiousDiseases/InfectionsAZ/EnterococciSpeciesAndGRE/GeneralInformation/ [Accessed 28.06.2011].

Hedin, G., Rynback, J. & Lore, B., (2010). *New technique to take samples from environmental surfaces using flocked nylon swabs*. Journal of Hospital Infection. **75:** 314-317.

Herrmann, J. M., Tahiri, H., Ait-Ichou, Y., Lassaletta, G., González-Elipe, A. R. & Fernández, A., (1997). *Characterization and photocatalytic activity in aqueous medium of TiO_2 and Ag-TiO_2 coatings on quartz*. Applied Catalysis B: Environmental. **13:** 219-228.

Hippocrates. (400 BC). *On Ulcers* [Online]. Available: http://classics.mit.edu/Hippocrates/ulcers.mb.txt [Accessed 30/05/2011].

Holloway, B. W., (1955). *Genetic recombination in Pseudomonas aeruginosa*. Journal of General Microbiology. **13:** 572-81.

Hota, B., (2004). *Contamination, disinfection, and cross-colonization: are hospital surfaces reservoirs for nosocomial infection?* Clinical Infectious Diseases. **39:** 1182-9.

Huang, S. S., Datta, R. & Platt, R., (2006). *Risk of acquiring antibiotic-resistant bacteria from prior room occupants*. Archives of Internal Medicine. **166:** 1945-51.

Huang, Z., Maness, P.-C., Blake, D. M., Wolfrum, E. J., Smolinski, S. L. & Jacoby, W. A., (2000). *Bactericidal mode of titanium dioxide photocatalysis*. Journal of Photochemistry and Photobiology A: Chemistry. **130:** 163-170.

Hughes Whitlock Ltd. (1995). *BioProbe operating guide*.

Huslage, K., Rutala, W. A., Sickbert-Bennett, E. & Weber, D. J., (2010). *A quantitative approach to defining "high-touch" surfaces in hospitals*. Infection Control and Hospital Epidemiology. **31:** 850-3.

Hyett, G., Green, M. A. & Parkin, I. P., (2007). *The use of combinatorial chemical vapor deposition in the synthesis of Ti(3-delta)O4N with 0.06 < delta < 0.25: a titanium oxynitride phase isostructural to anosovite*. Journal of the American Chemical Society. **129:** 15541-8.

Ida, Y., Watase, S., Shinagawa, T., Watanabe, M., Chigane, M., Inaba, M., Tasaka, A. & Izaki, M., (2008). *Direct electrodeposition of 1.46 eV bandgap silver(I) oxide semiconductor films by electrogenerated acid*. Chemistry of Materials. **20:** 1254-1256.

Instrument Glasses. (2000). *UV Filter - Optivex* [Online]. Available: http://www.instrumentglasses.com/uv_filter.html. [Accessed 30/05/2011].

International Organisation for Standardisation. (2011). *ISO Standards* [Online]. Available: http://www.iso.org/iso/iso_catalogue.htm [Accessed 13/11/2011].

Ireland, J. C., Klostermann, P., Rice, E. W. & Clark, R. M., (1993). *Inactivation of Escherichia coli by titanium dioxide photocatalytic oxidation*. Applied and Environmental Microbiology. **59:** 1668-70.

Irie, H., Watanabe, Y. & Hashimoto, K., (2003). *Nitrogen-concentration dependence on photocatalytic activity of $TiO_{2-x}N_x$ powders*. Journal of Physical Chemistry B. **107:** 5483-5486.

Ito, T., (1977). *Toluidine blue - Mode of photodynamic action in yeast cells*. Photochemistry and Photobiology. **25:** 47-53.

Ito, T. & Kobayashi, K., (1977). *In vivo evidence for photodynamic membrane damage as a determining step of inactivation of yeast cells sensitized by toluidine blue*. Photochemistry and Photobiology. **25:** 399-401.

Jacoby, W. A., Maness, P. C., Wolfrum, E. J., Blake, D. M. & Fennell, J. A., (1998). *Mineralization of bacterial cell mass on a photocatalytic surface in air*. Environmental Science & Technology. **32:** 2650-2653.

Jaeger, C. D. & Bard, A. J., (1979). *Spin trapping and electron spin resonance detection of radical intermediates in the photodecomposition of water at TiO_2 particulate systems*. Journal of Physical Chemistry. **83:** 3146-3152.

Jeanes, A., Rao, G., Osman, M. & Merrick, P., (2005). *Eradication of persistent environmental MRSA*. Journal of Hospital Infection. **61:** 85-6.

Jin, R., Cao, Y., Mirkin, C. A., Kelly, K. L., Schatz, G. C. & Zheng, J. G., (2001). *Photoinduced conversion of silver nanospheres to nanoprisms*. Science. **294:** 1901-3.

Johanson, W. G., Jr., Pierce, A. K., Sanford, J. P. & Thomas, G. D., (1972). *Nosocomial respiratory infections with Gram-negative bacilli. The significance of colonization of the respiratory tract*. Annals of Internal Medicine. **77:** 701-6.

Johnson, A. P., Aucken, H. M., Cavendish, S., Ganner, M., Wale, M. C., Warner, M., Livermore, D. M. & Cookson, B. D., (2001). *Dominance of EMRSA-15 and -16 among MRSA causing nosocomial bacteraemia in the UK: analysis of isolates from the European Antimicrobial Resistance Surveillance System (EARSS)*. Journal of Antimicrobial Chemotherapy. **48:** 143-4.

Johnston, C. P., Cooper, L., Ruby, W., Carroll, K. C., Cosgrove, S. E. & Perl, T. M., (2006). *Epidemiology of community-acquired methicillin-resistant Staphylococcus aureus skin infections among healthcare workers in an outpatient clinic*. Infection Control and Hospital Epidemiology. **27:** 1133-1136.

Jordan, S. J., Perni, S., Glenn, S., Fernandes, I., Barbosa, M., Sol, M., Tenreiro, R. P., Chambel, L., Barata, B., Zilhao, I., Aldsworth, T. G., Adriao, A., Faleiro, M. L., Shama, G. & Andrew, P. W., (2008). *Listeria monocytogenes biofilm-associated protein (BapL) may contribute to surface attachment of L. monocytogenes but is absent from many field isolates*. Applied and Environmental Microbiology. **74:** 5451-6.

Jori, G., Fabris, C., Soncin, M., Ferro, S., Coppellotti, O., Dei, D., Fantetti, L., Chiti, G. & Roneucci, G., (2006). *Photodynamic therapy in the treatment of microbial infections: Basic principles and perspective applications*. Lasers in Surgery and Medicine. **38:** 468-481.

Jung, W. K., Koo, H. C., Kim, K. W., Shin, S., Kim, S. H. & Park, Y. H., (2008). *Antibacterial activity and mechanism of action of the silver ion in Staphylococcus aureus and Escherichia coli*. Applied and Environmental Microbiology. **74:** 2171-2178.

Kawahara, K., Tsuruda, K., Morishita, M. & Uchida, M., (2000). *Antibacterial effect of silver-zeolite on oral bacteria under anaerobic conditions*. Dental Materials. **16:** 452-5.

Kawashita, M., Tsuneyama, S., Miyaji, F., Kokubo, T., Kozuka, H. & Yamamoto, K., (2000). *Antibacterial silver-containing silica glass prepared by sol-gel method*. Biomaterials. **21:** 393-398.

Keevil, B. & Warnes, S., (2011). *New insights into the antimicrobial mechanisms of copper touch surfaces*. BMC Proceedings. **5:** P39.

Kelly, P. J., Li, H., Whitehead, K. A., Verran, J., Arnell, R. D. & Iordanova, I., (2009). *A study of the antimicrobial and tribological properties of TiN/Ag nanocomposite coatings*. Surface and Coatings Technology. **204:** 1137-1140.

Kibbler, C. C., Quick, A. & O'Neill, A. M., (1998). *The effect of increased bed numbers on MRSA transmission in acute medical wards*. Journal of Hospital Infection. **39:** 213-219.

Kikuchi, Y., Sunada, K., Iyoda, T., Hashimoto, K. & Fujishima, A., (1997). *Photocatalytic bactericidal effect of TiO_2 thin films: Dynamic view of the active oxygen species responsible for the effect*. Journal of Photochemistry and Photobiology A-Chemistry. **106:** 51-56.

Kim, J., Pitts, B., Stewart, P. S., Camper, A. & Yoon, J., (2008). *Comparison of the antimicrobial effects of chlorine, silver ion, and tobramycin on biofilm*. Antimicrobial Agents and Chemotherapy. **52:** 1446-1453.

Kim, J. S., Kuk, E., Yu, K. N., Kim, J.-H., Park, S. J., Lee, H. J., Kim, S. H., Park, Y. K., Park, Y. H., Hwang, C.-Y., Kim, Y.-K., Lee, Y.-S., Jeong, D. H. & Cho, M.-H., (2007). *Antimicrobial effects of silver nanoparticles*. Nanomedicine: Nanotechnology, Biology and Medicine. **3:** 95-101.

Klevens, R. M., Edwards, J. R., Richards, C. L., Jr., Horan, T. C., Gaynes, R. P., Pollock, D. A. & Cardo, D. M., (2007). *Estimating health care-associated infections and deaths in U.S. hospitals, 2002*. Public Health Reports. **122:** 160-6.

Kloos, W. E. & Bannerman, T. L. (1999). *Staphylococcus and micrococcus*. *In:* Murray, P. R., Baron, E. J., Pfaller, M. A., Tenover, F. C. & Yolken, R. H. (eds.) *Manual of Clinical Microbiology.* 7 ed. Washington D.C.: ASM Press.

Kollef, M. H., Afessa, B., Anzueto, A., Veremakis, C., Kerr, K. M., Margolis, B. D., Craven, D. E., Roberts, P. R., Arroliga, A. C., Hubmayr, R. D., Restrepo, M. I., Auger, W. R., Schinner, R. & Grp, N. I., (2008). *Silver-coated endotracheal tubes and incidence of ventilator-associated pneumonia - The NASCENT Randomized Trial*. JAMA - Journal of the American Medical Association. **300:** 805-813.

Kolobow, T., Berra, L., Li Bassi, G. & Curto, F., (2005). *Novel system for complete removal of secretions within the endotracheal tube: the Mucus Shaver*. Anesthesiology. **102:** 1063-5.

Komerik, N. & Wilson, M., (2002). *Factors influencing the susceptibility of Gram-negative bacteria to toluidine blue O-mediated lethal photosensitization*. Journal of Applied Microbiology. **92:** 618-623.

Kowal, K., Wysocka-Król, K., Kopaczyńska, M., Dworniczek, E., Franiczek, R., Wawrzyńska, M., Vargová, M., Zahoran, M., Rakovský, E., Kuš, P., Plesch, G., Plecenik, A., Laffir, F., Tofail, S. A. M. & Podbielska, H., (2011). *In situ photoexcitation of silver-doped titania nanopowders for activity against bacteria and yeasts*. Journal of Colloid and Interface Science. **In Press, Corrected Proof**.

Kraemer, H., (1905). *The oligodynamic action of copper foil on certain intestinal organisms*. Proceedings of the American Philosophical Society. **44:** 51-65.

Laborde, D. J., Weigle, K. A., Weber, D. J. & Kotch, J. B., (1993). *Effect of fecal contamination on diarrheal illness rates in day-care centers*. American Journal of Epidemiology. **138:** 243-255.

Landrin, A., Bissery, A. & Kac, G., (2005). *Monitoring air sampling in operating theatres: can particle counting replace microbiological sampling?* Journal of Hospital Infection. **61:** 27-29.

Leape, L. L., Brennan, T. A., Laird, N., Lawthers, A. G., Localio, A. R., Barnes, B. A., Hebert, L., Newhouse, J. P., Weiler, P. C. & Hiatt, H., (1991). *The nature of adverse events in hospitalized patients. Results of the Harvard Medical Practice Study II*. New England Journal of Medicine. **324:** 377-84.

Lewis, T., Griffith, C., Gallo, M. & Weinbren, M., (2008). *A modified ATP benchmark for evaluating the cleaning of some hospital environmental surfaces*. Journal of Hospital Infection. **69:** 156-63.

Li, B. & Logan, B. E., (2005). *The impact of ultraviolet light on bacterial adhesion to glass and metal oxide-coated surface*. Colloids and Surfaces B: Biointerfaces. **41:** 153-161.

Li, Q., Xie, R., Li, Y. W., Mintz, E. A. & Shang, J. K., (2007). *Enhanced visible-light-induced photocatalytic disinfection of E. coli by carbon-sensitized nitrogen-doped titanium oxide*. Environmental Science & Technology. **41:** 5050-5056.

Li, Y., Leung, P., Yao, L., Song, Q. W. & Newton, E., (2006). *Antimicrobial effect of surgical masks coated with nanoparticles*. Journal of Hospital Infection. **62:** 58-63.

Lin, Y.-S. E., Vidic, R. D., Stout, J. E. & Yu, V. L., (1996). *Individual and combined effects of copper and silver ions on inactivation of Legionella pneumophila*. Water Research. **30:** 1905-1913.

Lipovsky, A., Nitzan, Y., Friedmann, H. & Lubart, R., (2009). *Sensitivity of Staphylococcus aureus strains to broadband visible light*. Photochemistry and Photobiology. **85:** 255-260.

Liu, J., Sonshine, D. A., Shervani, S. & Hurt, R. H., (2010). *Controlled release of biologically active silver from nanosilver surfaces*. ACS Nano. **4:** 6903-13.

Lu, Z.-X., Zhou, L., Zhang, Z.-L., Shi, W.-L., Xie, Z.-X., Xie, H.-Y., Pang, D.-W. & Shen, P., (2003). *Cell damage induced by photocatalysis of TiO_2 thin films*. Langmuir. **19:** 8765.

Lundin, A., (2000). *Use of firefly luciferase in ATP-related assays of biomass, enzymes, and metabolites*. Methods in Enzymology. **305:** 346-70.

Lv, M., Su, S., He, Y., Huang, Q., Hu, W., Li, D., Fan, C. & Lee, S. T., (2010). *Long-term antimicrobial effect of silicon nanowires decorated with silver nanoparticles*. Advanced Materials. **22:** 5463-7.

Ma, H., Winslow, C. J. & Logan, B. E., (2008). *Spectral force analysis using atomic force microscopy reveals the importance of surface heterogeneity in bacterial and colloid adhesion to engineered surfaces*. Colloids and Surfaces B: Biointerfaces. **62:** 232-237.

Maclean, M., MacGregor, S. J., Anderson, J. G. & Woolsey, G., (2008). *High-intensity narrow-spectrum light inactivation and wavelength sensitivity of Staphylococcus aureus*. FEMS Microbiology Letters. **285:** 227-32.

Maclean, M., MacGregor, S. J., Anderson, J. G. & Woolsey, G., (2009). *Inactivation of bacterial pathogens following exposure to light from a 405-nanometer Light-Emitting Diode array*. Applied and Environmental Microbiology. **75:** 1932-1937.

Maclean, M., Macgregor, S. J., Anderson, J. G., Woolsey, G. A., Coia, J. E., Hamilton, K., Taggart, I., Watson, S. B., Thakker, B. & Gettinby, G., (2010). *Environmental decontamination of a hospital isolation room using high-intensity narrow-spectrum light*. Journal of Hospital Infection. **76:** 247-51.

Malik, R. E., Cooper, R. A. & Griffith, C. J., (2003). *Use of audit tools to evaluate the efficacy of cleaning systems in hospitals*. American Journal of Infection Control. **31:** 181-7.

Malik, Z., Hanania, J. & Nitzan, Y., (1990). *Bactericidal effects of photoactivated porphyrins--an alternative approach to antimicrobial drugs*. Journal of Photochemistry and Photobiology B: Biology. **5:** 281-93.

Maness, P. C., Smolinski, S., Blake, D. M., Huang, Z., Wolfrum, E. J. & Jacoby, W. A., (1999). *Bactericidal activity of photocatalytic TiO2 reaction: Toward an understanding of its killing mechanism*. Applied and Environmental Microbiology. **65:** 4094-4098.

Manheimer, W. A. & Ybanez, T., (1917). *Observations and experiments on dish-washing*. American Journal of Public Health. **7:** 614-618.

Marcus, S. L. & McIntyre, W. R., (2002). *Photodynamic therapy systems and applications*. Expert Opinion on Emerging Drugs. **7:** 321-34.

Martinez-Gutierrez, F., Olive, P. L., Banuelos, A., Orrantia, E., Nino, N., Sanchez, E. M., Ruiz, F., Bach, H. & Av-Gay, Y., (2010). *Synthesis, characterization, and evaluation of antimicrobial and cytotoxic effect of silver and titanium nanoparticles*. Nanomedicine : nanotechnology, biology, and medicine. **6:** 681-688.

Matsunaga, T., Tomoda, R., Nakajima, T., Nakamura, N. & Komine, T., (1988). *Continuous-sterilization system that uses photosemiconductor powders*. Applied and Environmental Microbiology. **54:** 1330-1333.

Matsunaga, T., Tomoda, R., Nakajima, T. & Wake, H., (1985). *Photoelectrochemical sterilization of microbial cells by semiconductor powders*. FEMS Microbiology Letters. **29:** 211-214.

McCarthy, A., (1997). *Methods of analysis and detection,* Cambridge, Cambrdge University Press.

McFarland, L. V., Mulligan, M. E., Kwok, R. Y. & Stamm, W. E., (1989). *Nosocomial acquisition of Clostridium difficile infection*. New England Journal of Medicine. **320:** 204-10.

McHugh, G. L., Moellering, R. C., Hopkins, C. C. & Swartz, M. N., (1975). *Salmonella typhimurium resistant to silver nitrate, chloramphenicol, and ampicillin*. Lancet. **1:** 235-40.

McKeating, J. A., Zhang, L. Q., Logvinoff, C., Flint, M., Zhang, J., Yu, J., Butera, D., Ho, D. D., Dustin, L. B., Rice, C. M. & Balfe, P., (2004). *Diverse hepatitis C virus glycoproteins mediate viral infection in a CD81-dependent manner*. Journal of Virology. **78:** 8496-505.

Mears, A., White, A., Cookson, B., Devine, M., Sedgwick, J., Phillips, E., Jenkinson, H. & Bardsley, M., (2009). *Healthcare-associated infection in acute hospitals: which interventions are effective?* Journal of Hospital Infection. **71:** 307-313.

Medina-Ramirez, I., Luo, Z., Bashir, S., Mernaugh, R. & Liu, J. L., (2011). *Facile design and nanostructural evaluation of silver-modified titania used as disinfectant*. Dalton Transactions. **40:** 1047-1054.

Melaiye, A. & Youngs, W. J., (2005). *Silver and its application as an antimicrobial agent*. Expert Opinion on Therapeutic Patents. **15:** 125-130.

Merz, W. G. & Roberts, G. D. (1999). *Algorithms for detection and identification of fungi*. *In:* Murray, P. R., Baron, E. J., Pfaller, M. A., Tenover, F. C. & Yolken, R. H. (eds.) *Manual of Clinical Microbiology.* 7 ed. Washington D.C.: ASM Press.

Miller, M. A., Arndt, J. L., Konkle, M. A., Chenoweth, C. E., Iwashyna, T. J., Flaherty, K. R. & Hyzy, R. C., (2010). *A polyurethane cuffed endotracheal tube is associated with decreased rates of ventilator-associated pneumonia*. Journal of Critical Care. **26:** 280-6.

Mills, A., Elliott, N., Parkin, I. P., O'Neill, S. A. & Clark, R. J., (2002). *Novel TiO_2 CVD films for semiconductor photocatalysis*. Journal of Photochemistry and Photobiology A: Chemistry. **151:** 171-179.

Mills, A. & LeHunte, S., (1997). *An overview of semiconductor photocatalysis*. Journal of Photochemistry and Photobiology A: Chemistry. **108:** 1-35.

Mills, A., Lepre, A., Elliott, N., Bhopal, S., Parkin, I. P. & O'Neill, S. A., (2003). *Characterisation of the photocatalyst Pilkington Activ™: a reference film photocatalyst?* Journal of Photochemistry and Photobiology A: Chemistry. **160:** 213-224.

Mills, A. & McGrady, M., (2008). *A study of new photocatalyst indicator inks*. Journal of Photochemistry and Photobiology A: Chemistry. **193:** 228-236.

Mills, A. & Wang, J., (2006). *Simultaneous monitoring of the destruction of stearic acid and generation of carbon dioxide by self-cleaning semiconductor photocatalytic films*. Journal of Photochemistry and Photobiology A: Chemistry. **182:** 181-186.

Mock, J. J., Barbic, M., Smith, D. R., Schultz, D. A. & Schultz, S., (2002). *Shape effects in plasmon resonance of individual colloidal silver nanoparticles*. The Journal of Chemical Physics. **116:** 6755-6759.

Monteiro, D. R., Gorup, L. F., Takamiya, A. S., Ruvollo, A. C., de Camargo, E. R. & Barbosa, D. B., (2009). *The growing importance of materials that prevent microbial adhesion: antimicrobial effect of medical devices containing silver*. International Journal of Antimicrobial Agents. **34:** 103-110.

Moore, G. & Griffith, C., (2002). *A comparison of surface sampling methods for detecting coliforms on food contact surfaces*. Food Microbiology. **19:** 65-73.

Moore, G. & Griffith, C., (2007). *Problems associated with traditional hygiene swabbing: the need for in-house standardization*. Journal of Applied Microbiology. **103:** 1090-103.

Moore, G., Griffith, C. J. & Fielding, L., (2001). *A comparison of traditional and recently developed methods for monitoring surface hygiene within the food industry: A laboratory study*. Dairy, Food and Environmental Sanitation. **21:** 478-488.

Morgan, T. D. & Wilson, M., (2001). *The effects of surface roughness and type of denture acrylic on biofilm formation by Streptococcus oralis in a constant depth film fermentor*. Journal of Applied Microbiology. **91:** 47-53.

Moyer, C. A., Brentano, L., Gravens, D. L., Margraf, H. W. & Monafo, W. W., Jr., (1965). *Treatment of large human burns with 0.5 per cent silver nitrate solution.* Archives of Surgery. **90:** 812-67.

Mulvey, D., Redding, P., Robertson, C., Woodall, C., Kingsmore, P., Bedwell, D. & Dancer, S. J., (2011). *Finding a benchmark for monitoring hospital cleanliness*. Journal of Hospital Infection. **77:** 25-30.

Munoz-Price, L. S., Ariza-Heredia, E., Adams, S., Olivier, M., Francois, L., Socarras, M., Coro, G., Adedokun, A., Pappas, T., Tamayo, M., McDade, R. & Cameron, D., (2011). *Use of UV powder for surveillance to improve environmental cleaning*. Infection Control and Hospital Epidemiology. **32:** 283-285.

Nastri, L., Donnarumma, G., Porzio, C., De Gregorio, V., Tufano, M. A., Caruso, F., Mazza, C. & Serpico, R., (2010). *Effects of toluidine blue-mediated photodynamic therapy on periopathogens and periodontal biofilm: in vitro evaluation*. International journal of immunopathology and pharmacology. **23:** 1125-32.

NHS Estates, (2004). *The NHS Healthcare Cleaning Manual*.

NHS National Patient Safety Agency. (2004). *NHS National Patient Safety Agency cleanyourhands campaign* [Online]. Available: http://www.npsa.nhs.uk/cleanyourhands [Accessed 15.05.2011].

Nitzan, Y., Balzam-Sudakevitz, A. & Ashkenazi, H., (1998). *Eradication of Acinetobacter baumannii by photosensitized agents in vitro*. Journal of Photochemistry and Photobiology B: Biology. **42:** 211-8.

Noble, W. C., (1975). *Dispersal of skin microorganisms*. British Journal of Dermatology. **93:** 477-85.

Noimark, S., Dunnill, C. W., Wilson, M. & Parkin, I. P., (2009). *The role of surfaces in catheter-associated infections*. Chemical Society Reviews. **38:** 3435-3448.

Noyce, J. O., Michels, H. & Keevil, C. W., (2006). *Potential use of copper surfaces to reduce survival of epidemic meticillin-resistant Staphylococcus aureus in the healthcare environment*. Journal of Hospital Infection. **63:** 289-97.

O'Neill, S. A., Parkin, I. P., Clark, R. J. H., Mills, A. & Elliott, N., (2003). *Atmospheric pressure chemical vapour deposition of titanium dioxide coatings on glass*. Journal of Materials Chemistry. **13:** 56-60.

Obee, P., Griffith, C. J., Cooper, R. A. & Bennion, N. E., (2007). *An evaluation of different methods for the recovery of meticillin-resistant Staphylococcus aureus from environmental surfaces*. Journal of Hospital Infection. **65:** 35-41.

Ohko, Y., Tatsuma, T., Fujii, T., Naoi, K., Niwa, C., Kubota, Y. & Fujishima, A., (2003). *Multicolour photochromism of TiO_2 films loaded with silver nanoparticles*. Nature Materials. **2:** 29-31.

Ohtani, B., Okugawa, Y., Nishimoto, S. & Kagiya, T., (1987). *Photocatalytic activity of titania powders suspended in aqueous silver nitrate solution: correlation with pH-dependent surface structures*. The Journal of Physical Chemistry. **91:** 3550-3555.

Oie, S., Suenaga, S., Sawa, A. & Kamiya, A., (2007). *Association between isolation sites of methicillin-resistant Staphylococcus aureus (MRSA) in patients with MRSA-positive body sites and MRSA contamination in their surrounding environmental surfaces*. Japanese Journal of Infectious Diseases. **60:** 367-9.

Olson, M. E., Harmon, B. G. & Kollef, M. H., (2002). *Silver-coated endotracheal tubes associated with reduced bacterial burden in the lungs of mechanically ventilated dogs*. Chest. **121:** 863-870.

Paardekooper, M., Vandenbroek, P. J. A., Debruijne, A. W., Elferink, J. G. R., Dubbelman, T. M. A. R. & Vansteveninck, J., (1992). *Photodynamic treatment of yeast cells with the dye toluidine blue - All-or-none loss of plasma membrane barrier properties*. Biochimica Et Biophysica Acta. **1108:** 86-90.

Page, K., (2009). *Photocatalytic thin films: their characterisation and antimicrobial properties.* PhD, UCL.

Page, K., Palgrave, R. G., Parkin, I. P., Wilson, M., Savin, S. L. P. & Chadwick, A. V., (2007). *Titania and silver-titania composite films on glass - potent antimicrobial coatings*. Journal of Materials Chemistry. **17:** 95-104.

Page, K., Wilson, M., Mordan, N. J., Chrzanowski, W., Knowles, J. & Parkin, I. P., (2011). *Study of the adhesion of Staphylococcus aureus to coated glass substrates*. Journal of Materials Science. **In Press**.

Page, K., Wilson, M. & Parkin, I. P., (2009). *Antimicrobial surfaces and their potential in reducing the role of the inanimate environment in the incidence of hospital-acquired infections*. Journal of Materials Chemistry. **19:** 3819-3831.

Paramasivam, I., Macak, J. M., Ghicov, A. & Schmuki, P., (2007). *Enhanced photochromism of Ag loaded self-organized TiO_2 nanotube layers*. Chemical Physics Letters. **445:** 233-237.

Parkin, I. P. & Palgrave, R. G., (2005). *Self-cleaning coatings*. Journal of Materials Chemistry. **15:** 1689-1695.

Percival, S. L., Bowler, P. G. & Russell, D., (2005). *Bacterial resistance to silver in wound care*. Journal of Hospital Infection. **60:** 1-7.

Percival, S. L., Woods, E., Nutekpor, M., Bowler, P., Radford, A. & Cochrane, C., (2008). *Prevalence of silver resistance in bacteria isolated from diabetic foot ulcers and efficacy of silver-containing wound dressings*. Ostomy Wound Management. **54:** 30-40.

Perni, S., Piccirillo, C., Pratten, J., Prokopovich, P., Chrzanowski, W., Parkin, I. P. & Wilson, M., (2009a). *The antimicrobial properties of light-activated polymers containing methylene blue and gold nanoparticles*. Biomaterials. **30:** 89-93.

Perni, S., Piccirillo, C., Prokopovich, P., Pratten, J., Parkin, I. P. & Wilson, M., (2011). *Antimicrobial properties of light-activated polyurethane containing indocyanine green*. Journal of Biomaterials Applications. **25:** 387-400.

Perni, S., Prokopovich, P., Piccirillo, C., Pratten, J., Parkin, I. P. & Wilson, M., (2009b). *Toluidine blue-containing polymers exhibit potent bactericidal activity when irradiated with red laser light*. Journal of Materials Chemistry. **19:** 2715-2723.

Phoenix, D. A., Sayed, Z., Hussain, S., Harris, F. & Wainwright, M., (2003). *The phototoxicity of phenothiazinium derivatives against Escherichia coli and Staphylococcus aureus*. FEMS Immunology and Medical Microbiology. **39:** 17-22.

Pittet, D., Allegranzi, B. & Boyce, J. M., (2009). *The World Health Organization guidelines on Hand Hygiene in Health Care and their consensus recommendations*. Infection Control and Hospital Epidemiology. **30:** 611-22.

Plowman, R., Graves, N., Griffin, M., Roberts, J. A., Swan, A. V., Cookson, B. & Taylor, L. (2000). *The socio-economic burden of hospital acquired infection*. London: PHLS.

Pneumatikos, I. A., Dragoumanis, C. K. & Bouros, D. E., (2009). *Ventilator-associated pneumonia or endotracheal tube-associated pneumonia? An approach to the pathogenesis and preventive strategies emphasizing the importance of endotracheal tube*. Anesthesiology. **110:** 673-80.

Pollini, M., Paladini, F., Catalano, M., Taurino, A., Licciulli, A., Maffezzoli, A. & Sannino, A., (2011). *Antibacterial coatings on haemodialysis catheters by photochemical*

deposition of silver nanoparticles. Journal of Materials Science: Materials in Medicine. 1-8.

Poulis, J. A., de Pijper, M., Mossel, D. A. & Dekkers, P. P., (1993). *Assessment of cleaning and disinfection in the food industry with the rapid ATP-bioluminescence technique combined with the tissue fluid contamination test and a conventional microbiological method*. International Journal of Food Microbiology **20:** 109-16.

Prado, V., Durán, C., Crestto, M., Gutierrez, A., Sapiain, P., Flores, G., Fabres, H., C, T. & Schmidt, M. (2010). *Effectiveness of copper contact surfaces in reducing the microbial burden (MB) in the intensive care unit (ICU) of hospital del Cobre, Calama, Chile. 14th International Conference on Infectious Diseases.* Miami, USA.

Pyle, B. H., Broadaway, S. C. & McFeters, G. A., (1995). *Factors affecting the determination of respiratory activity on the basis of cyanoditolyl tetrazolium chloride reduction with membrane filtration*. Applied and Environmental Microbiology. **61:** 4304-9.

Raad, II, Mohamed, J. A., Reitzel, R. A., Jiang, Y., Dvorak, T. L., Ghannoum, M. A., Hachem, R. Y. & Chaftari, A. M., (2011). *The prevention of biofilm colonization by multidrug-resistant pathogens that cause ventilator-associated pneumonia with antimicrobial-coated endotracheal tubes*. Biomaterials. **32:** 2689-94.

Ragas, X., Dai, T. H., Tegos, G. P., Agut, M., Nonell, S. & Hamblin, M. R., (2010). *Photodynamic inactivation of Acinetobacter baumannii using phenothiazinium dyes: In vitro and in vivo studies*. Lasers in Surgery and Medicine. **42:** 384-390.

Raju, N. R. C., Kumar, K. J. & Subrahmanyam, A., (2009). *Physical properties of silver oxide thin films by pulsed laser deposition: effect of oxygen pressure during growth*. Journal of Physics D: Applied Physics. **42:** 135411.

Rampaul, A., Parkin, I. P., O'Neill, S. A., DeSouza, J., Mills, A. & Elliott, N., (2003). *Titania and tungsten doped titania thin films on glass; active photocatalysts*. Polyhedron. **22:** 35-44.

Rampling, A., Wiseman, S., Davis, L., Hyett, A. P., Walbridge, A. N., Payne, G. C. & Cornaby, A. J., (2001). *Evidence that hospital hygiene is important in the control of methicillin-resistant Staphylococcus aureus*. Journal of Hospital Infection. **49:** 109-116.

Reitzel, R. A., Dvorak, T. L., Hachem, R. Y., Fang, X., Jiang, Y. & Raad, I., (2009). *Efficacy of novel antimicrobial gloves impregnated with antiseptic dyes in preventing the adherence of multidrug-resistant nosocomial pathogens*. American Journal of Infection Control. **37:** 294-300.

Rello, J., Afessa, B., Anzueto, A., Arroliga, A. C., Olson, M. E., Restrepo, M. I., Talsma, S. S., Bracken, R. L. & Kollef, M. H., (2010). *Activity of a silver-coated endotracheal tube in preclinical models of ventilator-associated pneumonia and a study after extubation*. Critical Care Medicine. **38:** 1135-40.

Rello, J., Kollef, M., Diaz, E., Sandiumenge, A., del Castillo, Y., Corbella, X. & Zachskorn, R., (2006). *Reduced burden of bacterial airway colonization with a novel silver-coated endotracheal tube in a randomized multiple-center feasibility study*. Critical Care Medicine. **34:** 2766-72.

Report by the Comptroller and Auditor General - HC 230 Session 1999-2000, (2000). *The management and control of hospital acquired infection in acute NHS Trusts in England*.

Report by the Comptroller and Auditor General - HC Session 2003-2004. (2004). *Improving patient care by reducing the risk of hospital acquired infection: A progress report*.

Rewa, O. & Muscedere, J., (2011). *Ventilator-associated pneumonia: Update on etiology, prevention, and management*. Current Infectious Disease Reports. **13:** 287-295.

Richards, M. J., Edwards, J. R., Culver, D. H. & Gaynes, R. P., (1999). *Nosocomial infections in medical intensive care units in the United States. National Nosocomial Infections Surveillance System*. Critical Care Medicine. **27:** 887-92.

Rivero, P., Urrutia, A., Goicoechea, J., Zamarreño, C., Arregui, F. & Matías, I., (2011). *An antibacterial coating based on a polymer/sol-gel hybrid matrix loaded with silver nanoparticles*. Nanoscale Research Letters. **6:** 305.

Rockson, S. G., Lorenz, D. P., Cheong, W. F. & Woodburn, K. W., (2000). *Photoangioplasty: An emerging clinical cardiovascular role for photodynamic therapy*. Circulation. **102:** 591-6.

Rosenthal, M. B., (2007). *Nonpayment for performance? Medicare's new reimbursement rule*. New England Journal of Medicine. **357:** 1573-5.

Ruparelia, J. P., Chatteriee, A. K., Duttagupta, S. P. & Mukherji, S., (2008). *Strain specificity in antimicrobial activity of silver and copper nanoparticles*. Acta Biomaterialia. **4:** 707-716.

Rupp, M. E., Fitzgerald, T., Marion, N., Helget, V., Puumala, S., Anderson, J. R. & Fey, P. D., (2004). *Effect of silver-coated urinary catheters: efficacy, cost-effectiveness, and antimicrobial resistance*. American Journal of Infection Control. **32:** 445-50.

Rutala, W. A., Katz, E. B., Sherertz, R. J. & Sarubbi, F. A., Jr., (1983). *Environmental study of a methicillin-resistant Staphylococcus aureus epidemic in a burn unit*. Journal of Clinical Microbiology. **18:** 683-8.

Rutala, W. A., Weber, D. J. & Healthcare Infection Control Practices Advisory Committee. (2008). *Guideline for disinfection and sterilization in healthcare facilities*. Atlanta, GA.: Centers for Disease Control and Prevention.

Saito, T., Iwase, T., Horie, J. & Morioka, T., (1992). *Mode of photocatalytic bactericidal action of powdered semiconductor $Ti0_2$ on mutans Streptococci*. Journal of Photochemistry and Photobiology B: Biology. **14:** 369-379.

Salmon-Divon, M., Nitzan, Y. & Malik, Z., (2004). *Mechanistic aspects of Escherichia coli photodynamic inactivation by cationic tetra-meso(N-methylpyridyl)porphine*. Photochemical & Photobiological Sciences. **3:** 423-9.

Salo, S., Storgards, E. & Wirtanen, G., (Year). *Alternative methods for sampling from surfaces*. *In:* Wirtanen, G., Salo, S. & Mikkola, A., eds. 30th R3-Nordic Contamination Control Symposium, 1999 Espoo, Finland. VTT Offsetpaino, 187-198.

Salo, S. & Wirtanen, G. (1999). *Detergent based blends for swabbing and dipslides in improved surface sampling*. *In:* Wimpenny, J., Gilbert, P., Walker, J., Brading, M. & Bayston, R. (eds.) *Biofilms: The Good, The Bad and The Ugly.* Cardiff: BioLine.

Samore, M. H., Venkataraman, L., DeGirolami, P. C., Arbeit, R. D. & Karchmer, A. W., (1996). *Clinical and molecular epidemiology of sporadic and clustered cases of nosocomial Clostridium difficile diarrhea*. American Journal of Medicine. **100:** 32-40.

Sanborn, L. W., (1963). *The relation of surface contamination to the transmission of disease*. American Journal of Public Health. **53:** 1278-1283.

Sandel, M. K. & McKillip, J. L., (2004). *Virulence and recovery of Staphylococcus aureus relevant to the food industry using improvements on traditional approaches*. Food Control. **15:** 5-10.

Schierholz, J. M., Lucas, L. J., Rump, A. & Pulverer, G., (1998). *Efficacy of silver-coated medical devices*. Journal of Hospital Infection. **40:** 257-262.

Schmidt, M. & Initiative, C. T. S., (2011). *Copper surfaces in the ICU reduced the relative risk of acquiring an infection while hospitalized*. BMC Proceedings. 5: O53.

Schreckenberger, P. C. & von Graevenitz, A. (1999). *Acinetobacter, Achromobacter, Alcaligenes, Moraxella, Methylobacterium, and other nonfermentative Gram-negative rods*. *In:* Murray, P. R., Baron, E. J., Pfaller, M. A., Tenover, F. C. & Yolken, R. H. (eds.) *Manual of Clinical Microbiology.* 7 ed. Washington D.C.: ASM Press.

Sclafani, A., Mozzanega, M.-N. & Pichat, P., (1991). *Effect of silver deposits on the photocatalytic activity of titanium dioxide samples for the dehydrogenation or oxidation of 2-propanol*. Journal of Photochemistry and Photobiology A: Chemistry. **59:** 181-189.

Scott II, R. D. (2009). *The direct medical costs of Healthcare-Associated Infections in U.S. hospitals and the benefits of prevention*. Division of Healthcare Quality Promotion, Centers for Disease Control and Prevention.

Seal, G. J., Ng, Y. L., Spratt, D., Bhatti, M. & Gulabivala, K., (2002). *An in vitro comparison of the bactericidal efficacy of lethal photosensitization or sodium hyphochlorite irrigation on Streptococcus intermedius biofilms in root canals*. Internation Endodontic Journal. **35:** 268-74.

Selan, L., Berlutti, F., Passariello, C., Thaller, M. C. & Renzini, G., (1992). *Reliability of a bioluminescence ATP assay for detection of bacteria*. Journal of Clinical Microbiology. **30:** 1739-1742.

Semmelweis, I. F., (1861). *The etiology, the concept and the prophylaxis of childbed fever,* Birmingham, Alabama., The Classics of Medicine Library.

Shahverdi, A. R., Fakhimi, A., Shahverdi, H. R. & Minaian, S., (2007). *Synthesis and effect of silver nanoparticles on the antibacterial activity of different antibiotics against Staphylococcus aureus and Escherichia coli*. Nanomedicine-Nanotechnology Biology and Medicine. **3:** 168-171.

Sharma, M., Visai, L., Bragheri, F., Cristiani, I., Gupta, P. K. & Speziale, P., (2008). *Toluidine blue-mediated photodynamic effects on Staphylococcal biofilms*. Antimicrobial Agents and Chemotherapy. **52:** 299-305.

Sharma, S. K., Vishwas, M., Rao, K. N., Mohan, S., Reddy, D. S. & Gowda, K. V. A., (2009). *Structural and optical investigations of TiO_2 films deposited on transparent substrates by sol-gel technique*. Journal of Alloys and Compounds. **471:** 244-247.

Shaughnessy, M. K., Micielli, R. L., DePestel, D. D., Arndt, J., Strachan, C. L., Welch, K. B. & Chenoweth, C. E., (2011). *Evaluation of hospital room assignment and acquisition of Clostridium difficile infection*. Infection Control and Hospital Epidemiology. **32:** 201-206.

Shiomori, T., Miyamoto, H., Makishima, K., Yoshida, M., Fujiyoshi, T., Udaka, T., Inaba, T. & Hiraki, N., (2002). *Evaluation of bedmaking-related airborne and surface methicillin-resistant Staphylococcus aureus contamination*. Journal of Hospital Infection. **50:** 30-35.

Shorr, A. F., Zilberberg, M. D. & Kollef, M., (2009). *Cost-effectiveness analysis of a silver-coated endotracheal tube to reduce the incidence of ventilator-associated pneumonia*. Infection Control and Hospital Epidemiology. **30:** 759-63.

Silver, S., (2003). *Bacterial silver resistance: molecular biology and uses and misuses of silver compounds*. FEMS Microbiology Reviews. **27:** 341-353.

Silver, S., Phung, L. T. & Silver, G., (2006). *Silver as biocides in burn and wound dressings and bacterial resistance to silver compounds*. Journal of Industrial Microbiology & Biotechnology. **33:** 627-634.

Simpson, J. A., Smith, S. E. & Dean, R. T., (1989). *Scavenging by alginate of free radicals released by macrophages*. Free Radical Biololgy and Medicine. **6:** 347-53.

So, C. W., Tsang, P. W., Lo, P. C., Seneviratne, C. J., Samaranayake, L. P. & Fong, W. P., (2010). *Photodynamic inactivation of Candida albicans by BAM-SiPc*. Mycoses. **53:** 215-20.

Sökmen, M., Candan, F. & Sümer, Z., (2001). *Disinfection of E. coli by the Ag-TiO_2/UV system: lipidperoxidation*. Journal of Photochemistry and Photobiology A: Chemistry. **143:** 241-244.

Sottile, F. D., Marrie, T. J., Prough, D. S., Hobgood, C. D., Gower, D. J., Webb, L. X., Costerton, J. W. & Gristina, A. G., (1986). *Nosocomial pulmonary infection: possible etiologic significance of bacterial adhesion to endotracheal tubes*. Critical Care Medicine. **14:** 265-70.

Spronk, P. E., Rommes, J. H. & Schultz, M. J., (2006). *Comment on "Antibacterial-coated tracheal tubes cleaned with a Mucus Shaver" by Berra et al*. Intensive Care Medicine. **32:** 2080-1; author reply 2082-3.

Stathatos, E., Petrova, T. & Lianos, P., (2001). *Study of the efficiency of visible-light photocatalytic degradation of basic blue adsorbed on pure and doped mesoporous titania films*. Langmuir. **17:** 5025-5030.

Stobie, N., Duffy, B., McCormack, D. E., Colreavy, J., Hidalgo, M., McHale, P. & Hinder, S. J., (2008). *Prevention of Staphylococcus epidermidis biofilm formation using a low-temperature processed silver-doped phenyltriethoxysilane sol-gel coating*. Biomaterials. **29:** 963-969.

Storgards, E., Simola, H., Sjöberg, A. M. & Wirtanen, G., (1999). *Hygiene of gasket materials used in food processing equipment part 2: Aged materials*. Food and Bioproducts Processing. **77:** 146-155.

Sunada, K., Kikuchi, Y., Hashimoto, K. & Fujishima, A., (1998). *Bactericidal and detoxification effects of TiO_2 thin film photocatalysts*. Environmental Science & Technology. **32:** 726-728.

Sunada, K., Watanabe, T. & Hashimoto, K., (2003). *Studies on photokilling of bacteria on TiO_2 thin film*. Journal of Photochemistry and Photobiology A: Chemistry. **156:** 227-233.

Swanepoel, R., (1983). *Determination of the thickness and optical constants of amorphous silicon*. Journal of Physics E - Scientific Instruments. **16:** 1214-1222.

Syed, M. A., Babar, S., Bhatti, A. S. & Bokhari, H., (2009). *Antibacterial effects of silver nanoparticles on the bacterial strains isolated from catheterized urinary tract infection cases*. Journal of Biomedical Nanotechnology. **5:** 209-14.

Talon, D., (1999). *The role of the hospital environment in the epidemiology of multi-resistant bacteria*. Journal of Hospital Infection. **43:** 13-17.

Tauc, J., (1968). *Optical Properties and Electronic Structure of Amorphous*. Materials Research Bulletin. **3:** 37-46.

Tauc, J., (1970). *Absorption Edge and Internal Electric Fields in Amorphous Semiconductors*. Materials Research Bulletin. **5:** 721-&.

Taylor, L., Phillips, P. & Hastings, R., (2009). *Reduction of bacterial contamination in a healthcare environment by silver antimicrobial technology*. Journal of Infection Prevention. **10:** 6-12.

Technical publication for the 2D series lamp. (2005). Available: http://www.gelighting.com/eu/resources/literature_library/prod_tech_pub/downloads/biax2d_datasheet_0506.pdf [Accessed 01/06/2011].

Thompson, T. L. & Yates, J. T., (2006). *Surface science studies of the photoactivation of TiO_2 - New photochemical processes*. Chemical Reviews. **106:** 4428-4453.

Tolker-Nielsen, T., Brinch, U. C., Ragas, P. C., Andersen, J. B., Jacobsen, C. S. & Molin, S., (2000). *Development and dynamics of Pseudomonas sp. biofilms*. Journal of Bacteriology. **182:** 6482-6489.

Torres, A., Ewig, S., Lode, H. & Carlet, J., (2009). *Defining, treating and preventing hospital acquired pneumonia: European perspective*. Intensive Care Medicine. **35:** 9-29.

Tseng, S. P., Teng, L. J., Chen, C. T., Lo, T. H., Hung, W. C., Chen, H. J., Hsueh, P. R. & Tsai, J. C., (2009). *Toluidine blue O photodynamic inactivation on multidrug-resistant Pseudomonas aeruginosa*. Lasers in Surgery and Medicine. **41:** 391-397.

Tuomanen, E., Cozens, R., Tosch, W., Zak, O. & Tomasz, A., (1986). *The rate of killing of Escherichia coli by β-lactam antibiotics is strictly proportional to the rate of bacterial growth*. Journal of General Microbiology. **132:** 1297-1304.

Uttley, A. H., Collins, C. H., Naidoo, J. & George, R. C., (1988). *Vancomycin-resistant enterococci*. Lancet. **1:** 57-8.

van Schothorst, M., Huisman, J. & van Os, M., (1978). *Salmonella-onderzock in huishoudens met salmonellose bij zuigelingen*. Nederlands Tijdschrift voor Geneeskunde. **122:** 1121-1125.

Vermeulen, N., Keeler, W. J., Nandakumar, K. & Leung, K. T., (2008). *The bactericidal effect of ultraviolet and visible light on Escherichia coli*. Biotechnology and Bioengineering. **99:** 550-556.

Verran, J., (2010). *Antimicrobial surfaces: addressing the intended application*. Chimica oggi/Chemistry today. **28:** 36-38.

Verran, J., Boyd, R. D., Hall, K. E. & West, R., (2002). *The detection of microorganisms and organic material on stainless steel food contact surfaces*. Biofouling: The Journal of Bioadhesion and Biofilm Research. **18:** 167 - 176.

Verran, J., J.Redfern, Smith, L. A. & Whitehead, K. A., (2010a). *A critical evaluation of sampling methods used for assessing microorganisms on surfaces*. Food and Bioproducts Processing. **88:** 335-340.

Verran, J., Lees, G. & Shakespeare, A. P., (1991). *The effect of surface roughness on the adhesion of Candida albicans to acrylic*. Biofouling. **3:** 183-191.

Verran, J., Packer, A., Kelly, P. & Whitehead, K. A., (2010b). *The retention of bacteria on hygienic surfaces presenting scratches of microbial dimensions*. Letters in Applied Microbiology. **50:** 258-63.

Wagenvoort, J. H., Sluijsmans, W. & Penders, R. J., (2000). *Better environmental survival of outbreak vs. sporadic MRSA isolates*. Journal of Hospital Infection. **45:** 231-4.

Wainwright, M., (1998). *Photodynamic antimicrobial chemotherapy (PACT)*. Journal of Antimicrobial Chemotherapy. **42:** 13-28.

Wainwright, M., (2003). *The use of dyes in modern biomedicine*. Biotechic and Histochemistry. **78:** 147-55.

Wainwright, M., Phoenix, D. A., Marland, J., Wareing, D. R. & Bolton, F. J., (1997). *A study of photobactericidal activity in the phenothiazinium series*. FEMS Immunology and Medical Microbiology. **19:** 75-80.

Wakayama, Y., Takagi, M. & Yano, K., (1980). *Photosensitized inactivation of Escherichia coli cells in toluidine blue light system*. Photochemistry and Photobiology. **32:** 601-605.

Warnes, S. L. & Keevil, C. W., (2011). *Mechanism of copper surface toxicity in vancomycin-resistant enterococci following wet or dry surface contact*. Applied and Environmental Microbiology. **77:** 6049-59.

Watts, R. J., Kong, S. H., Orr, M. P., Miller, G. C. & Henry, B. E., (1995). *Photocatalytic inactivation of coliform bacteria and viruses in secondary waste-water effluent*. Water Research. **29:** 95-100.

Weaver, L., Noyce, J. O., Michels, H. T. & Keevil, C. W., (2010). *Potential action of copper surfaces on meticillin-resistant Staphylococcus aureus*. Journal of Applied Microbiology. **109:** 2200-5.

Weber, D. J. & Rutala, W. A., (1997). *Role of environmental contamination in the transmission of vancomycin-resistant enterococci*. Infection Control and Hospital Epidemiology. **18:** 306-9.

Weber, D. J. & Rutala, W. A., (2011). *The role of the environment in transmission of Clostridium difficile infection in healthcare facilities*. Infection Control and Hospital Epidemiology. **32:** 207-209.

Weber, D. J., Rutala, W. A., Sickbert-Bennett, E. E., Samsa, G. P., Brown, V. & Niederman, M. S., (2007). *Microbiology of ventilator-associated pneumonia compared with that of hospital-acquired pneumonia*. Infection Control and Hospital Epidemiology. **28:** 825-31.

Wei, C., Lin, W. Y., Zainal, Z., Williams, N. E., Zhu, K., Kruzic, A. P., Smith, R. L. & Rajeshwar, K., (1994). *Bactericidal activity of TiO_2 photocatalyst in aqueous media: toward a solar-assisted water disinfection system*. Environmental Science & Technology. **28:** 934-938.

Wendt, C., Wiesenthal, B., Dietz, E. & Ruden, H., (1998). *Survival of vancomycin-resistant and vancomycin-susceptible enterococci on dry surfaces*. Journal of Clinical Microbiology. **36:** 3734-6.

Wenzel, R. N., (1936). *Resistance of solid surfaces to wetting by water*. Industrial & Engineering Chemistry. **28:** 988-994.

Wenzel, R. P., (1995). *The Lowbury Lecture. The economics of nosocomial infections*. Journal of Hospital Infection. **31:** 79-87.

West, A. R., (1999). *Basic Solid State Chemistry,* Chichester, John Wiley & Sons, Ltd.

White, R. J., (2002). *An historical overview of the use of silver in wound management.* British Journal of Nursing. **6:** Suppl 1, 3-8.

Whitehead, K. A., Smith, L. A. & Verran, J., (2008). *The detection of food soils and cells on stainless steel using industrial methods: UV illumination and ATP bioluminescence*. International Journal of Food Microbiology. **127:** 121-8.

Whyte, W., Hambraeus, A., Laurell, G. & Hoborn, J., (1992). *The relative importance of the routes and sources of wound contamination during general surgery. II. Airborne*. Journal of Hospital Infection. **22:** 41-54.

Whyte, W., Hodgson, R. & Tinkler, J., (1982). *The importance of airborne bacterial contamination of wounds*. Journal of Hospital Infection. **3:** 123-135.

Wilcox, M. H., (1996). *Cleaning up Clostridium difficile infection*. Lancet. **348:** 767-8.

Wilcox, M. H., Finch, R. G., Smith, D. G., Williams, P. & Denyer, S. P., (1991). *Effects of carbon dioxide and sub-lethal levels of antibiotics on adherence of coagulase-negative staphylococci to polystyrene and silicone rubber*. Journal of Antimicrobial Chemotherapy. **27:** 577-87.

Willis, C., Morley, J., Westbury, J., Greenwood, M. & Pallett, A., (2007). *Evaluation of ATP bioluminescence swabbing as a monitoring and training tool for effective hospital cleaning*. British Journal of Infection Control. **8:** 17-21.

Wilson, M., (1993). *Photolysis of oral bacteria and its potential use in the treatment of caries and periodontal disease*. Journal of Applied Bacteriology. **75:** 299-306.

Wilson, M., (1996). *Susceptibility of oral bacterial biofilms to antimicrobial agents*. Journal of Medical Microbiology. **44:** 79-87.

Wilson, M., (2003). *Light-activated antimicrobial coating for the continuous disinfection of surfaces*. Infection Control and Hospital Epidemiology. **24:** 782-784.

Wilson, M., Dobson, J. & Sarkar, S., (1993). *Sensitization of periodontopathogenic bacteria to killing by light from a low-power laser*. Oral Microbiology and Immunology. **8:** 182-7.

Wilson, M. & Mia, N., (1993). *Sensitisation of Candida albicans to killing by low-power laser light*. Journal of Oral Pathology and Medicine. **22:** 354-7.

Wilson, M. & Mia, N., (1994). *Effect of environmental factors on the lethal photosensitization of Candida albicans in vitro*. Lasers in Medical Science. **9:** 105-109.

Wilson, M. & Pratten, J., (1995). *Lethal photosensitisation of Staphylococcus aureus in vitro: effect of growth phase, serum, and pre-irradiation time*. Lasers in Surgery and Medicine. **16:** 272-6.

Wilson, M. & Yianni, C., (1995). *Killing of methicillin-resistant Staphylococcus aureus by low-power laser light*. Journal of Medical Microbiology. **42:** 62-6.

Wolfrum, E. J., Huang, J., Blake, D. M., Maness, P. C., Huang, Z., Fiest, J. & Jacoby, W. A., (2002). *Photocatalytic oxidation of bacteria, bacterial and fungal spores, and model biofilm components to carbon dioxide on titanium dioxide-coated surfaces*. Environmental Science & Technology. **36:** 3412-9.

Wong, M.-S., Chu, W.-C., Sun, D.-S., Huang, H.-S., Chen, J.-H., Tsai, P.-J., Lin, N.-T., Yu, M.-S., Hsu, S.-F., Wang, S.-L. & Chang, H.-H., (2006). *Visible-light-induced bactericidal activity of a nitrogen-doped titanium photocatalyst against human pathogens*. Applied and Environmental Microbiology. **72:** 6111-6116.

Wong, M. S., Sun, D. S. & Chang, H. H., (2010). *Bactericidal performance of visible-light responsive titania photocatalyst with silver nanostructures*. PLoS One. **5:** e10394.

Wong, V., Staniforth, K. & Boswell, T. C., (2011). *Environmental contamination and airborne microbial counts: a role for hydroxyl radical disinfection units?* Journal of Hospital Infection. **78:** 194-199.

Yamanaka, M., Hara, K. & Kudo, J., (2005). *Bactericidal actions of a silver ion solution on Escherichia coli, studied by energy-filtering transmission electron microscopy and proteomic analysis*. Applied and Environmental Microbiology. **71:** 7589-93.

Yan, G., Chen, J. & Hua, Z., (2009). *Roles of H_2O_2 and OH radical in bactericidal action of immobilized TiO_2 thin-film reactor: An ESR study*. Journal of Photochemistry and Photobiology A: Chemistry. **207:** 153-159.

Yang, M.-C., Yang, T.-S. & Wong, M.-S., (2004). *Nitrogen-doped titanium oxide films as visible light photocatalyst by vapor deposition*. Thin Solid Films. **469-470:** 1-5.

Yoshida, Y., Furuta, S. & Niki, E., (1993). *Effects of metal chelating agents on the oxidation of lipids induced by copper and iron*. Biochimica et Biophysica Acta (BBA) - Lipids and Lipid Metabolism. **1210:** 81-88.

Yu, F. P. & McFeters, G. A., (1994). *Rapid in situ assessment of physiological activities in bacterial biofilms using fluorescent probes*. Journal of Microbiological Methods. **20:** 1-10.

Yu, J. C., Ho, W., Yu, J., Yip, H., Wong, P. K. & Zhao, J., (2005). *Efficient visible-light-induced photocatalytic disinfection on sulfur-doped nanocrystalline titania*. Environmental Science & Technology. **39:** 1175-1179.

Zanetti, G., Blanc, D. S., Federli, I., Raffoul, W., Petignat, C., Maravic, P., Francioli, P. & Berger, M. M., (2007). *Importation of Acinetobacter baumannii into a burn unit: a recurrent outbreak of infection associated with widespread environmental contamination*. Infection Control and Hospital Epidemiology. **28:** 723-725.

Zanin, I. C., Lobo, M. M., Rodrigues, L. K., Pimenta, L. A., Hofling, J. F. & Goncalves, R. B., (2006). *Photosensitization of in vitro biofilms by toluidine blue O combined with a light-emitting diode*. European Journal of Oral Sciences. **114:** 64-9.

Zhao, G., Kozuka, H. & Yoko, T., (1996). *Sol-gel preparation and photoelectrochemical properties of TiO_2 films containing Au and Ag metal particles*. Thin Solid Films. **277:** 147-154.

Zita, J., Krýsa, J. & Mills, A., (2009). *Correlation of oxidative and reductive dye bleaching on TiO_2 photocatalyst films*. Journal of Photochemistry and Photobiology A: Chemistry. **203:** 119-124.

Zubkov, T., Stahl, D., Thompson, T. L., Panayotov, D., Diwald, O. & Yates, J. T., (2005). *Ultraviolet light-induced hydrophilicity effect on TiO_2(110)(1x1). Dominant role of the photooxidation of adsorbed hydrocarbons causing wetting by water droplets*. The Journal of Physical Chemistry B. **109:** 15454-15462.